In Vivo Use of Monoclonal Antibodies for Radiolabelling Blood Cells

A Study Using Lymphocyte and Platelet Specific Antibodies Labelled with Indium-111

Thesis submitted for the degree of Doctor of Philosophy (PhD)

Faculty of Medicine - University of London

by

Issa LOUTFI
MD, MSc

Nuclear Medicine Unit and Immunology Department
Royal Postgraduate Medical School
Hammersmith Hospital
Du Cane Road
London
UK

1990

Abstract

This thesis explores the use of indium-111 labelled monoclonal antibodies (McAb) for specific radiolabelling of cells in blood and solid tissues. Various ^{111}In McAbs reacting with platelets, lymphocytes or molecules of the major histocompatibility complex (MHC) have been tested in vitro then injected in vivo to image the cell population expressing the relevant antigen using the scintillation camera.

Experimental work involving an ^{111}In anti-platelet McAb includes in vitro tests for antibody binding and effect on platelet aggregation. Injection of the ^{111}In McAb in man has resulted in imaging platelet distribution in the body and detection of abnormal platelet deposition in thrombus.

^{111}In McAbs have also been used for labelling the main subsets of lymphocytes (T & B). Testing of ^{111}In anti-lymphocyte McAbs with normal lymphocytes and cell lines has indicated their range of binding and effect on the cells. The injection of an ^{111}In anti-T cell McAb in the rat has resulted in antibody binding to T cells in blood, lymph nodes and spleen. Antigen modulation after administration of the antibody has also been observed. Additionally, ^{111}In McAb cell labelling in the rat has been compared to the use of ^{111}In tropolone labelled lymphocytes in terms of imaging lymphoid tissues, following lymphocyte kinetics and radiodosimetry.

In vivo use of ^{111}In McAbs is also presented in an experimental model of allogeneic kidney transplant in the rat. Immunopathological events of lymphocyte infiltration and induction of Class I and II MHC molecules in the graft during acute rejection have been traced using in vivo ^{111}In anti-T cell, activated T cell, Class I or Class II MHC McAbs and scintillation camera imaging. Images of rejecting and cyclosporine treated transplants have been obtained. The implications of the findings for the detection and discrimination of rejection are discussed.

Contents

List of Tables in the Thesis

List of Figures in the thesis

List of Abbreviations Used in the Thesis

Ab : Antibody
Abd : Abdomen
ACD : Acid citrate dextrose
Ag : Antigen
Ant : Anterior
APAAP : Alkaline phosphatase anti-alkaline phosphatase
BG : Background
BM : Bone marrow
B/T : Bound/Total
CD : Cluster of differentiation
CEA : Carcinoembryonic antigen
CLL : Chronic lymphatic leukaemia
CLN : Cervical lymph nodes
Con A : Concanavalin A
Conc : Concentration
Cont : Continued
Cpm : Count per minute
C1q : First component of the complement
CsA : Cyclosporine
Ct : Count
CTCL : Cutaneous T cell leukaemia
CTL : Cytotoxic T lymphocyte
Ctrl : Control
d : day
Deion : Deionized
Dist : Distilled
DTPA : Diethylene-triamine-pentaacetic acid
DVT : Deep venous thrombosis
$\overline{E}\beta$ (MeV) : Mean energy of β emissions in mega electron-volts
Expt : Experiment
F : Female
FITC : Fluorescein isothiocyanate
GPIIb, IIIa : Glycoprotein IIb, IIIa
HAMA : Human anti-mouse antibody
Hb : Haemoglobin
Hct : Haematocrit
ICRF : Imperial Cancer Research Fund
IF : Immunofluorescence

Ig : Immunoglobulin
Int : intestine
ITP: Idiopathic thrombocytopenic purpura
kDa : Kilo dalton
KeV : Kilo electron-volt
Kid : Kidney
L : Left
LAK : Lymphokine activated killer
LAO : Left anterior oblique
LFOV : Large field of view
LM : Lymphocytes-Monocytes
LN : Lymph nodes
LNC : Lymph node cells
LPO : Left posterior oblique
M : Male
McAb : Monoclonal antibody
MeV : Mega electron-volt
MHC : Major histocompatibility complex
min : Minute
MLN : Mesenteric lymph nodes
MW : Molecular weight
NA : Not applicable
ND : Not done
OD : optical density
PA : Platelet aggregation
PAK : Phytohaemagglutinin activated killer
PBMNC : Peripheral blood mononuclear cells
PBS : Phosphate buffered saline
PHA : Phytohaemagglutinin
PI : Post injection
pl : Plasma
PMT : Photomultiplier tube
Post : Posterior
PP : Peyer's patches
PPP : Platelet poor plasma
PRP : Platelet rich plasma
Ptlt : Platelet
R : Right
RAM : Rabbit anti-mouse
RAO : Right anterior oblique

RBC : Red blood cells
RBE : Relative biological effectiveness
ROI : Region of interest
RPMS : Royal Postgraduate Medical School
RPO : Right posterior oblique
RT : room temperature
SD : Standard deviation
SDS-PAGE : Sodium dodecyl sulphate polyacrylamide gel electrophoresis
se : Standard error of the mean
Spl : Spleen
Std : Standard
$T_{1/2}$: Half-life
$T_{1/2b}$: Biological half-life
$T_{1/2eff}$: Effective half-life
TDL : Thoracic duct lymphocytes
Thy : Thymus
TIL : Tumour infiltrating lymphocytes
Tx : Transplant
UV : Ultraviolet
Vol : Volume
vs : Versus
vWF : von Willebrand factor
WB : Whole blood, or whole body (in images)
WBC : White blood cell
yr : Year

Acknowledgements

In writing this thesis, I owe a great debt of gratitude to Professor JP Lavender, my supervisor. His understanding and encouragement as well as his excellent advice and criticism have been invaluable to me in the achievement of this work.

To Professor JR Batchelor and Dr AA Epenetos, I also owe much. Professor Batchelor for his innovative ideas on the exploration of transplant rejection and his practical contribution in performing the delicate transplant operations, and Dr Epenetos for his enthusiasm for scientific research on monoclonal antibodies and faith in the work of young scientists from all over the world.

I also acknowledge the valuable help and great assistance offered by Dr PM Chisholm in the achievement of the experimental aspect of labelling lymphocytes in vivo. She provided an excellent research approach and a firm scientific opinion based on honesty, knowledgeability and deliberation.

I am most thankful to Dr MJ Myers who advised me on the dosimetry and statistical aspects of this work. In Dr AM Peters, I have found the Nuclear Medicine Scientist that is able to instigate new ideas and make tracer kinetics look simpler with informal and instructive debates.

The staff at Hammersmith Hospital and the Royal Postgraduate Medical School deserve a special mention and recognition of their efforts in providing a friendly, professional and responsible milieu for the performance of scientific research of a very high standard.

My warmest thanks go to Miss B Henderson for the efficient and orderly performance of patient imaging using the scintillation camera at the Nuclear Medicine Unit. I also recognize the untiring efforts of Ms G Webb

and Mr M Braun, a friend and colleague, in giving technical assistance and stimulating discussions. I am grateful as well to the staff in Dr M Ritter's laboratory, Dr G Sivolapenko, Mrs H Ladyman and Dr M Larche' for technical advice and help.

In the Hammersmith Oncology Group, I have made strong ties and lasting friendships. Dear colleagues I would like to mention : Dr NS Courtenay-Luck, Miss D Snook, Mr B Dhokia, Dr C Kosmas, Dr H Kalofonos, Dr S Pervez and Mr AWJ Stuttle.

I am also extremely grateful to the staff at the Wellcome library especially Miss E Davies and the staff at the Department of Medical Illustration for the great trouble they have taken over the preparation of my photographs.

The generous gifts of monoclonal antibodies and reagents from the Imperial Cancer Research Fund-London and antibodies from Unipath-Oxoid-Basingstoke, the MRC-Cellular Immunology Unit-Oxford and the Blond McIndoe Centre-Queen Victoria Hospital-East Grinstead are very much appreciated. Also, the supply of ^{111}Indium by the ICRF, Amersham International plc and the Medical Research Council-Cyclotron Unit, especially Dr H Danpure and Miss S Osman, has been instrumental in the achievement of the research work using radiolabelled McAbs.

The contribution of Dr P Lumley, Glaxo Research Group, in the performance of platelet aggregation studies has been most useful.

Finally, words of thanks to the Syrian Atomic Energy Commision, the body sponsoring my studies in the UK. I appreciate the great efforts that staff at this establishment have put to ensure adequate sponsorship for my studies.

The moral support of my family and my friends in Syria and Britain is unforgettable.

Statement of Originality and Authenticity; Disclaimer; Publications Based on Work in the Thesis

The research work presented in this thesis is original and has been authentically performed by the candidate Dr I Loutfi. Experiments have been done either by the candidate alone or by the candidate working as a member of a team of researchers. Work that has been done jointly with other investigators includes :

Measurement of platelet aggregation in whole blood, in vivo use of the unlabelled anti-T cell McAb in the rat and experimental kidney transplantation in the rat.

Experimentation on live animals was done under a personal licence and a corresponding project licence and aimed at causing the least possible distress to the animal under study.

Reference is made to recognised publications and all personal communications are documented in writing. The inclusion of published material from other sources is mainly for clarification purposes and is fully acknowledged.

Finally, parts of the research work in this thesis have been published in scientific papers and presented as oral papers or posters at scientific meetings, as listed below :

1) Peters AM, Lavender JP, Needham SG, Loutfi I, Snook D, Epenetos AA, Lumley P, Keery RJ and Hogg N, Imaging thrombus with radiolabelled monoclonal antibodies to platelets. Br Med J 293 : 1525-1527, 1986.

2) Stuttle AWJ, Peters AM, Loutfi I, Lumley P, George P and Lavender JP, Use of anti-platelet monoclonal antibody $F(ab')_2$ fragment for imaging thrombus. Nucl Med Comm 9 : 647-655, 1988.

3) Loutfi I, Batchelor JR, Lavender JP and Epenetos AA, Lymphocyte targeting with ^{111}In labelled monoclonal antibodies. Int J Cancer Suppl 2, 45-49, 1988.

4) Loutfi I, Batchelor JR, Chisholm PM, Epenetos AA and Lavender JP, Targeting of lymphocytes with ^{111}In labelled monoclonal antibodies. Nucl Med Comm 9 : 1787-1796, 1988.

5) Loutfi I, Chisholm PM, Bevan D and Lavender JP, In vivo imaging of rat lymphocytes with an indium-111 labelled anti-T cell monoclonal antibody : A comparison with indium-111 labelled lymphocytes. Eur J Nucl Med 16 : 69-76, 1990.

6) Loutfi I, Batchelor JR, and Lavender JP, In vivo imaging and quantitation of renal transplant rejection using indium-111 labelled anti-lymphocyte and anti-MHC Class I and II monoclonal antibodies in a rat model. In Nuclear Medicine, Quantitative Analysis in Imaging and Function, Proceedings of the European Association of Nuclear Medicine Congress 1989, Strasbourg-France, Schmidt HAE and Chambron J, eds, Schattauer, Stuttgart-New York pp429-431, 1990.

7) Loutfi I and Myers MJ, Dosimetry of an indium-111 anti-T lymphocyte monoclonal antibody in a rat model and its implications in man. Nucl Med Comm 10 : 246, 1989, Abst No 90, Eur J Nucl Med 15 : 569, 1989, Abst No 683.

8) Loutfi I, Batchelor JR, and Lavender JP, In vivo imaging and quantitation of renal transplant rejection using indium-111 labelled anti-lymphocyte and anti-MHC Class I and II monoclonal antibodies in a rat model. Nucl Med Comm 10 : 264-265, 1989 (Abst No 131), Eur J Nucl Med 15 : 414, 1989 (Abst No 61), British Transplantation Society Meeting , Liverpool 10 & 11 April 1990, Paper No 19.

Dedication

Sheherazade continued :

The fisherman cast his net for the third time and waited. Then, he pulled the net out of the sea and there was a brass carafe inside it. "Good fortune" said he, "For I could sell this at the market and get a few dinars in return". The carafe had a brass cap tightly fitted and when the fisherman prised it open using his knife, a cloud of smoke billowed out. As the smoke reached high in the sky, the full figure of a giant Ef'reet formed. The Ef'reet's head touched the clouds and his voice was like thunder. ..."Prepare yourself to die" said the Ef'reet, "For I have sworn to kill whoever released me from my imprisonment"..... The fisherman was very frightened, but he said : "O great Ef'reet, before I die, can you satisfy my curiosity and answer my question? How could you fit inside the little carafe and your body is like a mountain?"..."I cannot believe that you could fit in such a small place". The Ef'reet laughed and said "To satisfy your curiosity I'll show you how it is done". Then, the Ef'reet converted himself into smoke and reentered the vessel. Promptly, the fisherman replaced the cap and thanked God for his safety.

The dawn came so Sheherazade stopped talking.

From A Thousand and One Nights, Eastern Heritage to All Humanity.

To all those who use good judgement, knowledge and honesty to control the forces of nature and, particularly, those who employ nuclear energy for peace and prosperity of mankind, I dedicate this thesis.

I Loutfi

Section One :

Aims and Relevant Background

Chapter 1 :

Aims and Objectives

1.1 Introduction :

Radioactive tracers provide tools for non-invasive evaluation of organ function. As examples one may take the accumulation of ^{131}I by the thyroid, the excretion of simple chelates by the kidney, and the use of radioactive gases to examine regional ventilation.

One field of active research in the use of such tracers is the labelling of circulating blood cells. Radionuclides such as ^{51}Cr have been in use for many years to label circulating red blood cells and record red cell mass and cell survival (Sterling and Gray 1950, Ebaugh et al 1953). Further examples are the labelling of lymphocytes with tritium (Gowans 1959) and leucocytes with ^{32}P (Grob et al 1947, Athens et al 1959).

With the advent of a gamma emitter, ^{111}In oxine in 1976 (McAfee and Thakur 1976a), it became possible to quantitate whole body distribution and image cell accumulation in vivo. This was applied to migrating granulocytes (Thakur et al 1977a) and also to platelets localisation in thrombus (Goodwin et al 1978).

However, cell labelling with ^{111}In oxine requires separation of the cells from whole blood before labelling. This cell separation is necessary due to non-selectivity of cell labelling with this agent. The method, therefore, suffers from certain limitations :

1) Cell damage during separation.
2) Cell damage due to irradiation of a small population.
3) Circulating cells may not be representative of effector cells in tissues.

Hence, the use of a cell specific tracer has some obvious advantages :

1) In vivo use, without need for cell manipulation in vitro.
2) Labelling a large cell population.
3) Specific labelling of cell subgroups, eg T & B lymphocytes.

One further point arises from this outline and that is the possibility of labelling fixed cells with a specific tracer. This possibility has been fairly widely explored in the use of monoclonal antibodies for imaging tumours. Relatively little attempt, however, has been made to look at non-neoplastic disease.

1.2 Aims of the thesis :

To explore the use of radiolabelled monoclonal antibodies for in vivo labelling of platelets and lymphocytes and, in the case of lymphocytes, to investigate labelling subsets of cells.

Lastly, as an approach to labelling antigens developed by fixed cells, to look at monoclonal antibodies directed against the major histocompatibility complex molecules, Class I & Class II, as exhibited by organs undergoing rejection.

Accordingly, the experimental work in this thesis covers the following points :

1) The use of an ^{111}In anti-platelet McAb : This involves :

- Testing in vitro the binding characteristics of the antibody to platelets and studying its effect on platelet aggregation.
- In vivo use in a human clinical situation for imaging thrombus.

2) The use of ^{111}In anti-lymphocyte McAbs, involving :

- In vitro tests of two ^{111}In anti-human T and B cell McAbs with lymphoid cell lines and blood.
- In vitro testing and in vivo use of an ^{111}In anti-T cell McAb in the rat as an experimental model for imaging lymphoid tissue.

3) The use of ^{111}In anti-lymphocyte and anti-Class I & II MHC McAbs in a rat model of allogeneic kidney transplant for imaging graft rejection.

Note :

The use of radiolabelled anti-granulocyte McAbs has not been attempted in this work as application of these reagents for labelling granulocytes has been reported with some depth in the medical and scientific literature.

Chapter 2 :

The Value of Cell Radiolabelling in Lymphocyte- and Platelet-in-Vivo Physiology

2.1 Introduction :

The guidelines for use of cell tracers and the criteria of an ideal cell label for quantitative analysis have been discussed by many authors (Brownell et al 1968, Ford 1975, Ansell and Micklem 1986). Such a tracer would be fixed and localised to the cell; not secreted or eluted, it would be stable for the period of the study, easy to detect and to measure with some precision and functionally neutral not affecting a cell's behaviour or conferring any physiological advantage or disadvantage. In addition, the tracer should be readily available without recourse to complex preparatory procedures.

2.2 β emitters as early cell labels :

Radiolabels incorporating beta emitters have been used as the first cell radiolabelling agents (Jones et al 1940, Bond et al 1958). Examples of using β emitters for labelling blood cells include, among others, erythrocyte labelling with radioactive phosphorus (Hahn and Hevesy 1940), the use of ^{3}H-thymidine to trace lymphocytes in the thoracic duct (Everett et al 1960) and the measurement of lymphocyte life-span in humans using ^{32}P (Ottesen 1954). Table 2.1 shows β radionuclides that have been used for blood cell labelling.

Table 2.1, β emitters for cell labelling.

Radionuclide	Half-life	Radiation	$\overline{E}\beta$ (MeV)	Chemical form/Radiopharmaceutical
^{3}H	12.46 yr	β^-	0.006	Nucleosides : adenosine, uridine, thymidine, etc. Amino acids : glycine, leucine, etc. Others : DFP.
^{14}C	5570.0 yr	β^-	0.050	Same as ^{3}H (see above). Serotonine (Platelets).
^{32}P	14.3 d	β^-	0.700	DFP, inorganic phosphate.
^{35}S	87.0 d	β^-	0.049	Amino acids : L-cystine, methionine.

yr : year, d : day, DFP : di-isopropyl fluorophosphate.

2.3 Cell radiolabelling with γ-ray emitters :

2.3.1 Chromium-51

Chromium-51 was first used by Gray and Sterling in 1950 to label red blood cells. Radioactive chromate can penetrate the cells and bind principally to intracellular protein (Pearson 1963, Steiner and Baldini 1970). Chromium-51 decays by electron capture with a half-life of 27.8 days emitting 320 KeV gamma rays. These undergo, however, a high degree of internal conversion so that only 10% of the nuclear transformations result in useful photonic emissions.

Chromium-51 has been used both in experimental animals and man to follow the kinetics of lymphocytes in vivo by recording whole body distribution after intravenous administration of the labelled cells and observing their recirculation by thoracic duct cannulation (see Chapter 7).

Platelet radiolabelling with ^{51}Cr has also been used to establish the kinetics of these cells in man (Aas and Gardner 1958, ICSH 1977) in normal and disease conditions such as idiopathic thrombocytopenic purpura (ITP).

Although the use of chromium-51 as a cell label has resulted in insight into blood cell kinetics and sites of cell localisation in the body, its application is presently restricted to experimental research in animals and a few haematological investigations in man such as red cell survival studies (ICSH 1971 & 1980, Dacie and Lewis 1984, Bentley and Miller 1986).

The main reasons for the unpopularity of chromium-51 as a radiolabel for white cells stem primarily from the physical characteristics of the radionuclide. Chromium-51 has a long half-life (28 days) and a low abundance of γ emissions due to the internal conversion phenomenon. Also, its 320 keV γ ray is not suitable for imaging with the scintillation camera due to its relatively high energy.

2.3.2 Indium-111 lipophilic chelating agents

In 1976 McAfee and Thakur (1976a & b), having tried a number of compounds, reported the suitability of ^{111}In oxine for radiolabelling white blood cells.

This agent (8-hydroxyquinoline) is highly lipophilic and readily forms a complex with ^{111}In. The complex penetrates the cell membrane then once inside the cell, it dissociates and ^{111}In binds intracellularly giving a stable radiolabel (Thakur et al 1977b). ^{111}In is a gamma-emitting radionuclide with energies 173 KeV (99%) and 247 KeV (94%) very suited to external detection by scintillation cameras. Other lipophilic chelates of ^{111}In have also been reported such as acetyl acetone (Sinn and Silvester 1979) and tropolone

(Dewanjee et al 1981, Danpure et al 1982). The advantage of using the latter lies in labelling white cells in plasma instead of saline.

Although ^{111}In oxine was introduced primarily for radiolabelling neutrophils (McAfee and Thakur 1976a), the use of this agent to radiolabel platelets and lymphocytes came soon afterward.

Studies in vitro and in vivo comparing ^{51}Cr- and ^{111}In-oxine-labelled platelets (Schmidt et al 1983a & b) have shown rather similar results. Clinically, ^{111}In oxine labelling has been used to image platelet localisation in thrombus (Goodwin et al 1978, Davis et al 1980a & b) and in the diagnosis of organ transplant rejection (Smith et al 1979a, Martin-Comin et al 1983).

Lymphocyte labelling with ^{111}In oxine has also been used. Experimental studies in rats (Rannie et al 1977) and in sheep (Frost et al 1979, Issekutz et al 1980) involving intravenous injection of ^{111}In oxine labelled lymphocytes, scintillation camera imaging and tissue sampling have shown kinetics of the ^{111}In labelled cells similar to those reported using other cell tracers such as ^{51}Cr. Scintillation camera scanning of the animals produced images of lymph nodes and spleen. In man, the method has been applied to a limited extent for following lymphocyte kinetics and lymph node imaging (see chapter 7 for details).

2.3.3 Other gamma labels

Cell labelling using technetium-99m has been tried extensively due to the availability and wide application of this radionuclide in various nuclear medicine investigations.

Successful tagging of red blood cells has been achieved by very simple methods involving this radionuclide (Stokely et al 1975, Pavel et al 1977). This application has been useful mainly in nuclear cardiology studies and in

the detection and localisation of gastrointestinal bleeding (Hegge et al 1978, Winzelberg et al 1979). However, the use of ^{99m}Tc and other gamma-emitting radionuclides such as the radioisotopes of iodine and ^{67}Ga for leucocyte labelling has not proved successful in general. The main problem has been lack of suitable chemical vehicles for these radionuclides to ensure stable and safe cell labelling (McAfee and Thakur 1976a & b). More recently, the introduction of ^{99m}Tc-HMPAO (hexamethyl propyleneamine oxime) white cell labelling has proven as reliable as ^{111}In oxine/tropolone leucocyte labelling in the investigation of sepsis especially inflammatory bowel disease and infected hip prostheses (Peters et al 1986 & 1988). However, due to the relatively short experience in using this tracer for white cell labelling, its value in platelet and lymphocyte labelling remains to be tested. Having said that, non-selectivity of cell labelling by ^{99m}Tc-HMPAO and the high cell toxicity of intracellular ^{99m}Tc (Rannie and Donald 1977, Merz et al 1986) would still restrict its use as a routine platelet or lymphocyte cell labelling agent.

2.4 Radiation damage to cells

Damage incurred on blood cells by the radiolabelling method has been studied by many workers in the field (Rannie and Donald 1977, Rannie et al 1977, Segal et al 1978, Kraal and Geldof 1979, Watson 1983).

Radiotoxicity to lymphocytes from ^{111}In oxine has been found to be the limiting factor for the obtention of the required radioactivity necessary for imaging the labelled cells with preservation of their normal physiology. Various functional end points have been tested including in vivo studies of lymphocyte homing and migration to lymphoid organs and reactive sites (Issekutz et al 1980, Sparshott et al 1981, van Dinther-Janssen and Scheper 1981), in vitro assays on the proliferative capacity of the cells (ten Berge et al 1983) or both in vivo and in vitro tests (Chisholm et al 1979).

Chemical toxicity from oxine, tropolone, indium, cadmium which results from ^{111}In radioactive decay, and other metal contaminants has also been implicated in affecting cellular function after labelling (Sparshott et al 1981, Balaban et al 1986 & 1987).

Those experimental studies and various reports dealing with cell and body dosimetry (Segal et al 1978, Goodwin et al 1981a & b, Silvester and Waters 1983, Goodwin and Meares 1985) have produced limits for the amount of indium-111 that can be used per lymphocyte in order to achieve cell labelling without significant toxic effect. The upper limit generally accepted is 7.4 MilliBq (0.2 pCi) per lymphocyte.

Other blood cells show less radiosensitivity than lymphocytes. Granulocytes and platelets can be labelled with ^{111}In radioactivity which is adequate for imaging without apparent effect on their function (Greenberg et al 1968, Bassano and McAfee 1979).

Cell radiotoxicity from ^{111}In oxine has been considered the result of Auger-electron energy deposition in the cell causing damage to the nucleus mainly and to a lesser extent the cytoplasm (Hofer et al 1975, Hofer 1984, Goodwin and Meares 1985).

Body dosimetry shows that the spleen is the target organ using ^{111}In-oxine-labelled lymphocytes, granulocytes or platelets. However, doses to other organs especially the bone marrow can also be important (Table 2.2)

Table 2.2. Organ and whole body dosimetry for ^{111}In labelled leucocytes (granulocytes mainly), lymphocytes or platelets[a].

Preparation[b]	Radiation dose (mGy/MBq)			Effective dose equivalent mSv/MBq
	Spleen	Liver	Bone marrow	
Mixed leucocytes (mainly neutrophils)	4.7	0.8	1.3	0.65
Lymphocytes	3.7	0.4	0.8[c]	0.65
Platelets	4.8	1.8	1	0.68

a Data from Goodwin et al 1981b.
b Labelled cells were injected intravenously.
c Dose to bone marrow and lymph nodes.

2.5 Summary

Presently, cell labelling with ^{111}In oxine is widely used for granulocyte radiotracing. However, due to technical difficulties in separating lymphocytes, especially lymphocyte subsets, and the radiosensitivity of these cells, ^{111}In oxine use has been limited to a few research applications. Also, platelet labelling with ^{111}In oxine is fraught with technical complexities restricting its widespread use.

Experience in using this agent in labelling blood cells, however, will serve as background knowledge in the testing and implementation of the new cell labelling approach using ^{111}In-labelled-cell-specific monoclonal antibodies.

Chapter 3 :

Monoclonal Antibodies

3.1 Introduction :

The era of Monoclonal Antibody Technology in biology began with the report by Kohler and Milstein (1975), which won them the Nobel Prize in Medicine in 1984, of a method to produce antibodies of a single specificity (clonality) in unlimited amounts. They achieved this monoclonal antibody (McAb) production by fusing B lymphocytes with myeloma cells grown in culture and isolating the hybridomas secreting the antibody by the timely use of selective media. The hybridoma incorporated the properties of the B cell that rearranged its immunoglobulin gene in specific antibody production and the unlimited expansion ability of the myeloma cell.

3.2 Monoclonal antibodies : Structure, production and preparation of antibody fragments

The immunoglobulin secreted by the hybridoma, whether in tissue culture or into the ascites fluid of a mouse or rat in which it is growing, retains normally the four-chain structure of these proteins, consisting of two pairs of identical heavy and light chains, held together by non-covalent bonds and disulfide bridges (see Figure 3.1). In general, monoclonal antibodies are homogenous reagents, available in potentially unlimited supply and are produced in response to defined antigen stimuli by planned immunisation of the animal source of B cells (mouse or rat) (Campbell 1984).

Figure 3.1 Antibody structure, antigenic determinants and effector functions

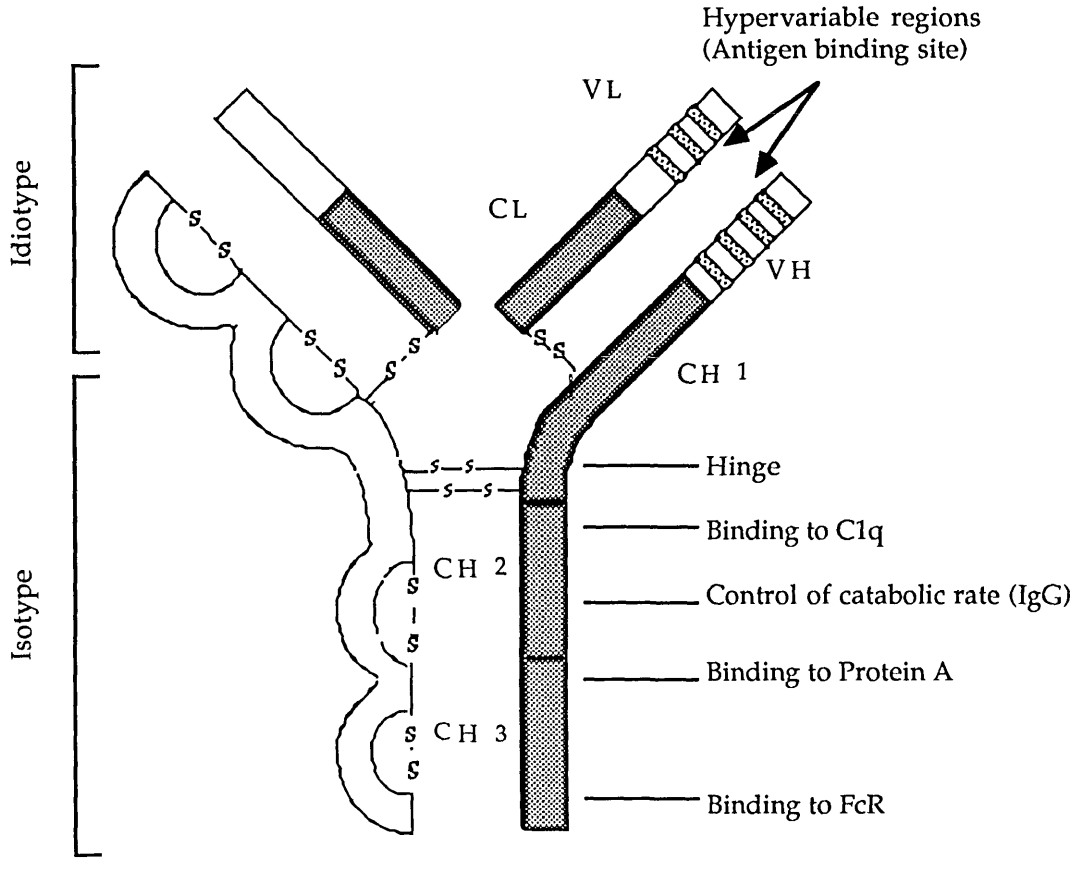

CH : constant domain of the heavy chain, VH : Variable domain of the heavy chain, CL : constant domain of the light chain, VH : Variable domain of the light chain, C1q : First component of the complement, FcR : Fc portion receptor.

Methods for the isolation, purification and fragmentation of monoclonal antibodies derive from the basic concepts of the four-chain and domain structure of immunoglobulins, and the experimentation in preparation and use of antibodies for various reasons (Parnham et al 1982). For instance, isotypic determinants correlate with biological activities (Oi et al 1984), such as binding to staphylococcal protein A (Ey et al 1978), C1q (Neuberger and Plasensky 1981) or specific Fc receptors (Unkeless et al 1981), that may be important for purification. The specific antibody reactivity generated in the hybridoma provides an additional property that can be utilised to advantage in selecting clones and purifying material. Antibody fragments (see Figure 3.2), ie $F(ab')_2$, Fab', Fab/c, etc, can be produced by antibody digestion with

various enzymes mainly pepsin or papain (Lamoyi and Nisonoff 1983, Parnham 1986).

Figure 3.2. Antibody fragments.

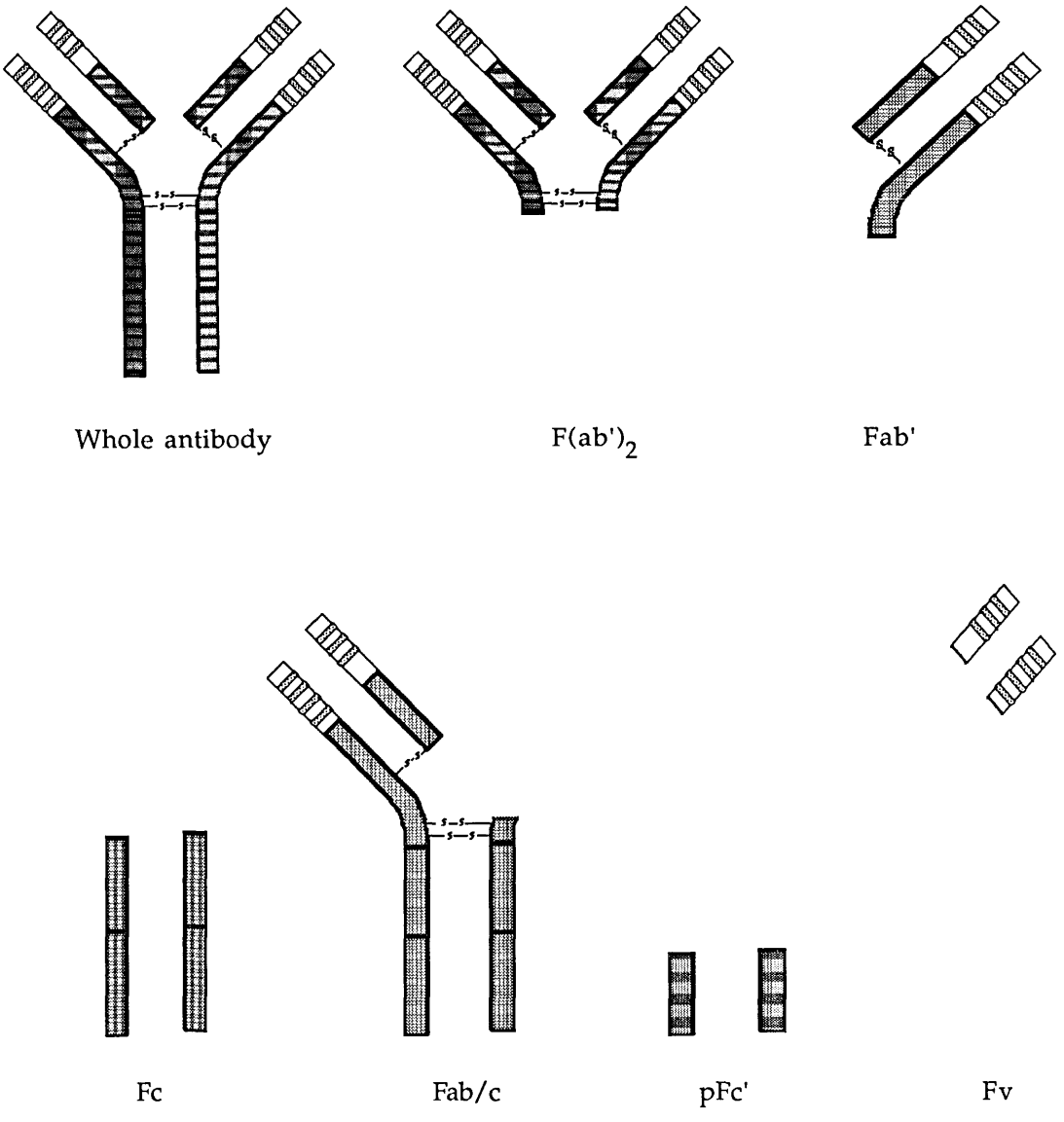

In addition to basic monoclonal antibody methodology, the development of somatic mutants and chimaeric molecules produced by transfectomas (Morrison 1985) presents novel alternatives for producing artificial constructs of antibody which can be useful for specific applications such as in vivo use (Neuberger et al 1984).

3.3 Monoclonal antibodies to blood cells

Within a period of less than ten years, the use of monoclonal antibodies in the identification and classification of biological structures has become a recognised and reliable approach. In the case of leucocytes and platelets, cellular structures have been identified in vitro by monoclonal antibodies. Monoclonal antibodies reactive with blood cells can be lineage- (lymphoid, myeloid etc), subset- (T cell, B cell, etc), or clone- (anti-idiotype) specific (Greaves et al 1981, Beverley 1984, Catovsky et al 1985, Janossy and Campana 1989).

Recently, a unified nomenclature classifying the majority of monoclonal antibodies reacting with leucocytes and platelets as well as their malignant counterparts has been agreed upon in what is presently known as the cluster of differentiation nomenclature (CD) (Bernard et al 1984, Reinherz et al 1986, McMichael et al 1987, Knapp et al 1989).

The fact that monoclonal antibodies recognise molecules specifically by binding to distinct epitopes on them makes the idea of specific targeting of these molecules quite attractive. Not only does this apply to the scientist in the laboratory for in vitro fingerprinting of different structures, but also to clinicians who would find it very useful a tool for in vivo targeting of certain tissues especially tumours.

3.4 In vivo use of monoclonal antibodies :

In practice, this question has been broadly addressed in two ways. The first has applied monoclonal antibodies on their own making use of their properties as biologicals with effector function for the defence of the organism against foreign antigens (Waldmann 1988). This application can be considered an extention of the erstwhile use of polyclonal antibodies in the immunotherapy of cancer (Hericourt and Richet 1895, Murray 1958,

Buinauskas et al 1959). The other line of research has been concerned with the delivery of different reagents to desired sites in the body by injecting reagent-coupled monoclonal antibodies. Again, the use of monoclonal antibodies for this goal has followed early trials using polyclonal antibodies (Pressman and Korngold 1953, Ghose et al 1972, Goldenberg et al 1978). Different reagents have been employed including radionuclides (Mach et al 1980, Farrands et al 1982), cytotoxic drugs and different toxins (Thorpe et al 1982, Gallego et al 1982).

Radiolabelled monoclonal antibodies enable non-invasive imaging of the targeted tissue using the scintillation camera. A second application would come as a consequence of successful imaging of tumours in the form of local radiation from energetic particles emitted by beta or alpha radionuclides linked to the same antibody used for imaging (Carrasquillo et al 1984, Mausner et al 1988).

3.5 In vivo use of monoclonal antibodies; limitations :

3.5.1 Antibody specificity, antigen accessibility and antibody-antigen binding constant

Monoclonal antibodies for in vivo use are required to have specificity for the tissue, especially tumour, that they target. This absolute specificity, however, does not seem to apply for the majority of malignant tissues as many epitopes expressed in cancerous tissues are shared to some extent with their normal counterparts. Thus, many tumours associated antigens (TAA) have been identified (Price et al 1980, Stefanini 1985) and monoclonal antibodies have been generated to these antigens for use in vivo, eg anti-CEA McAb (Bosslet et al 1985) and antibodies to the components of the human milk-fat-globule membrane (Taylor-Papadimitriou et al 1981).

In vivo binding of the antibody to its antigen depends in the first instance on the accessibility of the antibody to that antigen. If the McAb has free access to antigen, as in circulating cells, then Ab distribution on the cells and in plasma will depend on :

a) The number of antigenic sites available and Ab concentration in blood.
b) The affinity of the antibody to its antigen (Ab binding constant) in conditions of in vivo Ab-Ag reaction, ie 37° C, pH 7.4, in plasma and in the presence of other blood cells.
c) Any other non-specific binding of the antibody (Fc portion binding and low affinity binding to other non-target tissues).

In the case of tumours in extravascular territory, antibody access becomes a major problem resulting in a low fraction of the injected antibody reaching target (Jain and Baxter 1988).

In both situations, the effect of the antibody used on its antigen can interfere with its binding conditions and can therefore alter the way antibody accumulates in target tissue. This is noted using antibodies that cause antigen modulation (Ritz et al 1980, Chatenoud and Bach 1984), complement activation (Masui et al 1986) or antibody-dependent cytotoxicity (Kipps et al 1985).

3.5.2 Stability of the label and its effect on McAb kinetics

Radiolabelling of antibodies causes protein denaturation and results in some loss of antibody reactivity (Lindmo et al 1984, Andres and Schubiger 1986). Also, elution of the radionuclide from radiolabelled antibodies occurs after storage in vitro (Evans 1984) or due to enzyme degradation in vivo. For example, radioiodine labelled antibodies undergo dehalogenation in vivo resulting in a rapid clearance of the radioactivity in the urine (Rainsbury and Westwood 1982).

In addition, the radiolabel can alter the distribution of the antibody in vivo. This is noted especially following injection of ^{111}In McAbs labelled by the bifunctional chelates such as DTPA (Perkins and Pimm 1985, Halpern et al 1988). High uptake in the liver is found, thus reducing the amount of antibody available for targeting tissue specifically and obscuring lesions present in the liver itself.

3.5.3 The human anti-mouse antibodies (HAMA)

The generation of a humoral anti-mouse response to murine monoclonal antibodies injected in vivo is a limitation to their repetitive use in the same individual (Shawler et al 1985, Schroff et al 1985). The immune response has been found to be directed mainly to the antibody isotype and its subtypes, and to the antibody idiotype (Herlyn et al 1985, Chatenoud 1986). The use of the less immunogenic antibody fragments, ie $F(ab')_2$ or Fab' fragment, has been shown to offer a partial solution to this problem (Courtenay-Luck et al 1986). Also, the introduction of human monoclonal antibodies or human-mouse hetero-antibodies would minimise immunisation against the administered xenogeneic antibodies (Boulianne et al 1984, Brown et al 1987).

Using a different strategy, manipulation of the immune response in man by induction of tolerance to rat or mouse McAbs or immunosuppression by using cyclosporine treatment have also been tried. However, results have been controversial and none of the methods reported so far has been efficient in eliminating completely the immune response to the administered mouse or rat antibodies (Benjamin et al 1986, Sivolapenko et al 1989).

Section Two :

In Vitro and in Vivo Use of an ^{111}In Anti-Platelet-Glycoprotein Monoclonal Antibody

Chapter 4 :
The Physiology of Platelets

4.1 The platelet : Origin, kinetics and life-span :

Early studies on thrombopoiesis have recognised platelet production from the megakaryocyte of the bone marrow (Wright 1906). Recently, the major cellular events that accompany the maturation of the megakaryocyte and the effect of various factors involved therein have been described in more detail (Feinendegen et al 1962, McPherson 1971, Levin and Evatt 1979). Less clear, however, is the process of platelet release in the circulation, which is generally thought to take place in the pulmonary vasculature, by fragmentation of mature megakaryocytes and the generation of proplatelets (Melamed et al 1966, Tingaard Pedersen 1974, Trowbridge et al 1982).

Circulating platelets have a finite life-span and their kinetics in the body are described in terms of blood circulation, normal splenic pooling and final removal from blood by the reticuloendothelial system (Harker 1977, Heyns et al 1980, Klonizakis et al 1980).

Normal platelet survival, determined by random radiolabelling using ^{51}Cr or ^{111}In, is almost linear and the mean platelet life-span is 9-10 days (Heaton et al 1979, Schmidt et al 1983a, Trowbridge and Martin 1983). In general, as platelet life-span becomes more severely reduced in disease, the survival deviates further from linearity. When platelet life-span is severely reduced as in ITP (as short as a few hours) the survival profile becomes approximately monoexponential implying random removal of platelets from the circulation (Branehog et al 1974, Heyns et al 1982).

Platelets are distributed between a circulating pool (60-70%), a splenic pool (30%) and a smaller liver pool (5-15%) in the normal human (Heyns et al

1980, Klonizakis et al 1980, Robertson et al 1981, Scheffel et al 1982). Platelets in the spleen are rapidly and freely exchangeable with their counterparts in blood as in a closed, well-mixed, two compartmental system (Peters et al 1980). Accordingly, the number of platelets in the spleen depends on the balance of input by the splenic blood flow and output, which is related to the mean platelet intrasplenic transit time (normal ≈ 6.5 min). In splenomegaly, the splenic platelet pool is expanded and blood recovery of injected radiolabelled platelets falls as low as 10%. In contrast, the recovery in asplenic individuals approaches 100% (Aster 1966, Harker and Finch 1969).

The reason why the spleen concentrates platelets in such large numbers is unclear. Macrophage function may play a role in platelet splenic pooling, as many platelets can be seen adhering to splenic macrophages by scanning electron microscopy (Weiss et al 1974).

4.2 Platelet activation and the role of platelet surface glycoproteins in platelet aggregation :

Platelets are primarily connected with haemostasis. Clot formation after the occurrence of a breach in normal vasculature or the development of thrombosis in a diseased vessel involves platelet interaction and deposition in the affected site (Mustard and Packham 1979, Kinlough-Rathbone et al 1983, Zucker and Nachmias 1985). Adhesion of platelets to sites of vascular injury occurs basically by binding of von Willebrand factor (vWF) and collagen in the subendothelium to platelet surface glycoprotein Ib (GPIb) (Bolhuis et al 1981, George et al 1984). Next, platelet aggregation may follow. This phenomenon is an active process requiring collision of platelets, extracellular Ca^{2+}, metabolic energy provided by intracellular ATP and fibrinogen and can be triggered by various stimuli, eg ADP, thromboxane A2 and thrombin. These aggregating agents interact with platelet membrane

components or specific receptors and the stimulus is transduced to trigger platelet activation.

It is known presently, that aggregation is the consequence of the mobilisation on the platelet surface of a fibrinogen receptor identified as the GPIIb/IIIa complex (Marguerie et al 1980, Nachman and Leung 1982, Bennett et al 1982, Coller et al 1983). Once this receptor is exposed, the fibrinogen molecule, by combining with receptors localised on adjacent platelets, is thought to form bridges which link the cells together. Exposure of the GPIIb/IIIa molecule is assumed to represent a change in either the conformation or the microenvironment of preexisting GPIIb/IIIa complexes in the platelet membrane (Coller 1980 & 1985).

Recently, more detailed studies on the expression and conformational changes of platelet surface molecules (GPIb, GPIIb/IIIa, etc) in various test conditions in vitro have confirmed the integral role of receptors in platelet physiology (Nurden and Caen 1975, Caen et al 1976, McEver et al 1980, Kunicki et al 1981, Pidard et al 1983). In these experimental systems the use of antibodies (poly or monoclonal) has been instrumental in providing tools for the identification and quantitation of platelet surface receptors and specific reagents for pharmacologic interventions directed to each type of receptors (McGregor et al 1983, Jennings et al 1985, Berndt et al 1985, Kunicki et al 1986). An example of such usefulness is an antibody to platelet membrane glycoprotein IIa, which binds only to activated platelets (McEver and Martin 1984), thus making a specific probe for activated platelets in vitro and potentially in vivo.

4.3 Experimental and clinical studies using radiolabelled platelets :

Platelet kinetic studies and mapping of platelet distribution by surface probe counting or scintillation camera imaging constitute the two major applications of radiolabelled platelets clinically and in research.

Survival studies including mean platelet life-span and the shape of the survival curve offer information on the likely cause and severity of a thrombopenic condition (Abrahamsen 1970, Murphy et al 1972, Peters et al 1984 & 1985). This has been most valuable in cases of idiopathic thrombocytopenic purpura (ITP) where shortened platelet life-span is associated with near-exponential survival curves (Heyns et al 1982).

Imaging the distribution of radiolabelled platelets has been used in various experimental and clinical conditions as a means to detect thrombus. This was well shown by Thakur et al (1976), who first described platelet labelling with ^{111}In oxine. They tested the effect of the radiolabelling procedure on the platelets in vitro and showed localisation of radioactivity in induced deep venous thrombosis, surgical wounds and arterial lesions in dogs. Human use of ^{111}In oxine labelled platelets has been reported for the early postoperative detection of venous thrombosis (Goodwin et al 1978, Fenech et al 1981). Also, ^{111}In labelled platelets have been used in the study of large arterial lesions such as those occurring in the carotids and in atherosclerotic aneurysms. Davies et al (1980b) reported ^{111}In platelet deposition in carotid atherosclerotic lesions. Abdominal aortic aneurysms showed also positive platelet scan (Ritchie et al 1981). The effect of drugs on the accumulation of platelets in different vascular lesions was studied as well (Fedullo et al 1982, Romson et al 1982). The method, however, suffered many limitations. In addition to complexity of the labelling technique, thrombus detection by imaging ^{111}In-oxine platelets proved to be of rather low sensitivity especially in small vessels (Powers et al 1982). High circulating radioactivity, or blood

pooling in aneurysms, prevented early detection of ^{111}In oxine platelets that localised in thrombus, although in selected cases, subtraction methods were employed to enhance lesion contrast (Sutherland et al 1982, Bergman et al 1983, Machac et al 1989).

^{111}In oxine labelled platelets have also been used for the diagnosis of organ transplant rejection (Wang et al 1982). Rejecting kidneys accumulated radioactivity as reported by Smith et al (1979a), Marcus et al (1986) Tisdale et al (1986) and Desir et al (1987). Again, the complexity of the technique and the difficulty in interpretation of the findings especially patients treated with cyclosporine made it far from being routinely applicable in the diagnosis of rejection.

Finally, the study of prosthetic vascular graft thrombogenicity has benefited from imaging using ^{111}In oxine labelled platelets (Agarwal et al 1982, Stratton et al 1982). Thrombosis of prosthetic vascular grafts or prosthetic valves was demonstrated by imaging and directly by tissue sampling (Dewanjee et al 1983, Dewanjee 1984). The generation of micro-emboli from the prosthesis surface was also shown (Dewanjee 1984). In this field, however, there is still little understanding of the clinical significance of early and late postoperative deposition of platelets in prosthetic material and the exact relationship of platelet deposition to thrombus formation on the vascular prosthesis.

Chapter 5 :

In Vitro Testing of an ^{111}In Anti-Platelet Glycoprotein Monoclonal Antibody

5.1 Introduction

In this thesis, a new method for platelet radiolabelling and in vivo localisation of thrombus has been investigated. It involves testing the use of an ^{111}In labelled anti-platelet glycoprotein McAb for specifically targeting platelets by experiments conducted in vitro and in vivo. This experimental work includes radiolabelling of the anti-platelet McAb P256 (Bai et al 1984) with ^{111}In, binding assays of the radiolabelled antibody to platelets in platelet rich plasma and in whole blood, testing antibody effect on platelet aggregation in whole blood and in vivo use of ^{111}In P256 in a normal volunteer and patients with deep venous thrombosis. The use of the ^{111}In $F(ab')_2$ fragment of the same antibody is also described.

5.2 Materials, methods and results

5.2.1 The Monoclonal antibody P256

P256 is a murine McAb of the IgG_1 subclass. It was derived from fusion of P3-NSI/-1-Ag4-1 myeloma cell line with spleen cells from BALB/c mice immunised with peripheral blood mononuclear cells (Bai et al 1984). The antibody reacts with the 135 kDa IIb component of the intact platelet membrane glycoprotein complex IIb/IIIa. It belongs to the CD41 cluster of differentiation (Horton and Hogg 1987, von dem Borne et al 1989). P256 reacts primarily with normal human platelets and the megakaryocytes in the bone marrow. P256 does not bind to platelets from patients with Glanzmann's thrombasthenia which are deficient in the glycoprotein

IIb/IIIa from their surface (Phillips and Agin 1977, Nurden and Caen 1979, Bai et al 1984).

Pure monoclonal antibody was prepared[1] from ascites fluid by Protein-A affinity chromatography (Ey et al 1978) and was kept in phosphate buffered saline (PBS) at 4° C.

5.2.2 Preparation of P256 $F(ab')_2$ fragments[1]

$F(ab')_2$ fragments of P256 were prepared by digestion with activated papain (Parnham et al 1982). Purified McAb was concentrated to 5 mg/ml in 0.1 M sodium acetate buffer, pH 5.5, containing 3 mM EDTA and was digested with 2% activated papain for 4 hr at 37° C. The reaction was terminated by addition of iodoacetamide and stored at 4° C. The digest was eluted on a protein-A Sepharose column[2] to remove any remaining intact antibody and Fc portions. Purity of the obtained $F(ab')_2$ fragments was checked by non-reducing SDS-PAGE and Coomassie Blue gel staining. Purified P256 $F(ab')_2$ preparation was kept in PBS at 4° C.

Both whole antibody and $F(ab')_2$ fragments described above were a kind gift of Dr N Hogg, Imperial Cancer Research Fund, London, England.

5.2.3 ^{111}In labelling of P256 and P256 $F(ab')_2$

The monoclonal antibody was labelled with ^{111}In using the method of the double chelating agent of Hnatowich et al (1982 & 1983).

---

1 P256 whole antibody and P256 $(Fab')_2$ have been prepared at Dr N Hogg's laboratory, Imperial Cancer Research Fund, London. The methods used for this purpose are described above (Dr N Hogg, personal communication).

2 Pharmacia, Sweden.

5.2.3.1 Coupling of P256 to DTPA[1] :

Batches of 5 mg of the antibody were used. The volume of stock solution containing the amount of antibody required (usually 3-5 ml containing 5 mg Ab) was dialysed[2] extensively in PBS[3], pH 7.5-8, prepared in double distilled deionised water (2 litres, 3 changes). Dialysis was necessary to eliminate any trace of metals that might have contaminated the antibody solution during preparation. After dialysis, the antibody solution was concentrated in an Amicon Concentrator (England) to a small volume (200 µl at 2 X 10^{-4} mole/l antibody[4]), then it was added to DTPA[5] (diethylene-triamine-pentaacetic acid) cyclic anhydride powder in a plastic bijou[6] at a molar ratio of 40 : 1, DTPA : Antibody[7]. The antibody was left to react with DTPA for 1 hour at room temperature. Afterwards, a volume of 10 µl of the reaction mixture was frozen in an LP3 tube at -20° C for later testing (see below). DTPA coupled antibody was then separated from unbound DTPA by elution of the reaction mixture DTPA-McAb on a size exclusion Sephadex G-50 column[8] prepared in a barrel of a 20 ml plastic syringe[9] . Two millilitre successive elution fractions were obtained and the optical density (photon absorption) at 280 nm wave-length through 1 cm light path was measured

---

1 Throughout the DTPA-Ab coupling procedure, disposable plasticware (bijou and universal containers) was used. Also, new unused glass Pasteur pipettes and extensively washed glassware with double distilled deionised water were used. The use of metal containers and tools was avoided whenever possible.

2 Dialysis tubing (Viskin, England) was heated to 70° C in double distilled deionised H_2O containing EDTA (BDH, England) 10 mg/100ml, then it was washed twice in X2 Dist Deion H_2O before use.

3 Dulbecco's Formula A modified, Flow Labs, England.

4 The concentration of protein was measured using photon absorption at 280 nm. The absorption coefficient (Extinction Coefficient $E_{280}1\%$) of whole IgG and IgG $F(ab')_2$ fragments was considered to be 13.6 (Johnstone and Thorpe 1987, Fasman 1976).

5 Sigma, England.

6 Sterilin, England.

7 MW : DTPA=357, IgG=15 $X10^4$, $F(ab')_2=10^5$. The amount of DTPA added to 5 mg whole IgG was 0.5 mg and to 5 mg $F(ab')_2$ fragments : 0.7 mg.

8 Pharmacia, Sweden. Sephadex G-50 fine; useful fractionation range MW peptides/globular proteins 1500-30000. Gel filtration was used as an alternative to dialysis.

9 Monoject, England. Column volume 20 ml, void volume 6 ml (measured by elution of Dextran Blue in PBS).

in each fraction using a spectrophotometer[1] (see Table 5.1)[2]. The fractions containing Ab were then pooled, the final optical density[3] measured and the solution was filtered through a 0.22 μm millipore filter[4] in a vial containing N_2[5]. The recovery of antibody after coupling ranged between 50-70%. DTPA-coupled P256 was kept for a period of up to six months at 4° C.

Table 5.1. Elution fractions of P256-DTPA reaction mixture on the Sephadex G-50 column in PBS. P256 : 5 mg, DTPA : 0.5 mg.

Fraction No	Fraction volume (ml)	OD	Protein content (mg/ml)
BG[a]	--	0.00	0
1	2	0.01	0[b]
2	2	0.01	0[b]
3	2	0.02	0.01
4	2	1.17	0.86[c]
5	2	1.04	0.77[c]
6	2	0.12	0.09[d]
7	2	0.01	0[b]
8	2	0.01	0[b]
9	2	0.01	0[b]

a Background level was set at zero with PBS. This gave 3 reproducible readings of 0.000 before starting to measure the OD of the elution fractions.
b Fractions giving low readings, OD <0.010 (<10μg), were considered to be non-different from background.
c Fractions 4 & 5 were pooled together; OD : 1.10, final McAb concentration : 0.81 mg/ml, total : 3.24 mg, recovery of protein : 68%.
d Fraction 6 was not pooled with fractions 4+5 in order to keep the antibody-DTPA solution as concentrated as possible.

1 Pye Unicam, England.
2 DTPA-coupling of P256 F(ab')$_2$ was performed using the same protocol used for P256 whole Ab (see Appendix, Table A5.1 page 292 for experimental data).
3 Optical density: OD.
4 Millex-GV, low protein binding. Millipore, England.
5 Amersham, England.

5.2.3.2 ^{111}In labelling of antibody-DTPA[1] :

Firstly, the number of DTPA molecules bound per molecule of antibody was calculated. This was done by reacting the sample of the reaction mixture (10 µl), which was frozen at the end of the coupling reaction Ab-DTPA (see above), with carrier free ^{111}In solution[2] (20-40 MBq; 0.5-1 mCi) having raised its pH to 6-6.5 by the addition of 3.8% sodium citrate BP[3] (usually 1 volume $^{111}In\ Cl_3$ in 0.04 M HCl to 2 volumes sodium citrate 3.8%). After 30 minute incubation at room temperature, the reaction mixture was eluted on a Sephadex G-50 column to separate ^{111}In labelled antibody from ^{111}In-DTPA using a similar protocol to that used for separating Ab-DTPA from DTPA, ie 2 ml elution fractions in PBS. The radioactivity in each fraction was measured immediately in a dose calibrator[4] and a radioactive count was obtained for each fraction using a manual gamma scintillation counter[5] (see Table 5.2). The fraction of DTPA that was Ab bound was calculated by taking the ratio of the count-rate in the early fractions (associated with the protein peak) to the count-rate in all fractions collected (usually 20 fractions of 2 ml) representing ^{111}In bound to DTPA (antibody associated or not[6]). This ratio was converted to the number of DTPA molecules bound per Ab since both

---

1 All radiolabelling procedures were done at the hot laboratory-Medical Physics Department RPMS, inside a fume cabinet having a lead-shielded working area. Precautions were taken to avoid contamination of work surfaces by using absorbing waterproof paper (Benchkote, Whatman, England). Also, careful monitoring of the working area was performed before and after the radiolabelling procedure to ensure safe working conditions for users of the radiolabelling facilities. Disposable rubber gloves as well as specially designed tongs and forceps were used to handle the unsealed source of radioactivity. Radioactive waste was disposed of through the hot-lab-waste-disposal unit.

2 $^{111}InCl_3$ in 0.04 M HCl (INS-1), 740 MBq/ml (20 mCi/ml) at calibration time, Amersham International, England.

3 Sodium citrate injection 3.8% in 2 ml, Phoenix Pharmaceuticals Ltd, England.

4 Siel Isotope Calibrator, England.

5 Gamma scintillation counter, Department of Medical Physics RPMS. Samples were counted at a fixed distance (reproducible geometry) from the counter's crystal. Energy discriminators were set at 100 KeV (lower level) and at 450 KeV (upper level). The distance between the crystal and the samples could be altered by moving the stand on which the samples were placed up or down in relation to the crystal's face.

6 ^{111}In reaction kinetics with DTPA was assumed to be same for free DTPA and DTPA-Ab (Hnatowich et al 1982).

concentrations of DTPA and Ab used were noted at the beginning of the procedure.

Table 5.2. Elution of ^{111}In+DTPA+P256 reaction mixture[a] on the Sephadex G-50 column in PBS. Test sample (10µl) for calculation of the number of DTPA molecules bound per Ab.

Fraction No	Fraction volume (ml)	Radioactivity (MBq)	Count-rate (cpm-BG[b])
1	2.11	0.0	5[c]
2	2.00	0.0	8[c]
3	2.00	0.0	27[c]
4	2.00	0.1	614[d]
5	2.00	0.5	3328[d]
6	2.00	0.1	557[d]
7	2.00	0.2	1405
8	2.00	0.3	1666
9	2.00	3.0	20147
10	2.00	6.1	42073
11	2.00	6.8	47380
12	2.00	3.7	26438
13	2.00	0.7	4504
14	2.00	0.2	1138
15	2.00	0.1	316
16	2.00	0.0	142
17	2.00	0.0	67
18	2.00	0.0	29[c]
19	2.00	0.0	4[c]
20	2.00	0.0	7[c]

a Reaction mixture 10 µl; 25 mg/ml P256, 2.5 mg/ml DTPA, Mol DTPA : Ab; 42 : 1, ^{111}In : 24 MBq (0.65 mCi) in 100 µl.

b Background (BG) was subtracted. Average BG : 150 cpm (n=3, se=7).

c Count-rates corrected for background and falling within 3 standard errors of the calculated difference (99% confidence limits) were considered to be non-significant and were ignored.

d Radioactivity in elution fractions 4, 5 & 6 (first peak) was associated with DTPA bound to Ab . The radioactive count in the following fractions 7-20 (second peak) was associated with free DTPA. The ratios Ab-DTPA/DTPA (MBq) = 0.65/21.6 = 0.03. Ab-DTPA/DTPA (cpm) = 4499/149775 = 0.03. The number of DTPA molecules bound per P256 molecule = 1.26 DTPA/Ab.

DTPA-coupled P256 was found to have 1.26 molecules of DTPA per molecule of Ab[1] (see Table 5.2).

1 The number of DTPA/Ab for the various DTPA coupled monoclonal antibodies included in the experimental work in this thesis will be given at the first mention of the ^{111}In labelled preparation of each DTPA-McAb.

Preliminary testing of the DTPA coupled antibody involved also radiolabelling of a sample of the final preparation in concentrations of McAb-DTPA and ^{111}In similar to those employed practically[1] to obtain ^{111}In-McAb for in vitro or in vivo use. Same conditions as those mentioned above were used, ie antibody-DTPA added to ^{111}In in citrate buffer pH 6-6.5, reacted for 30 minutes RT[2] then the mixture eluted on a Sephadex G-50 column to separate ^{111}In labelled McAb from free ^{111}In. The early elution fractions containing radiolabelled antibody were pooled and the resulting preparation was afterwards millipore-filtered into a rubber-capped vial[3], which was kept in a suitable lead container at 4° C until use[4].

The radiolabelled product, ie ^{111}In DTPA-P256 (^{111}In P256) was described finally in terms of antibody mass, volume of the Ab solution and the specific activity at the time of labelling (labelling date and calibration time noted with each preparation)[5].

^{111}Indium test labelling of P256-DTPA[6]; 0.1 mg with $^{111}InCl_3$-citrate; 115 MBq (3.1 mCi) gave 900 MBq/mg (24.3 mCi/mg) specific activity in 6 ml PBS at the time of labelling and test labelling of P256-F(ab')$_2$ -DTPA[7] ; 0.1 mg with ^{111}In; 97 MBq (2.6 mCi) gave 650 MBq/mg (17.6 mCi/mg) in 6 ml PBS.

---

1 The limiting factor for the obtention of a high specific activity ^{111}In McAb preparation was the availability of carrier free ^{111}In in sufficient amounts for labelling, ie 150-200 MBq (4-6 mCi) per 0.1 mg McAb-DTPA. Most of McAb labelling done with ^{111}In in this thesis used 40-80 MBq (1-2 mCi) of ^{111}In per 0.1 mg Ab as a rough guide.

2 RT : room temperature.

3 Amersham, England.

4 ^{111}In McAbs were kept at 4° C and were used within one week of radiolabelling, except preparations for in vivo human application that were prepared immediately before use.

5 Antibodies radiolabelled with ^{111} In mentioned in the experimental work to follow will be described in the terms mentioned above, ie Ab concentration and specific activity at the time of labelling or use.

6 See Appendix, Table A5.2, page 292 for experimental data.

7 P256-F(ab')$_2$ -DTPA contained 1.17 DTPA molecules/Ab, (see Appendix, Tables A5.3, A5.4, pp293 & 294 for experimental data.

5.2.4 Immunoreactivity testing of the ^{111}In labelled McAb

The assessment of the resulting ^{111}In-DTPA-McAb preparation for suitability for use experimentally involved also the measurement of its immunoreactive fraction.

The method reported by Lindmo and Bunn (1986) was applied. A radiobinding assay under conditions of antigen excess was set and the immunoreactive fraction was determined by curve extrapolation to x = 0, corresponding to infinite antigen excess, in a double inverse linear plot, where the X axis represented the reciprocal of antigen concentration and the Y axis the ratio of total antibody added, to that antigen bound (T/B). The source of antigen used for testing ^{111}In P256 or ^{111}In P256 F(ab')$_2$ was platelet rich plasma (see below).

Platelet rich plasma (PRP) was prepared by centrifugation[1] at 190g for 15 minutes of ACD[2] anticoagulated fresh whole blood (30 ml in two universal plastic containers[3]) obtained from a normal volunteer[4]. After centrifugation, platelet rich plasma above the cell pellet was carefully withdrawn with a syringe tipped with a large bore needle (19G)[5] and was transferred to a sterile 20-ml-universal-plastic container. The number of platelets in the resulting PRP was counted using an automatic counter[6] and manually using a haemocytometer[7]. Platelet rich plasma prepared this way was found to contain a very low number of contaminating cells (erythrocytes, monocytes and lymphocytes < 0.1% of the differential count).

---

1 Centaur 2 swinging-bucket centrifuge, MSE, England
2 Acid citrate dextrose NIH formula A BP. One part ACD to 6 parts blood was used.
3 Twenty ml capacity, Sterilin, England.
4 A total of 60 ml of blood drawn in a syringe containing 10 ml ACD was obtained for the preparation of PRP and PPP. Blood was taken from healthy volunteers who were not on any medication for at least two weeks before the study.
5 Sterican, Germany.
6 Coulter, USA, Haematology Dept RPMS.
7 Improved Neubauer, BDH, England.

^{111}In P256 was added to aliquots of PRP containing increasing platelet numbers in LP3[1] tubes (Table 5.3).

Table 5.3. Setting of the experiment for measurement of the immunoreactivity of ^{111}In P256[a] with PRP[b].

Tube No[c]	Ptlt/ml[d]	^{111}In P256 conc[e] µg/ml	^{111}In P256/ptlt	Cold P256[f] µg/ml (tubes C&D only)
1 A,B,C,D.	$2X10^8$	0.2	4000	20
2 A,B,C,D.	10^8	0.2	8000	20
3.A,B,C,D.	$5X10^7$	0.2	16000	20
4.A,B,C,D.	$2.5X10^7$	0.2	32000	20
5.A,B,C,D.	$1.25X10^7$	0.2	64000	20
6.A,B,C,D.	$6.25X10^6$	0.2	128000	20

a ^{111}In P256 ; 25 µg/ml, 173.6 MBq/mg (4.7mCi/mg).

b PRP obtained after centrifugation of whole blood contained $2.5X10^8$ ptlt/ml. Platelet poor plasma (PPP) was obtained by spinning 40 ml of anticoagulated blood at 1500 g for 10 min and was used for diluting PRP.

c Quadruplicate tubes were used for every tube number : 1A, 1B, 1C, 1D, 2A, etc. Two tubes (A&B) were used to measure the extent of binding of ^{111}In P256 to platelets, the other two (C&D) contained unlabelled P256 as well (dispensed in the tubes before addition of ^{111}In P256) and were used to measure the Ab non-specific binding.

d Doubling dilutions of PRP in PPP of the number of platelets in tubes No 1 were dispensed in tubes 2-6. The total volume of the reaction mixture was made up to 1 ml with PPP.

e ^{111}In P256 was added to all the tubes at 0.2 µg/ml in a volume of 8 µl. A reference standard was left for comparison.

f Unlabelled (cold) P256 was added to tubes C&D of every number group at 20 µg/ml (100 fold excess over ^{111}In P256) for measuring non-specific binding of ^{111}In P256.

The tubes were incubated for 2 hours at room temperature. Intermittently, they were gently shaken to keep the platelets in suspension. At the end of the incubation, the tubes were centrifuged at 1500 g for 10 min and aliquots of 500 µl of the supernatant in each tube[2] were transferred to gamma counting plastic vials[3], and counted in an automatic gamma counter[4].

1 Luckham, England.

2 Centrifugation of PRP or anticoagulated whole blood at 1500 g for 10 min yielded platelet poor plasma (PPP), which was virtually cell free plasma, and a cell pellet.

3 Sterilin, England.

4 Packard Autogamma, USA, Haematology Dept, RPMS.

Table 5.4 includes the results of the binding assay and the calculation of the ratio T/B :

$$\frac{\text{Total } ^{111}\text{In P256 added}}{^{111}\text{In P256 platelet bound}^{1}},$$

Table 5.4. ^{111}In P256 platelet bound and values of ^{111}In P256 T/B for the calculation of the antibody's immunoreactive fraction.

Tube No	^{111}In P256 ptlt bound[a,b] cpm ± 1 se	Non-specific binding[c] cpm ± 1 se	T/B[d] ± 1 se
1	37400 ± 170	200 ± 250[e]	1.15 ± 0.006
2	36100 ± 170	100 ± 250[e]	1.19 ± 0.007
3	33900 ± 180	200 ± 250[e]	1.27 ± 0.010
4	29500 ± 190	400 ± 250[e]	1.46 ± 0.011
5	24200 ± 200	300 ± 250[e]	1.78 ± 0.016
6	15800 ± 220	100 ± 250[e]	2.72 ± 0.039

a All radioactive counts were corrected for background (BG). Average BG=130 cpm (n=3, se=7).

b Count-rate from ^{111}In P256 platelet bound was obtained indirectly by counting the 500 µl aliquots of the supernatant in tubes (A&B), correcting the resulting count-rate for BG, taking the average of the two count-rates (A&B) and multipying this average by 2 to get a value for the total unbound count-rate in the supernatant (the volume of the platelet pellet was ignored). Subtraction of unbound count-rate from the count-rate in the reference standard resulted in the count-rate in the pellet (platelet-bound count).

c Same method described in b above was used to obtain cell bound count-rate in the presence of excess unlabelled P256.

d Reference standard count-rate was obtained by counting an equal amount of ^{111}In P256 to that added to the test tubes (count was obtained in duplicate). Std 43000, n=2, se=150.

e The values of radioactive count-rates, differences in count-rates, ratios etc, that did not lie within three standard errors (se) representing 99% confidence limits were considered to be non-significant and were ignored.

The final step in calculating ^{111}In P256 immunoreactive fraction was to plot values for T/B (total ^{111}In P256 added to platelet bound count-rate) from Table 5.4 against the inverse antigen concentration (ml/platelet). The curve

[1] This ratio is needed for the calculation of the Ab immunoreactive fraction (Figure 5.1).

obtained was fitted with a linear function the Y-axis intercept of which gave the reciprocal of the immunoreactive fraction, Figure 5.1.

P256 immunoreactive fraction was found to be 1/1.07 = 0.937 (93.7%). A similar experiment was performed on ^{111}In P256 F(ab')$_2$ (25 μg/ml, 218 MBq/mg; 5.9 mCi/mg) and the immunoreactive fraction of this preparation tested with PRP was found to be 92.4%[1].

Figure 5.1, ^{111}In P256 immunoreactive fraction, the double inverse plot.

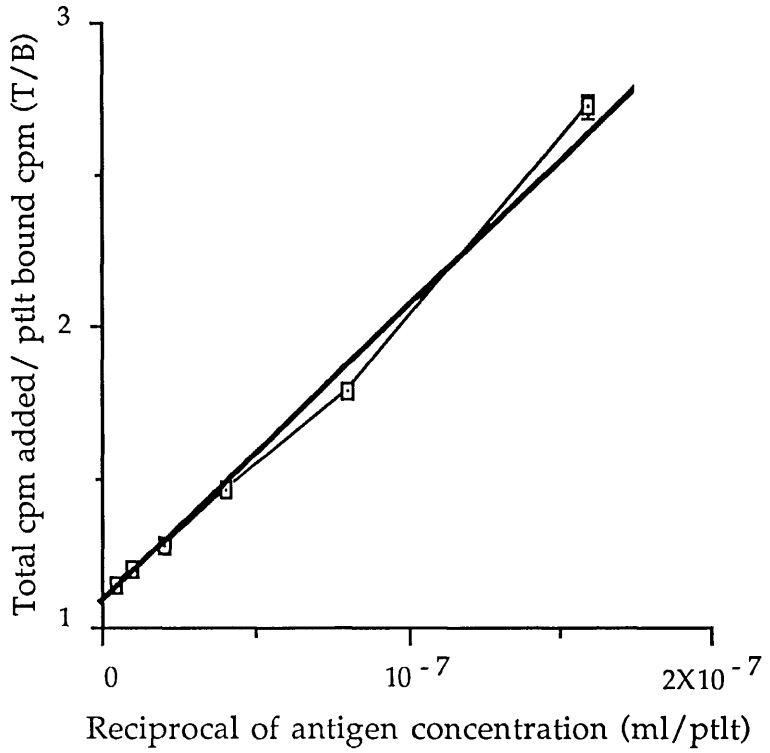

[1] The experimental data and the double inverse plot for the calculation of ^{111}In P256 F(ab')$_2$ are shown in Appendix, Tables A5.5, A5.6 and Figure A5.1 pp294 & 295.

5.2.5 In vitro binding of ^{111}In P256 or ^{111}In-P256-F(ab')$_2$ to human platelets in platelet rich plasma and whole blood

Radioimmunoassays of ^{111}In P256 or ^{111}In P256 F(ab')$_2$ with human platelets in near-physiological conditions (PRP, whole blood) were performed to define the extent of binding of the radiolabelled McAb to platelets over a defined range of McAb concentration.

5.2.5.1 Binding of ^{111}In P256 to platelet rich plasma

Platelet rich plasma was prepared as described above[1]. Aliquots of PRP containing 2X10^8 platelets were dispensed in LP3 tubes in duplicate. ^{111}In P256 in PBS was added to the tubes in decreased concentrations starting at 10^{6}Ab/ptlt and ending at ≈ 8000 Ab/ptlt, and the final volume was adjusted to 1 ml with PPP, see Table 5.5. Another set of eight tubes, containing 2X10^8 ptlt in each was prepared for measuring non-specific binding of ^{111}In P256. To each tube, P256 McAb (unlabelled) was added at a concentration yielding 20 fold excess over ^{111}In P256 before the addition of the labelled antibody, ie Tube 1 : 1000 µg/ml, Tube 2 : 500 µg/ml, etc. The tubes were incubated for 2 hr at 37°C in a water bath[2] with intermittent gentle shaking. Meanwhile, radioactivity was counted in all tubes in the manual radioactivity counter[3]. These counts represented the total radioactivity added to each tube[4]. At the end of the incubation time, the tubes were centrifuged at 1500 g for 10 min and aliquots of 500 µl PPP were transferred to LP3 tubes. The tubes were then counted in the same manual counter of radioactivity in exactly the same position as was done for the tubes containing the reaction mixture before centrifugation. The delay in time between counting before and after centrifugation did not exceed 30 minutes.

---

1 See Immunoreactivity testing of ^{111}In P256 page 55.
2 Grant, England.
3 Medical Physics Dept, RPMS.
4 No reference standard was prepared in this experiment. However, ^{111}In P256 added was directly measured in each tube.

Table 5.5. Setting and results of ^{111}In P256[a] vs PRP[b] radiobinding assay.

Tube No[c]	^{111}InP256 conc µg/ml	^{111}In P256 /ptlt	Std cpm[d] ± 1 se	Bound cpm[d] ± 1 se	B/T ± 1 se
1	50	10^6	84800 ± 210	13600 ± 340	0.16 ± 0.004
2	25	$5X10^5$	42600 ± 150	9800 ± 230	0.23 ± 0.006
3	12.5	$2.5X10^5$	21200 ± 100	7800 ± 160	0.37 ± 0.008
4	6.25	$1.25X10^5$	10500 ± 70	4700 ± 110	0.45 ± 0.011
5	3.13	$6.25X10^4$	5200 ± 50	3300 ± 70	0.64 ± 0.015
6	1.56	$3.13X10^4$	2600 ± 40	2000 ± 50	0.76 ± 0.022
7	0.78	$1.56X10^4$	1350 ± 30	1100 ± 40	0.80 ± 0.033
8	0.39	$7.8X10^3$	680 ± 20	570 ± 30	0.83 ± 0.053

a ^{111}In P256 : 150 µg/ml, 182 MBq/mg (4.9 mCi/mg). The volume of McAb added to the tubes was as small as possible (500-3.9 µl).

b PRP prepared in this experiment contained $3.5X10^8$ptlt/ml.

c Tubes prepared in duplicate. Each tube contained $2X10^8$ ptlt/ml. A separate set containing $2X10^8$ ptlt/ml + 20 fold excess of cold P256 over ^{111}In P256 was prepared to measure non-specific binding (see text).

d All count-rates were corrected for background. BG = 165, n = 3, se = 7.

Radioactivity platelet bound was calculated by subtraction of the count-rate remaining in platelet poor plasma (unbound radioactivity) at the end of the incubation time, from the total count-rate in each tube. Unbound radioactivity was obtained by correcting the count-rate in the 500 µl PPP aliquots taken after centrifugation of the tubes for background and multiplying the result by 2 (total volume of plasma = 1ml, the volume of the platelet pellet was ignored). Non-specific binding, calculated in the same way as above, was allowed for whenever statistically significant by subtracting the values of the count-rate non-specifically associated to platelets from the count-rate bound to platelets in the absence of excess

unlabelled antibody. The results were finally expressed as a ratio of the count-rate platelet bound to that totally added (B/T) (see Table 5.5[1]).

A repeat of this experiment using a different ^{111}In P256 preparation (same P256-DTPA stock, but ^{111}In labelling done on a different occasion) and PRP obtained from a different source than the one in the experiment above, showed essentially the same pattern of ^{111}In P256 binding to platelet having kept other reaction conditions equal to the previous experiment, ie concentration of reactants, incubation time and temperature etc (results summarised in Table 5.6[2]).

Table 5.6. Result of the repeat ^{111}In P256[a] vs PRP[b] radiobinding assay.

Ab/ptlt:	10^6	5X10^5	2.5X10^5	1.25X10^5	6.25X10^4	3.13X10^4	1.56X10^4	8X10^3
B/T :	0.16	0.22	0.36	0.47	0.65	0.78	0.82	0.86
± 1 se :	0.004	0.006	0.009	0.012	0.017	0.024	0.037	0.060

a ^{111}In P256 180 µg/ml, 348MBq/mg (9.4 mCi/mg).
b PRP was prepared from blood obtained from a normal volunteer. It contained 2.7X10^8ptlt/ml.

5.2.5.2 Binding of ^{111}In P256 F(ab')$_2$ to PRP

The same experimental protocol to that employed for ^{111}In P256 radio-binding assay was used, ie 2X10^8 ptlt in PRP + ^{111}In P256 F(ab')$_2$ (10^6Ab/ptlt-8X10^3 Ab/ptlt). Two experiments using PRP from two different donors were performed and the range of binding of the F(ab')$_2$ was determined[3].

Finally, the results[4] of ^{111}In P256 and ^{111}In P256 F(ab')$_2$ binding to platelets in PRP were plotted as a function of Ab concentration (Figure 5.2).

---

1 Non-specific binding of ^{111}In P256 was found to be non-significant (99% confidence limit) and was ignored (See Appendix, Table A5.7, page 296 for experimental data).
2 See Appendix, Tables A5.8, A5.9, pp296 & 297 for experimental data.
3 See page 59 for the method and Tables A5.10, A5.11, A5.12 and A5.13 Appendix, pp296 & 297 for the experimental data.
4 The ratio of platelet bound to total antibody added is shown in the graph.

Figure 5.2. Binding of ^{111}In P256 (Top) and ^{111}In P256 F(ab')$_2$ (Bottom) to platelets in platelet rich plasma.

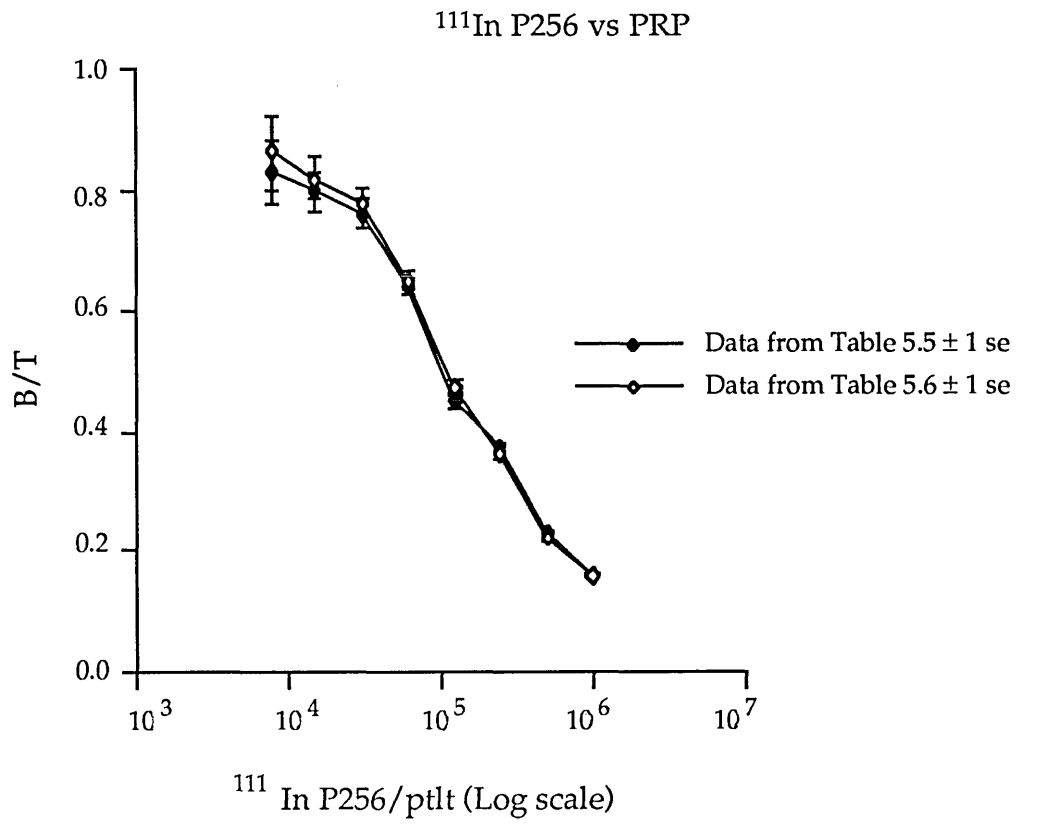

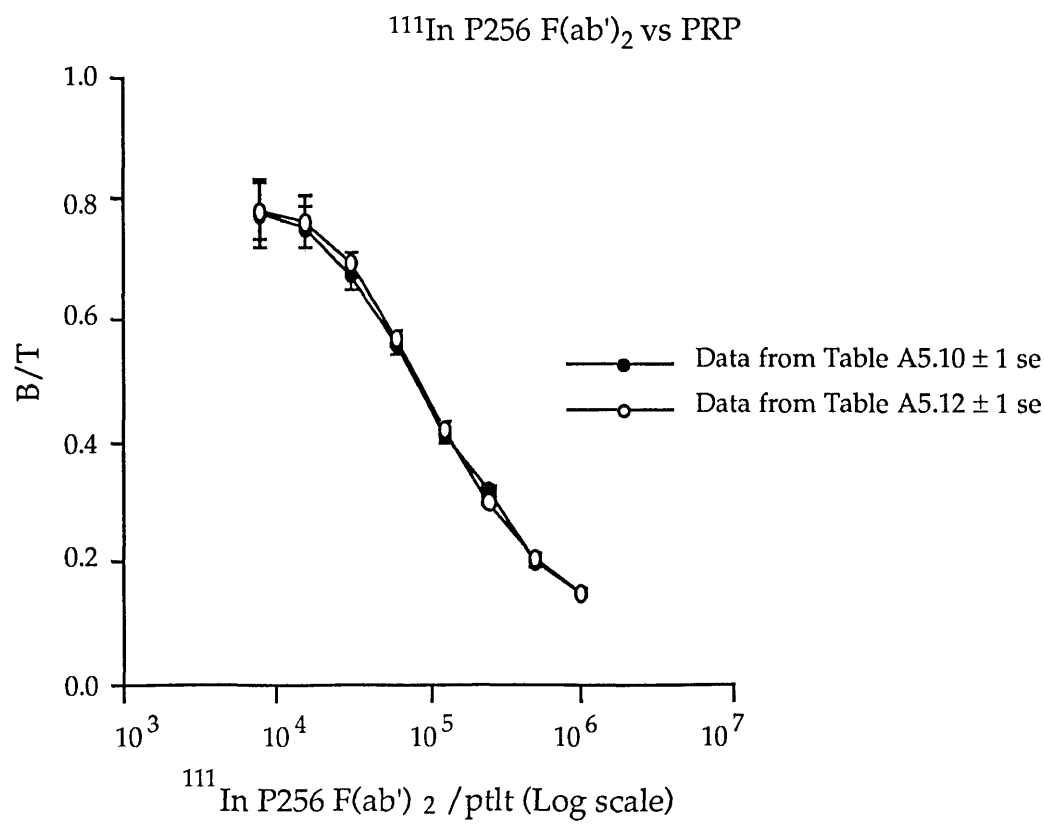

5.2.5.3 Binding of ^{111}In P256 to anticoagulated whole blood

Blood obtained from a normal volunteer was collected in ACD anticoagulant (1 part ACD to 6 parts blood)[1]. A complete blood count (RBC, WBC, platelets, Hb and Hct)[2] was obtained on a sample of the anticoagulated whole blood using an automatic Coulter counter[3]. Aliquots of 4 ml of ACD-anticoagulated blood were dispensed in sixteen 10 ml centrifuge tubes. ^{111}In P256 was added to eight tubes in concentrations similar to those added to PRP, ie 10^6 Ab/ptlt-8000 Ab/ptlt (see Table 5.7). Unlabelled P256 was added to the rest of the tubes at concentrations calculated to yield 20 fold excess over ^{111}In P256 which was added afterward in similar concentrations to the first eight tubes. The tubes were then sealed with Parafilm (USA) and fixed on a slowly rotating disc at 37° C[4]. After a 2 hr incubation period, aliquots of 500 µl ACD-blood from each tube were dispensed in gamma counting vials[5]. The tubes were then centrifuged at 190 g for 15 min and volumes of platelet rich plasma equal to those calculated to be contained in 0.5 ml ACD-blood + ^{111}In P256 in each tube[6] were dispensed in counting vials. Subsequently, the tubes were re-centrifuged at 1500 g for 10 min and similarly aliquots of PPP, calculated to be contained in 0.5 ml blood were transferred to gamma counting vials. Finally, all the counting vials were counted in an automatic gamma scintillation counter[7] . The count-rate in PPP was subtracted from

---

1 Sixty millilitre blood were withdrawn through a wide bore needle (G19) in a syringe containing 10 ml ACD.

2 RBC : red blood cells, WBC : white blood cells, Hb : Haemoglobin, Hct : Haematocrit.

3 Coulter counter , Haematology Dept RPMS.

4 Warm room (37° C), Immunology Department, RPMS.

5 Count-rates in these tubes represented the reference standards of the total ^{111}In P256 radioactivity added.

6 The volume of PRP (or PPP) obtained was calculated as follows : The volume of ^{111}In P256 added to 4 ml ACD-blood reduced the haematocrit value (Hct in ACD-blood was measured at the start of the experiment as part of the full blood count) in each tube according to the amount of solution added. Therefore, the volume of plasma in 0.5 ml ACD-blood + ^{111}In P256 was calculated from the following equation :

$$\text{Pl in 0.5 ml ACD-blood} + {}^{111}\text{In P256 (µl)} = \frac{(1\text{-Hct})\text{X}4000 + \text{vol Ab in µl}}{4000 + \text{vol Ab in µl}} \times 500 .$$

The volume of the platelets in PRP was ignored for the sake of this calculation.

7 Packard Autogamma, USA, Haematology Dept, RPMS.

the count-rate in whole blood to obtain cell bound count-rate, afterward, the ratio of cell bound radioactivity to activity in whole blood (B/T) was calculated (see Table 5.7)[1].

Table 5.7. Setting and results of the ^{111}In P256[a] vs ACD-blood[b] radiobinding assay[c].

Tube	^{111}In P256 conc µg/ml	^{111}In P256/ ptlt	cpm 500µl WB ± 1 se	cpm cell bound 500 µl WB ± 1 se	B/T ± 1 se
1	70	10^6	71200	7800	0.11
			± 270	± 400	± 0.005
2	35	$5X10^5$	35900	6500	0.18
			± 190	± 260	± 0.007
3	17.5	$2.5X10^5$	18000	5800	0.32
			± 130	±.180	± 0.010
4	8.75	$1.25X10^5$	8900	3400	0.38
			± 100	± 120	± 0.014
5	4.38	$6.25X10^4$	4500	2500	0.55
			± 70	± 80	± 0.020
6	2.19	$3.13X10^4$	2200	1400	0.64
			± 50	± 60	± 0.030
7	1.09	$1.56X10^4$	1100	800	0.70
			± 40	± 40	± 0.043
8	0.55	$7.8X10^3$	600	450	0.72
			± 30	± 30	± 0.062

a ^{111}In P256 : 300 µg/ml, 302 MBq/mg (8.2 mCi/mg).
b Hct = 0.40, Ptlt No = $2.85X10^8$/ml.
c All count-rates were corrected for background. BG = 110, n = 3, se = 6.

It was also found that PRP contained 80-95% of the activity present in whole blood. This pointed to a low binding of ^{111}In P256 to other blood cells (RBC, WBC) (see Table 5.8).

1 Non-specific binding was found to be statistically non-significant and was therefore ignored (see Appendix, Table A5.14, page 299).

Table 5.8. Radioactive counts in PRP and their ratio to ^{111}In P256 counts in ACD-Whole blood[a].

Tube	cpm 500µl WB ± 1 se	cpm PRP in 500 µl WB ± 1 se	PRP/T ± 1 se
1	71200	63400	0.89
	± 270	± 250	± 0.005
2	35900	33000	0.92
	± 190	± 180	± 0.007
3	18000	15500	0.86
	± 130	± 130	± 0.010
4	9000	8500	0.95
	± 100	± 90	± 0.015
5	4500	4000	0.90
	± 70	± 60	± 0.020
6	2200	1850	0.84
	± 50	± 40	± 0.028
7	1150	1000	0.86
	± 40	± 30	± 0.040
8	600	500	0.80
	± 30	± 30	± 0.055

a Same experiment as in the previous page.

The whole blood ^{111}In P256 binding experiment was repeated twice afterwards. The experimental conditions were kept the same at each time except for ^{111}In P256[1] that was labelled especially before each experiment and blood which was obtained from two different volunteers. The results of the repeat ^{111}In P256 versus ACD-whole blood radioimmunoassays are shown in Table 5.9[2].

1 Same batch of P256-DTPA was used as the one in the previous experiments.

2 See Appendix, Tables A5.15, A5.16, A5.17, A5.18, pp300 & 301 for experimental data.

Table 5.9. Result of the repeat ^{111}In P256 vs ACD-blood radiobinding assays.

Ab/ptlt:	10^6	5X10^5	2.5X10^5	1.25X10^5	6.25X10^4	3.13X10^4	1.56X10^4	8X10^3
Repeat I[a]								
B/T :	0.11	0.19	0.34	0.41	0.59	0.68	0.73	0.76
± 1 se :	0.005	0.006	0.009	0.012	0.018	0.025	0.037	0.055
PRP/T:	0.86	0.91	0.83	0.96	0.90	0.87	0.85	0.81
± 1 se :	0.004	0.006	0.008	0.013	0.017	0.023	0.034	0.048
Repeat II[b]								
B/T :	0.11	0.20	0.34	0.40	0.61	0.69	0.74	0.77
± 1 se :	0.004	0.006	0.008	0.011	0.016	0.023	0.035	0.051
PRP/T:	0.89	0.93	0.84	0.90	0.86	0.82	0.87	0.92
± 1 se :	0.004	0.006	0.008	0.011	0.015	0.021	0.033	0.049

a ^{111}In P256 : 260 µg/ml, 247 MBq/mg (6.7 mCi/mg), Hct : 0.42, Ptlt ct : 3X10^8ptlt/ml.
b ^{111}In P256 : 280 µg/ml, 276 MBq/mg (7.5 mCi/mg), Hct : 0.37, Ptlt ct : 2.45X10^8ptlt/ml.

5.2.5.4 Binding of ^{111}In P256 F(ab')$_2$ to anticoagulated whole blood

Three radiobinding assays of ^{111}In P256 F(ab')$_2$ were performed to assess the degree of Ab binding to platelets in whole blood over a range of increasing Ab concentrations. A similar protocol to that used for ^{111}In P256 versus whole blood radioimmunoassay (described above) was followed and the range of binding of ^{111}In P256 F(ab')$_2$ to platelets in whole blood was determined[1].

The results of ^{111}In P256 and ^{111}In P256 F(ab')$_2$ radioimmunoassays with whole blood were finally plotted as the antibody cell bound ratio versus antibody concentration (Figure 5.3).

1 See Appendix, Table A5.19, A5.20, A5.21, A5.22, A5.23, A5.24 and A5.25 pp302-305 for setting and results.

Figure 5.3. Binding of ^{111}In P256 (Top) and ^{111}In P256 F(ab')$_2$ (Bottom) to platelets in anticoagulated whole blood.

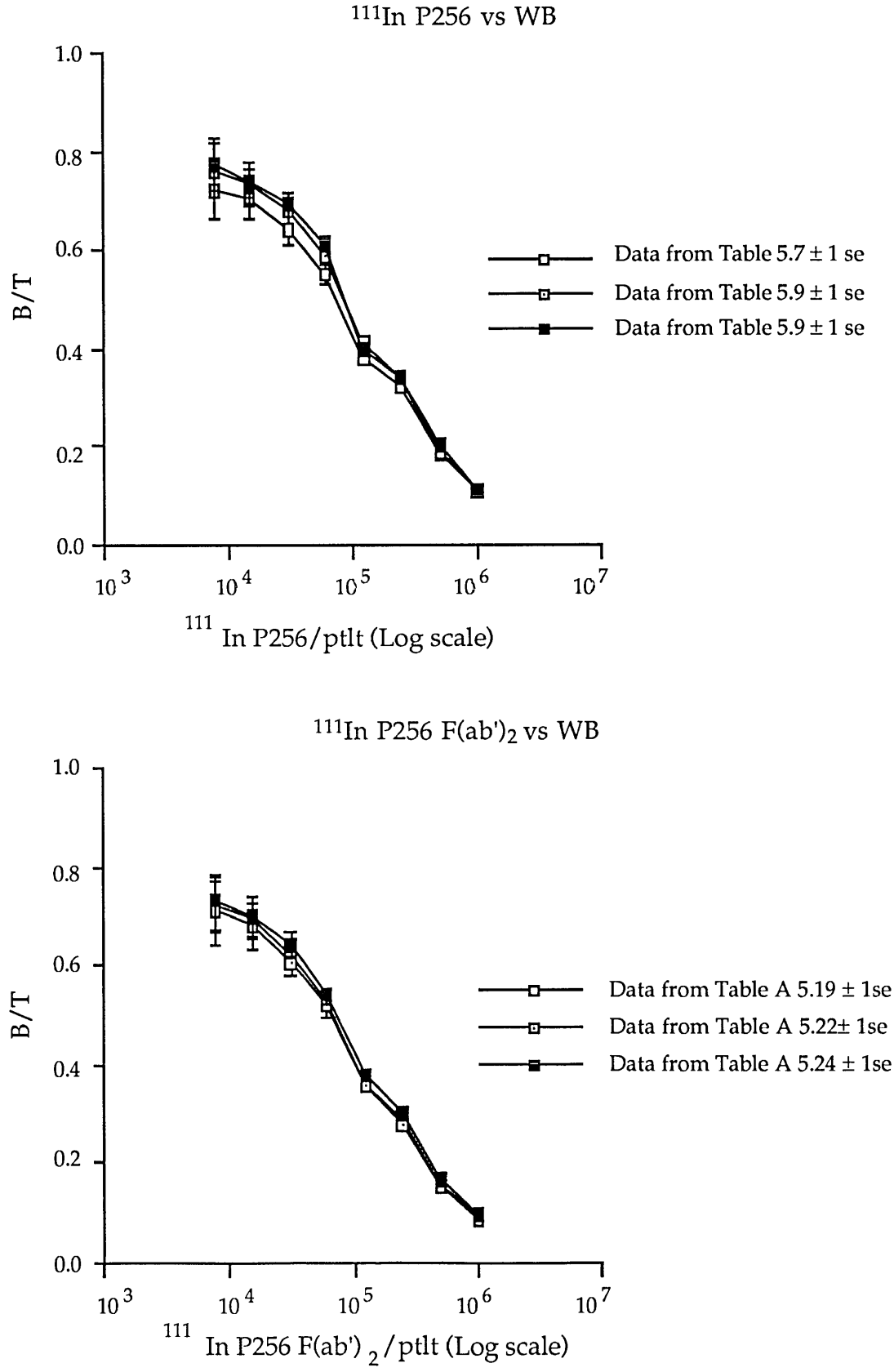

5.2.5.5 Summary of ^{111}In P256 or ^{111}In P256 F(ab')$_2$ versus PRP or whole blood radioimmunoassays

In vitro binding of the ^{111}In labelled monoclonal antibody P256 and its F(ab')$_2$ to PRP and whole blood are presented in Table 5.10.

Table 5.10. Summary of ^{111}In P256 and ^{111}In P256 F(ab')$_2$ radioimmunoassays

Ab/ptlt[a]	^{111}In P256		^{111}In P256 F(ab')$_2$	
	B/T (PRP)[b] ± 1 se	B/T (WB)[c] ± 1 se	B/T (PRP)[b] ± 1 se	B/T (WB)[c] ± 1 se
10^6	0.16 ± 0.003	0.11 ± 0.003	0.15 ± 0.003	0.10 ± 0.003
$5X10^5$	0.23 ± 0.004	0.19 ± 0.004	0.21 ± 0.004	0.16 ± 0.004
$2.5X10^5$	0.37 ± 0.006	0.33 ± 0.005	0.31 ± 0.005	0.29 ± 0.005
$1.25X10^5$	0.46 ± 0.008	0.40 ± 0.007	0.42 ± 0.007	0.37 ± 0.008
$6.25X10^4$	0.65 ± 0.011	0.58 ± 0.010	0.57 ± 0.010	0.53 0.011
$3.13X10^4$	0.77 ± 0.016	0.67 ± 0.015	0.68 ± 0.015	0.62 ± 0.015
$1.56X10^4$	0.81 ± 0.025	0.72 ± 0.022	0.76 ± 0.028	0.69 ± 0.023
$7.8X10^3$	0.85 ± 0.040	0.75 ± 0.032	0.78 ± 0.035	0.72 ± 0.023

a ^{111}In P256 or ^{111}In P256 F(ab')$_2$.

b Average of two values (see Tables 5.5 & 5.6 for ^{111}In P256, and Tables A5.10 & A5.12 for ^{111}In P256 F(ab')$_2$.

c Average of three values (see Tables 5.7 & 5.9 for ^{111}In P256 and Tables A5.19, A5.22 & A5.24 for ^{111}In P256 F(ab')$_2$.

Finally, Figure 5.4 shows the summary of the results in Table 5.10 plotted as antibody cell-bound ratio versus antibody concentration.

Figure 5.4. Summary of ^{111}In P256 / ^{111}In P256 F(ab')$_2$ radioimmunoassays

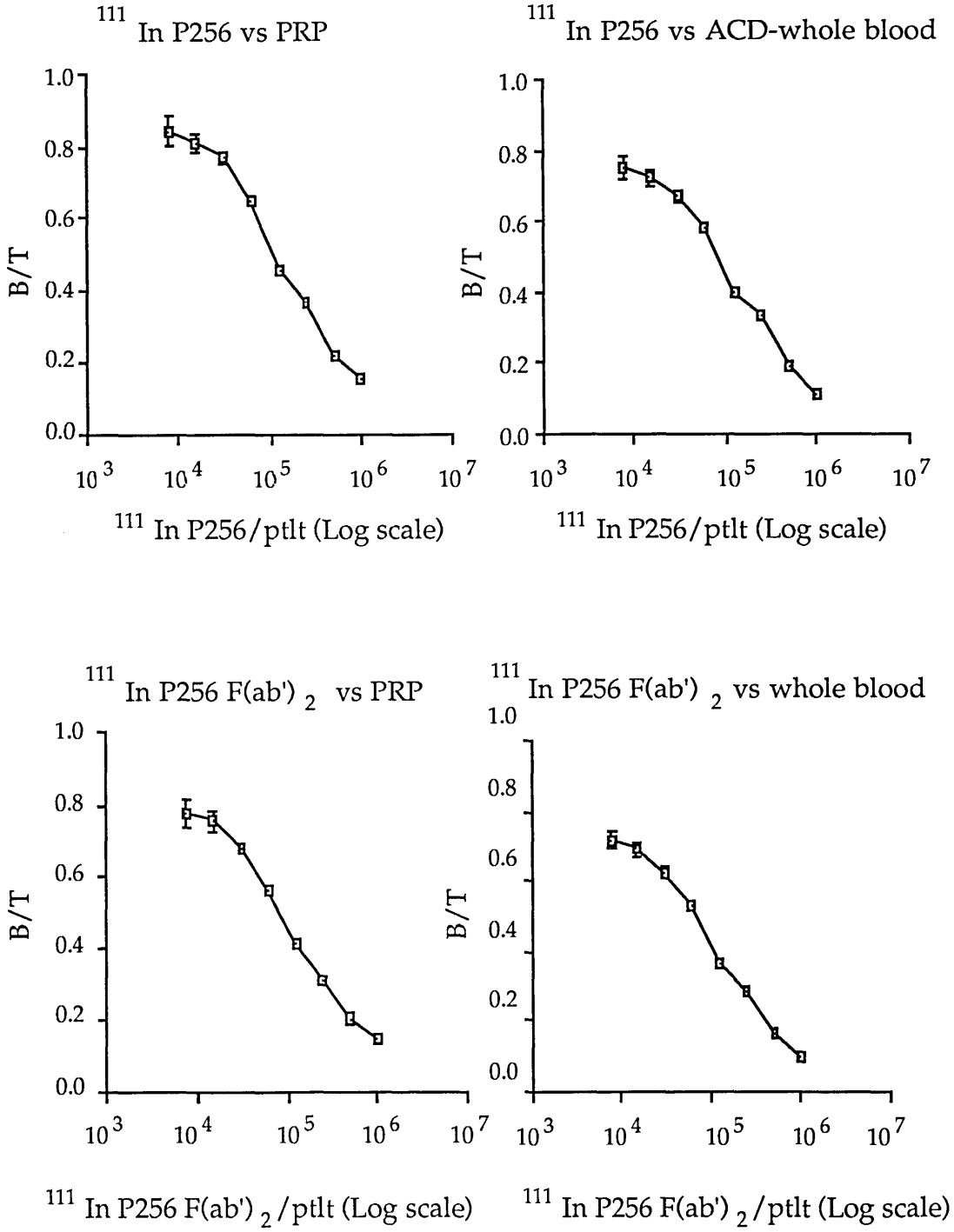

Notes : Each point is the arithmetic mean of values obtained in two experiments for ^{111}In P256 vs PRP and three experiments for ^{111}In P256 F(ab')$_2$ vs ACD-WB. The error bar at each point represents 1 se associated with that point.

5.2.6 In vitro testing of the effect of P256 or P256 F(ab')$_2$ on platelets

The effect of P256 or P256 F(ab')$_2$ on platelets at different McAb concentrations was assessed in vitro by visual recording of spontaneous aggregation in platelet rich plasma (PRP) under phase contrast microscopy. Measurement of spontaneous or induced aggregation in citrated whole blood was performed using the Ultraflo 100 whole blood platelet counter.

5.2.6.1 Platelet aggregation measured by microscopic counting

Blood collected from a normal volunteer was anticoagulated in ACD (30 ml blood taken in a syringe containing 5 ml ACD). Blood was dispensed equally in two universal plastic containers and centrifuged at 190 g for 15 minutes to obtain PRP and a pellet of erythrocytes and leucocytes as described earlier (see page 55). Platelet rich plasma was transferred to a third 20 ml-Universal and a platelet count was done[1].

Afterwards, aliquots of 1 ml PRP were dispensed in each of eight LP3 tubes. Each tube was tested at a time as follows :

A platelet count was performed, then P256 or P256 F(ab')$_2$ was added in a 50 µl volume from a dilution of antibody in PBS prepared immediately beforehand and calculated to yield the first Ab concentration set in Table 5.11.

---

1 50 µl volume of PRP was diluted X100 in 4950 µl normal saline in a 10 ml centrifuge tube. After mixing, platelet count was done using a haemocytometer (Improved Neubauer, BDH, England), a phase contrast microscope (X400 Magnification, M20 Wild-Leitz Switzerland) and a tally counter (Clay Adams, Becton and Dickinson USA). Platelets were allowed to settle for 15 min in the counting chamber before starting the count (the haemocytometer was placed in a humidified box). Count was done in duplicate using both counting chambers of the haemocytometer.

Table 5.11. Concentrations of P256[a] added to PRP.

Tube No	1	2	3	4	5	6	7	8
Ab conc (μg/ml)	56	28	5.6	2.8	0.56	0.28	0.056	0.028
Ab/ptlt	10^6	$5X10^5$	10^5	$5X10^4$	10^4	$5X10^3$	10^3	$5X10^2$

a The same molar concentrations of P256 $F(ab')_2$ as those of P256 were used for testing the effect of P256 $F(ab')_2$ on spontaneous aggregation in PRP.

The tube was then sealed and incubated at 37°C for 15 min with gentle intermittent mixing. At the end of the incubation time another platelet count was done. Single platelets and platelet aggregates were recorded separately using the tally counter.

The second tube was tested similarly except that the second Ab concentration in Table 5.11 was added this time. The method was repeated for each tube until the last Ab concentration was reached. The results of platelet counts before and after P256 addition at different concentrations are shown in Table 5.12[1].

The percentage platelet aggregation (PA) after addition of P256 was calculated as follows :

$$PA = [1-(\frac{N_{Ab}}{N_0})] \times 100$$

Where N_{Ab} : single platelet number after the addition of Ab, N_0 : single platelet number before the addition of the Ab (see Table 5.18 and Figure 5.5).

1 The results of platelet count before and after addition of P256 $F(ab')_2$ to PRP are shown in Tables A5.26 and A5.27 and Figure A5.2, Appendix, pp305 & 306.

Table 5.12. Platelet counts[a] pre and post P256 addition to PRP[b].

	Pre P256			Post P256		
Tube No	Single Ptlt[c]	Aggreg[d]	Total[e]	Single Ptlt[c]	Aggreg[d]	Total[e]
1	217 ± 10	3 ± 1.2	220 ± 10	3 ± 1.2	31 ± 4	34 ± 4
2	227 ± 11	6 ± 1.7	233 ± 11	5 ± 1.6	52 ± 5	57 ± 5
3	204 ± 10	3 ± 1.2	207 ± 10	7 ± 1.9	48 ± 5	55 ± 5
4	195 ± 10	14 ± 2.7	209 ± 10	10 ± 2.2	64 ± 6	74 ± 6
5	208 ± 10	9 ± 2.1	217 ± 10	43 ± 5	72 ± 6	115 ± 8
6	198 ± 10	8 ± 2	206 ± 10	77 ± 6	59 ± 5	136 ± 8
7	204 ± 10	5 ± 1.6	209 ± 10	193 ± 10	14 ± 3	207 ± 10
8	196 ± 10	6 ± 1.7	202 ± 10	191 ± 10	7 ± 1.9	198 ± 10

a Counts done in duplicate using the two chambers of the haemocytometer.
b Stock PRP contained $2.25X10^8$ptlt/ml.
c Single platelets counted in the 25 large square area of the haemocytometer.
d Aggregates of platelets (two or more platelets together) counted in the same area as c above.
e The total number of particles (single + platelet aggregates) counted in 25 large squares of the haemocytometer.

Table 5.13. Platelet aggregation after the addition of P256.

Tube No	1	2	3	4	5	6	7	8
PA (%) ± 1 se	99 ± 0.6	98 ± 0.7	97 ± 0.9	95 ± 1.2	79 ± 2.5	61 ± 3.7	5 ± 6.7	3 ± 7.0

Figure 5.5. Platelet aggregation versus P256 concentration in PRP.

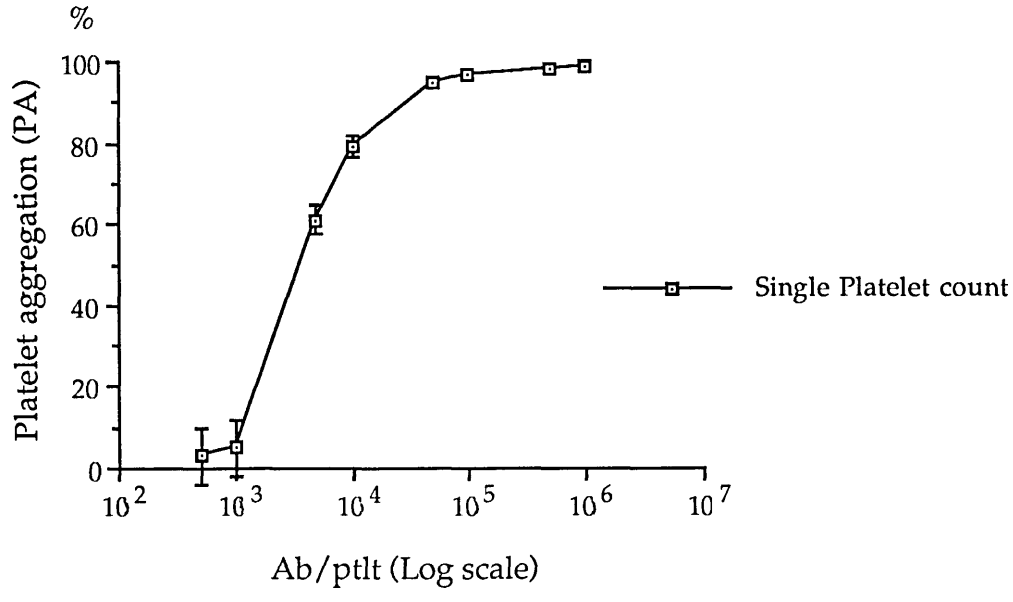

5.2.6.2 Measurement of spontaneous and induced platelet aggregation in whole blood in the presence of P256 or P256 F(ab')$_2$ using Ultraflo 100

The method employed an electronic particle counter, the Ultraflo 100[1], which counted single platelets in whole blood without the need to separate them from other blood cells (Lumley and Humphrey 1981). The results were recorded as a fall in individual platelet count denoting platelet aggregation[2].

5.2.7 Summary of the studies testing spontaneous or induced platelet aggregation by P256 or P256 F(ab')$_2$

Testing the effect of P256 or P256 F(ab')$_2$ on platelets in PRP and anticoagulated whole blood showed an increase in spontaneous aggregation of platelets in the presence of the antibody. This was especially noted with whole P256 antibody which caused massive platelet aggregation when its

1 Clay Adams.
2 For experimental details and results see Appendix, pp306-308.

concentration exceeded 3.5-4X10^3 Ab/ptlt. P256 concentration below that level caused little aggregation and no significant aggregation was observed at concentrations < 1000 ab/ptlt. In contrast, P256 F(ab')$_2$ showed a weaker effect on aggregation than the whole Ab. Concentrations less than 3500 Ab/ptlt caused no significant increase in aggregation and only high concentrations of the Ab (above 10^4 Ab/ptlt) led to a noticeable reduction in single platelet count.

Antibody effect on induced aggregation was less obvious than its effect on spontaneous aggregation in the experiments performed. Potentiation of the effect of U-46619[1] by preincubation of whole blood with P256 was seen in one experiment[2]. However, the effect of P256 or P256 F(ab')$_2$ on induced aggregation by ADP or collagen at the concentrations of Ab used was not markedly different from the control (no Ab)[3].

5.3 Discussion

5.3.1 In vitro radioimmunoassays of ^{111}In P256 or ^{111}In P256 F(ab')$_2$ vs PRP or whole blood

Labelling of P256 or P256 F(ab')$_2$ with ^{111}In using the method described yielded high specific activity up to 900 MBq/mg (24 mCi/mg), which was in agreement with levels of specific activity of ^{111}In McAbs reported earlier (Hnatowich et al 1982 & 1983). This level provided adequate radioactivity for imaging purposes using a low antibody mass (90 MBq/100μg) without significant effect on the immunoreactivity of the antibody.

Binding of ^{111}In labelled anti-platelet glycoprotein McAb P256 or its F(ab')$_2$ fragment to platelets was documented by direct radioimmunoassays in

---

1 A stable prostaglandin endoperoxide analog, Upjohn.
2 See Table A5.30, Appendix, page 308.
3 See Table A 5.31, Appendix, page 308.

platelet rich plasma and in anticoagulated whole blood. The design of the radioimmunoassays aimed at causing the least possible manipulation of platelets by avoiding platelet washing and at minimising aggregation by incubating the cells at room temperature or 37°C. This design necessitated an indirect calculation of the amount of antibody bound to platelets by measurement of non-cell-bound ^{111}In radioactivity in the supernatant after centrifugation of the cell suspension at 1500 g for 10 minutes and subtrating this amount from the total ^{111}In activity present therein. Non-specific binding of ^{111}In P256 to the tube wall or other cells (whole blood assay) was not found to be significant, indicating reliability of the calculation for the amount of antibody-platelet bound.

These tests, especially the one employing whole blood as a source of antigen and labelling medium, simulated in vivo conditions of antigen-antibody reaction and gave information on the range of binding of the antibody to platelets in that situation. Furthermore, specific binding of ^{111}In P256 or ^{111}In P256 F(ab')$_2$ to platelets was confirmed in the whole-blood assays as 80-96% of activity in whole blood was in platelet rich plasma both bound to platelets and free in plasma.

Thus, the main question binding assays helped to clarify was the extent of Ab binding to platelets at varying Ab concentrations. If the ratio of cell bound to total Ab added was considered, the optimal Ab concentration for the highest cell binding ratio would lie between $3X10^4$ and $8X10^3$ Ab/ptlt[1] (1-0.25 μg/ml).

---

[1] We chose to report antibody concentration as Ab molecules per platelet as it gave a more realistic idea on the amounts involved in each assay. The number of platelets in the media used (PRP & whole blood) lied usually within the range found in normal man, ie $2.50\text{-}4.00X10^8$/ml (exception was the case of the immunoreactivity testing of the ^{111}In McAbs).

5.3.2 Aggregometry studies employing P256 and P256 F(ab')$_2$

Serious effect of the antibody on platelets both in platelet rich plasma and whole blood was observed. P256 induced platelet aggregation when added at concentrations above 3.5-4X10^3 Ab/ptlt (0.2-0.22 μg/ml). This effect was negligible at concentrations of Ab below 10^3 Ab/ptlt. In comparison, the effect of P256 F(ab')$_2$ was less marked and platelet aggregation did not occur until Ab concentrations more than 10^4 Ab/ptlt were added to platelet rich plasma or whole blood.

In contrast to studies of spontaneous platelet aggregation by whole P256 Ab or F(ab')$_2$, testing of induced aggregation of platelets by proaggregants (U-46619, ADP and collagen) in the presence of the antibody (P256 or P256 F(ab')$_2$) did not result in a clear potentiation of the proaggregant effect.

This phenomenon could be explained by the antibody causing cross-linking of GP IIb/IIIa molecules, possibly leading to conformational changes in the heterodimer complex, and enabling them to interact with fibrinogen.

Evidence to support this hypothesis was in the reduced effect of F(ab')$_2$ fragment as compared to whole antibody and the total failure of monomeric Fab' of the same antibody to cause platelet aggregation under similar conditions (Stuttle et al 1988b). Thus, a pharmacological effect of P256 F(ab')$_2$, mediated by receptor-cross linking on platelet surface and Fc mediated functions such as Fc receptor binding and lattice formation, would be the main events to cause platelet aggregation by this antibody (Jennings et al 1985, Modderman et al 1986).

Chapter 6 :

In Vivo Use of ^{111}In P256 and ^{111}In P256 F(ab')$_2$ in Man

6.1 Introduction :

The problems posed by in vivo use of anti-platelet McAbs to radiolabel platelets are those related to direct effects of the antibody on platelet function, those seen in general upon injection of a foreign protein, like immediate or delayed immune reactions, and those concerning the radiation dose expected from such use in human to the whole body and target organs.

The effect of P256 and its F(ab')$_2$ on platelet aggregation was studied in vitro (see Chapter 5). ^{111}In P256 was subsequently applied in vivo and a pilot clinical study of its value in labelling platelets for the early imaging of thrombus was started[1].

In this chapter, the kinetics of radiolabelled platelets after injection of ^{111}In P256 or ^{111}In P256 F(ab')$_2$ are described and images of localisation in thrombus are shown.

6.2 Subjects, Materials and methods :

6.2.1 Subjects studied[2] :

One normal volunteer, a patient with leukaemia (megakaryoblastic, FAB : M7) and 16 patients suspected of thrombus (DVT, vascular graft thrombosis, arterial thrombi and vasculitis) were included in the study (see Table 6.1).

---

1 The study was approved by the local ethical committee and the Administration of Radioactive Substances Advisory Committee (ARSAC).

2 An informed consent was obtained from each subject undergoing the study.

Table 6.1. Subjects injected in vivo with ^{111}In P256 or ^{111}In P256 F(ab')$_2$

Patient	Sex (M/F)	Age (yr)	Complaint/diagnosis	Venography
I. ^{111}In P256				
1. JPL	M	59	Normal volunteer	ND
2. JW	M	27	Leukaemia (Megakaryoblastic, M7)	ND
3. GM	M	79	Total hip replacement, DVT L leg ?	Normal
4. AS	M	72	DVT L leg ?	Positive
5. SH	M	75	Ca bladder, DVT R leg ?	Negative
6. VH	F	48	Vasculitis, old venous thrombosis	ND
7. HQ	M	63	DVT R leg ?	Positive
8. DS	M	60	Thrombosed prosthetic aortic valve	ND
9. CN	M	63	Myocardiac infaction, LV thrombus	ND
10. CC	M	62	Thrombus in R subclavicular vein related to Hickman line	Positive
II. ^{111}In P256 F(ab')$_2$				
11. AM	F	89	DVT L leg ?	ND
12. ML	F	77	DVT L leg ?	Negative
13. EK	F	25	DVT L leg	ND
14. JC	M	63	DVT L leg	Negative
15. MD	M	81	DVT L Leg ?	ND
16. DA	F	87	DVT R leg	ND
17. WM	M	65	Carotid stenosis & aorto-bifemoral graft.	ND
18. RW	M	50	Narrowed carotids, transient ischaemic attacks.	ND

Notes : ND : not done, DVT : deep venous thrombosis, Ca : carcinoma, LV : left ventricle, L : left, R : right, ? : clinical suspicion of the abnormality.

Relevant medical history and clinical examination including the measurement of the person's height and weight were obtained for every

participating individual. Also, a full blood count[1] was done before the administration of the labelled antibody. All subjects studied were not on any anticoagulants at the time of the study. No other preparation was deemed necessary.

6.2.2 Labelling of P256 or P256 F(ab')$_2$ with ^{111}In :

The method of labelling was described in detail earlier (see page 49). The ^{111}In labelled preparation was filtered through a 0.22 μm Millipore filter after labelling and was used within 24 hr of preparation.

^{111}In P256 or ^{111}In P256 F(ab')$_2$[2] was injected intravenously in a small volume (2-4 ml) through a 21 G-butterfly-injection set over 3-5 minutes and flushed with 2 ml physiological saline BP. In all subjects injected with ^{111}In P256 or ^{111}In P256 F(ab')$_2$ no untoward reactions were noted

6.2.3 Blood sampling

Blood samples were taken from a vein other than that used for injection of ^{111}In P256 or F(ab')$_2$ (usually a vein in the contralateral arm to that injected with the antibody). Five millilitre samples of blood were taken at each time using a syringe tipped with a 19 G needle and blood was immediately transferred to vials containing EDTA anticoagulant and mixed. A 1 ml aliquot of blood was transferred to radioactivity-counting vial. The rest of the collected blood was centrifuged at 1500 g for 10 minutes and a 1 ml aliquot of plasma was taken into a second vial for radioactive counting.

In addition, separate blood samples for cell counting were collected in vials containing EDTA and a full blood count was obtained.

---

1 The full blood count included : haemoglobin (Hb) and haematocrit (Hct) measurements, erythrocyte, leucocyte and platelet counts.

2 Usually 100 μg labelled P256 or F(ab')$_2$ was used per patient, the normal volunteer was injected with 5 μg of P256 only.

Blood sampling[1] began early (5 minutes) after injection and followed at close intervals, eg 10 min, 30 min, 1 hr, then at more spaced times until 8 days after injection. Radioactive counting was performed for each sample in an automatic well counter[2] and the count was corrected for decay to the time of injection (t_0). Time activity curves for the radioactivity in whole blood and its cellular fraction[3] were based on the counts obtained from each of the cases studied.

6.2.4 Imaging using the scintillation camera :

All patients underwent imaging after the injection of the labelled antibody. A large field of view scintillation camera[4] equipped with a medium energy collimator and linked on-line to a computer[5] was used for acquisition, display and analysis of the data.

6.2.4.1 Dynamic imaging :

The early distribution of the labelled Ab was studied by rapid sequence imaging of the anterior upper abdominal area in 5 patients. One minute successive frames were acquired in a 64X64 pixel matrix for 30 minutes starting immediately after the injection of the tracer (see Figure 6.1).

---

1 The timing of blood sampling was dictated mainly by reasons of practicability (patients being on the ward, etc).

2 Packard Autogamma, USA, Haematology Dept, RPMS.

3 The count-rate cell associated was calculated by subtracting the count-rate in the plasma in 1 ml whole blood, ie (1-Hct) ml, obtained after centrifugation of blood, from the count-rate in 1 ml whole blood.

4 IGE Autotune, USA. Two energy windows centered around 170 KeV and 240 KeV, ± 10%, were used.

5 MDS Data system, USA.

Figure 6.1. Dynamic sequence imaging 1-32 min of the upper abdominal area after iv injection of ^{111}In P256 in patient SH. Frames 64X64 pixel matrix, 1 min duration, sequence from left to right and from top to bottom. Radioactivity is seen in the cardiac blood pool (centre), liver (left of each frame) and spleen (right of each frame).

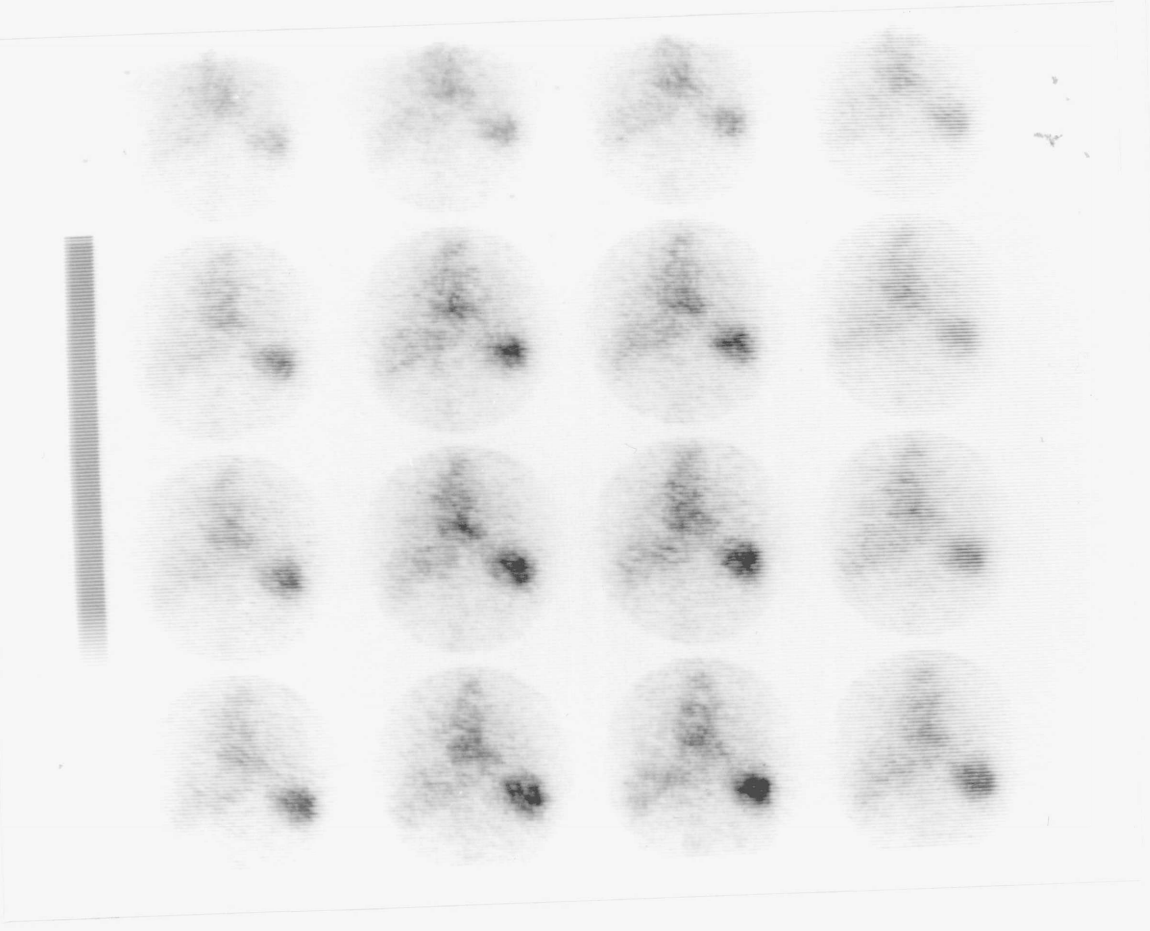

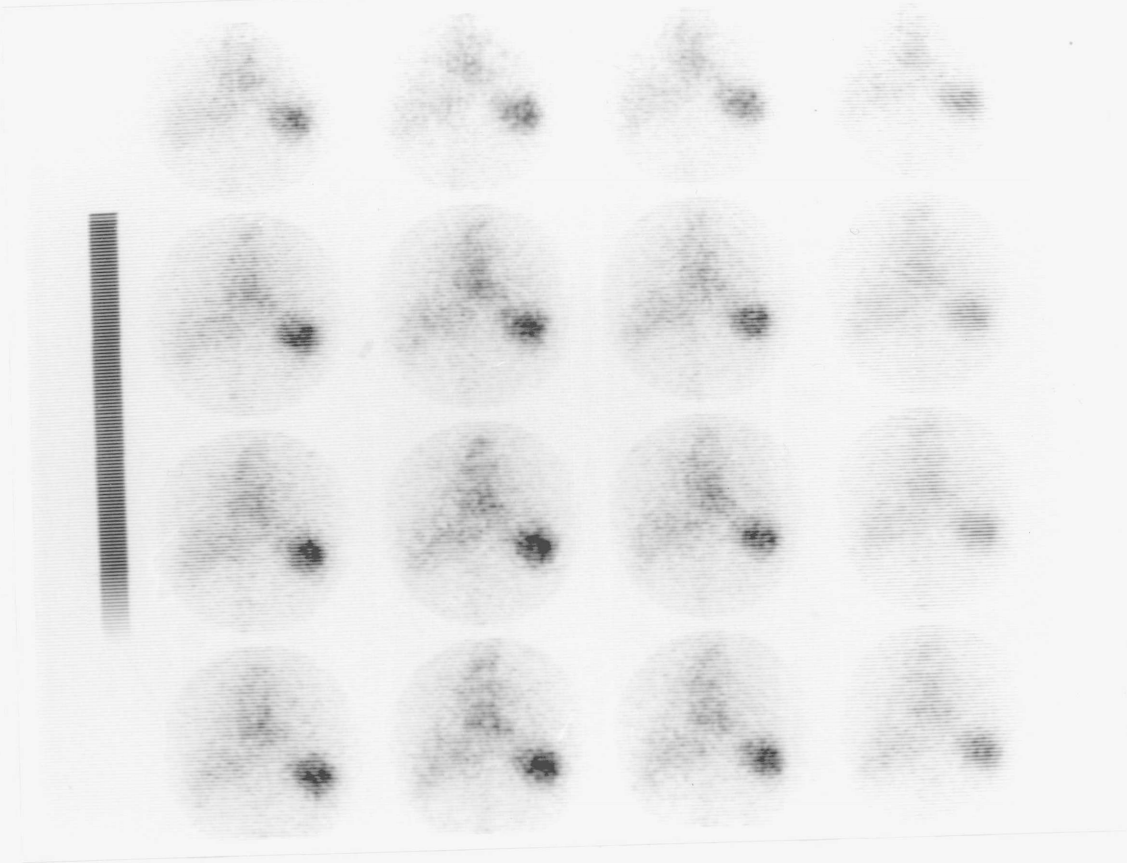

Analysis of this study involved drawing regions of interest (ROI) around the heart, liver and spleen on a composite image obtained by frame addition 1-30. The average count per pixel for every region was obtained for every frame and the resulting values[1] plotted as as function of time. The curves represented the kinetics of ^{111}In P256 or ^{111}In P256 F(ab')$_2$ in the spleen, liver and the blood pool (heart).

6.2.4.2 Static imaging

Images of the distribution of radioactivity after intravenous injection of ^{111}In P256 or ^{111}In P256 F(ab')$_2$ were taken to localise platelet deposition in thrombus. Delayed imaging up to 72 hr was performed to allow background radioactivity due to circulating radioactivity to decrease. Acquisition was performed in a 128X128 pixel matrix and the time duration of each frame was controlled manually depending on the count rate obtained. Multiple views were taken including anterior upper abdomen, pelvis and the lower limbs (2 views : upper legs & lower legs). In a few patients, a whole body scan (anterior or posterior) using the camera in scanning mode was done.

Analysis of the results involved visual inspection of the resulting images[2] by three experienced and independent observers and the outcome was reported as "positive" or "negative" for the presence of thrombus.

6.2.5 Contrast venography :

In patients suspected of deep venous thrombosis, venography studies[3] using a radiocontrast substance[4] were performed to document the presence of

---

1 The values were not corrected for radioactive decay of ^{111}In as it was negligible during the 30 min period of study.

2 A hardcopy of each scan was obtained directly on transparent nuclear medicine film (Kodak, USA) from the camera's oscilloscope. Also, images were checked using the computer monitor.

3 Department of Diagnostic Radiology, RPMS, Hammersmith Hospital.

4 Iohexol 240, England.

venous thrombus and to compare the result with the scans. Venography was done within 12 hr of the injection of the labelled antibody and was reported independently of the scan.

6.2.6 Reporting the results and clinical management of the patient :

All results (scans and radiographs) were reported to the clinicians in charge so that proper action could be taken for each patient.

6.2.7 The protocol used :

1) Label P256 or P256 $F(ab')_2$ with ^{111}In, dispense 100 μg.
2) Obtain from the patient informed consent, brief medical history and clinical examination (record weight and height).
3) Place a butterfly in a vein and take blood sample for blood count.
4) Inject labelled Ab iv.
5) Start dynamic acquisition for 30 min.
6) Sample blood (early 5-30', then up to one week or more) for radioactivity and cell count.
7) Static imaging (delayed 12, 24 ,48 & 72 hr).
8) Contrast venography (if applicable).

6.3 Results :

6.3.1 Kinetics of ^{111}In P256 or ^{111}In P256 F(ab')$_2$ labelled platelets :

6.3.1.1 ^{111}In P256

The time activity curve of whole blood or cell bound[1] ^{111}In activity after injection of ^{111}In P256 in the normal volunteer is shown in figure 6.2[2].

Figure 6.2. ^{111}In radioactivity in blood versus time after the injection of ^{111}In P256 in the normal volunteer (JPL).

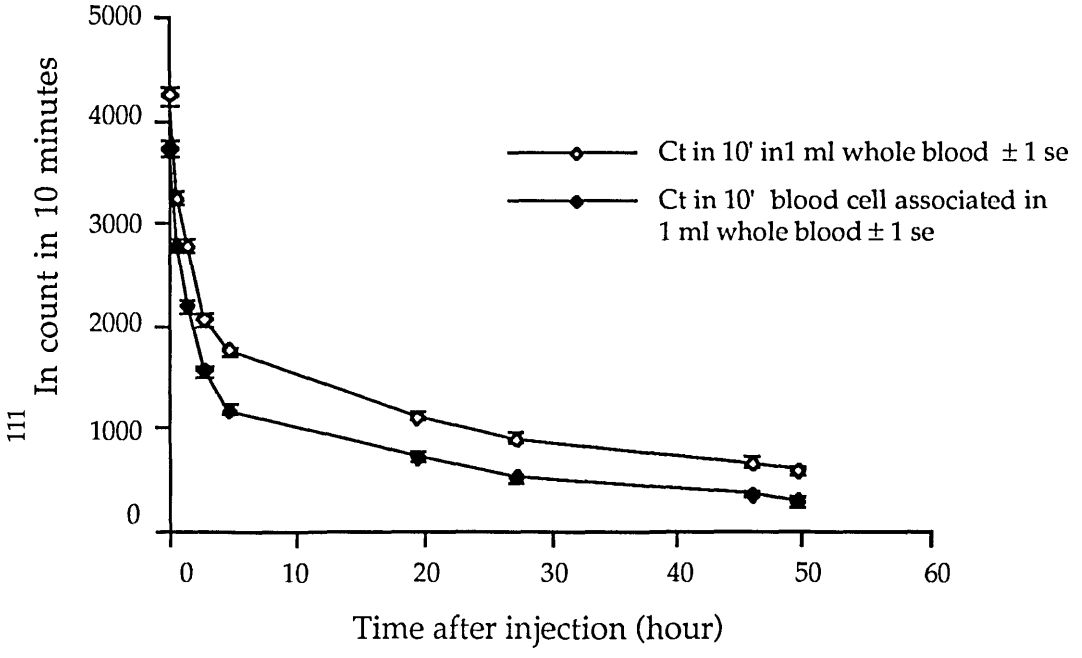

Two other blood time activity curves after the injection of ^{111}In P256 were obtained for two patients. The first patient (SH) was diagnosed clinically to have deep venous thrombosis and the second patient (CN), who had sustained a myocardial infarction earlier, was diagnosed to have a left

---

1 The count rate in the volume of plasma contained in 1 ml whole blood, ie (1-Hct) ml, was subtracted from the count rate in 1 ml whole blood and was plotted against time. Counting time was 10 minutes, all counts were corrected for background.

2 See Appendix, Table A6.1, page 309 for experimental data.

ventricular thrombus demonstrated on a 2D echo. A similar pattern of blood radioactivity to that seen in the normal volunteer was observed[1,2].

The distribution of ^{111}In radioactivity between the plasma and the cellular blood fraction was calculated from the radioactive counts in whole blood and plasma. The ratio of cell bound to total radioactivity in blood indicated that radioactivity was mainly associated with the cells, especially in the early fractions (JPL average 0.69 ± 0.019; SD= 0.143, SH average 0.76 ± 0.006; SD = 0.036, CN average 0.80 ± 0.007; SD = 0.070)[3].

The dynamic study of the early distribution of ^{111}In P256 after iv injection in patient (VH) using the scintillation camera computer system showed a decreasing count-rate in the blood pool, an increasing count-rate in the spleen and a steady count-rate in the liver (Figure 6.3). This pattern was seen in all the patients injected with ^{111}In P256 that had a dynamic scan as part of their study.

Figure 6.3. Kinetics of ^{111}In P256 uptake in the blood pool (heart), spleen and liver from 1-30 minutes after iv injection. A dynamic study using the scintillation camera.

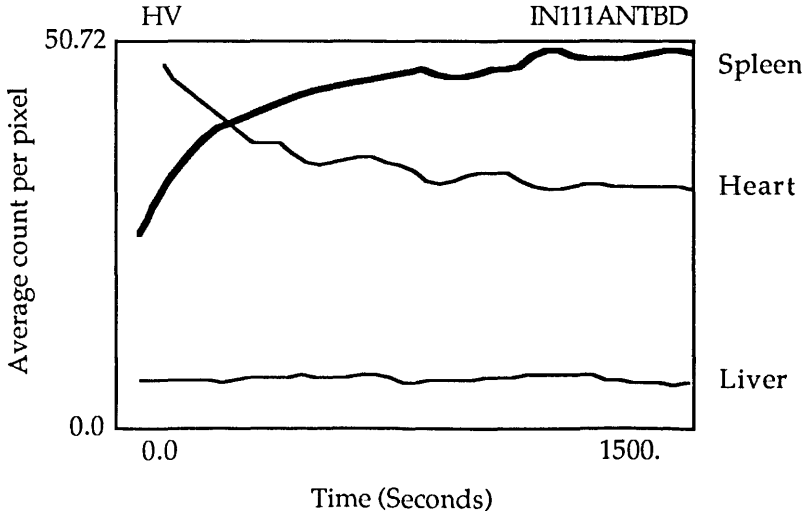

1 The experimental data and blood time activity curve on patient SH are shown in Table A6.2 and Figure A6.1, respectively, Appendix, pp 309 & 310.

2 The experimental data and blood time activity curve on patient CN are shown in Table A6.3 and Figure A6.2, respectively, Appendix, pp310 & 311.

3 See Tables A6.1, A6.2, A6.3, Appendix, pp309 & 310 for experimental details.

6.3.1.2 ^{111}In P256 F(ab')$_2$

The time activity curve of ^{111}In radioactivity (whole blood and cell associated) after injection of ^{111}In P256 F(ab')$_2$ in patient JC suspected of deep venous thrombosis in the left leg is shown in figure 6.4[1]

Figure 6.4. ^{111}In radioactivity in blood versus time after the injection of ^{111}In P256 F(ab')$_2$ in patient JC.

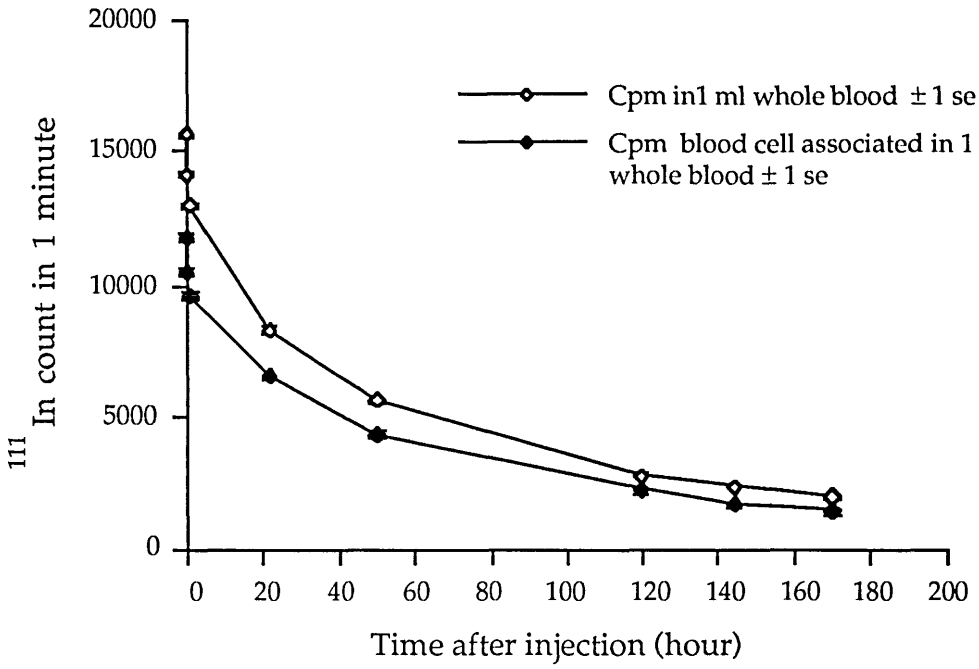

Similar findings were also noted in another patient (AM)[2] in whom deep vein thrombosis of the left leg was diagnosed clinically.

^{111}In radioactivity after ^{111}In P256 F(ab')$_2$ iv injection was found to be mostly cell associated[3]. The kinetics of ^{111}In P256 F(ab')$_2$ in blood, liver and spleen was found to be similar to that obtained with the whole antibody[4].

---

1 See Table A6.4, Appendix, page 311, for experimental details.

2 The experimental data and blood time activity curve on patient AM are shown in Table A6.5 and Figure A6.3, respectively, Appendix, page 312.

3 See Tables A6.4 and A6.5, Appendix, pp311 & 312 for experimental details.

4 See Figure A6.4, Appendix, page 313 for the kinetics of ^{111}In P256 F(ab')$_2$ in blood, liver and spleen studied in patient WM.

6.3.2 Delayed imaging

6.3.2.1 ^{111}In P256

Whole body distribution of radioactivity 24 and 48 hr after ^{111}In P256 injection in all patients imaged included intensive splenic uptake, low blood pool and low liver radioactivity (see figure 6.5).

Figure 6.5. Whole body image of the distribution of radioactivity 24 hr after the injection of ^{111}In P256 in patient GM. Posterior view showing intense uptake in the spleen (L) and relatively low uptake in the liver and blood pool (heart).

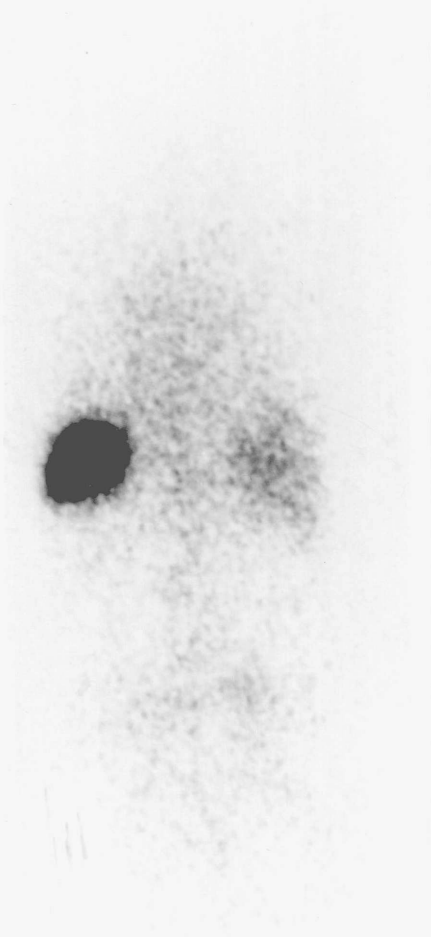

The uptake in various organs was assessed by drawing regions of interest around the selected organ on the anterior and posterior whole body images taken at various times after injection of the labelled antibody (1, 24 and 48 hr). The percentage uptake in each organ of the total present in the whole body was calculated for each view. Afterwards, the geometric mean of the anterior and posterior percentage uptake in each organ was taken as representative of the percentage uptake in that organ[1]. Accordingly, the spleen contained 30-40%, liver 10-15% and the blood pool 45-60% of the activity in whole body between 1 and 48 hr after antibody injection in patients GM and SH (see Table 6.2).

Table 6.2. Organ counts and percentage uptake in the spleen, liver and blood pool[a] in patients GM and SH at 1, 24 and 48 hr after injection of ^{111}In P256 taken from the anterior and posterior whole body scans[b].

	Ant ct	%total	Post ct	% total	% geometric mean
Patient GM					
Whole body					
1 hr	516260	100	568030	100	100
24 hr	362430	100	403750	100	100
Spleen					
1 hr	179140	34.7	228920	40.3	37.4
24 hr	116370	32.1	157060	38.9	35.3
Liver					
1 hr	65050	12.6	59080	10.4	11.4
24 hr	49730	13.7	41220	10.2	11.8
Patient SH					
Whole body					
48 hr	305270	100	347180	100	100
Spleen					
48 hr	108370	35.5	137830	39.7	37.5
Liver					
48 hr	47010	15.4	50690	14.6	15.0

a The percentage uptake in the blood pool was calculated by subtraction of the counts in liver and spleen from the whole body count.

b No abnormal uptake of radioactivity was observed in these patients.

1 This method assumed regular body geometry and uniform attenuation of γ rays throughout the body and therefore the values obtained were a rough estimate of the amounts actually present in each organ.

Three patients imaged 24 hr after injection of ^{111}In P256 showed abnormal localisation of radioactivity. In the first patient (HQ), two intense areas of radioactive uptake were seen in the right leg (above and below the knee). Contrast venograms of the same area showed a venous thrombus corresponding to the uptake seen on the scan (see Figure 6.6).

Figure 6.6. Positive uptake of radioactivity above and below the R knee (arrow) seen 24 hr after the injection of ^{111}In P256 in patient HQ of the anterior whole body scan (left panel) corresponding to the venous thrombus (arrow) seen on the venogram (right panel).

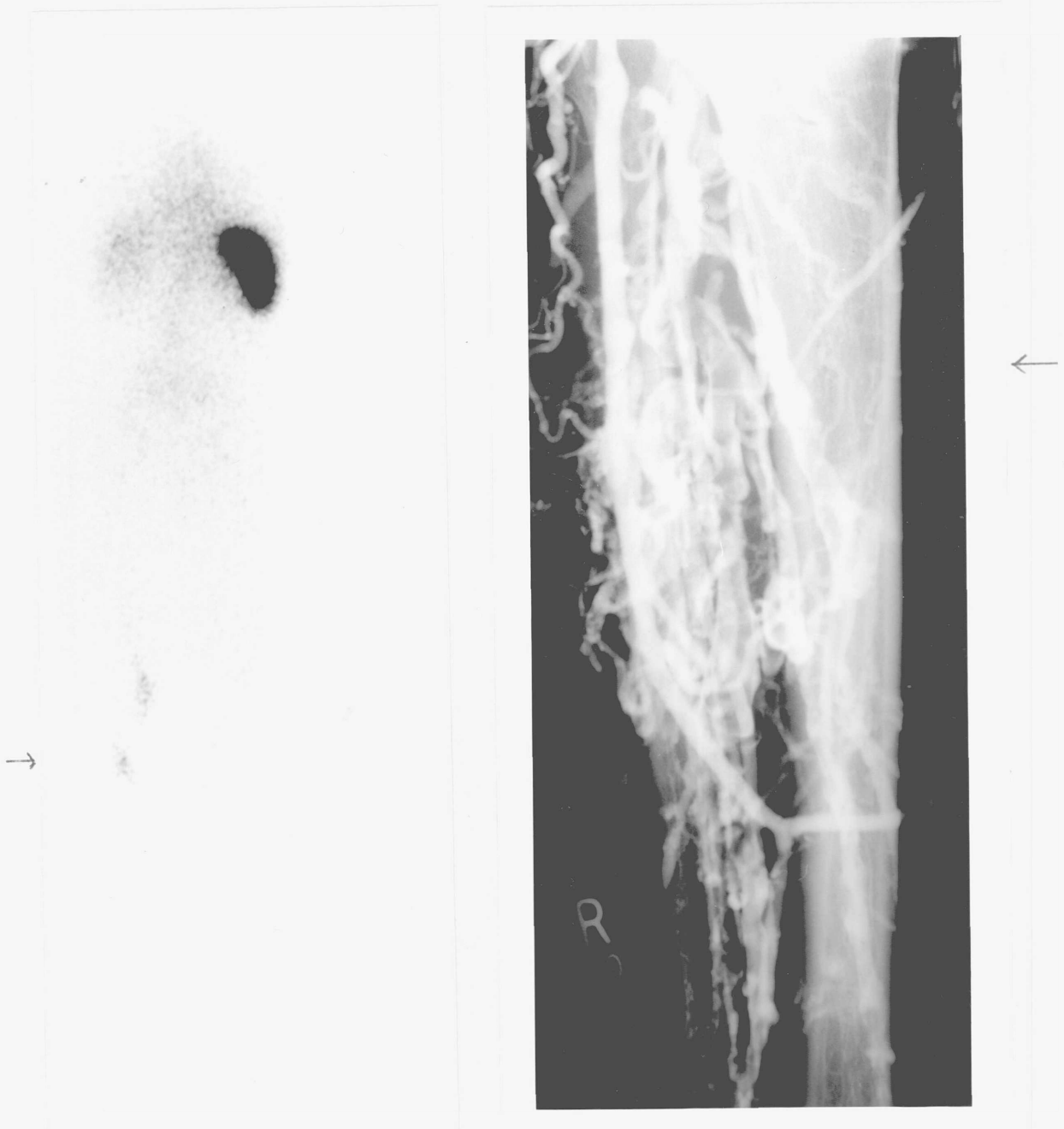

In the second patient (VH), intense positive uptake was seen in a thrombosed arteriovenous-access shunt previously used for haemodialysis in the management of the patient's chronic renal failure (see Figure 6.7). No other uptake was identified.

Figure 6.7. Posterior whole body scan of patient VH showing intense uptake of radioactivity in a thrombosed arteriovenous shunt in the right thigh (arrow).

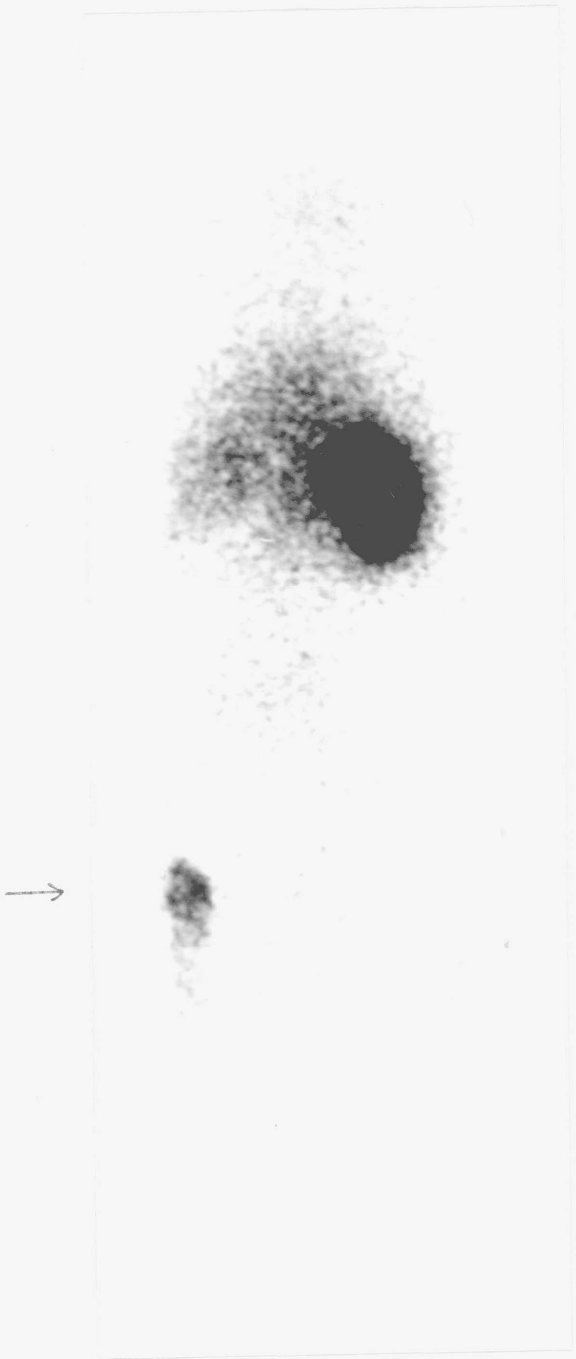

In the third patient (CC), localisation of activity was seen in the base of the neck, in the right axilla and in an intravenous line (Hickman line) put earlier in the subclavian vein. Venography of the right upper limb showed thrombus in the subclavian vein and the Hickman catheter. Scans in the rest of the patients (7 patients) were negative. This was in agreement with negative venograms in these patients. In the patient with leukaemia (JW), no abnormal localisation of radioactivity was noted after the injection of ^{111}In P256, but an enlarged spleen was depicted on the scan (Figure 6.8).

Figure 6.8. Anterior whole body scan of patient JW 24 hr after injection of ^{111}In P256 showing an enlarged spleen.

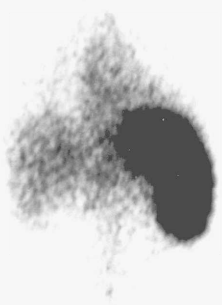

6.3.2.2 ^{111}In P256 F(ab')$_2$

The delayed (24 & 48 hr) whole body distribution of radioactivity in all patients studied resembled that obtained with the whole antibody, ie intense spleen uptake, low activity in blood pool and liver. The percentage uptake in spleen, liver and blood pool was similar to that obtained with the whole antibody.

Three patients imaged with this tracer showed positive uptake of radioactivity.

The first patient (ML) suspected of a left leg DVT showed three discrete areas of uptake one in the area of the left femoral vein and the other two in the area of the right femoral vein. Images taken at 4 days showed further accumulation of activity in these abnormal areas (Figure 6.9). The venogram of the left leg was, however, negative.

Figure 6.9. Uptake in areas of the left and right femoral veins after the injection of ^{111}In P256 F(ab')$_2$ in patient ML suspected of deep venous thrombosis. The venogram of the left leg was negative.

A) Anterior pelvis, 12 hr post Ab injection, abnormal uptake in R femoral vein (arrow). Note the high background in the iliac and femoral vessels.

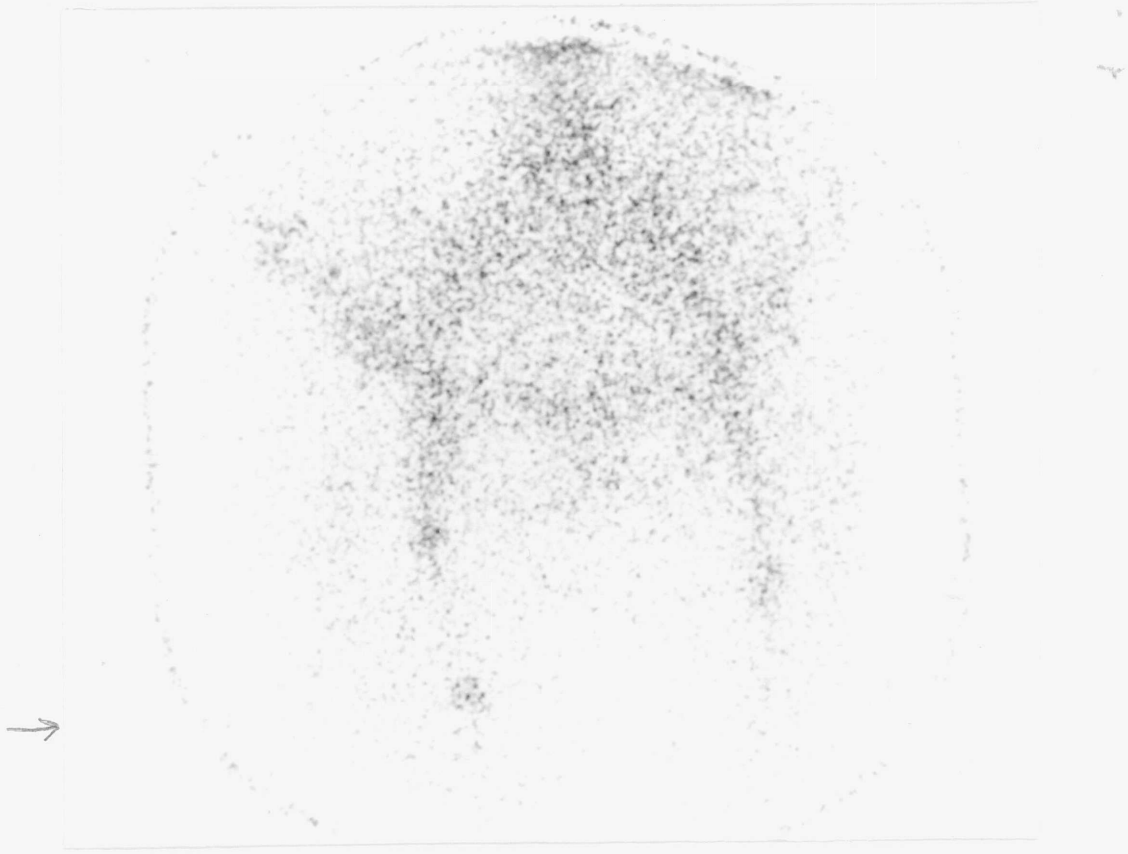

B) Ant pelvis at 24 hr PI showing two discrete areas of abnormal uptake in L & R femoral vein. Radioactivity in the blood pool is still noted.

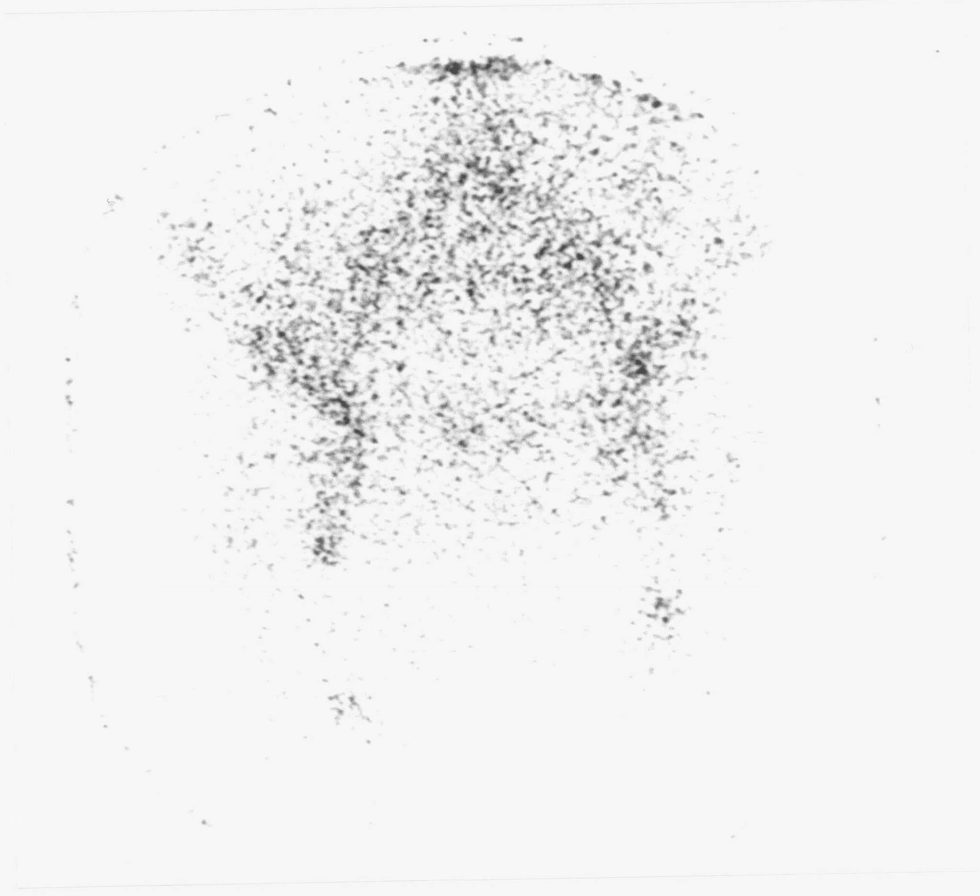

C) Ant pelvis 4 days PI showing 3 areas of abnormal accumulation of radioactivity. No background seen.

D) Negative venogram on the left leg.

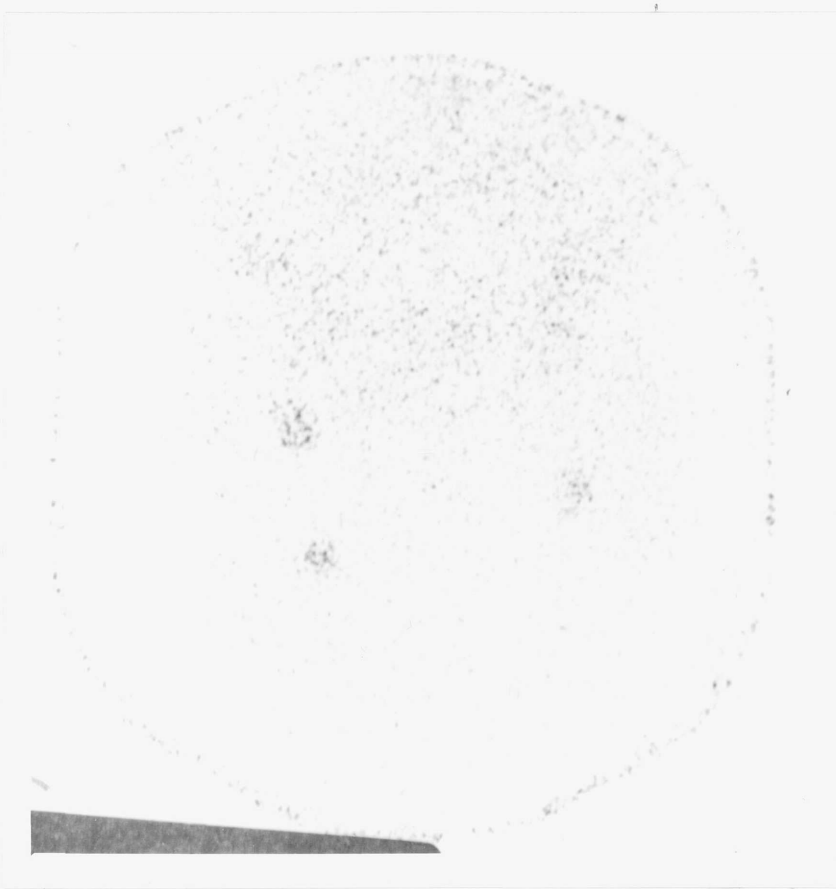


L

The second patient (MD), suspected of left leg DVT, showed increased activity in the upper left leg and two sites of increased activity in the line of the femoral vein.

The third patient (WC) suffering from narrowed carotid arteries showed increased uptake of ^{111}In activity in the lower abdominal aorta corresponding to a synthetic aorto-bifemoral graft put previously in that area (Stuttle et al 1988).

The other 5 patients showed no focal increase in uptake and their scans were considered negative.

6.3.3 Platelet counts before and after the injection of ^{111}In P256 or ^{111}InP256 F(ab')$_2$

In all patients, a platelet count was obtained immediately before the injection of the ^{111}In anti-platelet antibody. Monitoring of the platelet count followed after the injection of the antibody and no significant difference from pre-injection values was noted[1].

[1] See Table A6.4 for comparison of platelet counts before and after ^{111}In P256 or ^{111}In P256 F(ab')$_2$ injection, Appendix, page 313.

6.4. Analysis & Discussion :

6.4.1 Antibody dose and radioactivity

Based on the results of the radioimmunoassays and aggregation studies described in Chapter 5, a dose of 100 μg of Ab per patient was used. The starting point in the calculation of the dose was in deciding upon the number of Ab molecules to be injected per platelet without causing aggregation. A concentration of 500 Ab molecules per platelet corresponding approximately to 1% of the total number of GPIIb/IIIa on the platelet surface[1] was taken as the basis for dose calculation. This number was multiplied by the total number of circulating platelets[2] to obtain the dose (number of platelets/l known from the blood count and total blood volume calculated from a nomograph after measuring the weight and height of the individual, Hurley 1975) . The amount of radioactivity associated with 100 μg antibody used for scintillation camera imaging ranged between 7.4-10 MBq (200-300 μCi).

6.4.2 Kinetics of ^{111}In P256 or ^{111}In P256 F(ab')$_2$

The shape and time span of the blood clearance curve and the finding that most blood radioactivity was cell associated after the intravenous injection of ^{111}In P256 or ^{111}In P256 F(ab')$_2$ prompted a comparison of the ^{111}In Ab data with those obtained after the injection of ^{111}In oxine/tropolone labelled platelets; the standard method for platelet kinetic studies (ICSH 1988).

Firstly, recoverable blood radioactivity 30 min after injection of labelled antibody amounted to 77% of that measured at 5 min for ^{111}In P256 in the

---

1 The number of GPIIb/IIIa on the platelet surface was reported by many authors (Pidard et al 1983, Lombardo et al 1985, Ruggeri 1986). This number ranged between 20000-100000 per platelet; average 50000.

2 The platelet population in the splenic pool amounting normally to 30% of the total platelet pool was not included in the calculation. Circulating platelet number ≈ $1.25X10^{12}$ptlt.

normal volunteer (JPL) and in patient CN. In the case of ^{111}In P256 F(ab')$_2$, it was 83% of the value at 10 min in patient JC. In comparison, recovery of radioactivity in blood had been reported to be 60% approximately after the injection of ^{111}In oxine/tropolone labelled platelets[1].

Secondly, the shape of the blood time activity curve was similar in both methods showing a slow decrease in blood count-rate over 4-5 days. However, the time span of blood radioactivity after ^{111}In P256 injection was significantly shorter than that usually found using ^{111}In oxine labelled platelets in normal conditions (100-200 hr vs 2400 hrs).

Thirdly and from the dynamic studies using the scintillation camera computer system, the spleen was the main organ to accumulate radioactivity after injection of ^{111}In P256. Peak uptake was reached at about 30 minutes post-injection. Moreover, splenic uptake was paralleled by a decrease in the signal from blood pool; a picture similar to that obtained after ^{111}In oxine/tropolone platelet injection.

Thus, taking the above considerations into account and referring to previously reported kinetics of intravenously-injected ^{111}In-labelled murine McAbs in man (Pimm et al 1985, Hnatowich et al 1985, Rosenblum et al 1985, Eger et al 1987), the shape of the time activity curve can be related to three independent, although simultaneously acting events :

1) The kinetics of ^{111}In McAb itself in the circulation regardless of its specificity such as accumulation in liver, kidney and metabolism in peripheral tissues. The pattern of antibody clearance follows roughly a compartmental model and a half-life of 30 hr approximately in blood. This factor would affect the non-cell bound fraction of antibody in the circulation.

---

1 Assuming normal platelet splenic pool.

2) The kinetics of the ^{111}In P256-platelet entity, which is related in turn to the survival of the platelets and any effect of antibody binding to platelets may have on this survival.

3) The kinetics of the ^{111}In McAb vis a` vis its antigen present on the platelet surface. This would include the affinity of Ab binding to its antigen, degradation of the Ag-Ab complex on the surface and internalisation or shedding of the immune complex in the circulation.

In all, blood clearance of radioactivity after iv injection of ^{111}In P256 can be described as shown in figure 6.10.

Figure 6.10. Body distribution of ^{111}In P256 after injection intravenously.

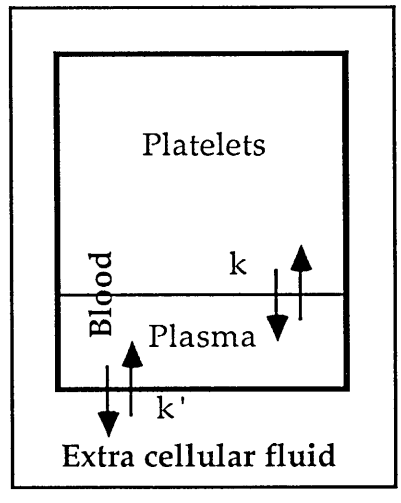

k : Binding constant of ^{111}In P256 to platelets and turnover rate of antibody on the platelet surface (see text).
k': Rate of exchange of ^{111}In P256 between blood and the extracellular fluid and rate of antibody loss in peripheral tissues.

^{111}In P256 distributes in a closed space comprising blood volume in the early period after antibody injection and both blood and extracellular fluid at a later stage. At every time point this large space is subdivided into two parts : the cell mass including all platelets and the plasma. Antibody distribution between the two parts (bound and free), assuming even mixing of the

antibody in the circulation (including liver and spleen parenchyma), will depend on the concentration of antibody and antigen, and the binding constant of the antibody to its antigen. In the conditions of reaction used, where antigen concentration exceeds that of the antibody by 100 fold, the Ag-Ab reaction is driven to completion (shift to the right). Therefore, the continuous presence of cell bound radioactivity in the circulation will depend mainly on the life-span of the intact Ab-platelet complex in the blood and spleen. Since platelets have a finite life-span, then this would be the major factor in determining the shape of blood time-activity curve after injection of ^{111}In P256. This is true provided the antibody does not cause any change in platelet life-span, undergo degradation itself or get shed from the platelet surface before the final removal of the platelet-Ab complex from the circulation (no Ab reutilisation). Events leading to loss, inactivation or degradation of the antibody from the surface of circulating platelets or the premature clearance of platelets from the circulation result in a shortened life-span of the platelet-Ab bound radioactivity as compared to the actual life-span of platelets and produce a different shape of the time-activity curve form the normal platelet survival curve.

All subjects studied using ^{111}In P256 or ^{111}In P256 F(ab')$_2$ showed shortened life-span of radioactivity as compared to standard ^{111}In oxine/tropolone platelets (normal : 9-10 days). In five studies, good fit of the time activity curves was obtained using exponential functions (Figure 6.11). In Table 6.3, the details of each curve and the corresponding exponential as well as linear curve fits are shown.

Figure 6.11. Exponential function fit to blood ^{111}In P256 and ^{111}In P256 F(ab')$_2$ radioactivity versus time data.

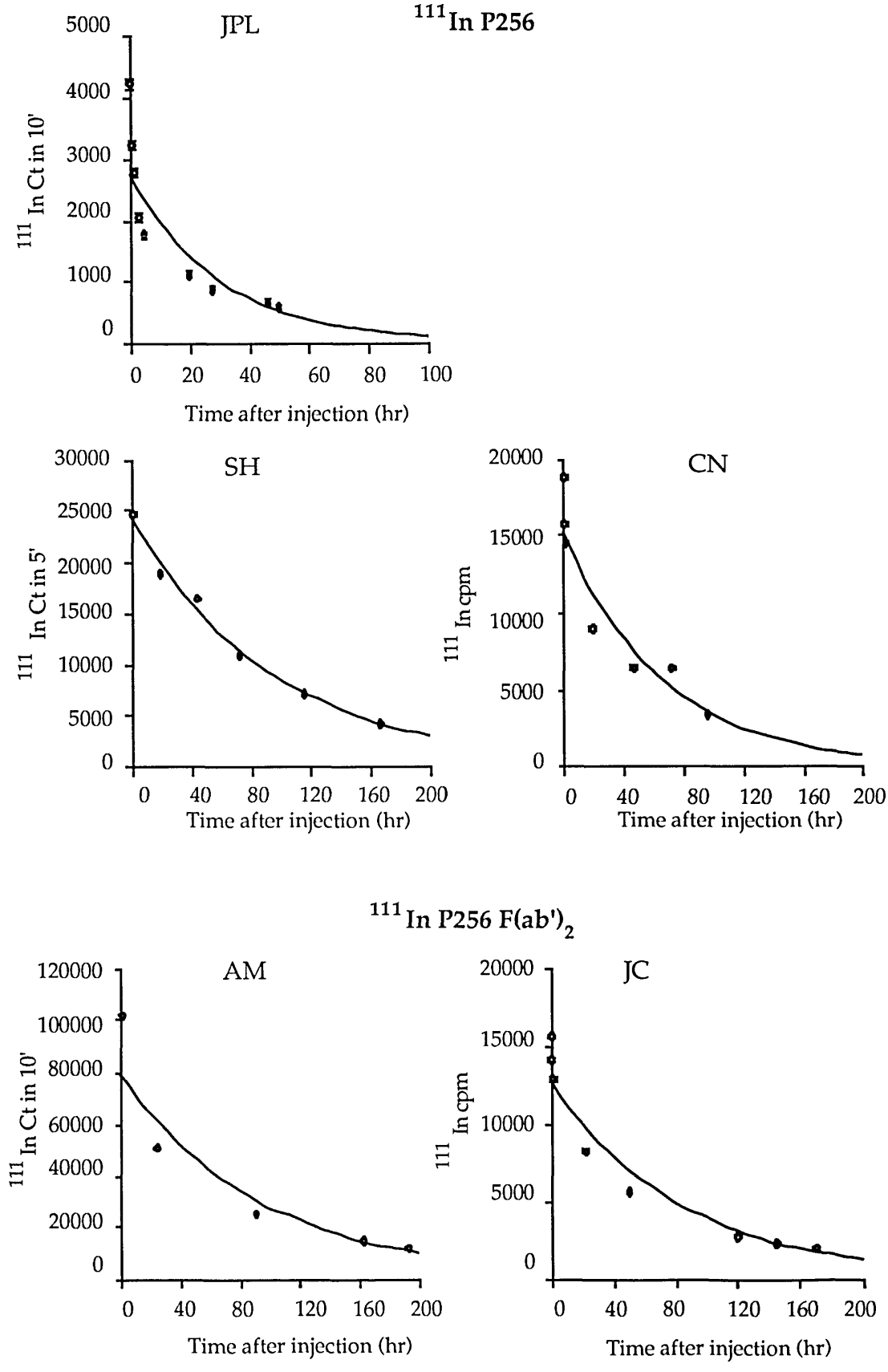

Table 6.3. Exponential and linear fit functions for blood radioactivity data after ^{111}In P256 or ^{111}In P256 F(ab')$_2$ injection.

Subject	Exponential data fit equation	$T_{1/2}$ (hr)	R^2	Linear data fit equation	$T_{1/2}$ (hr)	R^2
JPL[a]						
-WB[c]	$y=2745e^{-0.03x}$	21	0.88	y=2812-52x	26.9	0.68
-CAA[d]	$y=2205e^{-0.04x}$	15.8	0.89	y=2290-48x	24	0.63
SH[a]						
-WB	$y=24373e^{-0.01x}$	63	1.00	y=22011-119x	92.4	0.93
-CAA	$y=18885e^{-0.01x}$	63	1.00	y=16878-92x	91.8	0.95
CN[a]						
-WB	$y=15239e^{-0.02x}$	46.2	0.92	y=15151-135x	56.2	0.82
-CAA	$y=11566e^{-0.01x}$	49.5	0.85	y=11672-99x	58.8	0.75
JC[b]						
-WB	$y=12691e^{-0.01x}$	57.8	0.97	y=12564-73x	86.1	0.84
-CAA	$y=9655e^{-0.01x}$	57.8	0.98	y=9464-55x	85.9	0.86
AM[b]						
-WB	$y=79081e^{-0.01x}$	63	0.96	y=77981-396x	98.4	0.76
-CAA	$y=49454e^{-0.01x}$	77	0.98	y=47211-225x	105.1	0.87

a ^{111}In P256
b ^{111}In P256 F(ab')$_2$
c WB : whole blood.
d CAA : cell associated activity.

For each time activity curve, the closeness of the fit using the exponential or the linear function can be judged by the value of R^2 (coefficient of determination) which denotes the percentage of the variation in the data that can be explained by the curve. Accordingly, the exponential curve fit has been adopted as the best model for describing the observed kinetics. The half-life of blood radioactivity (whole blood or cell associated) has been calculated for each case; average[1] 57.5 hr, and the corresponding mean life 83 hr (3.5 days).

1 Data from the normal volunteer were not included due to inadequate delayed sampling.

It is clear from Table 6.3 that in vivo use of ^{111}In P256 or ^{111}In P256 F(ab')$_2$, in the way described, has led to a peculiar pattern of blood radioactivity. Although platelet labelling is evident, the kinetics of blood and cell associated radioactivity have diverged from that obtained with in vitro ^{111}In oxine/tropolone labelled platelets. It is not clear, however, whether the short life-span of blood radioactivity after ^{111}In McAb use be due to random removal of platelets coated with Ab from the circulation or to gradual loss of the Ab from platelet surface by mechanisms related to protein turnover or degradation in vivo. The former possibility is more likely, based on the fact that anti-platelet antibodies are known to cause platelet immune mediated destruction such as that seen in ITP, where platelet kinetic studies using in vitro labelled platelets show drastically shortened platelet survival and an exponential time activity curve of blood clearance. In the case of ^{111}In-P256-platelet labelling, however, the shortening of platelet life span is less marked than that usually observed in ITP. In addition, the platelet counts obtained before and after ^{111}In P256 injection do not show significant alteration of platelet numbers (see Table A6.6, Appendix, page 313) pointing to effective compensation of any possible loss of platelets due to antibody binding and reticuloendothelial system clearance.

Thus, the question of the shape and time span of the blood radioactivity clearance after the injection of ^{111}In McAb remains unresolved. More studies are required to substantiate the observations obtained so far. Also, the use of platelet dual labelling techniques such as sodium ^{51}chromate in vitro and ^{111}In McAb in vivo would enable the follow-up of in vitro labelled platelets (^{51}Cr) that had bound ^{111}In McAb in vivo and subsequently establish their fate.

6.4.3 Thrombus imaging using ^{111}In P256 or ^{111}In P256 F(ab')$_2$

Whole body images taken 1-72 hr after the injection of ^{111}In P256 or ^{111}In P256 F(ab')$_2$ gave a mapping of platelet distribution similar to that obtained using ^{111}In oxine/tropolone labelled platelets, ie high uptake in the spleen, lower uptake in liver and activity in the blood pool. These images indicated the efficiency of ^{111}In P256 or ^{111}In P256 F(ab')$_2$ in radiolabelling platelets in vivo. In some patients, the use of the radiolabelled antiplatelet antibody enabled to localise clinically suspected thrombus. In two patients (HQ & CC), the findings were corroborated by positive venograms showing thrombus in the same area seen on the scan. There were also areas localised by scintillation camera imaging which did not show on the venogram. This pointed to the value of the method in detecting sites of on-going platelet localisation, ie active thrombus formation which would be most important for the institution of anticoagulant therapy. Uptake was more pronounced as delayed images of the affected area were taken indicating most probably deposition of more platelets bearing the ^{111}In McAb in the thrombus.

In addition, positive uptake was seen in prosthetic vascular grafts which had been known to attract platelet deposition and thrombosis.

These findings were in agreement with data from experimental work in dogs involving the use of other antiplatelet monoclonal antibodies or antibody fragments radiolabelled with ^{123}I, ^{111}In or ^{99m}Tc (Oster et al 1985, Som et al 1986).

Using the ^{111}In McAb method, areas not easily accessible to conventional venography such as the pelvis and neck could be investigated for thrombus formation. Furthermore, thrombus in arteries, heart and main vessels could be amenable to investigation using the new technique without recourse to complicated and rather invasive procedures.

A more detailed study including more patients is necessary, however, to establish the clinical usefulness of the labelled antibody application in terms of sensitivity, specificity and accuracy in detecting thrombus even though early indications show promise for its application in this area[1].

6.4.4 Dosimetry of ^{111}In P256 or ^{111}In P256 F(ab')$_2$

Radiation dosimetry of ^{111}In labelled anti-platelet McAb was studied both at the cellular (single platelet) and whole body level.

Maximum radioactivity per platelet assuming even distribution of ^{111}In McAb[2] among the platelet population in blood and spleen was calculated to be in the order of $4X10^{-6}$ Bq[3]. This was very much lower than radioactivity associated with ^{111}In oxine/tropolone labelled platelets ($5X10^{-4}$Bq/ptlt).

Furthermore, the platelet being a cell devoid of a nucleus makes damage to DNA, that potentially leads to mutation and malignancy, unlikely to occur using ^{111}In labelling of these cells although damage to the cytoplasm will still be a factor to consider.

Whole body dosimetry using the kinetics and distribution of ^{111}In McAb radioactivity presented above[4] (see page 84), showed that the spleen was the target organ. Localisation in the spleen was calculated to be 30-40% of the radioactivity in the whole body, which reflected the proportion of platelets normally present in that organ. The amount of radioactivity in the spleen, after an initial increase up to 30 min post ^{111}In McAb injection was assumed to follow closely the kinetics of blood radioactivity (exponential decrease

---

1 It is worth mentioning that Amersham International plc has adopted development and further testing of P256 antibody for the diagnosis of thrombus in man.

2 Amount of radioactivity used per patient 7.5-10 MBq (200-300 μCi) ^{111}In.

3 This amount was simply calculated by supposing a freely exchangeable pool of blood and splenic ^{111}In McAb, a consideration of the number of platelets in blood and spleen ($1.75X10^{12}$ ptlt) and cell binding ratio of 75%.

4 Early and delayed imaging of whole body using the scintillation camera.

$T_{1/2b}$ 60 hr). The effective half-life in the spleen was therefore $T_{1/2\ eff}$ 45 hr and the maximum dose expected from a dose of 10 MBq (≈ 300 μCi) of ^{111}In McAb would be 37 mGy. Radiation doses to other organs were also calculated. The liver was found to contain 10% of the injected activity which gave a radiation dose of 1.7 mGy[1] and the bone marrow dose was assumed to come mainly from blood radioactivity (20% of the injected dose) amounting to 2.3 mGy[1]. The effective dose equivalent was calculated to be 3 mSv (Snyder et al 1975). These doses compared favourably with doses caused by the use of ^{111}In oxine/tropolone labelled platelets (see Table 2.2, page 34).

---

1 Same $T_{1/2eff}$ was assumed for radioactivity in liver and bone marrow.

Section Three :

^{111}In Anti-Lymphocyte Monoclonal Antibodies, in Vitro and in Vivo Tests.

Chapter 7 :
Lymphocyte Physiology

7.1 Lymphocyte origin and circulation :

In the domain of lymphocyte physiology there have been many controversies concerning lymphocyte origin and fate. Until the mid 1950s, lymphoid organs, especially the lymphoid tissues of the gut, and lymph nodes associated with the gastrointestinal tract, were thought to be the major sites of lymphopoeisis. Once generated, lymphocytes are released in efferent lymph, they then join the blood stream and subsequently enter different tissues of the body where they end a short life cycle. These concepts were based on experimental data obtained mainly by cannulation of various lymphatic vessels and analysis of collected lymph in terms of output of lymphocytes and type of cells present (Yoffey and Courtice 1956). However, experimental findings on the long life-span of lymphocytes (Ottesen 1954) and the confirmation of lymphocyte recirculation from blood to lymph (Gowans 1959) came to rectify these postulates and to add new insights into the functional role of these cells.

The outlines of the major physiologic pathways that lymphocytes followed in the body were laid down soon afterwards as discoveries concerning the functions of the thymus (Miller 1961a & b) and the bursa of Fabricius (Kincade and Cooper 1971), were added to the body of information on lymphocyte circulation and localisation. A schematic representation in Figure 7.1, drawn by Micklem et al 1966, summarised the knowledge of that subject at the close of the Sixties.

Figure 7.1. Diagram of cell migration pathways in the lymphomyeloid complex as envisaged by Micklem et al 1966. The broken lines are putative lymphocyte migratory pathways.

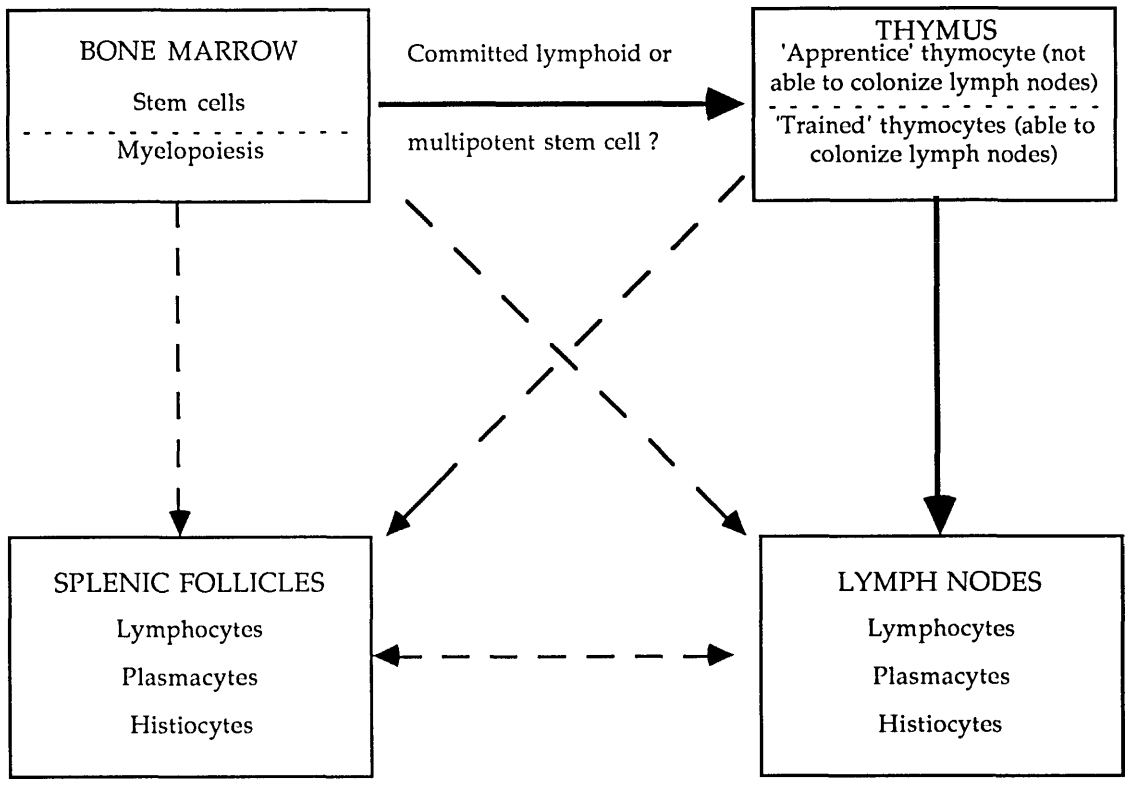

7.2 Lymphocyte subsets and specific microenvironments for lymphocyte interaction :

Observations on lymphocyte involvement in reactive events have indicated the presence of two main functional subsets of lymphocytes called T and B cells.

Lymphocytes, depending on their origin, thymus derived or not, have been found to localise into distinctive areas in lymph nodes and spleen in what is known as segregation of thymus dependent and non-thymus dependent lymphocytes (Parrott et al 1966). This segregation is thought to have an important bearing on the way cells such as lymphocytes, dendritic cells and

macrophages interact with each other, and in providing micro-environments for these interactions (Parrott and de Sousa 1971).

7.3 Lymphocyte kinetics in pathology :

Central to their physiology, lymphocytes mount immune responses to challenges by foreign (non-self) substances. The outcome of these reactions depends on a multitude of factors. Some of them are related to the type and nature of the antigen triggering the response, and others relate to the host in which the reaction occurs. Conventionally, immune responses have been studied under two main categories :

The first is the so called humoral response in which antibodies directed to the antigen are produced. The second, namely, the cellular response encompasses events that involve lymphocytes interacting directly with antigen (cytotoxicity, delayed type hypersensitivity reactions, etc).

Generally, research into the progression and establishment of immune responses has relied heavily on in-vitro tests, which have recently provided insight into the minutiae of cellular involvement in each type of response studied. Major discoveries in this field include, among others, the role of the dendritic cell and the macrophage in antigen presentation (Fishman 1961), lymphokine secretion and effects (Isaacs and Lindemann 1957, Bloom and Bennett 1966), and the condition of major histocompatibility complex restriction in lymphocyte interactions (Zinkernagel and Doherty 1975).

In contrast to in-vitro experimentation, research into the kinetics of various lymphocytes and other blood cells in vivo during the development of immune responses has been limited to a relatively small number of experimental studies in animals and a few observations in man.

It is presently known that lymphocytes distribute randomly in lymphoid tissues according to regional blood flow, or fraction of cardiac output, that supplies each organ (Ottaway and Parrott 1979). This random distribution is generally associated with a non-selective migration or localisation of lymphocyte populations, mainly small lymphocytes, in lymphoid tissues or reactive sites (Parrott and Wilkinson 1981). However in a few cases, increased localisation of lymphoblasts has been found in reactive sites and thought to be related to the presence of specific antigen (Asherson and Allwood 1972, MacGregor and Logie 1974, Ottaway and Parrott 1979). In other situations, non-random migration of large lymphoblasts has been related to the source of cells studied. Lymphoblasts from mesenteric lymph nodes or thoracic duct lymph share a marked preferential accumulation in lymphoid tissue within or adjacent to the intestine, whereas cells from peripheral nodes accumulated preferentially in peripheral lymph nodes (Griscelli et al 1969, Guy-Grand et al 1974, Parrott and Fergusson 1974, Rose et al 1976, Hall et al 1977). Recently, more evidence has been emerging on non-random migration of lymphocyte subpopulations to lymphoid tissues associated with different organs such as intestines and skin (Chin and Hay 1980, Reynolds et al 1982), or after specific immunisation (Baine et al 1981, Drayson 1986). However, more studies are still needed to establish the exact patterns of migration attributable to each lymphocyte subpopulation.

The kinetics of lymphocytes in malignancies affecting the immune system, ie lymphomas, Hodgkin's disease and certain leukaemias, is another subject of interest in the field of lymphocyte migration in pathology (Crowther et al 1969, Spivak and Perry 1970, Zatz et al 1974, Warnke et al 1979). Observations on lymphoma spread and the propensity of many of its types to affect certain organs such as T cell lymphoma of the skin and lymphoma of the small bowel have suggested that malignant cells may follow to a great extent the migratory pattern of their normal counterparts (T & B cells,

immunoblasts, etc) (Strykmans et al 1977, Miller et al 1980, Crowther and Wagstaff 1983).

These observations have been supported by limited research work involving mainly radiolabelled (^{3}H, ^{51}Cr or ^{111}In) circulating lymphocytes from patients with Sezary syndrome or B-chronic-lymphocytic leukaemia (Strykmans et al 1968, Hersey 1971, Bremer et al 1973a & b, Flad et al 1973, Scott et al 1973, Engeset et al 1974, Wagstaff 1981a, b & c).

7.4 Experimental and clinical studies using radiolabelled lymphocytes :

Research into lymphocyte-in-vivo physiology has benefited to a great extent from the application of radionuclides for labelling these cells.

Early experimentation in this field has employed β emitters and many examples of this application are found in the literature (Gowans 1959, Ottesen 1954, Everett 1960, Bremer et al 1973a)

More recently, quantitation and mapping of the distribution of the radiolabelled lymphocytes have relied on the use of γ-ray emitters.

Chromium-51 chromate has been used extensively to label lymphocytes in experimental studies and, to a lesser extent, clinically in man. Smith and Ford (1983) gave a multi-aspect account of in-vivo lymphocyte physiology in the rat using ^{51}Cr-labelled thoracic duct lymphocytes. After iv injection of ^{51}Cr labelled lymphocytes (the cells were passaged from blood to lymph in intermediate animals prior to injection), the immediate distribution of radioactivity was in the lungs, blood and liver. Rapid localisation of radioactivity followed in the spleen, lymph nodes and Peyer's patches, and increased steadily with time as the radioactivity in the lungs, blood and liver declined. The tempo of recirculation from blood to lymph was also determined. The labelled cells peaked in thoracic-duct lymph between 8 and

15 hr after injection, the average transit time from blood to lymph was 12 hr and the cell recovery in lymph was 40% in the 24 hr period after injection.

Hersey (1971) injected sodium ^{51}chromate-labelled autologous lymphocytes purified by sedimentation and density gradient centrifugation of blood in man. Using blood sampling, urine collection and external surface probe counting at set times after injection of the labelled cells, he followed their kinetics in normal volunteers and patients with chronic lymphatic leukaemia (CLL). Clearance of radioactivity from blood followed a bi-exponential pattern $T_{1/2}$ (1) : 15 min, $T_{1/2}$ (2) : 7 hr. The percentage of labelled cells remaining in the circulation 4 hours after injection was 2% in normals and 20% in patients with CLL. Surface counting showed maximum uptake in the spleen at 2-3 hr after injection (6-8 % of injected radioactivity), at 30 min in the liver (2%) and at a later time beyond 4 hr over the iliac crest (representing bone marrow). In leukaemia patients, early bone marrow uptake was absent and a delayed peak was seen at 24-48 hr.

A more detailed study in humans was reported by Scott et al (1972 & 1973). These authors were able to demonstrate by careful analysis of cell kinetic data obtained with ^{51}Cr labelled leucocytes or lymphocytes, patterns of blood clearance, as well as splenic and bone marrow uptake, which were compatible with lymphocyte recirculation observed previously in experimental animals. The recirculating lymphocyte pool was calculated to be 23 $X10^9$ cells having a turnover through blood of 12 times/day. Mean lymphocyte life-span was found to be 18 days. In CLL patients, the blood clearance of CLL cells was slower than normal and equilibrium with the marrow pool was delayed and became complete only after 24-72 hr. A mean $T_{1/2}$ of 3.8 days in blood was found for the labelled cells in CLL.

Bazerbashi et al (1978) also studied the kinetics of ^{51}Cr-labelled lymphocytes in patients with chronic lymphocytic leukaemia. They showed that

leukaemic lymphocytes left the circulation for the tissues less rapidly than lymphocytes in normal individuals. However, the average number of cells transferred per day was of the same order of magnitude as normal because of the higher circulating lymphocyte count. They speculated that blood and lymph nodes might accumulate lymphocytes in response to a transport defect, which hindered the progress of these cells from one pool to another.

The introduction of the ^{111}In lipophilic chelating agent oxine for leucocyte labelling in 1976 (McAfee and Thakur 1976a) gave researchers a more suitable lymphocyte labelling method and a great advantage over the use of ^{51}Cr in enabling imaging of the labelled-cells with the scintillation camera.

An experimental study in the rat (Rannie et al 1977) comparing different lymphocyte radiolabelling agents including ^{51}Cr, ^{99m}Tc and ^{111}In, concluded that ^{111}In oxine was the most promising agent, among labelling agents available at the time, for the study of lymphocyte migration and in imaging the distribution of the labelled cells using a scintillation camera. Frost et al (1979) succeeded in imaging lymph nodes in various parts of the body of sheep injected with ^{111}In-oxine-labelled lymphocytes. They postulated that labelling with ^{111}In oxine would provide a means for imaging lymphoid tissue in man and following the migration of lymphocyte populations into lymphoid and non-lymphoid tissues in a variety of pathological conditions.

In man, Lavender and co-workers (1977) used ^{111}In oxine lymphocytes in two normal subjects and two patients with Hodgkin's disease. They showed localisation of the labelled cells during the first four hours after injection in the spleen, liver and bone marrow. After 19-26 hours, uptake of radioactivity could be observed in cervical, external iliac and inguinal lymph nodes as well as mediastinal and hilar lymph nodes in the patients with Hodgkin's disease. Blood radioactivity in two subjects dropped to 50%

the starting value shortly after injection and 25% was left at 12 hrs, then there was a 10 % rise in activity followed by further much slower clearance.

Wagstaff and co-workers (1981a, b & c) employed a rather complicated technique by elutriation of lymphocytes in great numbers in order to get 200-450 μCi (7.4-17 MBq) of ^{111}In radioactivity on the cells. They reported successful imaging of lymphoid organs and cell kinetics in two normal volunteers that were similar to those observed in the experimental animal. Patients with lymphoid leukaemia, lymphoma, Hodgkin's disease and osteogenic sarcoma were also studied, and it was possible to localise areas of tumour involvement as well as identify abnormal lymphocyte kinetics in some of them. For example, ^{111}In labelled lymphocytes in CLL patients cleared from the circulation without any sign of reappearance therein (in normals, reentry of the cells to blood after initial transit in the spleen would cause a late blood-radioactivity peak). Lymph node localisation was less well defined in CLL patients than in normals and the uptake in bone marrow appeared to be higher in those patients. The authors explained this pattern as reflecting the migratory behaviour of the type of lymphocytes labelled in CLL which was mainly B cells, while in normals, T cells were the majority in the labelled lymphocyte population collected from blood (70%) and thus their kinetics were recorded primarily in such studies.

Employing a similar lymphocyte-labelling method by automated apheresis, Read et al (1990) reproduced earlier findings by Wagstaff et al (1981a, b & c) and pointed to the potentiality of ^{111}In-oxine-labelled-human lymphocytes in studying normal and abnormal lymphocyte traffic.

Other authors (Goodwin et al 1981a, Milgram and Goodwin 1985) reported uptake of radioactivity in chronic osteomyelitis, rheumatoid arthritis and cystitis after injection of ^{111}In oxine lymphocytes. However, the sensitivity of the method in detecting these lesions was low in the order of 50%.

7.5 Radiolabelling lymphocyte subsets :

Mariano Garcia et al (1988) studied the localisation of rat lymphocytes prepared from different organs and labelled with ^{111}In tropolone. They found similar pattern of distribution using labelled peripheral blood lymphocytes or T-enriched-splenic cells (collected by running spleen cells on a nylon-wool column). Localisation was observed in lymph nodes and spleen at 24 hr, while labelled splenic cells (unfractionated) showed a different pattern by localising mainly in liver and spleen, and relatively less in lymph nodes. Thymus cells failed completely to migrate and localised in the liver. No mention was made, however, of any morphological identification of the labelled cells, ie surface markers or rosetting properties.

Attempts in the direction of effector lymphocyte radiolabelling have been reported recently in conjunction with the use of lymphokine-activated lymphocytes (lymphokine activated killers; LAK cells) for the immunotargeting of tumours (Rosenberg 1985). Immediately after intravenous injection, ^{51}Cr or ^{111}In oxine labelled LAK cells localised mainly in the lung. Progressive localisation in the liver followed and little or no localisation in the tumour site was seen (Lotze 1980). Mitogen (phytohaemagglutinin; PHA) stimulated lymphocytes (PAK cells) have also been tried for immunotherapy (Mazumder et al 1984). The localisation pattern of these cells was studied by following their distribution after ^{111}In oxine labelling and was found to be in liver, spleen and lungs. In a tumour mass in one thigh, day-one count rate increased by only a factor of 2 by day 8 after infusion of the cells. The use of tumour infiltrating lymphocytes (TIL) after expansion in vitro with interleukin-2 and mitogen (PHA) was also tested (Rosenberg et al 1986). ^{111}In oxine TIL (Kradin et al 1987) were found to localise mainly in the lung, liver and spleen. Areas of metastatic involvement did not accumulate, however, any radioactivity.

Chapter 8 :

In Vitro Tests and in Vivo Use of an ^{111}In Anti-T Lymphocyte Monoclonal Antibody in the Rat

A Model for Cell Binding, Antigen Modulation, Lymph Node Scanning and Radiation Dosimetry of in Vivo Injected ^{111}In Anti-T Cell McAbs

8.1 Introduction :

Two strategies can be used to image lymphoid tissue with radionuclides[1]. In the first, lymphocytes or leucocytes are labelled in vitro with a suitable radionuclide before reinjection into the autologous recipient. In the second, and more recently, monoclonal antibodies with specificity for cell surface molecules on lymphocytes or on lymphocyte subpopulations have been radiolabelled and infused into recipients.

Studies using indium-111 labelled lymphocytes (Lavender et al 1977, Wagstaff et al 1981a, b & c) have been limited by the extreme radiosensitivity of this cell type (Anderson et al 1974, Sprent et al 1974, Chisholm et al 1979, Sprent 1985). In order to obtain satisfactory external images of lymphoid tissues without exceeding the limits imposed by this radiosensitivity, it has been necessary to isolate large numbers of cells for labelling and this is not generally practicable. Although the exact mechanism by which radiation damage is inflicted on lymphocytes by indium-111 is not known, it is likely that a major cause of damage is the release within the labelled cells of the short range Auger electrons associated with radionuclide decay (Silvester and Waters 1983). If so, then the alternative strategy of using indium-111 labelled antibodies directed only at the cell surface should reduce the likelihood of radiation damage.

---

1 Lymph node scanning using radioactive nanocolloids is not considered here. Only methods employing specific cell radiolabelling techniques are discussed.

Furthermore, the specificity of radionuclide binding in vivo using labelled antibodies is dictated by the specificity of the antibody itself; this strategy has therefore the additional practical advantage of not requiring in vitro preparation and purification of the target cells before labelling.

In the experiments described below, a rat model has been used to analyse in vivo labelling of T lymphocytes with an indium-111 labelled monoclonal antibody MRC OX-19 (Dallman et al 1984) which reacts with a cell surface molecule analogous to the CD5 glycoprotein of human T cells. In vivo distribution of indium-111 labelled antibody has been tested by indirect immunofluorescence analysis of cells obtained from a variety of lymphoid tissues, by counting tissues for indium-111 and by scintillation camera imaging. ^{111}In McAb distribution has also been compared to ^{111}In labelled lymphocytes by scintillation camera imaging and tissue counting. Finally, an estimation of the radiation dosimetry involved for the use of a similar application in man is presented.

8.2 Materials and Methods :

8.2.1 Animals

Adult Wistar rats bred in closed colonies[1] were used as recipients of unlabelled or ^{111}In-labelled monoclonal antibodies. AO (RT1^{u}) inbred rats[2] were used as donors of lymphocytes for ^{111}In labelling in vitro and as recipients of the labelled cells.

BALB/c mice[2] were used for immune-ascites production.

---

1 RPMS Biological Services Unit and King's College Zoology Dept.
2 Harlan-Olac, England.

8.2.2 Monoclonal antibodies

8.2.2.1 MRC OX-19

MRC OX-19 is a mouse anti-rat CD5 monoclonal antibody of the IgG_1 subclass which reacts with a surface glycoprotein present on all rat thymocytes and peripheral T cells and on a small proportion (2%) of B cells (Dallman et al 1984). It was purchased as ascites fluid from Serotec Ltd, England. Immunoascites was also produced on site[1] after growing the hybridoma cell line[2] producing the antibody in RPMI 1640 tissue culture medium[3] supplemented with 10% foetal calf serum in a humidified atmosphere of 5% CO_2 in air at 37°C in a tissue culture incubator[4]. Hybridomas were injected (10^7 cells in 1 ml PBS per mouse) intraperitoneally in four Pristane[5]-conditioned-BALB/c mice and ascites was obtained by tapping the peritoneal cavity of ascites-affected mice daily until death of the animals (3-5 ml of immunoascites was obtained per mouse on average). MRC OX-19 was purified by ion exchange chromatography (see below) and stored at 0.5 mg/ml in phosphate buffered saline (PBS) at 4° C in a vial containing nitrogen gas.

8.2.2.2 W3/13

W3/13 is a mouse monoclonal antibody which reacts with all rat thymocytes and peripheral T cells (Williams et al 1977). Tissue culture supernatant was obtained as a gift from Dr AF Williams, MRC Cellular Immunology Unit, Oxford, England.

---

1 Immunology Department RPMS.

2 The cell line was a kind gift from Dr AF Williams MRC Cellular Immunology Unit , Oxford, England.

3 RPMI (Roswell Park Memorial Institute) 1640 medium contained 20mM Na_2HCO_3, 2 mM L-glutamine, 1 mM sodium pyruvate, 50 iu penicillin and 50 µg/ml streptomycin.

4 Leec, England.

5 Pristane (2,6,10,14-tetramethylpentadecane): Sigma England. Pristane was injected intraperitoneally at 0.5 ml in BALB/c mice and the animals were left for 10 days before inoculation with hybridoma cells.

8.2.2.3 H17E2

H17E2 is a mouse monoclonal antibody of the IgG_1 subclass with specificity for human placental alkaline phosphatase (Travers and Bodmer 1984). It does not bind to rat tissues and was used as a control (irrelevant) antibody in these studies. Purified ascites was obtained from the Imperial Cancer Research Fund, London, England.

8.2.3 Purification of MRC OX-19

Firstly, a sample of the ascites fluid (10 µl, 1/100 dilution) was analysed by SDS-PAGE[1] for its protein content. This showed 4 protein bands one of which corresponded to mouse IgG (see Figure 8.1).

Figure 8.1. Photograph of the SDS-PAGE of MRC OX-19 ascites showing 4 bands in the left lane. Control mouse IgG sample is shown in the right lane.

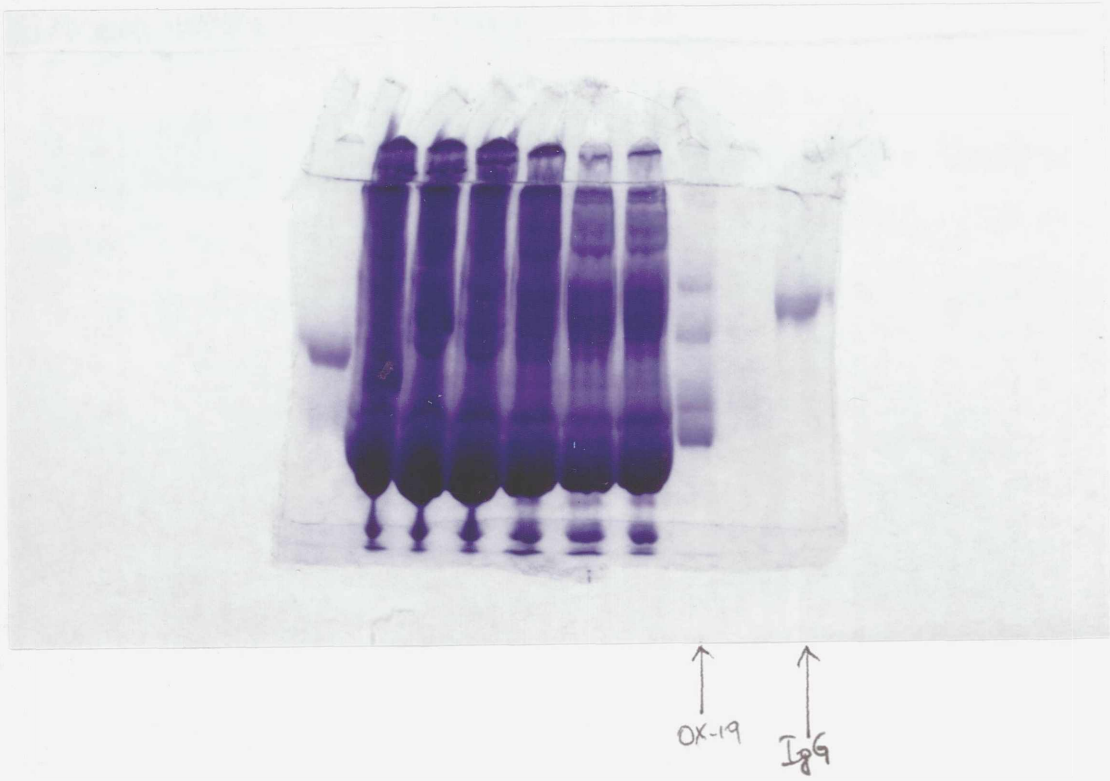

1 Sodium dodecyl phosphate polyacrylamide gel electrophoresis. See Appendix, page 314 for experimental details.

Next, the monoclonal antibody was purified by running the ascites fluid produced on the anion exchange chromatography column Mono Q of a Fast Protein Liquid Chromatography system[1] (FPLC). A sample (100 µl of 1:10 dilution of ascites in 20 mM TEA buffer; see below) was loaded on the column equilibrated with 20 mM of triethanolamine (TEA)[2] pH 7.7. The column was then eluted using a salt gradient of 1M NaCl[3] in 20 mM TEA and the elution fractions were collected using an automatic fraction collector set to collect separate protein peaks as detected by the system's UV cell in separate tubes (total of 4 corresponding to those on SDS-PAGE), Figure 8.2.

Figure 8.2. Photograph of the FPLC trace upon elution of MRC OX-19 ascites (pilot run). Four peaks of protein eluting separately (blue line) are seen. The red line denotes application of the salt gradient

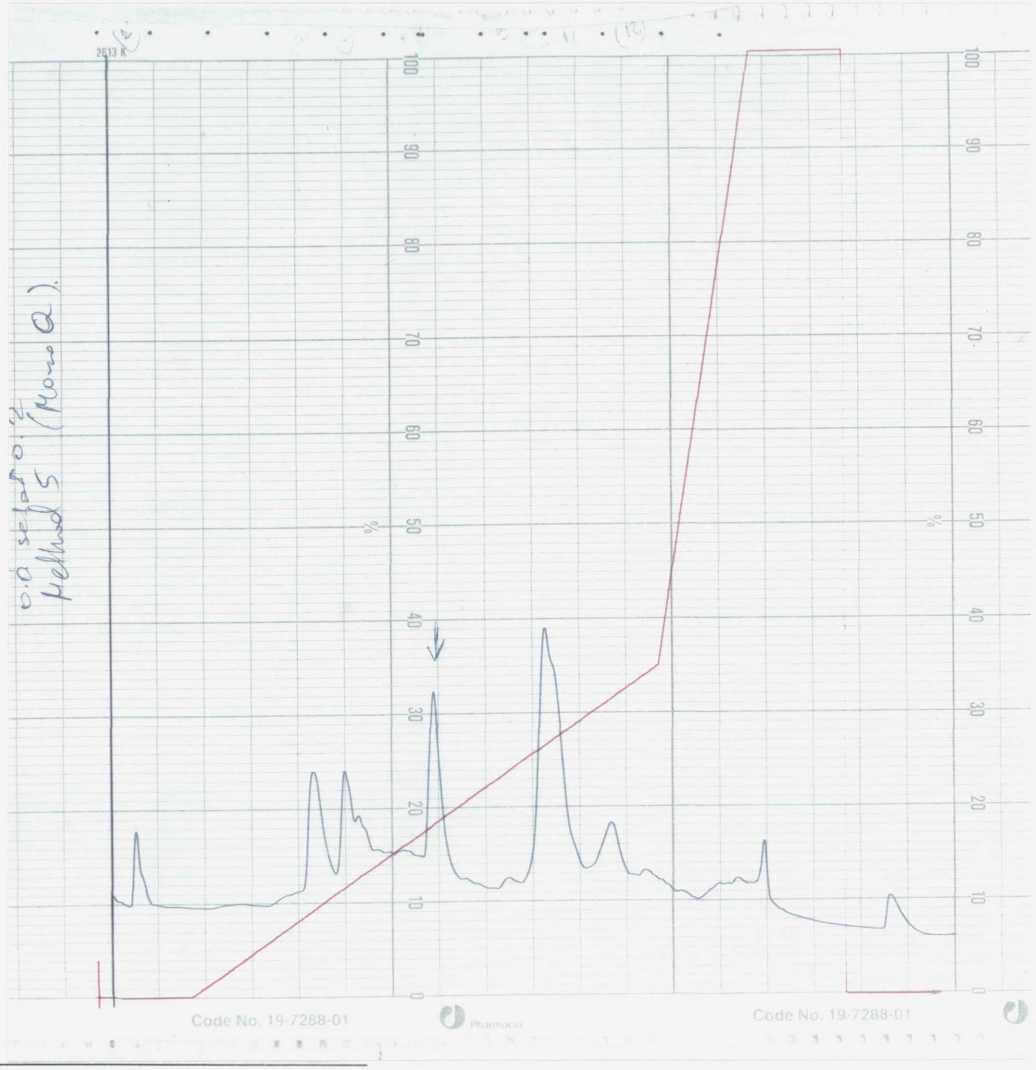

1 Pharmacia, Sweden.
2 Sigma, England.
3 BDH, England.

Each fraction was tested for antibody presence by an indirect immunofluorescence assay using rat lymph node cells (see the Immunofluorescence section page 131 for details of the staining procedure). Fluorescence on the cells was examined under a fluorescent microscope[1] and scored as negative, weak positive and strong positive[2]. One positive fraction was identified and was confirmed to contain MRC OX-19 McAb by running the cells in the corresponding test tube in a fluorescence-activated-cell sorter[3]. The antibody was located in protein peak No 3 (see Figure 8.2). Afterwards, a second run of a larger volume of ascites fluid (2 ml) dialysed against 20 mM TEA using similar conditions to the ones used before, ie 20 mM TEA loading buffer, 1 M NaCl gradient in 20 mM TEA eluting buffer etc, was performed and the fraction containing the antibody was collected[4]. This was then dialysed against phosphate buffered saline (PBS)[5] pH 7.5-8 and finally kept at 4°C in a vial containing nitrogen gas[6].

8.2.4 Monoclonal antibody labelling with ^{111}In and testing antibody immunoreactivity

MRC OX-19 and H17E2[7] McAbs were labelled with ^{111}In using the method of the double chelating agent DTPA of Hnatowitch et al (1982)[8]. The specific activity obtained was 650 MBq/mg (18 mCi/mg) of MRC OX-19 and 250 MBq/mg (7 mCi/mg) of H17E2.

---

1 Dialux 20, Leitz, Wetzlar, Germany.

2 For details of the findings, see Appendix, pp314 & 315.

3 Epics C flow cytometer, Coulter USA. For details of the experimental setting and results see Appendix, pp314 & 315.

4 A volume of 6 ml was obtained, OD (280nm) : 0.47, protein content : 0.35 mg/ml.

5 Dulbecco's Formula A modified, Flow Labs, England.

6 Amersham, England.

7 H17E2-DTPA coupled antibody was taken from a stock preparation intended for use in patients. It contained 1.2 DTPA molecules per antibody and its immunoreactivity was 75%; ICRF Oncology Group, Hammersmith Hospital, London.

8 For details on the labelling procedure see Chapter 5 Page 49. For experimental details on DTPA-coupling, measuring the number of DTPA/Ab and test labelling of MRC OX-19 see Tables A8.1, A8.2 and A8.3, Appendix, pp315-317. For test labelling H17E2 see Table A8.4, Appendix, page 317.

Immunoreactivity after labelling was tested by a radiobinding assay under conditions of antigen excess (Lindmo and Bunn 1986). The immunoreactive fraction was determined by extrapolation in a linear plot of the inverse relative cell associated activity versus the inverse cell concentration[1].

8.2.5.Binding of ^{111}In MRC OX-19 to rat lymph node cells and blood

Cervical lymph nodes were dissected form an adult Wistar rat. A cell suspension was prepared by teasing the lymph nodes in a plastic Petri dish containing Tris balanced salt solution 1% BSA, pH 7.45 using two 21 G needles mounted on two 5 ml plastic syringes[2]. The clumps were allowed to settle in a 20 ml plastic Universal tube[3] for 5 minutes, then the resulting cell suspension was washed once in the buffer. Finally, the cells were resuspended in 5 ml buffer and their number counted in a haemocytometer. LP3 tubes were prepared in duplicate, each contained $4X10^6$ lymph node cells in Tris-buffered balanced salt solution 1% BSA. ^{111}In MRC OX-19 was added in increasing concentrations ($5X10^3$-10^6 Ab/cell see Table 8.1 and the volume adjusted to 1 ml using buffer. After 2 hr incubation at 37° C the cells were washed twice[4] and the radioactivity bound to the cell pellet counted in a gamma scintillation counter (Packard Autogamma-USA).

Radiobinding of the ^{111}In MRC OX-19 to whole blood was performed in LP3 tubes by adding the antibody in 100 µl PBS to 1 ml ACD[5] anticoagulated Wistar rat blood (1 part ACD to 6 parts blood) in increasing concentrations (see Table 8.1). The haematocrit (0.25 in this case) and lymphocyte count ($4X10^6$/ml) were measured in a sample having a similar dilution before the assay, ie 1 ml ACD-blood + 100 µl PBS.

---

1 For details of the experimental procedure, see Appendix pp317 & 318.
2 Monoject, England.
3 Sterilin, England.
4 Centrifugation at 150 g for 7 minutes and washing in buffer.
5 Acid Citrated Dextrose NIH Formula A BP.

Table 8.1. Concentration of ^{111}In MRC OX-19 added to lymph node cells or ACD-whole blood.

Tube No	Ab/lymphocyte	Ab (µg)/ml
1	10^6	1
2	$5X10^5$	0.5
3	10^5	0.1
4	$5X10^4$	0.05
5	$2.5X10^4$	0.025
6	10^4	0.01
7	$5X10^3$	0.005

The tubes were left to incubate for 2 hr at 37°C in a water bath with intermittent gentle mixing. Then, they were centrifuged at 1000 g for 10 min, a 200 µl volume of plasma was transferred to counting vials and the radioactivity counted in an automatic well counter[1]. Cell bound radioactivity was calculated by subtracting the amount in the plasma from the total added (see Results page 136).

In both cases (whole blood & lymph node assay), standards of the added radiolabelled antibody were prepared for calculation of the relative cell bound activity.

8.2.6 ^{111}In labelling of lymphocytes

Lymph node cell suspensions were prepared from the superficial cervical lymph nodes of normal AO rats and the lymphocytes were labelled with indium-111 in vitro (Chisholm et al 1979). The cells at 10^8/ml in saline were incubated with ^{111}In-tropolonate[2] at 370 kBq (10 µCi)/10^8 cells for five minutes at room temperature. The cells were washed three times by

1 Packard Autogamma USA, Haematology Department RPMS.

2 Tropolone (2-hydroxy-2,4,6-cycloheptatriene-1-one), Fluka, Switzerland, was used as a $4.4X10^{-3}$ M solution in 20 mM Hepes saline buffer, pH 7.6. $^{111}InCl_3$ in 0.04 M HCl (10 µl, 3.7 MBq, 100 µCi) was mixed with 100 µl tropolone solution and the mixture was added to the cells and incubated for 5 minutes.

centrifugation in PBS containing 1% foetal calf serum to remove unbound ^{111}In and were resuspended in PBS for injection. A standard of the injected dose containing a known radioactivity and number of cells was left for reference.

8.2.7 In vivo administration of antibody or labelled cells and tissue sampling

8.2.7.1 The experimental setting (Figure 8.3)

Three different groups of experiments were performed to test binding of in vivo injected antibodies to lymphocytes and compare the injected ^{111}In-anti-T cell antibody with ^{111}In tropolone lymph node cells (Figure 8.3).

Figure 8.3. The experimental setting for in vivo administration of antibodies and labelled lymphocytes in the rat.

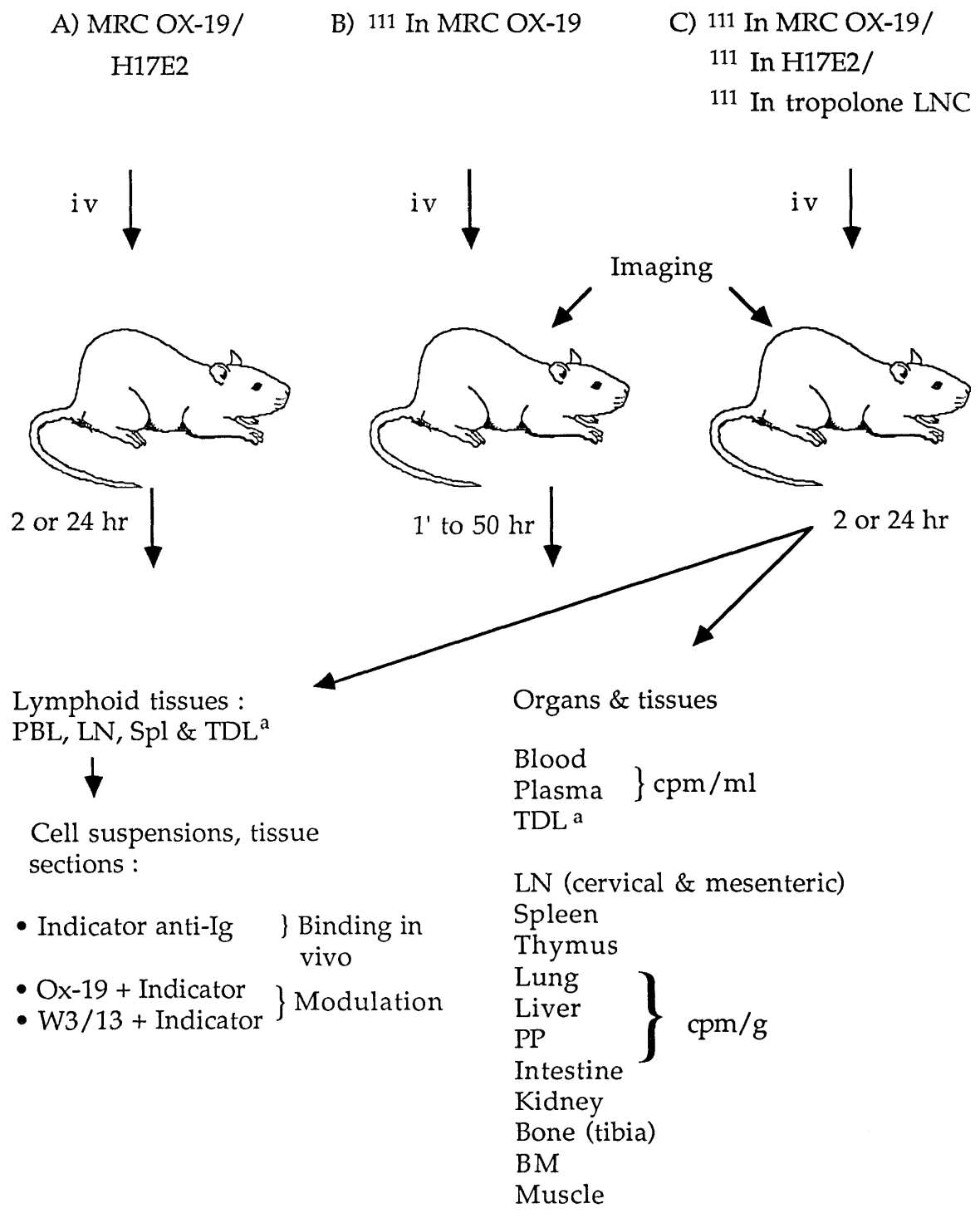

[a] Thoracic duct lymphocytes collected from cannulated rats (in Group A & B).
Abbreviations : PBL : Peripheral blood lymphocytes, LN : Lymph node, Spl : Spleen, PP : Peyers patches, BM : Bone marrow, LNC : Lymph node cells, 1' : 1 minute, Cpm : Count per minute, Ig : Immunoglobulin.

Group A :

In the first set of experiments, unlabelled MRC OX-19 in PBS was injected intravenously in increasing doses into Wistar rats. The animals were killed at 2 or 24 hr after injection and in vivo antibody binding to lymphocytes in blood, lymph nodes and spleen was tested by indirect immunofluorescence or immunochemistry. This experimental group included also rats which had indwelling thoracic duct cannulae to test antibody binding to thoracic duct lymphocytes, and rats injected with the negative control (irrelevant) H17E2 monoclonal antibody (see Table 8.2).

Table 8.2. List of experiments performed using unlabelled MRC OX-19 or H17E2 McAb, Group A.

Expt.	Rat	Preparation used	Dose	Time of sacrifice
A1	A1a	MRC OX-19	400µg/kg	2 hr
	A1b	MRC OX-19	400µg/kg	24 hr
	A1c	H17E2	400µg/kg	2 hr
	A1d	H17E2	400µg/kg	24 hr
A2	A2a	MRC OX-19	20µg/kg	2hr
	A2b	MRC OX-19	20µg/kg	24 hr
	A2c	MRC OX-19	80 µg/kg	2 hr
	A2d	MRC OX-19	80 µg/kg	24 hr
	A2e	MRC OX-19	400µg/kg	2 hr
	A2f	MRC OX-19	400µg/kg	24 hr
	A2g	H17E2	400µg/kg	2 hr
	A2h	H17E2	400µg/kg	24 hr
A3[a]	A3a	MRC OX-19	20 µg/kg	24 hr
	A3b	MRC OX-19	40 µg/kg	24 hr

a McAb injected into cannulated rats.

Group B :

The second set of experiments involved intravenous injection of ^{111}In MRC OX-19 in Wistar rats, imaging the animals at different times afterwards then sampling various tissues for the amount of radioactivity localised in each of them. This group included, also, thoracic duct cannulated rats in order to test the amount of ^{111}In MRC OX-19 reaching central lymph (Table 8.3).

Table 8.3. List of experiments performed using ^{111}In MRC OX-19 and details of the dose, radioactivity and time of injection, Group B.

Expt.	Rat	Dose	Radioactivity	Time of sacrifice
B1	B1a	20 µg/kg	4.8 MBq (130 µCi)	2 min
	B1b	20 µg/kg	3 MBq (80 µCi)	10 min
	B1c	20 µg/kg	2.5 MBq (70 µCi)	20 min
	B1d	20 µg/kg	2.3 MBq (63 µCi)	30 min
B2	B2a	25 µg/kg	6 MBq (160 µCi)	1 hr
	B2b	25 µg/kg	4.7 MBq (130 µCi)	3 hr
	B2c	25 µg/kg	3.8 MBq (60 µCi)	24 hr
B3	B3a	40 µg/kg	3.5 MBq (95 µCi)	2 hr
	B3b	40 µg/kg	3.5 MBq (95 µCi)	24 hr
	B3c	40 µg/kg	2 MBq (50 µCi)	36 hr
	B3d	40 µg/kg	2 MBq (50 µCi)	50 hr
B4[a]	B4a	40 µg/kg	4 MBq (110 µCi)	7 hr
B5[a]	B5a	40 µg/kg	4 MBq (110 µCi)	12 hr

[a] McAb injected into cannulated rats.

Group C :

The third experimental setting involved comparison of rats injected with ^{111}In MRC OX-19, ^{111}In H17E2 (negative control) or ^{111}In tropolone lymph node cells by scintillation camera imaging and tissue sampling at 2 or 24 hr after injection of the label. In vivo binding of ^{111}In MRC OX-19 to lymphocytes in blood, lymph nodes and spleen was also tested by indirect immunofluorescence or immunochemistry (Table 8.4).

Table 8.4. List of experiments performed, rats included and details of injected antibodies or cells, Group C.

Expt.	Rat	Preparation used	Dose	Radioactivity	Time of sacrifice
C1[a]	C1a	^{111}In MRC OX-19	40 µg/kg	3.5 MBq (95 µCi)	2 hr
	C1b	^{111}In MRC OX-19	40 µg/kg	3.5 MBq (95 µCi)	24 hr
	C1c	^{111}In LNC	5X10^8 cell	1.5 MBq (40 µCi)	2 hr
	C1d	^{111}In LNC	5X10^8 cell	1.5 MBq (40 µCi)	24 hr
C2	C2a	^{111}In H17E2	40 µg/kg	1.5 MBq (40 µCi)	2 hr
		^{111}In H17E2	40 µg/kg	1.5 MBq (40 µCi)	24 hr

[a] Rats C1a and C1b were also included in Table 8.3 as B3a and B3b, respectively, for the sake of completion of ^{111}In MRC OX-19 sampling data.

8.2.7.2 Injection of the antibodies or ^{111}In labelled cells.

^{111}In-labelled or unlabelled antibodies were injected in adult Wistar rats and ^{111}In-tropolone lymph node cells were injected in AO rats. Injections (≈1ml) were given intravenously in a lateral tail vein under ether anaesthesia. A standard of the injected radioactivity was kept for comparison.

The amounts of antibody or cells used, radioactivity injected and the times of sacrifice of the animals after injection are given in Tables 8.2, 8.3 and 8.4.

8.2.7.3 Thoracic duct cannulation

The method described by Ford (1977) was applied[1]. Lymph was collected in separate fractions in 10 ml centrifuge tubes after injection of the antibody (two hourly fractions after the injection of MRC OX-19 and one hourly fractions after the injection of ^{111}In MRC OX-19).

8.2.7.4 Tissue sampling

Group A experiments

The injection of the antibodies was described above (see Table 8.2). At the set time of killing of each animal (2 or 24 hr after injection of the antibody), blood, lymph nodes and the spleen were sampled and suspensions of mononuclear cells were prepared. Samples of lymph nodes and spleen were also frozen for cutting tissues sections at a later time (for details of sampling and tissue suspension preparation see Appendix page 319). Staining of the cells (PBMNC[2], spleen cells and lymph node cells) by immunfluorescence followed. Also, multiple cytospin slides of each of the cell populations were prepared for immunocytochemistry staining.

The thoracic duct cannulated rats, injected with MRC OX-19 after an overnight collection of lymph, were sacrificed 24 hr post antibody injection. Before that, two hourly lymph fractions up to 12 hr post antibody injection were collected in 10 ml centrifuge tubes containing 1 ml DAB-20[3] and cytospins were immediately prepared for each fraction without cell washing for immunocytochemistry staining at a later stage (see preparation of cytospins, Appendix, page 319 and immunochemistry staining page 132). At

---

1 For details of the procedure see Appendix, page 318.
2 PBMNC : peripheral blood mononuclear cells.
3 Dulbecco's phosphate buffered saline (A) containing calcium and magnesium (B) and 20 unit of heparin per ml.

the time of sacrifice, the rats were treated in the same way described above for the intact rats injected with unlabelled antibodies.

Group B

At set times after injection of ^{111}In labelled antibodies, blood was taken into a 10 ml syringe containing heparin through a cardiac puncture under terminal anaesthesia. Samples of various lymphoid (cervical lymph nodes, thymus, mesenteric lymph nodes, spleen and Peyers patches) and non-lymphoid tissues (lung, liver, kidney, intestine, bone, bone marrow and muscle) were then removed and cleaned. The tissue samples were kept on a wet tray, then they were weighed in preweighed gamma scintillation counting vials[1]. Finally, the vials were counted for ^{111}In radioactivity in an automatic well scintillation counter[2]. The amount of radioactivity in each tissue was expressed as the percent injected dose of ^{111}In present per gramme wet weight of tissue. A known volume of blood was transferred to a counting vial and another aliquot of heparinised blood was centrifuged (1000 g, 15 min) and a known volume of plasma was also obtained for counting.

Tissue sampling in the rats which had indwelling thoracic duct cannulae involved collection of lymph in LP3 tubes (containing 10 units of heparin in 10 µl) immediately after the intravenous injection of ^{111}In MRC OX-19. One-hourly fractions were collected and the volume, cell number and radioactivity in the lymph and that cell associated were measured for each fraction. After the last lymph fraction, the rats were killed and treated in the same way as the other ^{111}In McAb injected rats, ie tissue sampling for counting radioactivity.

---

1 Sterilin, England.
2 Packard Autogamma, Haematology Dept, RPMS.

Group C

Tissue sampling in this group of animals involved a combination of blood and lymphoid organ sampling for immunofluorescence and immunochemistry staining (see Group A above) as well as lymphoid and non-lymphoid tissue sampling for radioactivity counting (Group B protocol). This was done in rats injected with ^{111}In MRC OX-19.

The animals injected with ^{111}In tropolone lymph node cells and ^{111}In H17E2 were sampled only as was done in Group B, ie sampling lymphoid and non-lymphoid tissues for radioactivity counting.

Sampling in each pair of experimental animals in this group was done at 2 or 24 hr after injection of the labelled antibodies or cells (see Table 8.4).

8.2.8 Immunofluorescence analysis by flow cytometry

Indirect immunofluorescence staining was performed on mononuclear cell suspensions from peripheral blood, spleen and lymph nodes. In LP3 tubes prepared in triplicate, the cells (2-4 X10^6 cells in a pellet), were incubated with monoclonal antibody MRC OX-19 or W3/13 added in 100 µl for 30 minutes on ice, washed[1] to remove excess antibody and then incubated with fluorescein isothiocyanate (FITC)-conjugated rabbit anti-mouse immunoglobulin[2] for 30 minutes. The cells were then washed, fixed in paraformaldehyde[3] and stored at 4° C until analysed by flow cytometry.

Flow cytometry analysis was performed by a Coulter EPICS C flow cytometer using 90° and forward angle light scatter to gate on the lymphocyte

---

1 Washing was done using PBS containing 1% BSA and 1% sodium azide (pH 7.4).

2 QB.AR9 F(ab')$_2$ Rabbit-anti-mouse Ig fluorescein conjugate, Serotec, England. This reagent was used at 1/120 dilution in PBS containing 20% normal Wistar rat serum (the mixture was centrifuged for 10 minutes in a microfuge before use).

3 1% paraformaldehyde (BDH, England) in PBS pH 7.4. The cells were fixed for 15 minutes at room temperature then washed in PBS 1% BSA-azide.

population and single parameter fluorescence analysis to identify FITC positive cells. For each population at least 10^4 cells were analysed and the proportion of the cells positive as well as the intensity of fluorescence was recorded.

Assessment of in vivo MRC OX-19 binding was made by staining cell suspensions with FITC-conjugated anti-mouse Ig alone. The proportion of CD5-positive cells in each tissue which had bound MRC OX-19 in vivo was then calculated as :

$$\frac{\%\text{ cells stained with FITC anti-mouse Ig alone}}{\%\text{ cells stained with MRC OX-19 and FITC anti-mouse Ig}} \times 100$$

The extent to which in vivo MRC OX-19 caused modulation, ie T cells that had lost the CD5 molecule from their surface was calculated by comparing the proportion of T cells stained in vitro with W3/13 monoclonal with the proportion stained with MRC OX-19 in vitro, ie

$$1 - \frac{\%\text{ cells stained with MRC OX-19 and FITC anti-mouse Ig}}{\%\text{ cells stained with W3/13 and FITC anti-mouse Ig}} \times 100$$

8.2.9 Immunoalkaline phosphatase staining of cytospins, touch imprints & tissue sections

Cytospins were prepared from the suspensions of PBMNC, LNC, TDL or spleen cells[1]. The slides were stained for MRC OX-19 or W3/13 by an indirect alkaline phosphatase/anti-alkaline phosphatase (APAAP) technique (Bevan & Chisholm 1986). Assessment of in vivo MRC OX-19 binding was done by staining the preparations without addition of a first layer antibody, while identification of CD5- or W3/13-positive cells in the preparation was done using MRC OX-19 or W3/13, respectively, as the primary antibody followed, in sequence, by rabbit anti-mouse Ig[2], APAAP[2]

---

1 For details of the technique see Appendix, page 319.

2 Dako, Denmark.

complex and a chromogenic substrate (Fast Red[1]). The touch imprints were fixed in acetone and stained in the same way as above.

Tissue sections from spleen and lymph nodes were prepared by cutting the frozen blocks of tissue in a cryotome[2]. Five-µm-thick sections were cut and mounted on microscope slides. After overnight drying, the sections were fixed with acetone and stained using APAAP as described above.

8.2.10 Scintillation camera imaging

8.2.10.1 Instrumentation and relevant performance characteristics of the system used for imaging

A large field of view scintillation camera[3] (crystal diameter = 35 cm, PMT No 30) was equipped with a pinhole collimator (conic shape, pinhole diameter = 5 mm , height = 30 cm, diameter at base = 33 cm). The camera was linked to a dedicated on-line computer for acquisition, display and analysis of the data (Medical Data System, USA), see Figure 8.4.

Figure 8.4. The scintillation camera with the pinhole collimator in place.

1 Sigma, England.
2 Bright, England.
3 Toshiba GCA-202, Japan.

A test using a phantom of the thyroid gland[1] was done to check the ability of the system to pick small variations in radioactivity in the field of view at various pinhole positions ranging between 2 cm from the plane of the object studied giving maximum magnification and the pinhole at ≈ 15 cm from the object (minimum magnification). The energy of acquisition of the camera was set at 240 keV± 20% window. The test showed that the system's resolution was 10 mm (diameter of the smallest resolvable circle) in the centre of the field of view at the position of minimum magnification. Resolution was 6 mm at the position of maximum magnification. Spatial distortion did not affect the quality of the image obtained and was mainly noticeable at the edge of the field of view. Quantitation of the relative amounts of radioactivity in different compartments of the phantom by drawing regions of interest on the images obtained showed approximately the same results regardless of the collimator's distance from the phantom[2].

8.2.10.2 Rat imaging after the injection of ^{111}In McAb or ^{111}In labelled cells.

Imaging of the rats injected with ^{111}In McAbs (MRC OX-19 or H17E2) was carried out on animals under intraperitoneal anaesthesia.

Static acquisition was performed immediately before the animal was killed taking multiple views (128 X 128 pixel matrix) of 10 minute duration. Views of the whole animal were taken as well as spot views of the head and neck, chest and abdomen. Analysis of the data was by visual examination of the images.

---

1 3602 Thyroid phantom, Picker Nuclear USA. See Figure A8.2, Appendix, page 319.

2 See Table A8.6, Appendix, page 319 for details.

8.2.11 In vivo testing of lymphocyte recirculation after in vitro ^{111}In MRC OX-19 cell binding and fluorescein labelling.

Three experiments[1] were performed to test the ability of thoracic duct lymphocytes which had been radiolabelled in vitro by incubation with ^{111}In MRC OX-19 to localise in lymphoid tissue and recirculate from blood to lymph. In the last experiment, fluorescence labelling of TDL (Butcher and Ford 1986) was performed in addition to in vitro labelling with ^{111}In MRC OX-19.

Each experiment involved an overnight collection of TDL from a thoracic-duct-cannulated Wistar rat in DAB-20 (see rat cannulation, Appendix page 318). The cells were washed once in Hank's balanced salt solution containing 1% BSA then were incubated with ^{111}In MRC OX-19 at 10^5 Ab/cell in the same buffer at 37°C for 2 hours. Afterwards, the cells were washed, resuspended in a small volume of medium and reinjected into the same rat. In the last experiment only (Expt D3), the incubation of TDL with ^{111}In MRC OX-19 was followed immediately by another incubation with fluorescein solution[2] at 40 µg/ml FITC for 15 min the cells were then washed and the extent of ^{111}In MRC OX-19 binding was measured in a gamma well counter and the labelling with FITC checked under a fluorescence microscope.

The cells were reinjected in the same rat via an indwelling venous port in a lateral tail vein. One hourly lymph fractions were collected immediately

---

1 Experimental group D, Expt D1; Rat D1a was injected with $7X10^8$ TDLs that had bound 2.3 µg MRC OX-19 and radioactivity of 0.1 MBq (3 µCi) ^{111}In, the rat was sacrificed at 2 hr after injection of the cells. Expt D2; Rat D2a injected with : $4X10^8$ TDLs bearing 1.7 µg MRC OX-19 and 0.1 MBq (3 µCi) ^{111}In, the rat was sacrificed at 24 hr after injection of the cells. Expt D3; Rat D3a injected with $6.5X10^8$ TDLs bearing 1 µg MRC OX-19, 0.33 MBq (9 µCi) ^{111}In and labelled with FITC (dual labelling), the rat was sacrificed at 19 hr after injection of the cells. Rat D3b injected with: $5X10^8$ TDLs, 1.66 µg MRC OX-19, 0.2 MBq (5.5 µCi) ^{111}In, FITC labelled, time of killing of the animal 43 hr after cell injection.

2 Fluorescein isothiocyanate, Isomer I, Sigma, England. FITC was dissolved in PBS then it was filtered through a 0.45 µm filter and a stock solution of 500 µg/ml was prepared.

afterwards and ^{111}In radioactivity was measured in each (cell bound and unbound). The cells were also examined for fluorescence under the fluorescence microscope in the experiment using double labelled cells . The presence of fluorescent cells in the collected lymph was recorded as positive or negative and their percentage was determined whenever their number was statistically significant. At the end of the lymph collection the rats were sacrificed and their tissues sampled for radioactivity counting (see experimental setting B page 130).

8.3 Results

8.3.1 Immunoreactivity and binding of ^{111}In MRC OX-19 to blood and lymph node cells

The immunoreactive fraction was 50% for ^{111}In MRC OX-19 and 75% for ^{111}In H17E2.

The results of the in-vitro assays of ^{111}In MRC OX-19 with rat blood and lymph node cells are shown in Figure 8.5 and Table 8.5 (refer to paragraph 8.2.5 and Table 8.1 pp 122 & 123 for experimental details and setting).

Figure 8.5. Binding of ^{111}In MRC OX-19 to rat blood and lymph node cells.

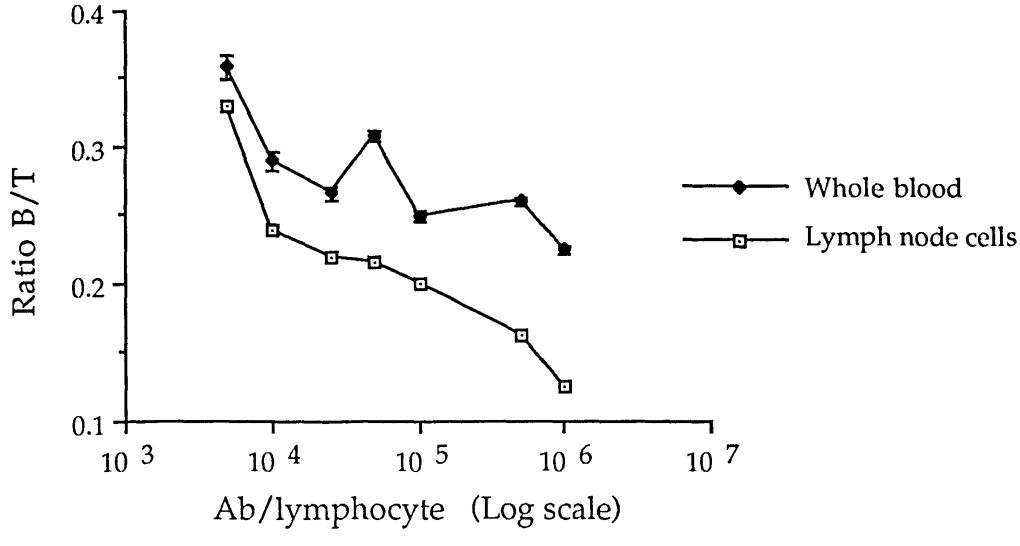

Table 8.5. Binding of ^{111}In MRC OX-19[a] to rat blood and lymph node cells.

Tube No	Std added[b]	Cpm bound LNC[c]	Ratio B/T[d]	Cpm in 1-Hct Pl[e]	Cpm cells (1ml WB)[f]	RatioB/T (WB)[g]
1	3600000 ±8500	450000 ±700	0.125 ±0.0004	2790000 ±6400	811000 ±10600	0.225 ±0.003
2	1800000 ±4250	290000 ±460	0.162 ±0.0005	1333800 ±3000	467800 ±5200	0.260 ±0.003
3	360000 ±850	72200 ±130	0.200 ±0.0006	271000 ±700	89600 ±1100	0.249 ±0.003
4	180000 ±420	38700 ±100	0.215 ±0.0007	124900 ±500	55300 ±650	0.307 ±0.004
5	90000 ±210	19700 ±70	0.219 ±0.0009	66000 ±350	24000 ±410	0.266 ±0.005
6	35600 ±130	8550 ±50	0.240 ±0.001	25240 ±220	10300 ±260	0.290 ±0.007
7	15640 ±90	5100 ±40	0.329 ±0.002	10040 ±100	5600 ±140	0.358 ±0.009

a ^{111}In MRC OX-19 : 163 MBq/mg (4.40 mCi/mg).
b Cpm added to each tube containing lymph node cells.
c Cpm bound to lymph node cells in each tube.
d Ratio of bound to total radioactivity added.
e Cpm present in the volume of plasma in 1 ml whole blood, ie (1-Hct) ml.
f Cpm cell associated in 1 ml whole blood.
g Ratio of cell bound to total added radioactivity in whole blood.

In Table 8.5, the binding of ^{111}In MRC OX-19 to lymph nodes cells ranged between 12.5 to 33% of the total amount of Ab added in the assay. Binding of the antibody to cells in whole blood was in the range of 23-36% of the total for the same concentrations of Ab added above.

8.3.2 In vivo binding of McAb to lymphocytes, Studies with unlabelled MRC OX-19 or H17E2 antibodies, Group A experiments

The extent to which intravenously injected MRC OX-19 antibody bound to lymphocytes in lymphoid tissues was tested in three separate experiments in

which different amounts of antibody were injected and tissues were removed for analysis 2 or 24 hr after injection (see Table 8.2, page 126).

Lymphocyte populations obtained from peripheral blood, spleen and lymph nodes were tested by immunofluorescent staining for the presence of MRC OX-19 on their surface. Lymphocytes in all three tissues bound in vivo administered MRC OX-19, although to a different extent (see Table 8.6) and the degree of binding, ie the proportion of the available CD5-positive cells within any one tissue which bound the antibody was dose dependent (see Table 8.7). Doses of antibody above 20 μg/kg resulted within two hours in a high proportion of the CD5-positive cells in spleen and peripheral blood being labelled; binding to lymph node cells was more limited and more variable. There was also a reduction in the extent of in vivo binding demonstrable in cells taken at 24 hours compared to cells taken at 2 hours.

Although in some experiments almost all the available CD5-positive cells in lymphoid tissues had bound antibody in vivo, ie the proportions of cells which were labelled in vitro with indicator (FITC anti-mouse Ig) alone was the same as the proportion labelled with MRC OX-19 and indicator, the intensity of immunofluorescence in cells labelled in vivo was substantially less. This relatively weak fluorescence in cell populations labelled in vivo compared to cells stained in vitro in antibody excess, suggested that by no means all the CD5 molecules on the positive cells had bound antibody in vivo (see Figure 8.6).

Figure 8.6. Comparison of the immunofluorescence staining profiles of cells which bound MRC OX-19 in vivo (a) and in vitro (b), Expt C, Rat C1a.

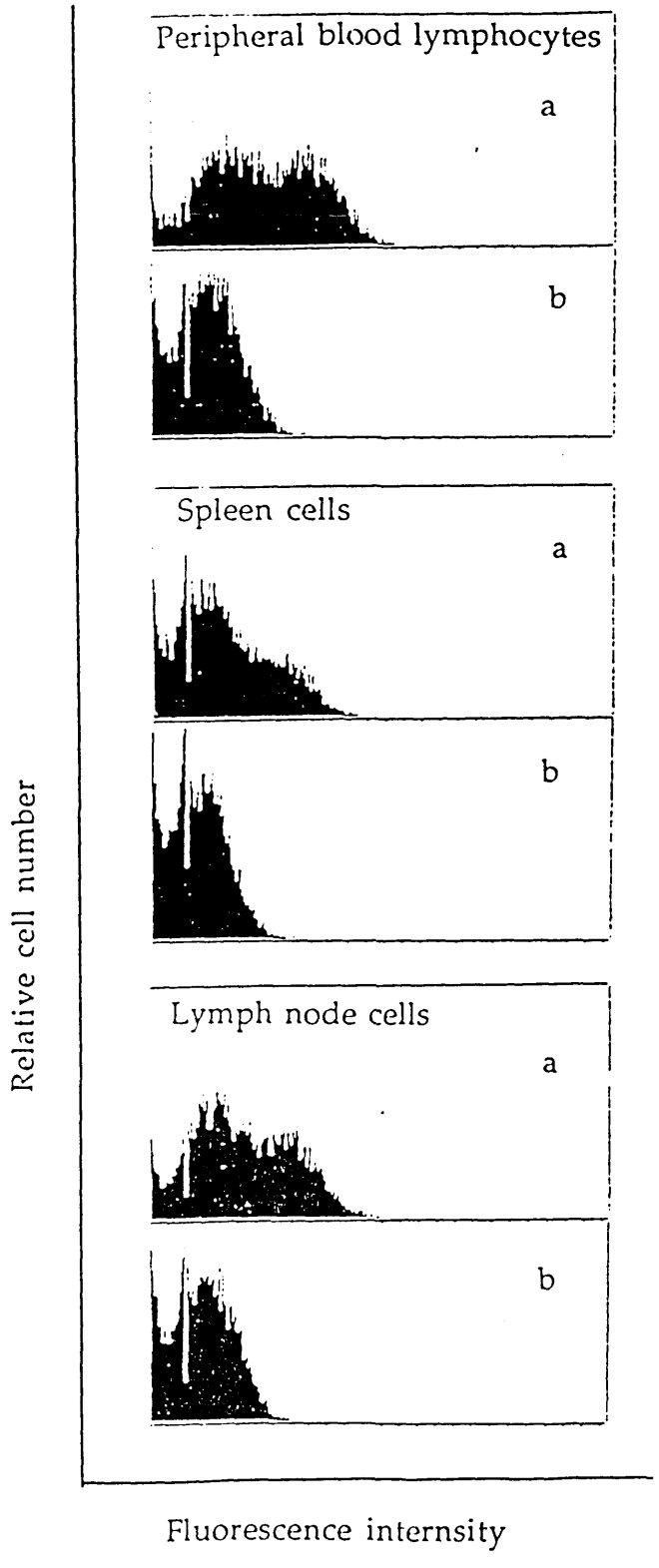

Table 8.6. Immunofluorescence staining of peripheral blood mononuclear cells, lymph node cells and spleen cells after injection of MRC OX-19, H17E2 or ^{111}In MRC OX-19 McAbs.

Expt[a]	Rat	Percentage of positive cells								
		No Ab added in vitro			MRC OX-19 added in vitro			W3/13 added in vitro		
		PBMNC	LNC	Spleen cells	PBMNC	LNC	Spleen cells	PBMNC	LNC	Spleen cells
A1	A1a	20	0.7	4	31	50	28	ND	ND	ND
	A1b	0.6	0.4	0.7	53	30	42	ND	ND	ND
	A1c	0.8	0.4	0.6	67	63	43	ND	ND	ND
	A1d	0.4	0.4	0.4	55	46	39	ND	ND	ND
A2	A2a	3	0.4	3	62	67	47	47	36	36
	A2b	1.1	2	0.6	67	54	60	71	46	39
	A2c	38	1	17	58	55	37	57	39	47
	A2d	1	2	0.6	53	48	54	68	45	41
	A2e	7	5	15	7	51	25	62	40	42
	A2f	14	2	3	27	7	30	69	33	29
	A2g	0.2	0.4	0.2	71	53	40	66	39	35
	A2h	0.2	0.2	0.6	85	64	74	73	41	48
A3	A3a	15	6	14	20	45	23	52	45	37
	A3b	18	8	9	18	47	30	51	47	38
C1	C1a	54	4	20	53	44	43	67	54	46
	C1b	5	6	5	57	55	42	70	55	42

a Experiments listed in Tables 8.2 and 8.4.
Abbreviations : PBMNC : peripheral blood mononuclear cells, LNC : lymph node cells, ND : not done.

Table 8.7. MRC OX-19 binding to rat lymphocytes in blood, lymph nodes and spleen and modulation of CD5 in vivo.

Expt[a]	Rat	% Binding to CD5 positive cells			% Modulation		
		PBMNC	LNC	Spleen cells	PBMNC	LNC	Spleen cells
A1	A1a	65	0	14	ND	ND	ND
	A1b	0	0	0	ND	ND	ND
	A1c	0	0	0	ND	ND	ND
	A1d	0	0	0	ND	ND	ND
A2	A2a	5	0	5	0	0	0
	A2b	0	0	0	6	0	0
	A2c	66	0	46	0	0	21
	A2d	0	0	0	22	0	0
	A2e	100	10	60	89	0	40
	A2f	52	0	0	61	79	0
	A2g	0	0	0	0	0	0
	A2h	0	0	0	0	0	0
A3	A3a	75	13	87	62	0	38
	A3b	100	17	19	65	0	21
C1	C1a	102	9	47	21	19	7
	C1b	9	11	12	19	0	0

a Experiments listed in Tables 8.2 and 8.4.
Abbreviations : PBMNC : peripheral blood mononuclear cells, LNC : lymph node cells, ND : not done.

Immunocytochemical analysis of cytospins prepared from the same tissues as used in the flow cytometry analysis confirmed these findings and, additionally, frozen tissue sections revealed that most of the labelled cells were confined to the T cell-dependent areas of spleen and lymph nodes, ie were T cells (Figure 8.7). As in the immunofluorescence analysis, it was clear that the intensity of staining of cells after in vivo binding was less than could be achieved with antibody excess in vitro (Figure 8.7B, D, F & H). In each of these experiments an irrelevant monoclonal antibody H17E2 anti-human placental alkaline phosphatase antibody of the same isotype as MRC OX-19 injected into control rats did not bind to lymphocytes neither did it affect the numbers of CD5-positive cells present in any tissue (see Tables 8.6 & 8.7).

Figure 8.7. Immunochemistry of cytospins, touch imprints and sections of lymph nodes and spleen taken from rats injected with MRC OX-19 in vivo and stained with APAAP.

Fig 8.7A. Cytospins of lymph node cells from rat A2c (2 hr post Ab injection) stained with indicator only to detect in vivo MRC OX-19 binding (APAAP, X1000) Note the faint red staining.

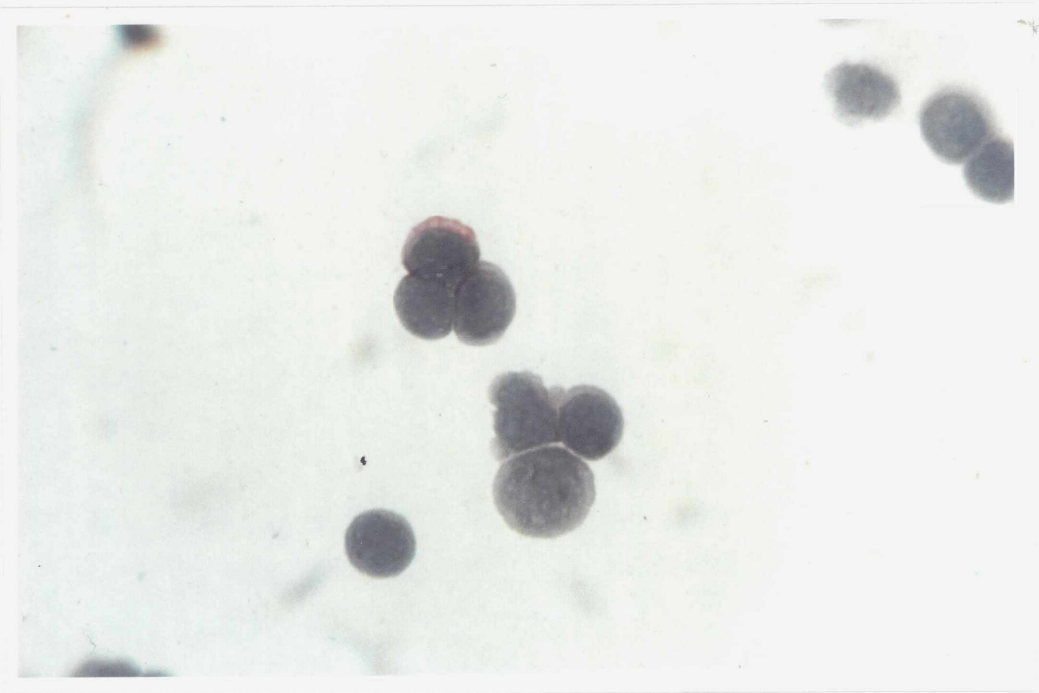

Fig 8.7B. Cytospins of lymph node cells from rat A2c (2 hr post Ab injection) stained with MRC OX-19 in vitro and indicator showing CD5-positive cells (APAAP, X1000). Note the strong red staining on the cells.

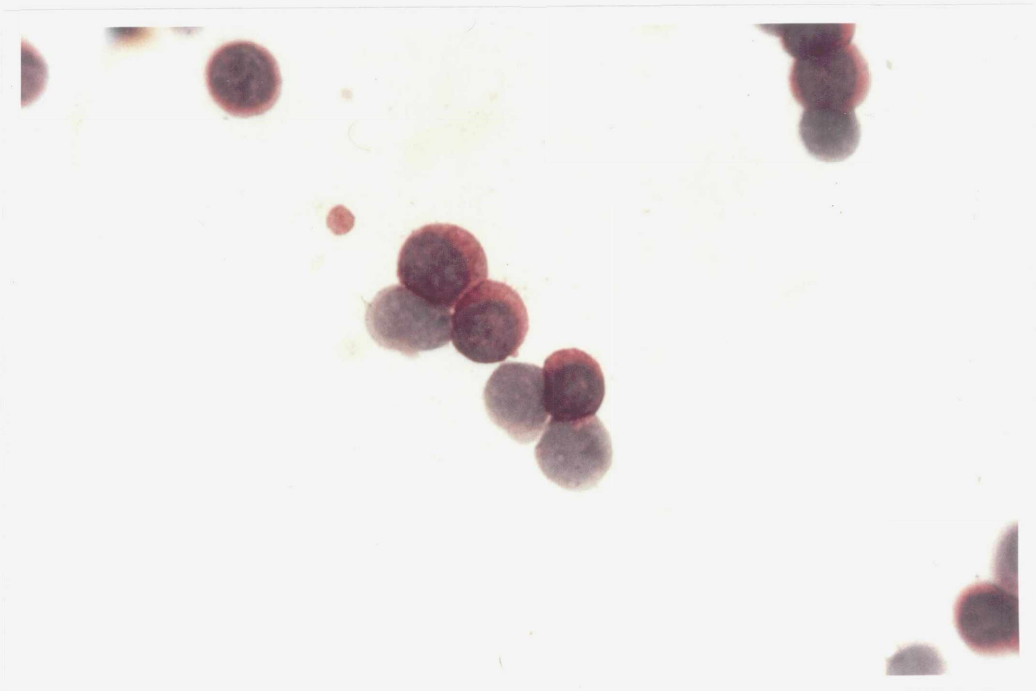

Fig 8.7 C. Touch imprints of a lymph node from rat A2d (24 hr post Ab injection) stained with indicator only to detect in vivo MRC OX-19 binding (APAAP, X400). Faint staining on the cells.

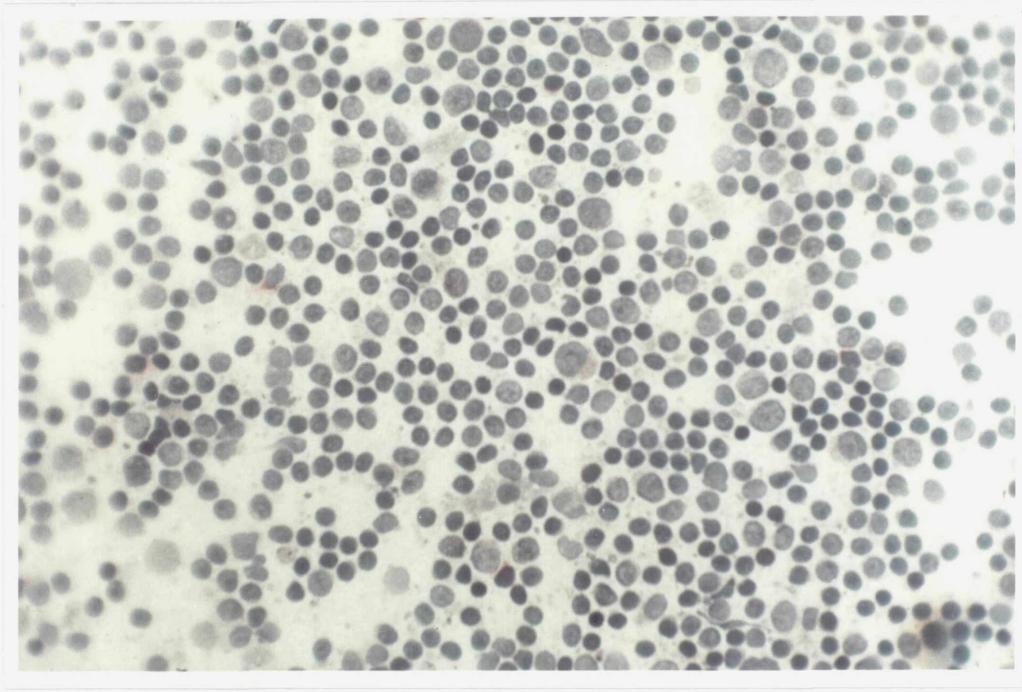

Fig 8.7D. Touch imprints of a lymph node from rat A2d (24 hr post Ab injection) stained with MRC OX-19 in vitro and indicator showing CD5-positive cells (APAAP, X400). Strong red staining on the cells.

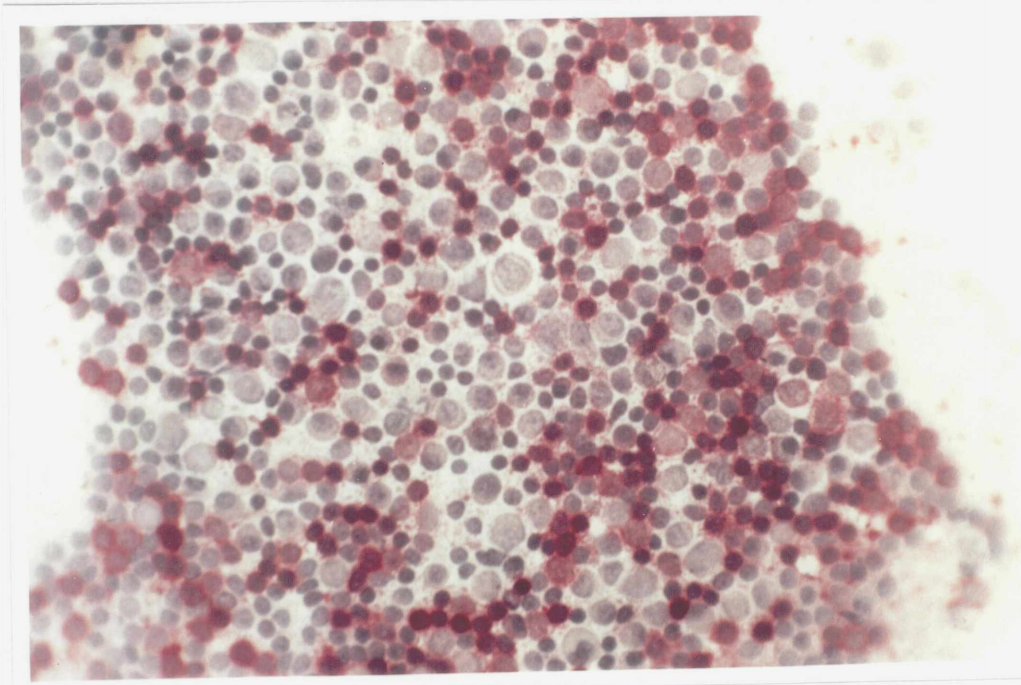

Fig 8.7E. Spleen section from rat A2e (2 hr post Ab injection) stained with indicator only to detect in vivo MRC OX-19 binding (APAAP, X400). Note the strong red staining around the central arteriole (T cell area).

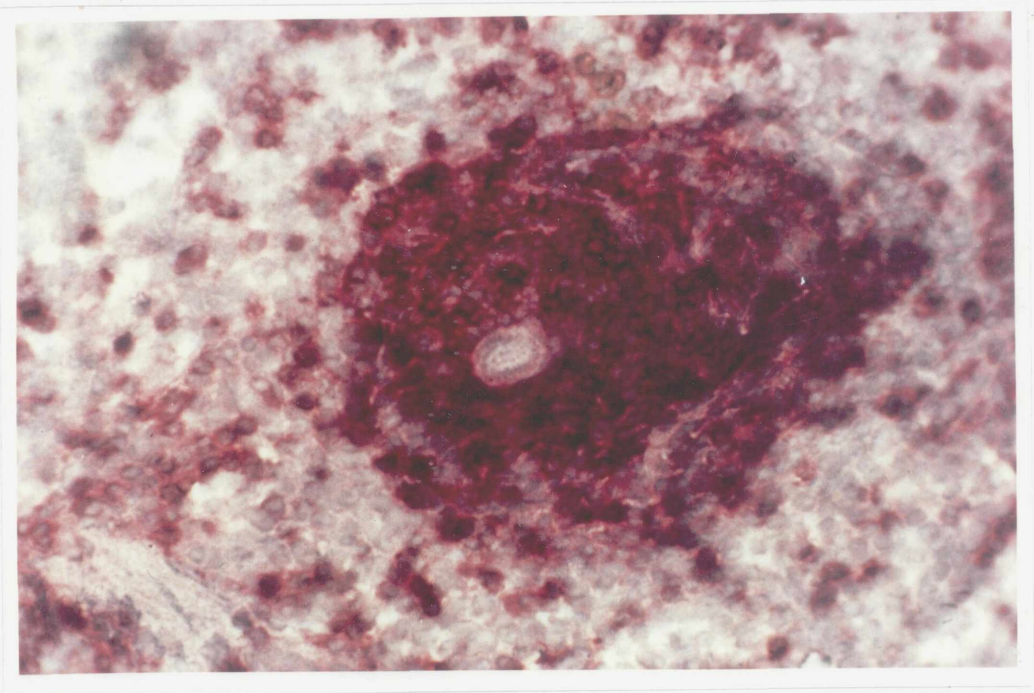

Fig 8.7F. Spleen section from rat A2e (2 hr post Ab injection) stained with MRC OX-19 in vitro and indicator showing CD5-positive cells (APAAP, X400). Note the very strong red staining around the central arteriole.

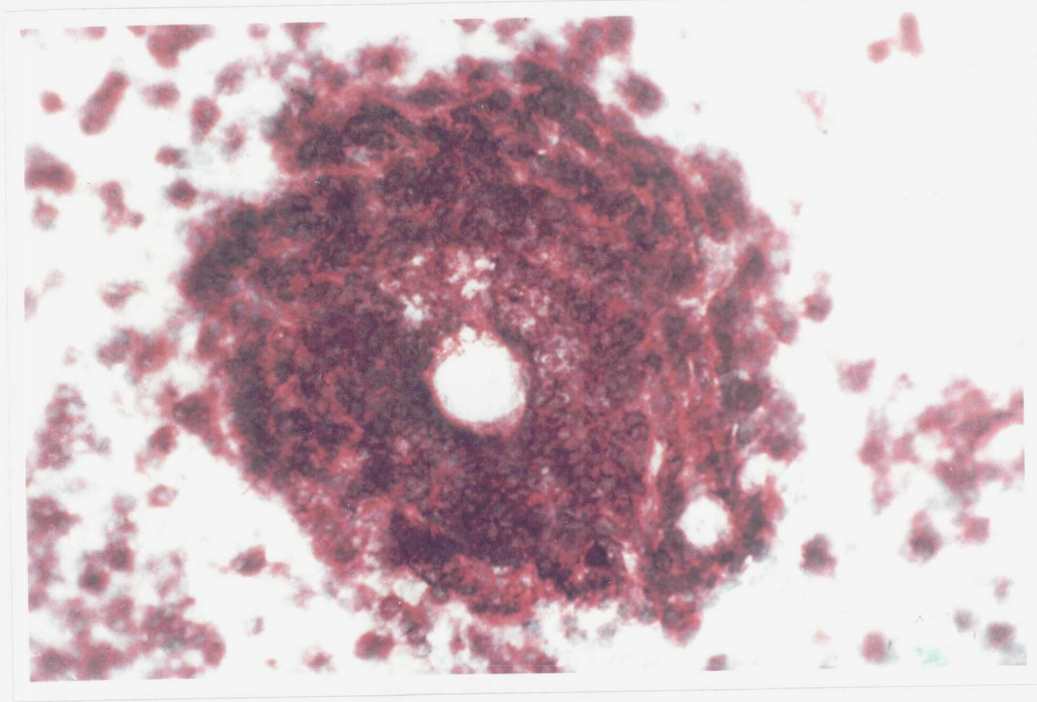

Fig 8.7G. Lymph node section from rat A2e (2 hr post Ab injection) stained with indicator only to detect in vivo MRC OX-19 binding (APAAP, X160). Note positive red staining around the high endothelial venule and paracortical zone (T cell area).

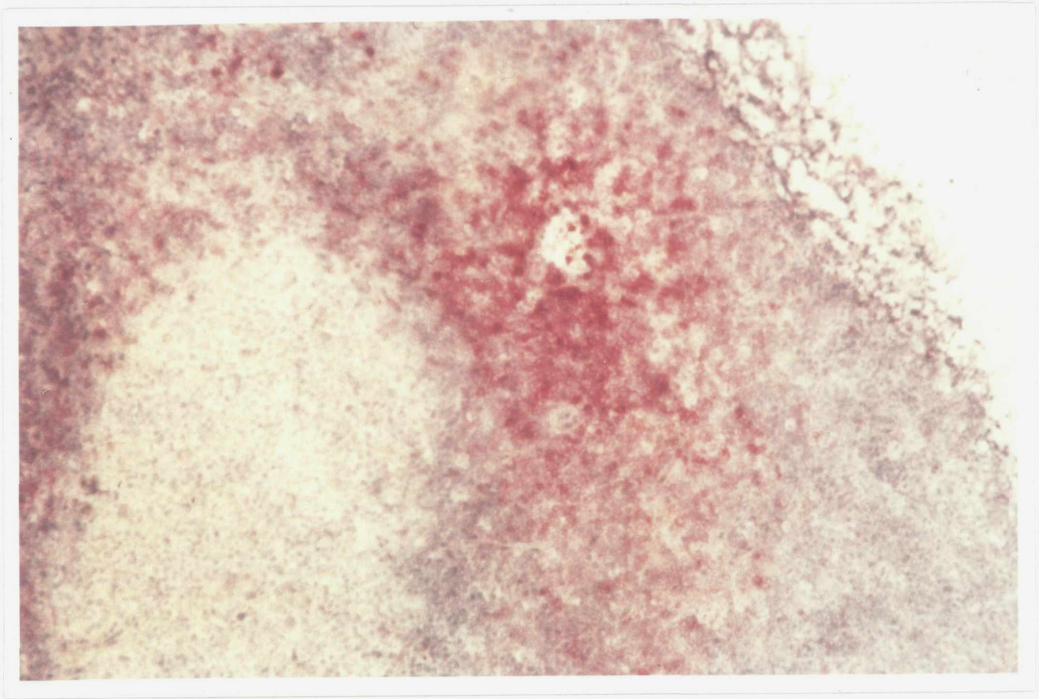

Fig 8.7H. Lymph node section from rat A2e (2 hr post Ab injection) stained with MRC OX-19 in vitro and indicator showing CD5-positive cells (APAAP, X160). Note the strong red staining in the paracortical zone.

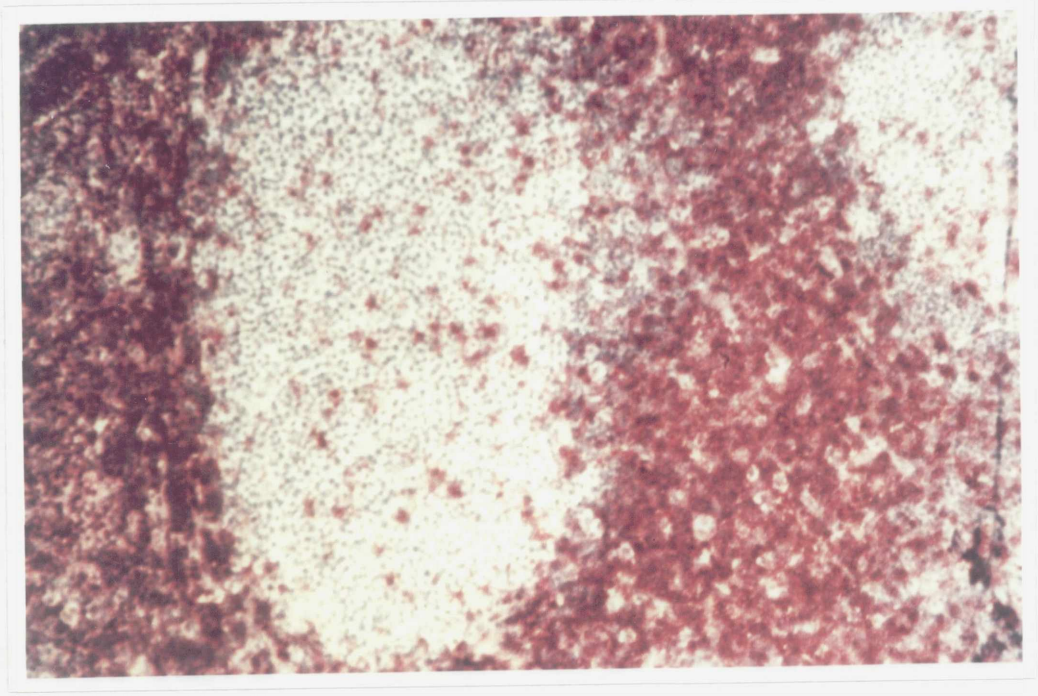

8.3.3 In vivo modulation of CD5

Binding of antibody at 37°C to lymphocytes surface molecules can result in a polar redistribution of the antibody-antigen complexes followed by exocytosis or shedding of the complexes from the cell. Internalisation of the complex inside the cells may also occur. This modulation or loss of surface markers can be induced by antibody following in vivo administration and can result in an apparent disappearance from the circulation or from tissues of cells for which the antibody has specificity. In reality, the cells may still be present but will be unable to bind further antibody until resynthesis of the surface molecule occurs. Whether or not modulation of the CD5 molecule had occurred was investigated in experiments by estimating the numbers of T cells present in the cell populations stained for CD5 by staining also with the McAb W3/13 which identified a T cell marker distinct from CD5. As shown in Table 8.7, doses of MRC OX-19 above 20 μg/kg resulted in in vivo binding to T cells, but in some experiments this was accompanied by a substantial loss of the CD5 molecule from the cells. A dose of 400 μg/kg of antibody resulted in the loss of the CD5 molecule from more than 80% of the T cells in the blood within 2 hours of injection (Expt A2). Doses of 40 and 80 μg/kg antibody produced high levels (70-100%) of binding to T cells with only relatively little modulation, ie 20% or less of the T cells had lost the CD5 molecule from their surface. The extent of modulation of CD5 from peripheral blood lymphocytes, although not the extent of binding, was comparable at 2 and 24 hours.

8.3.4 Studies with ^{111}In MRC OX-19, Experimental group B

The results of five experiments in which ^{111}In MRC OX-19 was injected intravenously and the distribution of the antibody was measured at various times after injection by counting various tissues for ^{111}In are presented in Table 8.8. In one of the experiments (Expt B3, Rats B3a & B3b) assessment of in vivo binding was also made by immunofluorescence analysis (Expt C1, rats C1a & C1b, Tables 8.6 and 8.7) which provided corroborative evidence of in vivo binding of the labelled antibody to T cells. Analysis of the tissue distribution of ^{111}In labelled antibody showed splenic uptake which increased progressively over the first 2 hours and did not alter sustantially thereafter (Figure 8.8). Localisation of labelled antibody within lymph nodes occurred more slowly and reached significant levels at 24 hours (Figure 8.8), at which time the superficial cervical nodes were clearly visible by scintillation camera. Activity in the blood declined rapidly over the first hour after injection and then decreased more slowly (Figure 8.9). Localisation of labelled McAb in muscle was low throughout (background level) and relatively low in liver (Figure 8.9).

Table 8.8. ^{111}In MRC OX-19 distribution in vivo; tissue sampling data

		%ID/ml		%ID/g											
Expt[a]	Rat	W B	Pl	CLN	MLN	Thy	Spl	Lung	Liver	Kid	PP	Int	Tib+BM	Tib	Muscle
B1	B1a	2.16	2.97	0.23	0.17	0.07	2.63	1.17	0.47	0.58	0.02	0.10	0.25	ND	0.06
		±0.005	±0.008	±0.003	±0.008	±0.0003	±0.006	±0.01	±0.003	±0.002	0.0001	0.0001	±0.002	ND	±0.0002
	B1b	1.75	2.25	0.95	0.40	0.13	7.26	1.64	0.54	0.78	0.37	0.12	0.51	0.17	0.05
		±0.004	±0.008	±0.003	±0.002	±0.0007	±0.0001	±0.004	±0.003	±0.002	±0.002	0.0006	±0.003	±0.001	±0.0003
	B1c	1.95	3.52	1.23	0.61	0.17	11.33	1.51	0.99	1.10	0.42	0.20	0.76	0.48	0.05
		±0.006	±0.01	±0.003	±0.002	±0.0009	±0.016	±0.004	±0.004	±0.002	±0.002	0.0008	±0.003	±0.001	±0.0003
	B1d	1.31	1.99	1.54	0.83	0.07	8.37	1.68	0.45	0.66	0.53	0.12	0.53	0.33	0.07
		±0.004	±0.007	±0.005	±0.002	±0.0004	±0.01	±0.004	±0.0009	±0.002	±0.002	±0.001	±0.002	±0.001	±0.0003
B2	B2a	1.99	3.32	0.64	0.35	0.08	10.01	0.84	3.51	0.99	0.23	0.17	0.25	0.11	0.04
		±0.004	±0.008	±0.001	±0.001	±0.0003	±0.016	±0.002	±0.007	±0.002	±0.001	±0.001	±0.001	0.0003	±0.0002
	B2b	0.96	1.40	4.82	4.59	0.73	13.51	1.53	2.54	0.69	3.74	0.26	0.28	0.17	0.06
		±0.001	±0.005	±0.011	±0.015	±0.003	±0.023	±0.004	±0.005	±0.002	±0.016	±0.001	±0.001	0.0001	±0.0006
	B2c	0.27	0.44	5.56	4.11	0.22	15.40	0.60	4.47	1.59	1.88	0.26	0.29	0.20	0.03
		±0.001	±0.002	±0.001	±0.001	±0.001	±0.031	±0.003	±0.013	±0.005	±0.016	±0.002	±0.001	±0.001	±0.0003

Table 8.8. (cont)

		%ID/ml		%ID/g											
Expt	Rat	WB	Pl	CLN	MLN	Thy	Spl	Lung	Liver	Kid	PP	Int	Tib+BM	Tib	Muscle
B3	B3a	1.25 ±0.006	1.82 ±0.010	4.11 ±0.017	ND ND	ND ND	12.96 ±0.038	ND ND	1.14 ±0.01	ND ND	ND ND	ND ND	ND ND	ND ND	0.04 ±0.001
	B3b	0.27 ±0.002	0.44 ±0.008	6.89 ±0.028	ND ND	ND ND	13.32 ±0.040	ND ND	1.63 ±0.063	ND ND	ND ND	ND ND	ND ND	ND ND	0.08 ±0.002
	B3c	0.25 ±0.001	0.33 ±0.001	4.60 ±0.008	4.57 ±0.042	0.30 ±0.017	13.85 ±0.042	0.89 ±0.004	1.48 ±0.007	1.98 ±0.007	1.52 ±0.009	0.36 ±0.002	0.49 ±0.004	0.42 ±0.002	0.03 ±0.0003
	B3d	0.14 ±0.0006	0.20 ±0.001	4.14 ±0.010	4.17 ±0.036	0.37 ±0.002	15.12 ±0.046	0.38 ±0.002	1.79 ±0.007	2.35 ±0.008	1.95 ±0.007	0.51 ±0.003	0.38 ±0.003	0.26 ±0.001	0.03 ±0.0003
B4[b]	B4a	1.14 ±0.009	3.05 ±0.024	0.93 ±0.016	0.60 ±0.017	0.27 ±0.003	18.28 ±0.22	0.98 ±0.012	0.98 ±0.008	1.62 ±0.013	0.50 ±0.01	0.40 ±0.01	1.00 ±0.01	0.38 ±0.005	0.03 ±0.008
B5[b]	B5a	0.27 ±0.0008	0.40 ±0.001	0.97 ±0.003	0.87 ±0.003	0.15 ±0.001	10.43 ±0.06	0.66 ±0.002	0.83 ±0.01	0.99 ±0.006	0.70 ±0.003	0.15 ±0.001	0.42 ±0.001	0.39 ±0.001	0.02 ±0.0001

a Expts listed in Table 8.3.
b Thoracic-duct-cannulated rat.

Figure 8.8. Uptake of radioactivity in the spleen and cervical lymph nodes in the rat after injection of ^{111}In MRC OX-19.

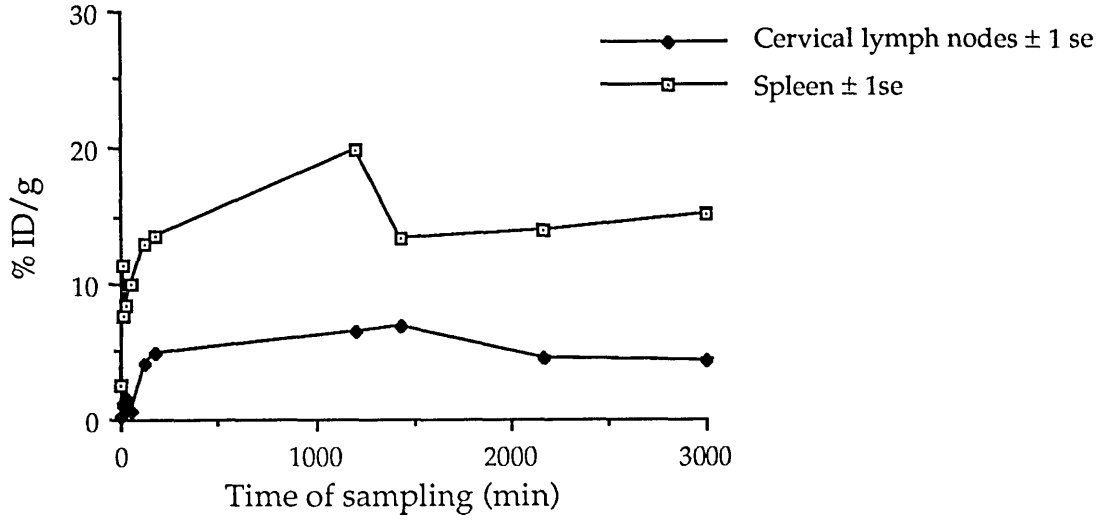

Figure 8.9. Blood kinetics of radioactivity and uptake in liver and muscle in the rat after injection of ^{111}In MRC OX-19.

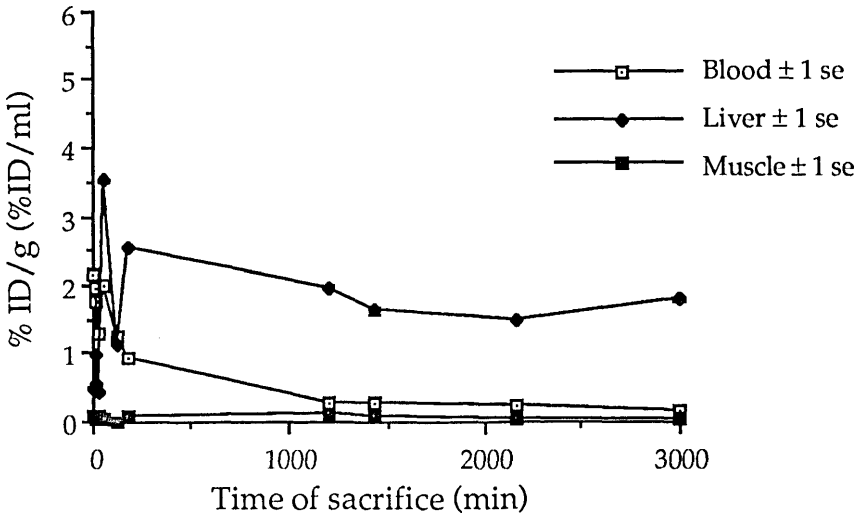

The injection of ^{111}In MRC OX-19 in two rats with indwelling cannulae in the thoracic duct resulted in radioactivity in the lymph very soon after injection. Part of this radioactivity was associated with the cell fraction in the lymph. In the first rat (Expt B4, Rat B4a), only two lymph fractions were collected over two hours (1 hr each fraction) after injection of ^{111}In MRC OX-19 and the cells were stained by immunofluorescence to check antibody binding to TDLs. The percentage fluorescence was 54.8% in fraction 1, 36.6% in fraction 2 and 64.9% in a positive control of lymph collected before Ab injection and stained with excess MRC OX-19 added in vitro. Fraction 1 contained 0.44±0.005 % ID/ml lymph and 0.04±0.001% ID was cell associated (≈ 10% of the radioactivity in the lymph). The corresponding values for fraction 2 were : 0.55±0.007%ID/ml; 0.06±0.001 cell associated. In the second rat, the collection of thoracic duct lymph continued until 12 hr after injection of ^{111}In MRC OX-19. Twelve one-hourly fractions were obtained and the radioactivity in the lymph and that cell associated were measured in each (Table 8.9).

Table 8.9. Radioactivity in thoracic duct lymph after injection of ^{111}In MRC OX-19 in the rat (Expt B5, Rat B5a).

Lymph Fraction[a]	%ID/ml	%ID cell associated in 1 ml
1	0.51±0.001	0.06±0.0003
2	0.55±0.001	0.05±0.0002
3	0.41±0.001	0.03±0.0002
4	0.34±0.001	0.02±0.0002
5	0.32±0.0009	0.02±0.0002
6	0.30±0.0009	0.01±0.0002
7	0.25±0.0008	0.01±0.0001
8	0.26±0.0008	0.02±0.0002
9	0.21±0.0007	0.01±0.0001
10	0.19±0.0006	0.01±0.0001
11	0.22±0.0007	0.01±0.0001
12	0.21±0.0008	0.01±0.0001

a Time after Ab injection in hours.

The results of tissue sampling of the two cannulated rats are shown in Table 8.8 where a much lower uptake in the lymph nodes is noted in comparison to the intact animals due to depletion of T lymphocytes by drainage through the cannulated thoracic duct.

8.3.5 Direct comparison of the in vivo distribution of ^{111}In after injection of labelled antibody or labelled lymphocytes

A comparison was made of the distribution of intravenously injected ^{111}In MRC OX-19 with the distribution of lymphocytes pre-labelled in vitro with ^{111}In tropolone and then injected intravenously. The cell population labelled with ^{111}In, ie lymph node lymphocytes, comprised 70-75% CD5-positive cells and the cells were labelled with a dose of ^{111}In well within the limits of radiotoxicity for lymphocytes and previously shown to permit normal migration of the labelled cells in vivo (Chisholm et al 1979). The dose of ^{111}In McAb chosen was 40 μg/kg which was thought on the basis of earlier experiments to be sufficient for binding to a majority of CD5-positive cells, at least in the blood, without causing modulation of the glycoprotein from the cells. As a control, some animals were injected with the same dose of ^{111}In H17E2 (irrelevant) antibody. The results of the experiment are presented in Figure 8.10[1].

[1] For the experimental details see Table A8.6, Appendix, page 320.

Figure 8.10. Comparison of radioactivity distribution after injection of ^{111}In MRC OX-19, ^{111}In tropolone labelled lymph node cells or ^{111}InH17E2 McAb in intact rats (sampling at 2 or 24 hr after injection).

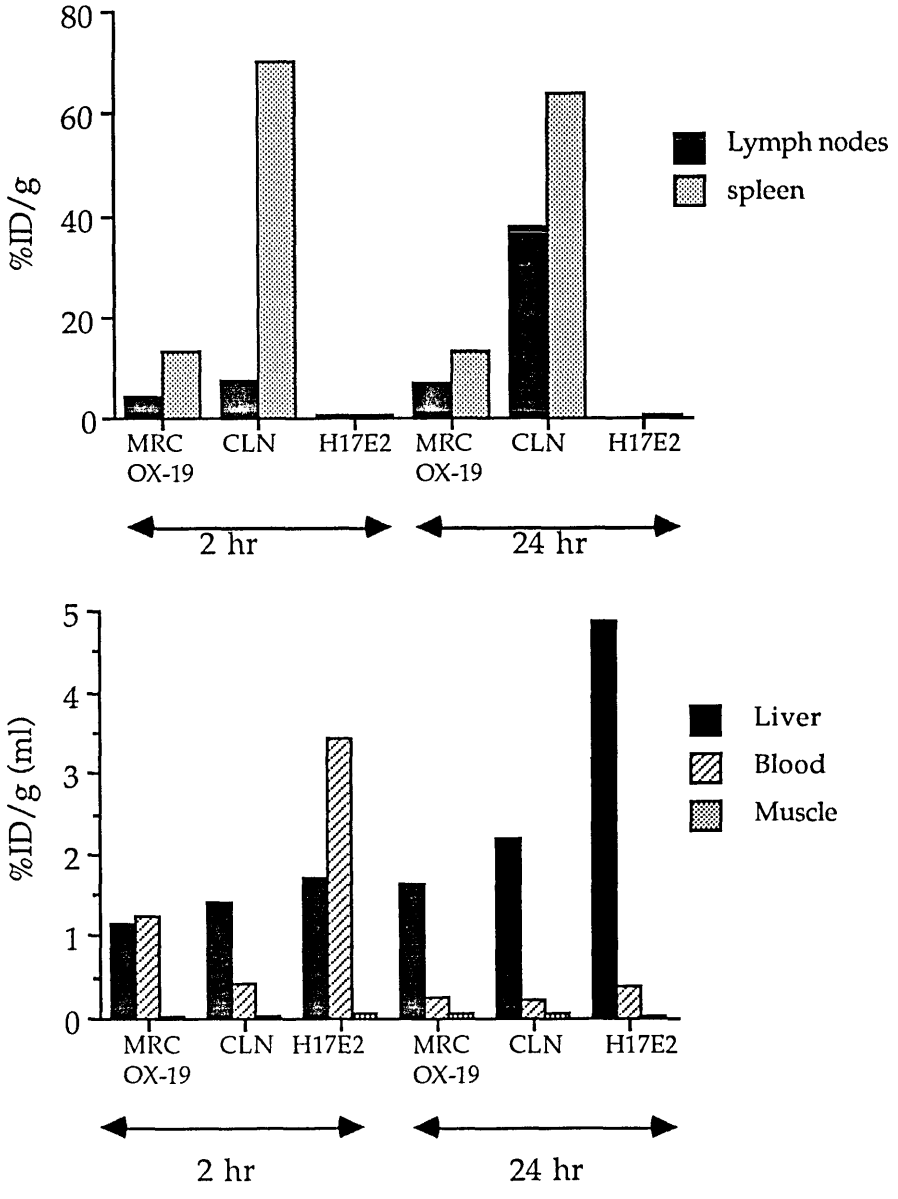

The findings with the labelled lymphocytes were exactly what one would expect from the results of numerous lymphocyte migration studies carried out in rats using many different radionuclides, including ^{111}In : Lymphocytes localised rapidly in the spleen, more slowly in lymph nodes and there was a concomitant loss of labelled cells from the blood which reflected this progressive accumulation in and migration through the

extravascular compartment of the lymphoid tissues. Injection of labelled MRC OX-19 antibody also resulted in localisation in the lymphoid tissues although the proportions of the injected ^{111}In found was less than was seen using cells pre-labelled in vitro. In contrast to the situation with labelled cells, in which almost all (90%) the radionuclide was and remained cell-associated, up to 70% of the ^{111}In found in the blood after injection of labelled antibody was in the plasma reflecting, presumably, an equilibrium between free and lymphocyte-bound antibody. The localisation of ^{111}In H17E2 (irrelevant) antibody was completely different : No localisation to lymphoid tissues, a substantial liver uptake and a high level of circulating antibody.

8.3.6 Scintillation camera imaging of rats injected with ^{111}In McAbs or cells

The animals used in the experiments described above were examined by scintillation camera early and up to 50 hours after injection. Whole body images taken soon (10-120 minutes) after injection of ^{111}In MRC OX-19 showed high localisation in the spleen and a substantial signal from the blood pool (Figure 8.11).

Figure 8.11. Static posterior view of rat B2a at 1 hr after injection of ^{111}In MRC OX-19. High radioactivity is seen in the spleen (red area), liver and blood pool in the heart. Radioactivity is also seen in the area of the bladder due ot secretion of non-Ab bound ^{111}In DTPA.

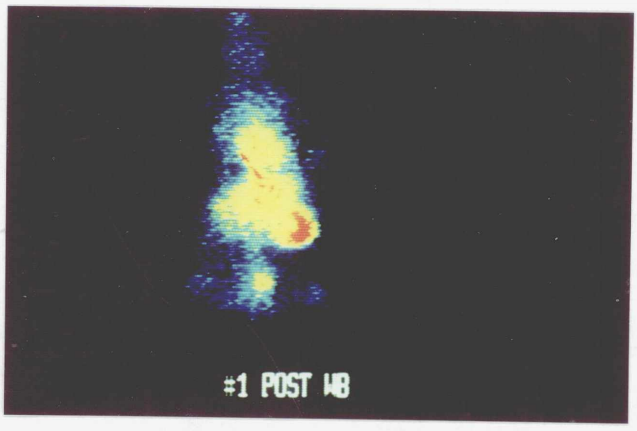

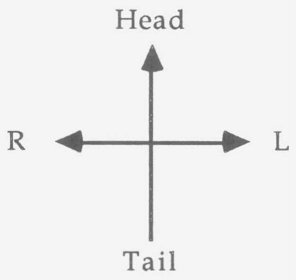

By 24 hours after injection of either labelled MRC OX-19 or labelled lymphocytes, the superficial cervical lymph nodes and the mesenteric chain of lymph nodes could be clearly visualised (Figure 8.12).

Figure 8.12. Uptake in lymph nodes 24 hr after injection of ^{111}In MRC OX-19 (rat C1b), left panel, and ^{111}In tropolone lymph node cells (rat C1d), right panel.

Fig 8.12A. Anterior view of the head and neck showing uptake in the cervical lymph nodes.

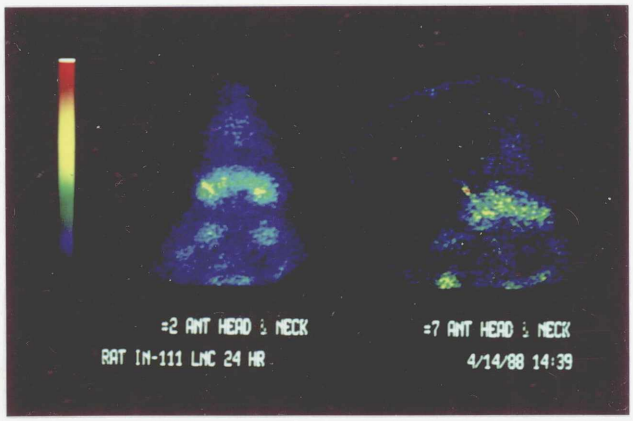

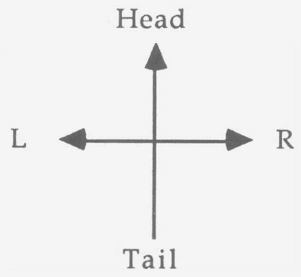

Fig 8.12B. Anterior view of the abdomen showing uptake in the mesenteric lymph nodes.

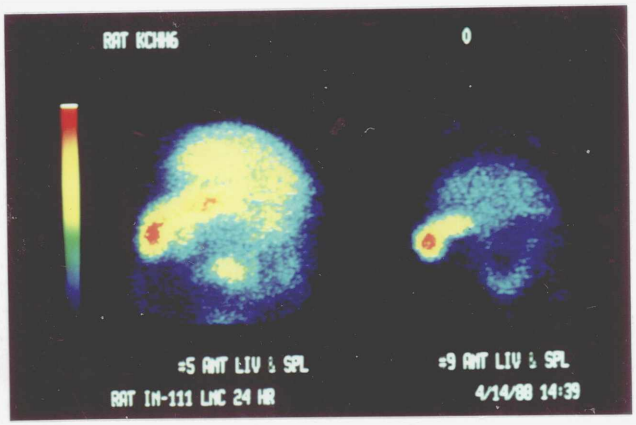

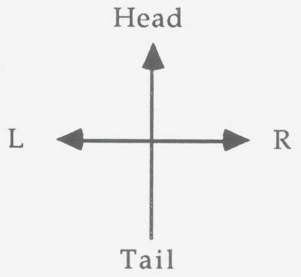

Whole body images taken at 24 hours (Figure 8.13) showed splenic uptake in animals injected with either ^{111}In MRC OX-19 or labelled cells and a rather high liver uptake in the animals injected with labelled McAb.

Figure 8.13. View of the posterior whole body 24 hr after injection of ^{111}In MRC OX-19 (rat C1b), left panel, and ^{111}In tropolone lymph node cells (rat C1d), right panel. Note the relatively high background and high liver uptake in the rat injected with McAb.

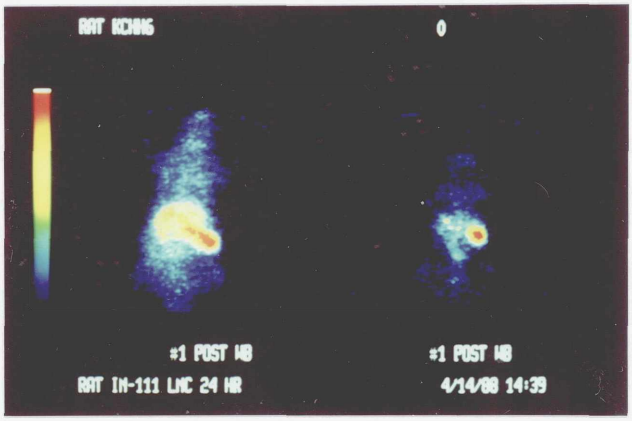

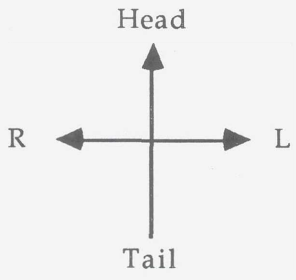

Images of animals injected with ^{111}In H17E2 demonstrated a gradually increasing localisation in the liver with a high blood pool persisting over 24 hours and no other tissue localisation.

8.3.7 Test of lymphocyte recirculation after labelling with ^{111}In MRC OX-19 in vitro; the dual labelling experiment

In the first two experiments[1] where TDLs were labelled in vitro with ^{111}In MRC OX-19 and injected into the same cannulated animal, radioactivity was detected in the lymph early after injection. Part of this radioactivity was cell associated.

In the third experiment, TDL double labelled (^{111}In MRC OX-19 and FITC) were followed in the lymph collected from the cannulated rats. Fluorescent

1 See paragraph 8.2.11 and Footnote 1 page 135.

cells were detected in the lymph pointing to recirculation of the double labelled cells. The results of lymph and tissue sampling are shown in Table 8.10.

Table 8.10. Results of lymph and tissue sampling in the experimental group D (testing of lymphocyte recirculation after ^{111}In MRC OX-19 labelling in vitro).

I. Lymph sampling

Expt D1, Rat D1a (2 hr after injection of ^{111}In MRC OX-19-TDL)

Lymph fraction[a]	Duration	%ID/ml	%ID/ml cell bound	IF[b]
1 (1)	1hr	0.044±0.010	0.005±0.0004	ND[c]
2 (2)	1hr	0.010±0.0001	0.0024±0.0007	ND

Expt D2, RatD2a (24 hr after injection of ^{111}In MRC OX-19-TDL)

Lymph fraction[a]	Duration	%ID/ml	%ID/ml cell bound	IF[b]
1 (2)	2hr	0.094±0.003	0.002±0.0007	ND
2 (3)	1hr	0.113±0.003	0.005±0.0008	ND
3 (4)	1hr	0.073±0.002	0.007±0.0008	ND
4 (12)	8hr	0.023±0.001	0.004±0.0008	ND
5 (14)	2hr	0.030±0.001	0.007±0.0008	ND
6 (15)	1hr	0.033±0.001	0.007±0.0008	ND
7 (16)	1hr	0.032±0.001	0.007±0.0008	ND
8 (17)	1hr	0.022±0.001	0.005±0.0008	ND
9 (18)	1hr	0.025±0.001	0.005±0.0007	ND
10 (19)	1hr	0.023±0.001	0.007±0.0008	ND
11 (20)	1hr	0.027±0.001	0.007±0.0008	ND
12 (21)	1hr	0.020±0.001	0.007±0.0008	ND

Expt D3, Rat D3a (19 hr after injection of ^{111}In MRC OX-19+FITC-TDL)

Lymph fraction[a]	Duration	%ID/ml	%ID/ml cell bound	IF[b]
1 (1)	1hr	0.073±0.001	0.002±0.0003	-ve
2 (2)	1hr	0.048±0.0008	0.002±0.0003	-ve
3 (3)	1hr	0.045±0.0008	0.001±0.0003	-ve
4 (4)	1hr	0.073±0.001	0.002±0.0003	-ve
5 (5)	1hr	0.053±0.008	0.002±0.0003	-ve
6 (6)	1hr	0.038±0.0007	0.002±0.0003	+ve
7 (8)	2hr	0.051±0.0009	0.002±0.0003	+ve
8 (16)	8hr	0.025±0.0006	0.002±0.0003	+ve
9 (19)	1hr	0.019±0.0006	0.003±0.0003	+ve

Table 8.10. Cont.

Expt D3, Rat D3b (43 hr after injection of ^{111}In MRC OX-19+FITC-TDL)

Lymph fraction[a]	Duration	%ID/ml	%ID/ml cell bound	IF[b]
1 (16)	16hr	0.005±0.0002	0.001±0.0001	+ve, 1%
2 (17)	1hr	0.006±0.0002	0.001±0.0001	+ve, 2%
3 (18)	1hr	0.006±0.0003	0.0007±0.0001	+ve, 2-3%
4 (19)	1hr	0.007±0.0003	0.0009±0.0001	+ve, 3%
5 (20)	1hr	0.005±0.0003	0.0008±0.0002	+ve, 2%
6 (22)	2hr	0.004±0.0003	0.001±0.0002	+ve, 1-2%
7 (24)	2hr	0.004±0.0003	0.001±0.0001	+ve, 5-6%
8 (26)	2hr	0.004±0.0002	0.0009±0.0001	+ve, 5%
9 (28)	2hr	0.004±0.0002	0.001±0.0001	+ve, 1-2%
10 (30)	2hr	0.003±0.0002	0.0007±0.0001	+ve, 1-2%
11 (32)	2hr	0.002±0.0001	0.0004±0.0001	+ve, 1%
12 (41)	9hr	0.003±0.0003	0.0006±0.0001	+ve, 1%
13 (43)	2hr	0.002±0.0001	0.0006±0.0001	+ve, 0.5%

a The numbers in brackets show the time after injection of the cells in hours.
b IF : Result of immunofluorescence testing (-ve : negative, +ve : positive).
c ND : Not done.

II. Tissue sampling

	%ID/g (ml)			
	Expt D1	ExptD2	ExptD3	
Tissue	Rat D1a	Rat D2a	Rat D3a	Rat D3b
W B	0.51±0.003	0.03±0.001	0.05±0.001	0.004±0.0005
Pl	0.70±0.004	0.04±0.002	0.062±0.001	0.007±0.0005
CLN	2.91±0.050	1.47±0.05	0.987±0.01	0.14±0.002
MLN	3.70±0.037	0.78±0.019	0.595±0.009	ND
Thy	0.09±0.003	0.06±0.002	0.063±0.002	0.005±0.0008
Spl	3.35±0.014	6.85±0.833	9.55±0.065	1.07±0.007
Lung	26.45±0.085	0.48±0.005	1.29±0.010	0.10±0.003
Liver	1.22±0.009	1.99±0.008	1.29±0.007	0.33±0.002
Kid	3.08±0.007	1.02±0.004	0.61±0.004	0.09±0.0006
PP	2.01±0.041	0.31±0.016	0.30±0.008	ND[c]
Int	0.17±0.017	0.05±0.006	0.023±0.002	ND
Tib+BM	1.58±0.009	0.21±0.002	0.924±0.006	ND
Tib	0.76±0.007	0.11±0.002	ND	ND
Muscle	0.03±0.002	0.006±0.001	0.005±0.0003	0.0008±0.0001

Early localisation of the cells was noted in the lungs in rat D1a. This lung uptake decreased at 24 hr and localisation in spleen and lymph nodes was observed in the other rats. Radioactivity in the lymph was noted in all animals and cell bound fraction ranged between 2-35%. Immunofluorescent cells in the lymph were mainly detected in the late fractions after 5 hours of the injection of the double labelled cells.

8.4 Discussion

8.4.1 Testing in vitro the immunoreactivity of ^{111}In MRC OX-19 antibody and its binding to blood and lymph node cells

MRC OX-19 was labelled with ^{111}In at a specific activity of 650 MBq/mg (18 mCi/mg). This was in agreement with earlier reports on antibody labelling using this method (Hnatowich et al 1982 & 1983). The antibody retained 50% of its immunoreactivity after purification and ^{111}In labelling, which was acceptable for use experimentally provided allowance for the non-reactive fraction be made in the interpretation of experimental data.

The binding of ^{111}In MRC OX-19 to blood and lymph node cells using similar lymphocyte numbers showed that 12-35% of the total antibody added was cell bound when Ab concentration was between $5X10^3$-10^6 Ab/cell. This finding pointed to the useful range of antibody concentration for the purpose of radiolabelling T lymphocytes by ^{111}In MRC OX-19, ie between $5X10^3$-$5X10^4$ Ab/lymphocyte.

8.4.2 In vivo tests

8.4.2.1 Studies using unlabelled antibodies; in vivo antibody binding and antigen modulation

Analysis of in vivo binding of monoclonal anti-CD5 antibody by indirect immunofluorescence established the following :

(1) Whether or not cells in different lymphoid compartments had bound the antibody,

(2) what proportion of the CD5-positive cells in any one compartment had bound the antibody,

(3) whether or not modulation, ie loss of the CD5 glycoprotein from the cells which bound the antibody had occurred and

(4) provided an estimate of the relative amounts of antibody bound per cell in different compartments by analysis of the intensity of fluorescence within the positive cell populations.

This strategy allowed a far more detailed analysis of in vivo binding of an anti-lymphocyte antibody than was possible using radiolabelled antibody and simply measuring the in-vivo distribution of the radionuclide. Using unlabelled antibody it was possible to identify by immunofluorescence a dose of antibody which gave good binding to lymphocytes, ie which bound to a high proportion of the cells in peripheral blood, spleen and lymph nodes, but which did not alter substantially the cell surface expression of the glycoprotein to which the antibody was directed. For the purpose of imaging lymphocytes, it was important that the antibody did not alter the function of the cells to which it bound. Cross-linking of cell surface glycoproteins on lymphocytes by antibodies could alter lymphocyte function in two ways : it could result in loss of function through loss of the molecule from the cell surface by exocytosis or internalisation, thus rendering the cell "invisible" for imaging purposes or, alternatively, it could activate the cell through delivery of a mitogenic signal (Clevers et al 1988). Modulation of CD3 glycoproteins from human peripheral blood lymphocytes regularly occurred following repeated injections of anti-human T cell McAbs to achieve reversal of transplant rejection (Russell et al 1984) but there had been little information on the likelihood of it occurring after a single imaging dose of antibody. Alternatively, cross-linking at the cell surface by antibody in vitro could activate the cell through delivery of a mitotic signal (Clevers et al 1988) although this would perhaps be less likely following in vivo administration of antibody. In the model presented in this thesis, a single dose of 400 μg/kg of antibody was sufficient to cause modulation on a

majority of peripheral blood lymphocytes within two hours. The experimental system used made it possible to measure the binding of radiolabelled antibody by radioactive counting and by immunofluorescence as well as determine whether or not modulation of the CD5 glycoprotein had occurred by using a second non-cross-reacting antibody with specificity for the same cell population in the immunofluorescence analysis. A similar strategy should be employed in clinical imaging studies since modulation would profoundly alter the in-vivo distribution of radiolabelled antibody and complicate interpretation of any images obtained.

8.4.2.2 Studies using ^{111}In McAbs and ^{111}In tropolone labelled lymphocytes

Direct comparison of ^{111}In distribution following injection of labelled anti-lymphocyte antibody or pre-labelled lymphocytes using the ^{111}In tropolone technique identified similarities and differences in the results obtained using the two methods. The amount of McAb injected in these experiments was a dose previously determined in experiments using unlabelled antibody to result in binding in vivo without modulation. The amount of ^{111}In used to label the antibody or the cells was estimated to be within the safety limits[1] for radiation damage to lymphocytes (Goodwin and Meares 1985) whether the cell bound the radionuclide at the cell surface in vivo or internally after labelling of the cells in vitro. Both injection of labelled antibodies and cells resulted in clear scintillation camera images of lymphoid tissues, ie of the spleen and some lymph nodes. The degree of labelling of superficial lymph nodes achieved with either method generated signal to background ratios on the scintillation camera comparable to those obtained in mice after injection of an ^{111}In anti-mouse histocompatibility alloantigen McAb (Goodwin et al 1985).

---

1 ^{111}In MRC OX-19 radioactivity up to 0.5 milliBq (0.01pCi) per cell from estimates in blood and lymph, ^{111}In tropolone radioactivity : 3 milliBq (0.08pCi)/cell.

Quantitative analysis by radiation counting in tissues showed significantly greater accumulation of ^{111}In labelled cells than ^{111}In labelled McAb in lymph nodes. The kinetics of ^{111}In-tropolonate-labelled lymph node cells followed the normal pattern of migration of labelled lymphocytes reported previously (Chisholm et al 1979, Rannie et al 1977). This pattern (see Figure 8.10, page 154) was of early splenic localisation and gradual increase of lymph node uptake after injection of the labelled cells. The decrease of activity in the spleen between 2 and 24 hr indicated lymphocyte migration from this organ to lymph nodes. The difference in the distribution of radioactivity between antibody and labelled cells could therefore reflect a difference in which the radionuclide reached the tissues; whereas the presence of radionuclide in lymph nodes after injection of labelled cells could be unambiguously attributed to migration of the labelled cells from the blood into the tissues, localisation of the radionuclide following injection of labelled antibody could be a consequence either of antibody binding to cells in the blood followed by their migration to the tissues, or alternatively, it could result from antibody binding to cells in situ after its perfusion into the tissues. This experimental system could not distinguish between these two possibilities. It was an important point, however, since in imaging studies the former would furnish a measurement of lymphocyte migration whereas the latter would provide only a static image of lymphocyte distribution. Comparative studies using labelled IgM and IgG McAbs with specificities for the same lymphocyte population should clarify this issue since IgM but not IgG immunoglobulins remain confined to blood.

The second difference in the scintillation camera images and radionuclide distribution in tissues between injection of labelled anti-T-cell antibody or labelled cells was that there was a greater blood (plasma) pool of radioactivity both early and late (24 hr) after injection of antibody. The

sensitivity of the labelled antibody system could perhaps be increased by injection of heterologous anti-Ig to clear the blood of unbound McAb immediately before scanning (Goodwin and Meares 1985) and this might allow detection of more deep-seated lymph nodes at an earlier time after injection of antibody .

8.4.2.3 Recirculation of in vitro ^{111}In MRC OX-19 labelled cells after injection in vivo

The use of an independent cell label (fluorescein) to check whether autologous thoracic duct lymphocytes that had bound ^{111}In MRC OX-19 in vitro recirculated back to lymph after intravenous injection gave support to the notion that lymphocytes kept their migratory capability after binding the antibody. In the experimental system used, however, the answer to the question of recirculation was given, essentially, as presence or absence of FITC labelled cells in the lymph and a rough estimate of their percentage therein by counting manually their number under a fluorescence microscope. The percentage was in the region of 0.5-6% and reflected most likely recirculation of lymphocytes that had bound the antibody in vitro. Although testing of the recirculation of lymphocytes that bound ^{111}In MRC OX-19 showed some evidence of this happening in the rat, the functional competence of these cells could not be ascertained in the experiments described. The functional testing would involve tracing of specific lymphocytes undergoing activation in a given condition, which would necessitate the use of another marker (other than CD5 present on all T cells) for cell detection. This condition was provided experimentally by the use of an anti-activated T cell monoclonal antibody in an allogeneic renal transplantation model described in detail in the next section.

8.4.3 Cellular and whole body dosimetric estimates; implications for use of a similar method in man

8.4.3.1 Microdosimetry of ^{111}In MRC OX-19

The radiation damage to lymphocytes by emissions from ^{111}In is mediated almost exclusively through damage to the DNA inside the nucleus (Anderson et al 1974, Sprent et al 1974). The efficiency of the transfer of energy from radioactive decay products to the genetic material varies enormously depending on the range, energy and location of the emissions. ^{111}In emits about 345 Auger-type electrons of various energies when any of its unstable nuclei disintigrates(Sastry and Rao 1984, Rao et al 1988). About 30% of these have an effective range (the distance over which most of the energy is dissipated) of 0.2 μm and if located in the cytoplasm can act only at the periphery of a 3.5 μm-diameter-lymphocyte nucleus. Five percent have a range of more than about 6 μm and can thus have an effect from anywhere in the cell or even from the cell surface. Sixty-seven percent have an energy of 600 eV and range of only 25 nm and can have very localised effects. It has been calculated (for cells slightly larger than lymphocytes) that the values of absorbed fractions, the ratio of energy absorbed in the nucleus to that emitted either in the nucleus or in the cytoplasm, vary over a range of 25 : 1 (Sastry et al 1987). Deposition of only a few hundred electron volts in the DNA of a cell is very likely to produce double strand breaks that lead to inactivation of the cell (Charlton 1987). The very low energy particles constituting the largest proportion of the spectrum of ^{111}In may therefore be extremely disruptive when emitted close to the nucleus. They have negligible effect, however, if produced even a few tens of nanometers away from the nucleus. Thus, for any attempt at calculating the microdosimetry of the radionuclide, it is essential to have an exact map of the localisation of the indium atoms in the nucleus and in the vicinity of the DNA.

The amount of damage due to loading the cells with indium labelled carrier is therefore dependent on the extent to which it is localised in the cell surface, cytoplasm or nucleus (Makrigiorgos et al 1989). As a rough guide, bearing in mind the difficulty of assessing the actual dose, the relative biological effectiveness (a measure of relative damage or relative effective dose) may be used as a proxy for cell damage. Since RBEs of 4.3 and 2 have been reported for ^{111}In oxine (80% nuclear) and ^{111}In citrate (30% nuclear) respectively (Sastry et al 1987), it would be expected that the radiation effect will be diminished even more in the case of ^{111}In MRC OX-19 (cell surface and probably low cytoplasmic localisation) compared to ^{111}In oxine and citrate. In order to measure the cell damage (and thus give a rough indication of dose to the cell in conventional terms) a cell survival curve for each radiopharmaceutical loading the cell could be established.

8.4.3.2 Whole body dosimetry using ^{111}In anti-T cell antibody in man based on ^{111}In MRC OX-19 data in the rat

Estimation of whole body dosimetry from the use of an ^{111}In anti-T cell McAb in man was attempted depending on the biolocalisation data of ^{111}In MRC OX-19 in the rat. This calculation was based on two assumptions :

The first considered the relative masses of organs to whole body mass to be same in the rat and man. This assumption was tested to be valid (especially for blood, spleen, lymph nodes, liver, lung and muscles) by referring to values of organ masses in man (ICRP 1975, Williams and Leggett 1989) and in the rat (Palou et al 1983, Smith and Ford 1983).

The second assumption was that the distribution of the putative ^{111}In anti-T cell McAb among different organs in the human would follow the pattern of ^{111}In MRC OX-19 in the rat after intravenous injection. The validity of this assumption was supported by the similarity in relative organ weights of

man and rat mentioned above and the similarity in the kinetics of ^{111}In labelled McAbs in the man and the rat in broad terms (blood clearance, localisation in liver, low excretion in the urine, etc).

Thus, based on the rat data for uptake and time course of localisation of ^{111}In MRC OX-19 in rat organs, a prediction could be made of the approximate dosimetry in human. The rat data showed highest uptake in the bone (equivalent to a maximum of 15% of the administered dose), liver (13%) spleen (8%) and Kidney (3%). The kinetics of ^{111}In indicated a maximum uptake within the first day with a long retention. Calculations of the effective dose equivalent, based on a worst case model considering instant uptake, infinite retention and complete decay inside the organ, were carried out for all the standard organs of interest (Snyder et al 1975). The results gave an effective dose equivalent of 0.2 mSv/MBq administered dose[1]. Most of the contribution to the total dose equivalent came from the spleen (65%), liver (18%) and kidney (15%) and little dose was associated with the bone marrow or gonads. The lymph nodes received a dose of about 20 μGy/MBq administered dose. The value found for the effective dose equivalent may be compared to figures published for ^{111}In labelled leucocytes, lymphocytes and platelets of about 0.65 mSv/MBq (Johansson 1984).

8.4.4 Summary

The ^{111}In anti-T lymphocyte antibody can be used to image lymphoid tissues by scintillation camera. Modulation, caused by antibody binding to the lymphocyte surface molecule for which it is specific within hours of a single injection, has identified a limitation on the amount of antibody which can be bound to the cell surface in vivo for imaging purposes. Nevertheless, a dose of antibody has been found which binds to lymphocytes in vivo without modulation and which is sufficient to enable external imaging of

---

1 For details see Table A8.7, Appendix page 320.

lymphoid tissues by scintillation camera. It should prove possible to raise the threshold dose at which modulation occurs by using fragments of antibody; this would also result in a more selective localisation within lymphoid tissues (Houston et al 1980) and, hence, better external images.

As well as measuring in vivo binding by radionuclide distribution and immunofluorescence analysis, the use of immunocytochemistry has identified exactly areas where the antibody has bound within lymph nodes and spleen. This confirmed that the anti-CD5 antibody localised selectively within the T-dependent areas of lymphoid tissues. The method should therefore enable in vivo localisation of antibodies directed against different lymphocyte subpopulations at the level of the lymphoid tissue microenvironment.

Finally, the experimental work presented in this study cannot directly compare the degree of radiation damage incurred on the cells by either of the two radiolabelling methods used : ^{111}In anti-lymphocyte McAb or ^{111}In tropolone in-vitro labelling. This makes judgement on the advantage of using one of the techniques rather than the other in terms of its relative innocuity and less damaging radiation effect hard to reach especially that function at the cellular level should be considered for this decision. However, the notion that antibodies bind to the cell surface, thereby rendering the nucleus less exposed to very short range Auger electrons of ^{111}In decay, would put radiolabelled antibodies in a better position than cell labelling with the lipophilic chelates in this respect. This could be amenable to study in a system where functional end-points as well as morphological changes, both cellular and at the DNA level, are tested after exposure of lymphocytes to different labelling agents including radiolabelled monoclonal antibodies.

Chapter 9 :

Radiolabelling Human T or B Lymphocytes with ^{111}In Monoclonal Antibodies

In Vitro Tests and Implications for Use in Vivo

9.1 Introduction

The rationale for in vivo use of radiolabelled monoclonal antibodies for cell labelling has been discussed previously[1]. For achieving this aim, background knowledge from experimental models such as that presented in the previous chapter and from in vitro tests of candidate antibodies is important to predict to some extent usefulness and practicability of in-vivo antibody use in man.

This chapter provides an active argument for the choice of antibody for lymphocyte targeting. Examples of in vitro tests employing T or B lymphocyte surrogates for testing the binding of anti-lymphocyte antibodies to cells and the implications of the findings for in vivo imaging of lymphocytes or radiotargeting tumours especially leukaemia and lymphoma are presented.

9.2 Anti-human lymphocyte monoclonal antibodies; reactivity, availability and previous experience in their use in vitro and in vivo

9.2.1 Antibody reactivity

Since the introduction of the monoclonal antibody technology, the number of anti-human lymphocyte McAbs has been increasing steadily. Various reactivities of the antibodies with normal and leukaemic/lymphomatous

---

1 See Aims and Objectives page 25 and Chapter 8 page 116.

lymphocytes have been reported and the specificity of such antibodies defined by various techniques including immunofluorescence, immunochemistry and radiobinding assays. The choice of an antibody for a specific purpose such as in vitro tests or in vivo use will depend in the first instance on its reactivity and range of cross-reactivity with cells and tissues. Accordingly, the planning of in vivo use of anti-lymphocyte specific McAbs would necessitate a strict identification of a number of antibodies that make suitable candidates which bind to normal lymphocytes, leukaemic or lymphomatous cells and do not cross-react with other cells or tissues. This situation is akin to that encountered in the case of anti-tumour-associated-antigen McAbs for the specific targeting of tumours.

Also, the effect of antibody binding on the cell in vivo is a factor to consider, especially that various preparations of antibodies bearing the same specificity can show different effects after binding. These effects have been shown to belong to one or a combination of the following four phenomena : no effect observed, cell activation or antigen modulation, complement activation and cell lysis, and the triggering of antibody-dependent cell-mediated cytotoxicity (ADCC).

Although each antibody preparation should be tested separately for these effects, knowledge of antibody origin (mouse, rat or human), class (IgG, IgM etc), subclass (IgG_1, IgG_{2a}) and whether used as whole antibody or fragments ($F(ab')_2$, Fab') would orientate towards the most likely effect to occur. For example, the anti-lymphocyte McAb CAMPATH-1G which is a rat IgG_{2b} has been shown to cause depletion of human T lymphocytes by ADCC, while IgM and IgG_{2a} which are McAbs of the same specificity cause cell depletion by complement activation (Dyer et al 1989). These antibodies (CAMPATH-1M) have been used in vitro to deplete T lymphocytes in bone marrow. Other antibodies show modulation of the surface molecule that they bind to (see previous chapter, Chatenoud et al 1982).

In general, the use of antibody fragments in targeting cells has resulted in partial or total loss of antibody effector functions by deleting reactions that necessitate Fc portion mediation such as complement activation or ADCC, or by avoiding receptor cross-linkage in the case of using monomeric Ab fragments (Fab') (Sedlacek et al 1983).

Finally, the effect of the radiolabel on antibody kinetics in the body and on the cell it binds to, would decide whether in vivo use of the radiolabelled antibody is worthwhile. This is important especially when imaging is concerned as the non-invasive nature of the procedure as well as the obtention of a high target to background ratio are among the conditions required for such use.

9.2.2 Antibody availability

This is a factor which should not be overlooked when planning the use of anti-lymphocyte antibodies in vivo having decided upon the suitable antibody for the purpose of the study. Ample and reasonably priced supply is necessary and stringent quality control tests of the preparation in terms of sterility and apyrogenicity etc should be performed.

9.2.3 In vitro and in vivo use of anti-human lymphocyte monoclonal antibodies in the medical and scientific literature

9.2.3.1 In vitro use of anti-human lymphocyte McAbs

Presently, it is rare to find scientific articles dealing with lymphocytes without the mention of anti-lymphocyte McAbs and the molecules they recognise in these cells. In clinical practice, the identification of structures using monoclonal antibodies has been applied in the classification of lymphocytes and leucocytes in general for the purpose of

leukaemia/lymphoma phenotyping and in patients infected with HIV to follow progression of the disease (value of T4, CD4, cell number in blood).

9.2.3.2 *In vivo use of anti-human lymphocyte McAbs*

In vivo administration of anti-lymphocyte antibodies has been used in different situations. Unlabelled anti-lymphocyte antibodies have been injected intravenously in patients affected with leukaemia to target the malignant cells (Dyer et al 1989). Also, anti-T cell McAbs have been used to reverse organ transplant rejection (Thistlethwaite et al 1984) and in the treatment of aplastic anaemia (Doney et al 1985). In the management of systemic autoimmune disease such as intensive rheumatoid arthritis and multiple sclerosis, anti-T cell monoclonal antibodies have caused immunosuppression in the patients receiving them and improvement of the clinical condition of the arthritic patients for variable lengths of time (Herzog et al 1987, Hafler et al 1988).

Radiolabelled anti-lymphocyte McAbs have also been used experimentally and clinically for imaging and treatment of lymphoid malignancies.

Few reports examined the use of an anti-T cell McAb; T101 (Roysten et al 1980) for imaging and treatment of cutaneous T-cell lymphoma (CTCL). For scintillation camera imaging, ^{131}I or ^{111}In radiolabelled T101 was injected intravenously or subcutaneously at various doses in the patients studied. Areas of skin involvement and especially lymph nodes affected by lymphoma could be visualised clearly on the images taken 1, 3 & 6 days after injection of the labelled antibody (Bunn et al 1984, Carrasquillo et al 1986, Keenan et al 1987, Rosen et al 1987, Zimmer et al 1988). For imaging purposes, the ^{111}In labelled T101 was found superior to ^{131}I T101 in localising tumour as reported by Carrasquillo et al 1987.

Therapy of CTCL and CLL using the T101 McAb has also been tried. An early study used unconjugated T101 (Dillman et al 1984) and documented a transient beneficial effect of antibody infusion on the clinical condition. Antigen modulation and the production of endogenous anti-mouse antibodies were also observed after in vivo use of T101 McAb in that study. Subsequently, various conjugates (radionuclides, cytotoxic drugs, etc) of the T101 McAb have been tried for the treatment of T cell malignancies and recently for depletion of T cells from bone marrow grafts (Laurent et al 1989). In vitro studies using T101 conjugated with radionuclides, toxins or both (Boven et al 1986, Dillman et al 1986, Buchsbaum et al 1987) pointed to an enhanced killing effect on leukaemic cell lines expressing the antigen recognised by the T101 McAb (CD5).

The response of CTCL to radioimmunotherapy using ^{131}I T101 (Rosen et al 1987, Zimmer et al 1988) was favourable in some patients and its duration ranged from 3 weeks to 3 months. Again, problems associated with this treatment in relation to the generation of human anti-mouse antibodies were observed despite the performance of plasmapheresis to reduce Ab levels in plasma in some of the patients studied.

Targeting malignant B cells has also been tried using radiolabelled anti-B cell McAbs. Experimentally, ^{67}Cu-labelled Lym-1 McAb has been found to localise significantly in tumour xenografts of RAJI cells[1] grown in nude mice (Deshpande et al 1988). B cells in Burkitt's lymphoma patients have been targeted using ^{131}I Lym-1 McAb (De Nardo et al 1986). These workers reported partial remission in a majority of patients treated using a fractionated-dose or a maximum-tolerated-dose protocol. Also, ^{131}I anti-CD7 McAb was used in a high dose regime for treating lymphoma (Bernstein et

---

[1] malignant human B cells expressing the Class II major histocompatibility complex molecules.

al 1990) and the use of ^{90}Y anti-idiotype monoclonal antibodies was tried with some success in patients with B cell malignancies (Parker et al 1990).

9.3 In vitro experiments for testing ^{111}In labelled two anti-human lymphocyte (T or B) monoclonal antibodies

9.3.1 Aim and experimental setting

Experiments were conducted in order to establish an optimal in vitro approach for testing reactions of two radiolabelled anti-T & B cell McAbs with lymphocytes including antibody binding and its range. Also, measurement of the relevant parameters of these reactions such as the antibody binding constant and Ab elution in an antibody free medium were performed. The possibility of the antibodies affecting the cells was tested in terms of the antibody causing antigen modulation or internalisation and the radiolabel-antibody entity altering induced cell proliferation in vitro.

Technically, there was a need for a readily available source of cellular antigen to conduct the various in-vitro tests. For in human, the main source of lymphocytes for testing purposes would be peripheral blood providing a limited number of cells. An alternative way of getting high yields of cellular antigen was to grow suitable lymphocyte cell lines (see below) and use them in the tests performed in vitro along with experiments on peripheral blood mononuclear cells.

9.3.2 Materials and Methods

9.3.2.1 Monoclonal antibodies

UCHT2 (Pan T) recognises a 67 kDa protein on T lymphocytes present on more than 95% of circulating human peripheral T cells, on 5-10% B cells and on cells of B-cell chronic lymphocytic leukaemia. It is an IgG_1 mouse

immunoglobulin, CD5 in the IUIS/WHO cluster nomenclature (Beverley and Callard 1981, McMichael et al 1987).

WR-17 (Pan B) recognises a 40-45 kDa glycoprotein antigen designated as representative of the CD37 cluster of anti-Pan B lymphocyte McAbs. It is a murine IgG_{2a} and reacts with all peripheral blood human B cells (Moore et al 1987, McMichael et al 1987).

Both antibodies were kindly provided free of charge by Unipath-Oxoid, Basingstoke-UK, purified in PBS buffer, pH 7.4 and were kept at 4°C.

The antibodies were radiolabelled with indium-111 using the double-chelating agent DTPA method[1]. The specific activity obtained after labelling was between 260-550 MBq/mg (7-15 mCi/mg). ^{111}In labelled McAbs were stored in PBS, pH 7.4. They were sterile and apyrogenic[2].

Immunoreactivity of each McAb was tested in a radiobinding assay using the appropriate lymphoid cell line for each antibody (see below) in similar conditions to the assay reported for ^{111}In MRC OX-19 antibody (see page 121)[3], ie incubation for 2 hr at 37°C and cells washed twice before counting radioactivity.

9.3.2.2 Lymphoid cell lines and whole blood[4]

T cell lines : Two T cell lines, MOLT4 a common thymocyte cell line and HPB ALL a mature thymocyte cell line, were used for testing the McAbs (Ferrero and Rovera 1984). Both T cell lines expressed the molecule

---

1 For details on the method, see Chapter 5 page 49. For experimental details, see Tables A9.1, A9.2, A9.3, A9.4, A9.5 and A9.6, Appendix, pp321-325.

2 Sterility testing was performed by the Quality Assurance Unit, Pharmacy Dept, Hammersmith Hospital, London, England.

3 See Table A9.7, Figure A9.1, Table A9.8, Figure A 9.2, Table A9.9, Figure A 9.3, Appendix, pp325-328 for experimental details.

4 Handling of the cell lines and blood was done under aseptic conditions in a laminar air flow cabinet (Medical Air Technology Ltd, England) Immunology Dept, RPMS.

recognised by UCHT2 (CD5) and some markers of the T cell lineage[1] (McMichael et al 1987).

The B cell line EBV PGF, an Epstein-Barr-virus transformed B cell line[2], was also used for in vitro testing of the antibodies. This cell line was positive for CD37 (60%) and negative for CD5 (<5%) and E-rosetting (CD2).

All three cell lines were grown in RPMI 1640 medium containing 10% foetal calf serum (FCS). They were incubated in an atmosphere of CO_2 in air at 37°C.

Whole blood from normal volunteers was anticoagulated in acid-citrate-dextrose (ACD) NIH formula A BP (1 part ACD to 6 parts blood). Alternatively, defibrinated blood was used.

9.3.2.3 Indirect immunofluorescence of the two anti-lymphocyte McAbs with the lymphoid cell lines

Cells from each lymphoid cell line (see above) were adjusted to 10^7 cell/ml in Tris buffered salt solution (Favour 1964) containing 1% FCS (Tris BSS 1% FCS). To aliquots of 100 µl cell suspension (10^6 cells), the McAb (Pan T or B) was added in 25 µl aliquots in decreasing concentrations : 2 µg/ml (10^6Ab/cell), 200 ng/ml (10^5 Ab/cell) or 20 ng/ml (10^4 Ab/cell) in LP3 tubes. Negative control tubes containing no Ab were also prepared. Two similar sets of tubes were obtained. The first set was incubated for 3 hr at 4°C and the other at 37°C. Then, the cells were washed 3 times in Tris BSS 1% FCS in the cold (4°C) and the cell pellet incubated for 1 hr at 4°C with 50 µl 1/10 dilution in PBS of rabbit anti-mouse immunoglobulin fluorescein

---

1 MOLT4 was tested by indirect immunofluorescence for binding to H17E2 (-ve control McAb) : 0.50%, CD3 :0.52%, CD5 : 98.53%, CD4 : 52.37%. It was positive for E-rosetting. HPB ALL testing gave : H17E2 : 0.53%, CD3 : 78.25%, CD5 : 91.50%, CD4 : 99.25%, E-rosetting : +ve.

2 Dr S Man, Immunology Dept, RPMS, personal communication.

conjugated[1] (RAM-FITC). Washing was repeated 3 times as above and the cells were examined immediately under a UV microscope[2].

9.3.2.4 Radioimmunoassay of ^{111}In Pan T or ^{111}In Pan B with the lymphoid cell lines

Binding of ^{111}In Pan T (or ^{111}In Pan B) to the lymphoid cell lines was tested in 10 ml plastic centrifuge tubes containing 10^7 lymphoid cells[3] in 5 ml ($2X10^6$ cell/ml) in Tris BSS 1% FCS. ^{111}In labelled antibodies, diluted in PBS, were added in 100 µl volume. The concentration of antibody ranged between 0.05 ng-5 µg McAb/ml[4]. The tubes were sealed with parafilm then, they were placed on a rotating disk with gentle continuous mixing for 2 hr at 37°C. At the end of incubation time, 3 aliquots of 1 ml volume of the cell suspension were taken from each tube and transferred to LP3 tubes. The first was considered a standard. The cells in the other two tubes were washed 3 times in Tris BSS 1% FCS in the cold, then they were counted for ^{111}In in a gamma well counter. This provided a direct comparison of the radioactive count-rate cell-bound to the total count-rate present in the cell suspension (count-rate in the standard). The 2 ml volume left was used for cell viability testing and for performing other procedures as necessary (immunocytochemistry staining or autoradiography).

Another set of tubes was prepared similarly to above and unlabelled antibody (Pan T or Pan B) was added at a 100-time excess over the labelled antibody to measure non-specific binding.

---

1 Dako-Denmark.
2 Dialux 20, Leitz, Wetzlar, Germany.
3 Cell viability was >95% by trypan blue exclusion.
4 0.05 ng : 10^2 Ab/cell, 0.5 ng : 10^3 Ab/cell, 5 ng : 10^4 Ab/cell, 50 ng : 10^5 Ab/cell, 500 ng : 10^6 Ab/cell, 5 µg : 10^7 Ab/cell.

9.3.2.5 Monitoring the fate of cell bound ^{111}In Pan T or ^{111}In Pan B; binding parameter measurement (binding constant, Ab elution & internalisation)

A) Antibody binding constants

The experiments performed to measure the binding parameter of each of the anti-lymphocyte monoclonal antibodies described above, ie UCHT2 and WR-17, were done following the method of Mason and Williams (1986).

Accordingly, the affinity of the interaction between the McAb and its cellular antigen was considered to follow Equation 9.1 :

$$\text{Equilibration Constant Keq } (M^{-1}) = \frac{K+1}{K-1} = \frac{[Ab\text{-}Ag]}{[Ab].[Ag]} \qquad \text{Eq 9.1}$$

Where : K+1 : The antibody association constant ($M^{-1}s$).
K-1 : The antibody dissociation constant (s^{-1}).
[Ab-Ag] : The concentration of bound Ab or Ag (M).
[Ab] : The concentration of free antibody.
[Ag] : The concentration of free antigen.

The association rate constant K+1 was calculated by measuring the initial rate of antibody binding when cells ($2X10^6$/ml) and ^{111}In labelled McAb (10^5 or $5X10^4$ Ab/cell) were incubated together for various intervals of time (1-6 min) at 37°C in Tris BSS 1% FCS. The fraction of radioactivity which had reacted at time t was experimentally determined and K+1 was calculated from Equation 9.2 :

$$K+1 = \frac{\text{Fraction of Ab binding}}{[Ag].t} \qquad \text{Eq 9.2}$$

The antibody dissociation constant K-1 was measured in an experiment involving firstly incubation of the lymphoid cells ($2X10^6$/ml) with the ^{111}In labelled McAb (Pan T or Pan B) at 10^5 or $5X10^4$ Ab/cell for 2 hr at 37°C. Unlabelled antibody (same as the radiolabelled Ab used in the first part) was

added in a large excess (X1000 times) over the radiolabelled Ab and the percentage radioactivity cell associated was measured over time. The values of the relative cell associated activity versus time were plotted on semilog graph paper and the dissociation rate was calculated from the $t_{1/2}$ of the curve, Equation 9.3

$$K\text{-}1 = \frac{0.693}{t_{1/2}} \qquad \text{Eq 9.3}$$

The equilibrium constant was calculated from Equation 9.1 after substitution of the values of K+1 and K-1 obtained from Eq 9.2 and 9.3 above.

B) Antibody elution :

This experiment, based on a report by Matzku et al 1986, was performed to give an idea on the rate of loss of cell bound antibody after initial incubation at an antibody concentration giving optimal cell binding (highest Bound/Total ratio) once the cells were resuspended in antibody free medium.

The experimental setting was the same as that used in the radioimmuno-assay described above (Paragraph 9.3.2.4, page 117). The cells from the HPB ALL or the EBV PGF cell line were incubated in 10-ml-centrifuge tubes with ^{111}In Pan T or ^{111}In Pan B, respectively at $5X10^4$ Ab/cell for 2 hr at 37°C with gentle intermittent mixing. Afterwards, 3 aliquots of 0.5 ml were collected (1 standard), the cells were washed in 2 aliquots and the radioactivity in all three tubes counted. The rest of the cell suspension was washed 3 times in Tris BSS 1% FCS, resuspended in 3.5 ml fresh medium and re-incubated at 37°C with mixing. At different time points, three 200 µl aliquots were collected (1 Std) and ^{111}In radioactivity in the supernatant and that cell bound (after 2 washes) were determined. The count-rates obtained showed

antibody elution as a decrease in cell bound radioactivity with a concomitant increase in the count-rate in the supernatant.

C) Antibody internalisation (Matzku et al 1986)

The same setting described in the radioimmunoassay of ^{111}In Pan T & Pan B was used (see Paragraph 9.3.2.4, page 117). Suspensions of cells in centrifuge tubes were left to incubate with ^{111}In Pan T or ^{111}In Pan B at a concentration of 25 ng/ml ($5X10^4$ Ab/cell) at 37°C with gentle intermittent mixing. Three aliquots (200µl each) were collected at various time points (1 Std) in LP3 tubes. The cells in 2 aliquots were washed twice in Tris BSS 1% FCS and the final pellet resuspended in 1 ml glycin buffer pH 2.8 for 20 minutes at room temperature (this caused dissociation of surface bound Ab). Meanwhile, ^{111}In radioactivity in the suspension was counted, then the cells were washed twice as before and the radioactivity measured again. The latter count indicated the amount of radioactivity internalised within the cells.

9.3.2.6 Radioimmunoassays of ^{111}In Pan T and ^{111}In Pan B versus whole blood

The experimental setting used to test binding of ^{111}In McAbs (Pan T or Pan B) to the cells and the corresponding lymphocyte subset in blood involved two parts :

The first included addition of the ^{111}In McAb (Pan T or B), diluted in 100 µl PBS in increasing concentrations, to 5 ml ACD anticoagulated whole blood in 10 ml centrifuge tubes. The tubes were sealed and left to incubate for 2 hr at 37°C with gentle mixing on a rotating disk. At the end of incubation time, 1 ml ACD-blood was taken from each tube and transferred to a counting vial. A volume of 1.5 ml ACD-blood was centrifuged at 1500 g for

10 minutes and a volume of plasma equal to (1-Hct) ml[1] was obtained and counted for ^{111}In radioactivity. Data from these samples gave information on the ratio of cell bound to total radioactivity present in the same volume of blood. Non-specific binding was allowed for by preparing a similar set of tubes containig 100-time excess of unlabelled antibody to the ^{111}In McAb added.

The second part of the experiment included isolating T and B lymphocytes from the volume of blood left after the first part (2.5 ml) and measuring ^{111}In radioactivity associated with each cell type.

Density gradient centrifugation on Lymphoprep[2] was used. Blood was diluted 1:1 in normal saline, then it was carefully layered on 4 ml of Lymphoprep in a 10 ml centrifuge tube. The tubes were centrifuged at 100 g for 25 minutes and the lymphocyte + the monocytes (LM) were collected at the interface Lymphoprep-blood. The LM were washed twice in the cold in physiologic saline (150 g for 7 min) and then they were resuspended in 1-1.5 ml physiological saline. Cell counts were obtained and an aliquot of known volume (300µl) was left for radioactive counting. Using AET[3]-treated sheep erythrocytes (SRBC), the remainder cells were rosetted for 1 hr at 4°C (Kaplan & Clark 1974). The rosettes were separated from non-rosetted cells using density gradient separation on Lymphoprep as above. Each cell population (T or B cells) was collected separately, washed in the cold and resuspended in 0.5-1ml saline. The number of cells was measured and ^{111}In radioactivity in a known volume counted. From the counts obtained and after correction from the number of cells in the counted samples to the

---

1 Volume of plasma contained in 1 ml ACD-blood, the haematocrit was measured as part of a full blood count performed at the beginning of the experiment.

2 Lymphoprep, Nyegaard Norway.

3 AET : 2-aminoethylisothiouronium bromide, Sigma, England. AET 40 mg/ml pH 9.0, 1 vol packed SRBC was added to 4 vols of AET solution, incubated for 15 min at 37°C. The cells were washed 3 times in saline and a 1% suspension was prepared. A volume of 0.1 ml AET-treated SRBC was added to 0.05 ml FCS and 0.05 ml of lymphocyte suspension. The mixture was centrifuged at 150 g for 5 min and allowed to stand for 1 hr at 4°C.

number present in 1 ml whole blood[1], radioactivity bound to T or B lymphocytes was estimated.

9.3.2.7 Testing the effect of ^{111}In Pan T and ^{111}In Pan B on mitogen induced cell proliferation

A whole blood culture technique was used (Pauly et al 1973). Two 96-well microtiter plates[2] were prepared for testing each ^{111}In McAb. Total reactant volume in each well was 200 µl. Defibrinated blood was added to give approximately $5X10^4$ cells of the relevant cell population (T or B) per well[3]. Each plate was divided into four parts, each containing 3 columns of wells as seen in Figure 9.1.

Figure 9.1. Setting of the microtiter plate for the testing of mitogen induced cell proliferation in whole blood in the presence of ^{111}In Pan T or Pan B, unlabelled Pan T or Pan B, HMFG2 or medium alone.

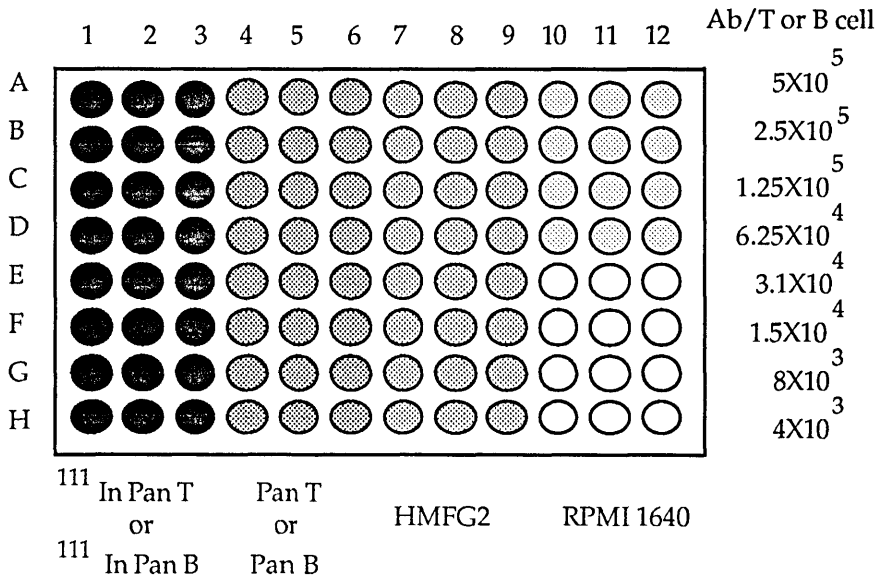

1 The ratio of T cells to all lymphocytes in blood was assumed to be 64% and for B cells 17.2% (Geigy Scientific Tables 1984).

2 Falcon, USA. U-shaped wells.

3 A full blood count was obtained for the defibrinated blood at the start of the experiment. T cell percentage of total lymphocytes was considered 64% and B cell percentage 17.2%.

To the first part, ^{111}In Pan T or ^{111}In Pan B in PBS was added in triplicate to the wells of the first row at a concentration of $5X10^5$ antibody/cell and in decreasing doubling dilutions to the next row and so on until the last row in the plate was reached. To the second part, the unlabelled Pan T or Pan B McAb was added in the same concentrations as the labelled McAbs and to the third part same antibody concentration as parts 1 & 2 of an irrelevant unlabelled antibody HMFG2 reacting with milk fat globules and no reactivity with blood cells (Taylor-Papadimitriou et al 1981). No antibody was added to the last part. The plates were left to incubate for 2 hr at 37°C in 5% CO_2 in air then the mitogen was added to the wells as follows :

1) In order to test the effect of ^{111}In Pan T, concanavalin A (Con A)[1] was added to all wells in one plate only (the other plate was left as control) at a concentration of 60 µg/ml. The plates were left to incubate (37°C, 5% CO_2 in air for 3 days), then [^{3}H] thymidine[2] was added at 1 µCi/well and the plates were left to incubate for a further 24 hr period before the cells were harvested.

2) To test the effect of ^{111}In Pan B, lipopolysaccharides (LPS)[3] from Escherichia coli 0111:B4 were added to all wells in one plate (the other was left as control) at a concentration of 15 µg/ml (Miller et al 1978, Smith et al 1979b). The plates were left to incubate overnight. Afterwards, pokeweed mitogen (PWM)[4] was added to the wells of the LPS stimulated plate at a concentration of 75 µg/ml and the plates were left to incubate for 5 days (Ault and Towle 1981). ^{3}H-thymidine was added to the plates at 1 µCi/well. They were then left to incubate for another 24 hr before the cells were harvested.

---

1 Lectin from Canavalia Ensiformis, Lot No : 85F8875, Sigma, England.
2 Amersham International, England.
3 Lot No. 57F-8845, Sigma , England.
4 Lectin from Phytolacca Americana, Lot No 96F-9675, Sigma, England.

At the end of the incubation with ^{3}H-thymidine all plates were treated as follows : The red blood cells were lysed in 3% acetic acid and the remaining leucocytes were harvested using a semi-automatic cell harvester[1] on glass-fiber paper[2]. The resulting paper discs were bleached with hydrogen peroxide, dipped in a vial containing liquid scintillation cocktail[3] and counted in a beta liquid scintillation counter[4].

9.3.3 Results of in vitro experiments

9.3.3.1 Binding of Pan T and Pan B to the lymphoid cell lines tested by indirect immunofluorescence; the effect of temperature

Indirect immunofluorescence of Pan T and Pan B McAbs versus the 3 cell lines tested : EBV PGF, MOLT4 and HPB ALL showed specific binding of Pan T to the T cell lines MOLT4 & HPB ALL and the Pan B to the EBV PGF B-cell line. The results of incubation at 4°C and 37°C were concordant in terms of number of positive cells stained and intensity of fluorescence[5]. However, the pattern of fluorescence showed some difference : diffuse pattern around the cells using both McAbs at 4°C and diffuse with discrete dots of fluorescence after incubation with the antibodies at 37°C. This effect was more pronounced using Pan T, in which case some cells displayed total capping of the fluorescence in one discrete dot in one pole of the cell.

---

1 Skatron, Norway.
2 Whatman, England.
3 ASC, Amersham International, UK.
4 LKB-Wallace, Sweden.
5 Immunofluorescence of the T cell-lines stained with UCHT2 was >95% and the B-cell line with WR-17 >90%. Fluorescence intensity ranged from weak positive, positive, to strong positive (arbitrary score).

9.3.3.2 Radioimmunoassays of ^{111}In Pan T and ^{111}In Pan B to the lymphoid cell lines and whole blood

The radioimmunoassays of ^{111}In Pan T and ^{111}In Pan B versus the 3 lymphoid cell lines showed specific binding of ^{111}In Pan T to the T cell lines (binding to the B cell line <1% at all Ab concentrations used) and specific binding of ^{111}In Pan B to the B cell line (binding to the T cell lines <1% at all Ab concentrations used). These results confirmed previous reports on the characterisation of the two McAbs (McMichael et al 1987).

Results of the radioimmunoassay of ^{111}In Pan T versus the T cell line HPB ALL & MOLT4 and ^{111}In Pan B versus the B cell line PGF are shown in Figure 9.2 and 9.3 respectively[1].

Figure 9.2. Binding of ^{111}In Pan T (UCHT2) to the T cell lines HPB ALL and MOLT4.

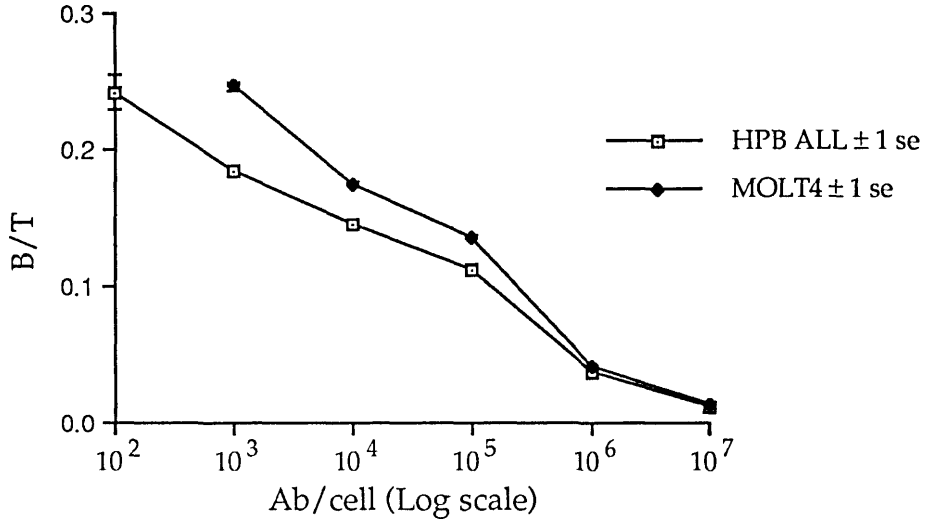

This graph shows very low relative binding at high Ab concentrations. The optimal binding ratio of 0.12-0.25 is obtained with Ab concentration of 10^5-10^3 Ab/cell.

---

1 For the experimental data, see Table A9.10, A9.11 and A9.12 Appendix, pp328 & 329.

Figure 9.3. Binding of ^{111}In Pan B (WR-17) to the B cell line EBV PGF.

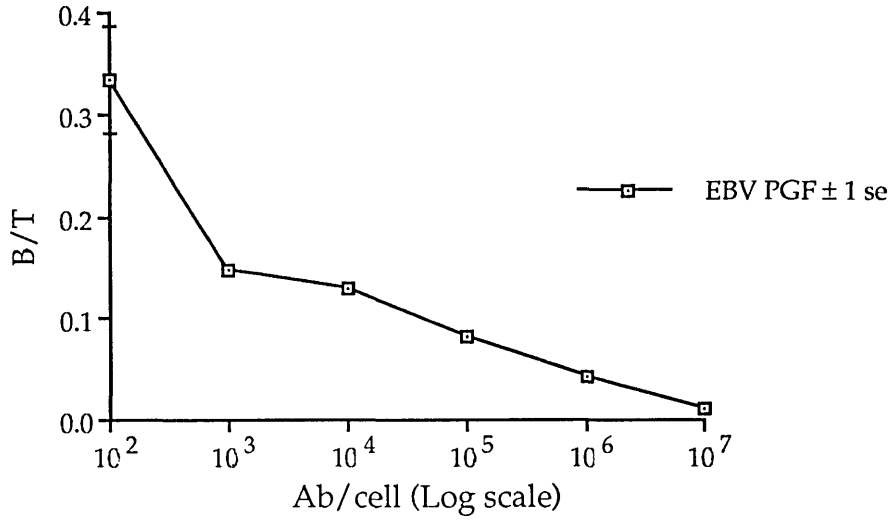

A similar pattern of binding to the above is also seen with this McAb.

The results of the radioimmunoassays of the ^{111}In McAbs versus ACD-blood are shown in Figure 9.4 (Pan T) and 9.5 (Pan B)[1].

Figure 9.4. Binding of ^{111}In Pan T (UCHT2) to ACD-whole blood.

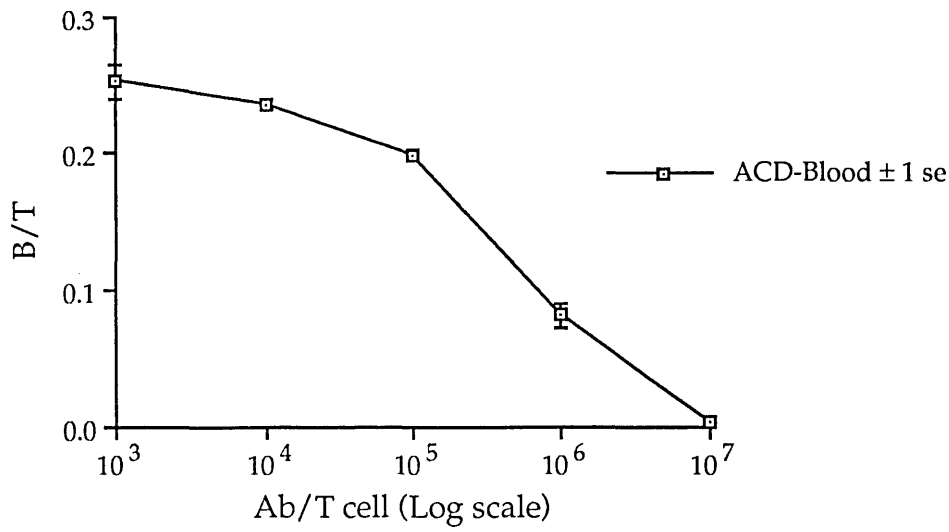

1 For the experimental data, see Tables A9.13, A9.14, A9.15 and A9.16, Appendix, page 330 & 331.

Figure 9.5. Binding of ^{111}In Pan B (WR-17) to ACD-whole blood.

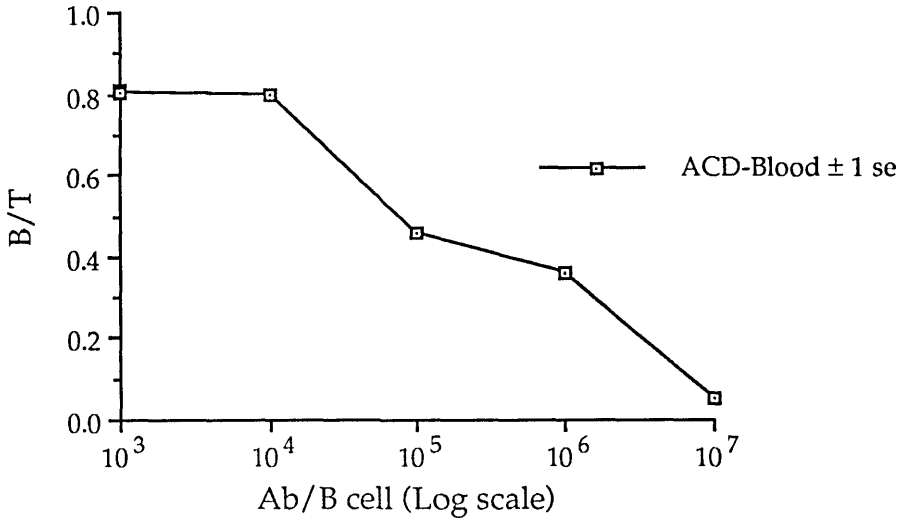

In these tests, the ratio of cell bound to total antibody added (B/T) for each antibody concentration used was taken to assess the efficiency of cell labelling in conditions similar to those found in vivo and to give an idea on the optimal range of antibody binding to the cells.

The whole blood assays for both antibodies showed higher ratios of cell bound to total antibody added than the assays using the cell lines as source of antigen (especially true for ^{111}In WR-17). Non-specific binding was generally low (<1% of cell bound antibody). Assessment of the distribution of radioactivity among the mononuclear cell by density gradient centrifugation and E-rosetting of blood after incubation with the labelled antibodies documented specific binding of ^{111}In UCHT2 to T cells and ^{111}In WR-17 to B cells (see Table A9.14 and A9.16, Appendix, page 330 & 331 for details).

9.3.3.3 Antibody binding parameters; binding constant, Ab elution and Ab internalisation

A) The binding constants of ^{111}In Pan T & ^{111}In Pan B

The equilibration constant of ^{111}In UCHT2 was calculated according to Equation 9.1 by substituting the values of K+1 (the association constant) and K-1 (the dissociation constant) therein. K+1 was found to be on average $1.6X10^{6}$ $M^{-1}S^{-1}$ (for the experimental data see Appendix, pp332-335). K-1 was calculated to be $2.4X10^{-5}$ s^{-1} and Keq $6.7X10^{10}$ M^{-1}. The same was applied for ^{111}In WR-17. Accordingly, K+1 (WR-17) was found to be on average $5.5X10^{5}$ $M^{-1}S^{-1}$, K-1 $3.9X10^{-5}$ s^{-1} and Keq $1.4X10^{10}$ M^{-1} (for the experimental data see Appendix, pp335-337).

B) Antibody elution :

The amount of ^{111}In McAb (^{111}In Pan T or B) bound to the relevant cell line[1] after 2 hr incubation at 37°C was taken to be 100% (cpm cell bound t_0). Elution of the antibody from the cells was calculated as :

$$\text{Ab elution (\%)} = 1 - \frac{\text{cpm cell bound}_t}{\text{cpm cell bound}_{t0}} \times 100$$

Where cpm cell bound$_t$: ^{111}In cpm cell associated at time t after resuspension of the cells in fresh medium.

The results of ^{111}In Pan T and ^{111}In Pan B elution are shown in Table 9.1[2].

---

1 For testing elution of ^{111}In UCHT2 the HPB ALL cell line was used. EBV PGF was used for testing elution of ^{111}In WR-17 (Pan B).

2 See Tables A9.23 and A9.24, Appendix, page 337 for the experimental data.

Table 9.1. Elution of ^{111}In UCHT2 (Pan T)[a] and ^{111}In WR-17 (Pan B)[b] from the lymphoid cell lines[c].

Time (hr)	^{111}In UCHT2 Elution (%)	^{111}In WR-17 Elution (%)
1	27.8±0.69	28.1±0.61
6	54.9±1.60	81.6±2.94
19	56.8±1.68	85.8±4.62
24	56.9±1.66	86.3±3.65

a ^{111}In UCHT2 : 47 MBq/mg (1.1 mCi/mg).
b ^{111}In WR-17 : 286 MBq/mg (7.7 mCI/mg).
c ^{111}In UCHT2 was tested on the HPB ALL T-cell line and ^{111}In WR-17 on the EBV PGF B-cell-line.

Accordingly, elution was a slow process for ^{111}In Pan T and ≈ 50% of the ^{111}In antibody was still cell associated after 24 hr. On the other hand, this process was faster for ^{111}In Pan B and less than 15% of the activity cell bound at 2 hr remained so at 24 hr.

C) Antibody internalisation

Early internalisation, ie cell associated activity remaining after incubation of the cells in acidic buffer, was noted for the lymphoid cells[1] that had been incubated with ^{111}In Pan T. This amounted to ≈ 20% of the activity cell associated before treatment with acidic buffer see Table 9.2[2]. In contrast, ^{111}In Pan B showed a rather low cell associated activity after treatment of the cells with low pH buffer and thus internalisation was not thought to occur significantly upon binding of this antibody to the EBV B cell line.

1 HPB ALL was used for testing the internalisation of ^{111}In UCHT2 and EBV PGF for testing the internalisation of ^{111}In WR-17.
2 See Tables A9.25 and A9.26, Appendix, page 338 for the experimental data.

Table 9.2. Internalisation of ^{111}In UCHT2 and ^{111}In WR-17 tested with the lymphoid cell lines HPB ALL and EBV PGF respectively.

Time (hr)[a]	^{111}In UCHT2 %Ab internalised	^{111}In WR-17 %Ab internalised
0	1.9±0.2	4.0±1.8
0.5	ND[b]	5.2±0.9
1	21.0±0.3	6.0±0.8
2	24.0±0.3	7.8±0.5
3	ND	8.3±0.5
20	18.0±0.3	ND
24	18.0±0.3	9.6±0.3

a Time after addition of the ^{111}In McAb to the cells.
b ND : Not done.

9.3.3.4 Effect of ^{111}In McAb on mitogen induced proliferation

Testing the effect of the ^{111}In anti-T or B cell monoclonal antibodies on mitogen induced proliferation in whole blood in vitro was done by comparing ^{3}H-thymidine incorporation in the wells containing labelled antibody with the other wells containing unlabelled, irrelevant or no antibody in the tested microtiter plate. Firstly, baseline proliferation, ie without the presence of mitogen, was measured. This was found to be low and non-significant (see Tables A9.28 and A9.30 Appendix, pp338 & 339 for experimental details). Secondly, control values for count-rates obtained in the wells containing no antibodies (well containing RPMI medium only) were noted and the mean was calculated (Control Value). Thirdly, count-rates in the wells containing HMFG2 (irrelevant McAb), unlabelled anti-lymphocyte (Pan T or Pan B) and ^{111}In-labelled anti-Pan T or Pan B were compared to the Control Value (see above) and the results were tabulated showing their significance to the 99% confidence limit (Table 9.3)[1].

[1] For the experimental details see Tables A9.27, A9.28, A9.29 and A9.30, Appendix, pp338 & 339.

Table 9.3. Comparison of ^{3}H-thymidine incorporation in the wells containing ^{111}In UCHT2 or ^{111}In WR-17, unlabelled UCHT2 or WR-17 and HMFG2 to ^{3}H-thymidine incorporation in the Control[a] wells (RPMI medium, no Ab).

^{111}In UCHT2 (Pan T)

Row	^{111}In UCHT2	Significance[b]	UCHT2	Signi-ficance	HMFG2	Signi-ficance
A	34100±900	S	4100±1600	NS	3000±3000	NS
B	1100±2300	NS	-152±3400	NS	1500±2400	NS
C	5000±2100	NS	350±1400	NS	-1600±2300	NS
D	160±2200	NS	2500±1600	NS	-1700±1700	NS
E	-1700±2400	NS	-390±1900	NS	-2400±1900	NS
F	3300±2900	NS	-3634±2700	NS	-960±2400	NS
G	-2100±1500	NS	3650±1650	NS	-4400±1800	NS
H	-5000±1960	NS	-1300±1600	NS	-2300±1550	NS

^{111}In WR-17

Row	^{111}In WR-17	Significance	WR-17	Signi-ficance	HMFG2	Signi-ficance
A	7300±11700	NS	15700±16800	NS	5600±14800	NS
B	9900±13900	NS	-1700±16400	NS	-3200±7100	NS
C	8200±16500	NS	12000±15700	NS	-2218±16400	NS
D	4140±13600	NS	1900±23000	NS	-3152±7650	NS
E	6030±8000	NS	14100±9700	NS	9300±13700	NS
F	6300±9800	NS	16300±10700	NS	2900±7100	NS
G	12700±11000	NS	12800±9000	NS	-8290±11000	NS
H	8000±27000	NS	-5000±10000	NS	10800±11600	NS

a The Control Value for the ^{111}In UCHT2 plate was 52000±870 and for the ^{111}In WR-17 plate 131300±7000 cpm.
b Significance to the 99% confidence limit, S : Significant, NS : non-significant.

The only effect noted was a reduction in ^{3}H-thymidine incorporation in the wells containing the highest concentration of ^{111}In Pan T (5X10^{5} Ab/T cell) see Table 9.3. No other effect was seen over the rest of the concentration range tested for ^{111}In Pan T or over that tested for ^{111}In Pan B. It was noted that the pattern of ^{3}H-thymidine incorporation with LPS+PWM stimulation

was more variable than with Con A stimulation[1]. However, no obvious negative effect on proliferation was seen in the wells containing ^{111}In Pan B when compared to the Control Value.

9.4 Discussion

9.4.1 Implications of antibody choice and in vitro tests for in vivo use of ^{111}In anti-lymphocyte McAbs in man

The Pan T McAb UCHT2 belonging to the CD5 cluster of differentiation and reacting with the majority of T cells and the Pan B (WR-17), CD37 reacting with B cells were chosen as examples of candidate anti-human lymphocyte McAbs for in vivo use. This was in view of radiolabelling subsets of lymphocytes for imaging lymphoid tissues using the scintillation camera. The choice of antibodies was based on a survey of anti-lymphocyte McAbs which would bind to T or B cells without known damaging effects on the cells especially in terms of complement activation[2]. Also, being specific for the two main subsets of lymphocytes (T & B), they gave a relatively simple model in vitro to establish the general binding characteristics of ^{111}In anti-lymphocyte McAbs and to study the effect of the radiolabel on the cells. However, the use of the two antibodies described was not considered to give a limitation by any means as other antibodies could have also been used for the same purpose.

The first investigations done confirmed specificity of the Pan T and Pan B McAbs to the respective cell lines. Then, the useful range of binding to the cell lines and more importantly to the lymphocyte population in question in whole blood was identified in view of potential use for cell radiolabelling and imaging. These tests, performed in conditions similar to in vivo

---

1 See Tables A9.27 and A9.29 for details, Appendix, pp338 & 339.
2 Supplier's note, personal communication.

situation, ie 37°C and cell concentration = $2X10^6$/ml, showed that relatively low concentrations of antibody (in the range of 10^3-10^5 Ab/cell) gave a higher percentage of cell binding, thence a better target to noise ratio. This range of antibody concentration reflected most likely equimolarity of cellular antigen and antibody in the conditions of assay used. The amount of radioactivity cell associated after antibody binding assuming average specific activity of the labelled antibody of 370 MBq/mg (10 mCi/mg) would be on average 0.25 milliBq/cell (range 0.15-4.6 milliBq/cell). The implications of this finding for lymphocyte radiolabelling were two fold. Firstly, maximum radioactivity cell bound would be much less than the upper level of 7.4 milliBq/cell (0.2 pCi/cell) recommended for lymphocyte radiolabelling with ^{111}In. Secondly, considering a minimum of ^{111}In activity of 4 MBq (100 μCi) for successful imaging using the scintillation camera, including reasonable imaging time and acceptable count-rate, the required number of cells bearing 0.25 milliBq each would be $1.6X10^{10}$, and this would not be far from in vivo applicability (labelling of the total circulating pool of T or B cells).

The effect of each antibody on lymphocytes was studied in experimental settings in vitro to check certain phenomena such as the alteration of expression of the antigen on the cell surface after binding the antibody, antibody internalisation and cell proliferation in the presence of the unlabelled or ^{111}In labelled antibody. Three effects were documented. The Pan T McAb caused redistribution of the CD5 molecule on the cell surface detected by indirect immunofluorescence. This phenomenon was seen to a lesser extent using the Pan B McAb. The possibility that the second layer of rabbit anti-mouse-immunoglobulin-fluorescein-conjugated antibody (RAM Ig FITC) could have caused the patching and capping observed was unlikely because capping occurred mainly in cells incubated with Pan T at 37°C and the incubation with RAM Ig FITC was done on ice. This finding was in

agreement with the earlier finding in the rat model (see previous chapter) where MRC OX-19 caused modulation in vivo. Also, the use of antibodies belonging to the CD5 cluster of differentiation had been known previously for causing antigen modulation both in vitro and in vivo (Shawler et al 1984). The significance of the loss of CD5 molecule in vivo was not clear with respect to alteration of T cell function. The only effect known was in vitro potentiation of mitogen induced proliferation of rat T cells after binding MRC OX-19 (anti-CD5 in the rat) (Dallman et al 1984). This effect could not be documented in the in-vitro experiments performed on the Pan T McAb in whole blood (see paragraph 9.3.3.4 page 190). Modulation would render the cell invisible to the radiolabelled antibody, hence adding a drawback to the lymphocyte-radiotracing method.

The second effect noted and which could be related to the first already discussed, was the internalisation of ^{111}In Pan T within the cells measured after elution of surface bound antibody using a low pH buffer. The testing of internalisation relied on the assumption that antibodies bound to the cell surface could be eluted by incubation of the cells in a low pH buffer (Matzku et al 1986, Tilgen et al 1987). Thus, about 25% of the ^{111}In Pan T McAb cell-bound remained so after incubation of the lymphoid cells in acidic buffer. No such residuum of ^{111}In radioactivity in the cells was found after using ^{111}In Pan B in the same way. The direct implication of antibody internalisation for the purpose of using ^{111}In anti-lymphocyte McAbs for cell radiolabelling would be in causing an increase in the radiation dose to the nucleus from radionuclides internalised inside the cytoplasm. This effect, although marginally detrimental to lymphocytes for imaging applications, could be used to benefit by targeting cell toxic agents on the same antibody and causing lethal hits inside the cells especially in the case of leukaemias and lymphomas.

The knowledge of the antibody binding constants and the results of the elution experiment gave a prediction of the time-span of antibody binding to the cells in standard (Ab binding constant expt) and in vivo simulated conditions (Ab elution Expt). In vitro experiments showed that binding of the whole antibody to the cells declined relatively slowly using ^{111}In Pan T (50% left after 24 hr, binding constant $6.7X10^{10}$ M^{-1}) and much more rapidly using ^{111}In Pan B (10% left after 24 hr, binding constant $1.4X10^{10}$ M^{-1}). Considering the $T_{1/2}$ of Ab dissociation (^{111}In Pan T : 8 hr, ^{111}In Pan B : 5 hr), $T_{1/2}$ of murine IgG in the plasma (30 hr), $T_{1/2}$ of ^{111}In (67 hr) and a long $T_{1/2}$ for lymphocytes, the radiolabelling of the main subsets of lymphocytes for imaging using ^{111}In McAb should be possible clinically and would follow closely Ab concentration in plasma. However, cell-survival studies requiring long-term follow-up of the radiolabelled cells would not be amenable to investigation using the same method (see discussion Chapter 6 and Chapter 8).

Finally, in vitro tests gave an indication of possible ^{111}In McAb effect on cell function by testing in vitro mitogen induced cell proliferation in the presence of ^{111}In Pan T or ^{111}In Pan B.

The setting used tried to mimic in vivo conditions by performing the test in whole blood. The effect of preincubation of the cells with the ^{111}In McAbs was also measured at the points of maximum proliferation in the assays employed (Con A at 3 days, LPS+PWM at 5 days). Both the effects of cell bound and non-cell bound (in the surrounding medium) ^{111}In radioactivity were assessed as antibody washing was not performed so that conditions of maximum exposure from the ^{111}In McAb were present.

The finding that ^{111}In Pan T at $5X10^5$ Ab/cell, 25 m[illegible]Bq/cell (0.67 pCi/cell) caused a reduction in ^{3}H-thymidine incorporation, pointed rather confidently to the damaging effect of radiation on the cells above a certain

threshold of ^{111}In antibody binding to the cells or presence around the cells. The main implication was in the identification of a "safe" range of antibody concentration for in vivo use. Its upper limits would be 10^5 Ab/T cell and the range for optimal cell binding and the least damaging effect would lie between 10^3 and 10^5 Ab/cell (T or B) in blood.

9.4.2 Summary

In this chapter, the use of ^{111}In anti-lymphocyte monoclonal antibody for lymphocyte radiolabelling was scrutinised and examples of in vitro tests that could lead to the final application of the method in vivo were given.

Although, to the best of our knowledge, none of the described ^{111}In anti-lymphocyte McAbs had been used in vivo in man, the experience presented in the rat and experience of others using a similar method gave support for applicability of radiolabelled anti-lymphocyte McAbs for imaging lymph nodes and lymphoid tissue in general in man. Caution would be still warranted in this kind of use. For antibody binding to a cell surface receptor would convey a signal to the cell which might cause a subtle change in cell function. Therefore, knowledge of this putative change would be important and that could only be achieved by performing tests more thoroughly down to the molecular level. Also, the damaging effect of radiation on lymphocytes, even at low level of exposure, would put some restriction on the use of radiolabelled anti-lymphocyte McAbs in vivo, especially in non-neoplastic conditions. In this context, long term effects of radiation such as induction of leukaemia or lymphoma would be the major concern. Therefore, a better understanding of cellular dosimetry and its relation to malignant changes in lymphocytes, in addition to observations in patients that had undergone previous investigations employing radiolabelled mixed-leucocyte preparations would provide a firmer basis for this application as a routine lymphocyte radiolabelling method in man.

Section Four :

^{111}In Monoclonal Antibodies against Lymphocytes, Activated Lymphocytes, Class I or II Major Histocompatibility Complex Antigens.

In Vitro Tests and in Vivo Use for the Imaging of Rejecting and Cyclosporine Treated Allogeneic Kidney Transplants in the Rat

Chapter 10 :

Organ Transplantation : Brief History and Problems Related to Early Diagnosis and Follow-up of Renal Transplant Rejection

10.1 Organ transplantation :

The grafting of tissues and transplantation of organs has developed to provide substitutes for damaged tissues or organs for which no man made agents can be used. In its simplest form, it is blood transfusion from one individual to another. In more sophisticated cases, whole organs or even parts of a system in the body have been removed from donors and surgically installed in recipients (kidney, liver, heart & lung, etc).

The development of tissue and organ transplantation went through three major steps to present day situation.

1) Early experimentation of transplanting tissues or organs between animals and work involving blood transfusion in man (Landsteiner and Levine 1930), established the need for using matched tissues for grafting. Autografts were accepted in the tested animals while allografts lost function and became necrotic within a short period of time after transplantation (Ullman 1902, Guthrie 1912, Schone 1912, Lexer 1914, Williamson 1923, Wu and Mann 1934). The role of the lymphocyte in graft rejection was also recognised by Murphy (1926).

2) Identification of transplantation antigens emerged from research work on tumour grafts. Tumour grafting was possible among the Japanese Walzing mice but not among hybrid mice (Little and Tizzer 1916). Gorer (1937 & 1938) discovered an antibody associated with the rejection of tumour grafts and the antigen involved was called antigen II. This antigen was linked to the product of the gene located at the locus H (Histocompatibility) discovered by Snell (1948) and intimately related to the rejection of tumour

grafts (Gorer et al 1948). The immunological nature of allograft rejection was finally established by Medawar (1944) from observations in man and experiments in the laboratory animal.

3) The ability to modify the recipient's immune response to avoid transplant rejection (Calne 1976) became possible by the introduction of immunosuppressive therapy (Murray et al 1963, Borel 1976) and by the trial of immunological manipulations such as passive or active enhancement (Brent and Medawar 1962, Stuart et al 1968, French and Batchelor 1969).

Presently, the improvement in the surgical techniques of transplantation has allowed the grafting of various organs (skin, kidney, liver, pancreas etc). In addition, organ rejection lends itself to treatment in most of the cases by available immuno-suppressive and modulatory regimens.

10.2 Immunopathological events during the progression of acute transplant rejection

While a variety of cells and humoral mediators have been implicated in the rejection responses, current evidence is that the T-cell is the principal mediator of primary rejection (Hall et al 1978a & b).

The pathological events that end in the acute rejection of an unmodified allogeneic kidney graft of an non-sensitised recipient are the following (Herbertson 1973) :

1) Infiltration of the graft with lymphocytes and other blood cells :

Cellular invasion starts early after transplantation and by its fourth day, the transplant is densely infiltrated mainly with lymphocytes, macrophages and plasma cells. Many activated lymphocytes are also detected including lymphoblasts and lymphocytes expressing high levels of interleukin 2 receptor (IL-2R). This cellular infiltration is accompanied by an

inflammatory exudate and vascular microemboli (Strom et al 1975, Busch et al 1976, Hancock 1984, Hall et al 1984).

2) Alteration of the graft tissue itself :

A prominent feature of acute rejection is the massive induction on graft cells of the major histocompatibility complex molecules (Milton and Fabre 1985, Milton et al 1986, Ahmed-Ansari et al 1988). This induction is caused by lymphokine secretion, mainly γ interferon, in the graft (Pober et al 1983, Wong et al 1984, Weetman and Rees 1988). Class I MHC induction occurs very early in the process of rejection while Class II de novo expression follows after 2-3 days of unmatched grafting.

3) Graft infarction and loss of function

Blood vessels in the rejecting graft become occluded by the deposition of fibrin and thrombosis. This leads to patchy infarction of the graft. In the end, thrombosis extends to the main vessels supplying the graft leading to total infarction and loss of function by 7-10 days after start of the rejection process (Kincaid-Smith 1967, Imbasciati et al 1987).

10.3 Diagnosis and follow-up of acute rejection of renal transplants

Early diagnosis of kidney transplant rejection is imperative as institution of effective treatment may reverse declining renal function and prevent irreversible damage. The condition is characterised clinically by fever, allograft tenderness, swelling, and significant reduction in urine output. Anti-rejection therapy involves usually immunosuppression using cytotoxic drugs, anti-lymphocyte antibodies and corticosteroids, which exposes the recipient to the risk of infection and induction of malignancy. Also, the use of cyclosporine can induce toxic nephropathy which can complicate the clinical picture in patients bearing kidney grafts. Presently,

positive diagnosis of kidney transplant rejection relies mainly on non-specific features such as the deterioration of renal function (increased serum creatinine, low urine output, abnormal ^{99m}Tc DTPA renography) and on the pathological diagnosis by performing a transplant biopsy or a fine needle aspiration (Pasternack 1968). Unfortunately, most of these tests are rather unsatisfactory due to their non-specificity for the diagnosis of rejection and the relatively invasive nature involved in obtaining repeated biopsies.

Other methods have also been reported to address the question of diagnosis of renal transplant rejection without gaining much popularity. For example, tests using various radiotracers including radiolabelled blood cells have been tried in various ways.

Radiolabelled granulocytes were injected in recipients of renal transplants and positive scans of the rejecting graft were obtained (Forstrom et al 1981). However, the technique suffered from lack of specificity. ^{111}In oxine lymphocyte scanning gave positive results in canine-(McKillop et al 1982) and rat-(Bergmann et al 1982, Lerch et al 1982) heart transplantation models and also in a human renal transplant study (Martin-Comin 1986). The method necessitated, however, the use of cumbersome techniques of separating and labelling lymphocytes. Also, the damaging effect of radioactivity on the cells added a drawback to using the technique safely in man. Another promising approach to the diagnosis of acute rejection was reported by Tisdale et al (1986) on the use of ^{111}In labelled platelet scanning. This method showed positive uptake in rejecting kidney grafts in human with high sensitivity and specificity. ^{111}In platelet scanning was also used for the follow-up of chronic rejection of renal transplants (Leithner et al 1982) and in the monitoring of human pancreatic transplants (Catafau et al 1989). Again, low specificity and the complicated technique of isolating and radiolabelling platelets did not encourage its use in routine clinical practice.

In summary, early detection and follow-up of kidney transplant rejection still lack the presence of a specific test. In next chapter, a new approach based on the immunopathology of acute rejection is presented for the early diagnosis and discrimination of rejection. This involves scintillation camera imaging and tissue quantitation of the distribution of ^{111}In-anti-lymphocyte and anti-major-histocompatibility-complex-molecule monoclonal antibodies in a rat kidney transplant model.

Chapter 11 :

^{111}In Radiolabelling and in Vitro Tests of Monoclonal Antibodies against Lymphocytes, Activated Lymphocytes and Class I and II Major Histocompatibility Complex in the Rat

11.1 Introduction

Based on immuno-pathological events occurring in the course of acute allogeneic-kidney-graft rejection, namely lymphocyte infiltration and the induction of MHC molecules (see previous chapter), a new method for the detection and monitoring of rejection has been tried. It involves in vivo use of ^{111}In anti-lymphocyte (CD5 & anti-IL-2 receptor), anti-Class I and anti-Class II MHC monoclonal antibodies in a rat kidney transplantation model (Milton and Fabre 1985).

In vitro tests for the determination of the specificity and binding of each ^{111}In McAb to the corresponding cell population are presented in this chapter. In vivo use of the ^{111}In labelled antibodies is shown in Chapter 12.

11.2 Materials and methods

11.2.1 Animals

Adult male DA ($RT1^{av1}$, $RT2^b$ & $RT3^a$) and PVG/c ($RT1^c$, $RT2^b$ & $RT3^{a)}$ rats were purchased from Harlan-Olac Ltd, England and used when they were between 200-350 g.

11.2.2. Monoclonal antibodies

MRC OX-19 was described earlier (see Paragraph 8.2.2.1, page 118). It is a mouse IgG_1 reacting with a 67 kDa glycoprotein on all rat T cells (CD5 in the rat) (Dallman et al 1984).

MRC OX-39 is a mouse IgG_1 which reacts with a glycoprotein of 45-50 kDa corresponding to the interleukin-2 receptor on activated rat T cells (Paterson et al 1989). Purified antibody was purchased from Serotec, England.

MN4-91-6 is a mouse IgG_1 which reacts with a polymorphic determinant on DA Class I MHC molecules. It is directed at the product of the RT1A locus and appears to be highly specific for the $RT1^a$ allele. It reacts with DA but not PVG, WAG or LEW (Milton and Fabre 1985).

F17-23-2 is a mouse IgG_1 which binds to a polymorphic determinant on DA Class II MHC encoded for by the RT1B region. It reacts with $RT1^a$, $RT1^l$ and $RT1^n$ but not $RT1^c$ (PVG) or $RT1^u$ (WAG) (Hart and Fabre 1981).

Both purified MN4-91-6 and F17-23-2 McAbs were a kind gift of Professor JW Fabre, Blond McIndoe Centre, East Grinstead, England.

11.2.3 Radiolabelling of the McAbs with indium-111

The method of ^{111}In labelling of McAbs by the double chelating agent DTPA was used[1]. The specific activity obtained ranged between 100-130 MBq/mg (2.7-3.5 mCi/mg)[2].

11.2.4 Immunoreactivity testing of the ^{111}In labelled McAbs

Immunoreactivity testing was performed using the double inverse plot described earlier (see page 55 for details of the method).

---

1 See page 49 for details of the procedure.

2 See Tables A11.1, A11.2, A11.3, A11.4, A11.5, A11.6, A11.7, A11.8 and A11.9 for details of DTPA coupling, measurement of the No of DTPA/Ab and ^{111}In test labelling of the three McAbs MRC-OX-39, MN4-91-6 and F17-23-2, Appendix, pp340-346. For details on the purification, DTPA coupling and ^{111}In labelling of MRC OX-19 McAb, see Paragraph 8.2.3 and 8.2.4, pp119-121.

11.2.4.1 ^{111}In MRC OX-19

The immunoreactivity of the antibody was tested with rat thoracic duct lymphocytes as source of antigen. Details of the test were described earlier (see pp121 & 317).

11.2.4.2 ^{111}In MRC OX-39

The source of cellular antigen for the testing of this McAb was mitogen-(Con A) activated-PVG-rat lymphocytes.

The spleen in a PVG rat was taken and a cell suspension was prepared (see page 319 for details). The red blood cells were lysed in a solution of Tris-buffered-ammonium chloride[1]. Then, the cells were resuspended in RPMI 1640 medium containing 10% FCS at 10^6 cell/ml (a total of 50 ml). In a 75 cm^2 flask[2], the cells were incubated with concanavalin A[3] at 2 µg/ml for 48 hr at 37°C in an atmosphere of 5% CO_2 in air. Afterwards, the cells were examined using an inverted microscope[4] to check proliferation, then they were washed once in Hank's balanced salt solution[5] containing 1% BSA and resuspended in buffer in preparation for the assay.

For testing immunoreactivity of ^{111}In MRC OX-39, the antibody was added at 10 ng to a series of LP3 tubes containing doubling dilutions of the stimulated lymphocytes in Hank's BSS 1% BSA starting with $2.5X10^7$ cell/ml. The cells were incubated for 2 hr at 37°C. Afterwards, cell bound radioactivity was measured, having washed the cells twice in the same buffer. An identical group of tubes was set with excess unlabelled antibody to measure non-

---

1 Stock solution 0.16 M NH_4Cl, 0.17 M Tris pH 7.65. Working solution : 90 ml 0.16 M NH_4Cl + 10 ml 0.17 M Tris, adjust pH to 7.2. The cell pellet was resuspended in 1 ml Tris-NH_4Cl for 2 minutes, then the cells were centrifuged over FCS at 300 g for 10 minutes. The cells were washed twice in buffer before use.

2 Falcon, USA.

3 Concanavalin A, Lot No 85F8875, Sigma, England.

4 Olympus, Japan.

5 Sigma, England.

specific binding, which was subtracted from the values obtained above. The data[1] obtained were plotted as the inverse relative cell-bound radioactivity versus the inverse cell concentration and the curve was extrapolated to intercept the Y axis at a point representing the inverse of the immunoreactive fraction.

11.2.4.3 ^{111}In MN4-91-6

The immunoreactivity of this McAb was tested on DA rat red blood cells as they express Class I MHC on their surface (Milton and Fabre 1985). DA rat blood was collected in a 10 ml-syringe containing 200 iu heparin by cardiac puncture under ether anaesthesia. The blood was washed three times in PBS by centrifuging at 500 g for 10 min and removing the buffy coat and upper layer of RBC after each wash. The cells were dispensed in a series of six LP3 tubes in doubling dilutions in PBS starting with 10^8 cell/ml. ^{111}In MN4-19-6 was added to each tube at 10 ng/ml and the tubes were left to incubate for 2 hr at 37°C in a water bath. Afterwards, the cells were washed twice in PBS in the cold and the cell bound radioactivity was measured in an automatic gamma well counter[2]. Another similar group of tubes containing excess unlabelled MN4-91-6 was prepared for measuring non-specific binding which was subtracted from the values obtained above. The data[3] obtained were plotted as the inverse relative cell bound radioactivity versus the inverse cell concentration and the curve was extrapolated to intercept the Y axis at a point representing the inverse of the immunoreactive fraction.

---

1 See Table A11.10 for the experimental setting and counting results and Figure A11.1 for the calculation of the immunoreactive fraction, Appendix, pp346 & 347.

2 Packard Autogamma, USA, Haematology Dept, RPMS.

3 See Table A11.11 for the experimental setting and counting results and Figure A11.2 for the calculation of the immunoreactive fraction, Appendix, pp347 & 348.

11.2.4.4 ^{111}In F17-23-2

DA rat spleen cells were used for this test as they contained relatively high numbers of B cells bearing Class II molecules on their surface. A suspension of spleen cells was prepared from the spleens of three DA rats. The red blood cells were lysed using Tris-buffered ammonium chloride as described above and the remaining cells were washed twice and resuspended in Hank's balanced salt solution containing 1% BSA. The cells were dispensed in LP3 tubes in doubling dilutions in buffer starting with $4X10^7$ cell/ml. ^{111}In F17-23-2 was added to the tubes at 10 ng/ml and the tubes were left to incubate for 2 hr at 37°C. At the end of the incubation time, the cells were washed twice with buffer in the cold and cell bound radioactivity was measured. Another similar set of tubes containing excess unlabelled F17-23-2 was prepared for measuring non-specific binding which was subtracted from the values obtained above. The data[1] obtained were plotted as the inverse relative cell bound radioactivity versus the inverse cell concentration and the curve was extrapolated to intercept the Y axis at a point representing the inverse of the immunoreactive fraction.

11.2.5 Radioimmunoassay of the ^{111}In McAbs versus the appropriate cell population; specificity and range of binding

11.2.5.1 ^{111}In MRC OX-19 vs rat lymph node cells and anti-coagulated blood

This test was described earlier in Chapter 8, page 122.

---

1 See Tables A11.12 for the experimental setting and counting results and Figure A11.3 for the calculation of the immunoreactive fraction, Appendix, pp348 & 349.

11.2.5.2 ^{111}In MRC OX-39 versus activated and non-activated lymphocytes

^{111}In MRC OX-39 was added to a set of four LP3 tubes containing $5X10^6$ mitogen-stimulated-PVG-rat-spleen cells (see Paragraph 11.2.4.2 above) in each at increasing concentrations : 10^3, 10^4, 10^5 and 10^6 Ab/cell. The antibody was also added in a similar way to another set of tubes containing unstimulated PVG rat spleen cells. The antibody was left to incubate with the cells for 2 hr at 37°C. Afterwards, the cells were washed twice in buffer and cell-bound radioactivity was counted in a gamma well counter[1]. Non-specifically bound radioactivity was allowed for by measuring cell associated activity in tubes containing excess of unlabelled MRC OX-39 McAb. The total volume in each tube was adjusted to 1 ml using buffer.

11.2.5.3 ^{111}In MN4-91-6 versus rat red blood cells

Radioimmunoassays of ^{111}In MN4-91-6 with either DA or PVG rat red blood cells were set in order to check the range of binding of the antibody to the cellular antigen and ensure the specificity of the ^{111}In labelled antibody to DA but not PVG rat Class I MHC.

Blood was taken from a DA or PVG rat by cardiac puncture and a suspension of red blood cells was prepared as described in Paragraph 11.2.4.3 above. Ten million rat-(DA or PVG) red-blood cells in PBS were dispensed in each of a set of four LP3 tubes. ^{111}In MN4-91-6 was added at 10^6, 10^5, 10^4 and 10^3 Ab/cell to the first, second, third and fourth tubes respectively. The volume in each tube was adjusted to 1 ml using buffer and the cells were incubated for 2 hr at 37°C. Afterwards, the cells were washed twice in PBS and cell bound radioactivity was measured. Corresponding tubes containing excess unlabelled MN4-91-6 were set to measure non-specific binding.

---

1 Packard Autogamma, USA, Haematology Dept, RPMS.

11.2.5.4 ^{111}In F17-23-2 versus spleen and B-lymphocyte-enriched-spleen cells

^{111}In F17-23-2 was tested for its specific binding to DA Class II MHC by radioimmunoassays set with rat (DA or PVG) spleen or B-enriched spleen cells. Cell suspensions were prepared from two spleens (DA or PVG) for each assay as described in Paragraph 11.2.4.4. In the first assay, spleen mononuclear cells in Hank's balanced salt solution 1% BSA were dispensed at 10^7 cell/ml in each of a set of four LP3 tubes. ^{111}In F17-23-2 was added at 10^6, 10^5, 10^4 and 10^3 Ab/cell to the first, second, third and fourth tubes respectively. After two-hour incubation at 37°C, the cells were washed twice in buffer and the cell associated radioactivity measured. In the second assay, enrichment of the spleen cell population with B cells by depletion of its T cells was done before addition of ^{111}In F17-23-2. This was achieved by incubation of the spleen mononuclear cell suspension (2 ml at $5X10^7$ cell/ml) with excess (12.5 μg/ml) MRC OX-19 monoclonal antibody (anti-CD5 in the rat) for 1 hr at 4°C. The cells were washed twice in buffer in the cold, resuspended in 2 ml buffer and sheep-anti-mouse-Ig coated magnetic beads (Dynabeads) (0.5 ml, 5-7 beads/T cell) were added to them in a 10 ml plastic centrifuge tube. After 30 minutes incubation time, the formation of rosettes[1] was checked under light microscopy. Then, by using a magnet on the outside of the tube the rosetted cells (CD5-positive cells; T cells) were separated from non-rosetted cells (CD5-negative cells; B cells). Afterwards, the non-rosetted cells were decanted, washed once in buffer and dispensed at $2X10^6$ cells in LP3 tubes for the assay which was done similarly to above, ie ^{111}In F17-23-2 added at 10^6, 10^5, 10^4 and 10^3 Ab/cell, 2 hr incubation at 37°C and measurement of cell-bound radioactivity. Non-specific binding was allowed for in the calculation of cell bound ^{111}In F17-23-2 by subtraction of cell associated activity obtained from similar tubes containing excess of unlabelled antibody in them.

---

1 Magnetic beads attached to T cell surface.

11.3 Results

11.3.1 Immunoreactivity of the ^{111}In F17-23-2 labelled McAbs

The Immunoreactive fractions of the ^{111}In McAbs were as follows : ^{111}In MRC OX-19 : 50%, ^{111}In MRC OX-39 : 77%, ^{111}In MN4-91-6 : 100% and ^{111}In F17-23-2 : 63%.

11.3.2. Specificity and range of binding of the ^{111}In McAbs to the respective cells

11.3.2.1 ^{111}In MRC OX-19 (anti-CD5; rat Pan T McAb)

The results of binding of this antibody to rat blood and lymph node cells were described earlier (see Chapter 8 page 136). Percentage cell binding was found to be in the range of 12-33% of the amount of antibody added in the assay[1].

11.3.2.2 ^{111}In MRC OX-39 (anti-IL2 receptor McAb in the rat)

^{111}In MRC OX-39 bound to mitogen (Con A) stimulated rat spleen cells but not to the same unstimulated cell population. This finding confirmed the specificity of the antibody for activated T cells bearing the interleukin-2 receptor.

The results of the radioimmunoassay of ^{111}In MRC OX-39 versus PVG-rat stimulated and unstimulated spleen cells are shown in Table 11.1.

---

1 No strain difference of binding of MRC OX-19 to rat T cells was assumed.

Table 11.1. Binding of ^{111}In MRC OX-39[a] to PVG-rat mitogen stimulated and non-stimulated spleen cells[b].

Ab/cell	Added cpm[c]	Bound cpm[d] St[e]	Ratio B/T St	Bound cpm NSt[f]	Ratio B/T NSt
10^6	591700 ± 400	47400 ± 100	0.080 ± 0.0002	10000 ± 60	0.017 ± 0.0001
10^5	59500 ± 140	9700 ± 60	0.163 ± 0.004	980 ± 20	0.017 ± 0.0003
10^4	5800 ± 40	1000 ± 20	0.180 ± 0.004	140 ± 10	0.025 ± 0.002
10^3	550 ± 15	120 ± 10	0.227 ± 0.018	30 ± 5	0.058 ± 0.013

a ^{111}In MRC OX-39 : 104 MBq/mg (2.8 mCi/mg).
b $5X10^6$ cell/ml.
c All count-rates were corrected for background (BG = 84, n =6, se = 4).
d Non-specific binding was allowed for in the cell-bound count-rate.
e Con A stimulated cells.
f Non-stimulated cells.

This shows that the percentage bound to total added Ab of 8-23% is obtained in the assay using stimulated cells, while using the same range of Ab concentration but unstimulated cells as targets, the percentage is ≈ 1-2% and does not exceed 6%.

11.3.2.3 ^{111}In MN4-91-6 (anti-Class I MHC in the DA rat)

Binding of ^{111}In MN4-91-6 to DA but not PVG rat red blood cells was confirmed in the radioimmunoassay performed using this antibody. Also, an idea on the range of binding of ^{111}In MN4-91-6 to cells bearing the relevant Class I MHC antigen was obtained. The results of this assay are shown in Table 11.2.

Table 11.2. Binding of ^{111}In MN4-91-6[a] to DA and PVG rat red blood cells[b].

Ab/cell	Added cpm[c]	Bound cpm[d] DA[e]	Ratio B/T DA	Bound cpm PVG[f]	Ratio B/T PVG
10^6	1986000 ± 4000	59000 ± 140	0.030 ± 0.0001	5700 ± 40	0.003 ± 0.00002
10^5	208000 ± 1300	37700 ± 100	0.181 ± 0.001	520 ± 15	0.003 ± 0.00009
10^4	19400 ± 80	5200 ± 40	0.267 ± 0.002	270 ± 10	0.014 ± 0.0006
10^3	2200 ± 30	750 ± 20	0.346 ± 0.009	80 ± 10	0.037 ± 0.004

a ^{111}In MN4-91-6 : 100 MBq/mg (2.7 mCi/mg).
b 10^7 cell/ml.
c All count-rates were corrected for background (BG = 93, n =6, se = 4) and for counting dead-time.
d Non-specific binding was allowed for in the cell-bound count-rate.
e DA red blood cells.
f PVG red blood cells.

In Table 11.2, relative binding of ^{111}In MN4-91-6 McAb to DA rat red blood cells ranged between 3-35% depending on the concentration of Ab in the assay. However, binding of the Ab to PVG RBC remained low and did not exceed 4% at best.

11.3.2.4 ^{111}In F17-23-2 (anti-Class II MHC in the DA rat)

The radioimmunoassay of ^{111}In F17-23-2 with spleen cells prepared from DA or PVG rats showed higher binding of the antibody to DA spleen cells thus confirming the specificity of this antibody. However, the difference between the extent of ^{111}In F17-23-2 binding to DA and PVG spleen cells was diminished especially when the lowest concentration of Ab in the assay was used. Similar findings were noted using B-enriched spleen cells as source of antigen. However in this case, higher percentage of cell binding was seen. The results of ^{111}In F17-23-2 assays versus rat (DA or PVG) spleen cells or B-enriched spleen cells are shown in Table 11.3.

Table 11.3. ^{111}In F17-23-2 binding to rat (DA or PVG) spleen-[a] or B-enriched[b] spleen cells.

I. Spleen cells[c]

Ab/cell	Added cpm[d]	Bound cpm[e] DA[f]	Ratio B/T DA	Bound cpm PVG[g]	Ratio B/T PVG
10^6	6618000 ± 12000	82700 ± 170	0.013 ± 0.0003	20500 ± 80	0.003 ± 0.00001
10^5	650000 ± 4000	11400 ± 60	0.018 ± 0.0001	4700 ± 40	0.007 ± 0.00007
10^4	63700 ± 150	2800 ± 30	0.044 ± 0.0005	1260 ± 20	0.020 ± 0.0003
10^3	6100 ± 50	390 ± 10	0.064 ± 0.002	170 ± 10	0.028 ± 0.002

II. B-enriched-spleen cells[h]

Ab/cell	Added cpm	Bound cpm DA	Ratio B/T DA	Bound cpm PVG	Ratio B/T PVG
10^6	4220000 ± 8000	127500 ± 200	0.030 ± 0.00008	31400 ± 100	0.007 ± 0.0003
10^5	403000 ± 2500	47200 ± 130	0.117 ± 0.0008	14300 ± 70	0.035 ± 0.0003
10^4	37000 ± 100	5800 ± 40	0.157 ± 0.001	3100 ± 30	0.084 ± 0.0009
10^3	3900 ± 40	830 ± 20	0.213 ± 0.005	430 ± 15	0.109 ± 0.004

a ^{111}In F17-23-2 : 132 MBq/mg (3.6 mCi/mg).
b ^{111}In F17-23-2 : 213 MBq/mg (5.7 mCi/mg).
c Spleen cell 10^7 cell/ml.
d All count-rates were corrected for background (BG_1 = 72, n =6, se = 3, BG_2 = 81, n = 6, se = 4) and for counting dead-time.
e Non-specific binding was allowed for in the cell-bound count-rate.
f DA cells.
g PVG cells.
h B-enriched-spleen cells 2X10^6 cell/ml.

In this table, ^{111}In F17-23-2 binding was higher to cells originating from the DA than cells from the PVG rat. However, relative Ab binding to PVG B-enriched spleen cells was rather high in absolute terms ≈ 10%.

11.4 Discussion

In this chapter, basic in vitro tests for confirming the specificity of each antibody used to the respective cell population were performed.

Particularly important were the tests done to check specific reactivity of the ^{111}In anti-Class I MHC (MN4-91-6) and anti-Class II MHC (F17-23-2) McAbs in that they both had reacted with cells that originated from DA but not PVG rats. This was in view of using donor specific antibodies in vivo to detect any alteration in Class I or Class II MHC expression on the rejecting kidney graft. The results of the tests confirmed the specific antibody reactivity expected although ^{111}In F17-23-2 binding to DA compared to PVG cells did not show the clear-cut difference seen with ^{111}In MN4-91-6 McAb. The reason for that was most likely due to the rather weak affinity of F17-23-2 to its antigen, which was also observed by Milton and Fabre (1985).

The range of binding of the individual antibodies to the tested cell population was found to be related to the antibody and the cell source of antigen used in the assay. In general, the percentage cell bound activity to the cells expressing the relevant antigen was in the range of 10-30% using concentrations of antibody between 10^3-10^5 Ab/cell and incubation for 2 hr at 37°C. However, binding of ^{111}In anti-Class I and Class II antibodies to their cellular antigens in vitro, would be expected to vary more in vivo depending on the type of cells binding the antibody and whether MHC molecules had been induced as in rejecting grafts. Therefore, it was not possible to predict from the experimental work presented the extent of antibody binding to renal parenchymal cells or vascular endothelium in those conditions.

In summary, in vitro tests of four ^{111}In labelled McAbs : MRC OX-19 (anti-CD5; Pan T in the rat), MRC OX-39 (anti-IL-2R in the rat), MN4-91-6 (anti-

Class I DA specific) and F17-23-2 (anti-Class II MHC DA specific) showed suitability of the radiolabelled antibodies for further application in vivo.

The details of the experimental application of these ^{111}In McAbs in an allogeneic-kidney-transplant-model in the rat are presented in next chapter.

Chapter 12 :

In Vivo Use of ^{111}In Anti-Lymphocyte, Activated Lymphocyte, Anti-Donor Class I & II MHC Monoclonal Antibodies for Scintillation Imaging of Rejection in Kidney Transplanted Rats.

A Rat Model for the Early Diagnosis and Discrimination of Rejection in Unmodified and Cyclosporine Treated Allogeneic Kidney Transplants

12.1 Introduction

A rat model for allogeneic kidney transplantation, previously reported in the literature (Milton and Fabre 1985), was adopted for the sake of specific detection of transplant rejection by imaging using the scintillation camera. This model, involving transplantation of DA rat kidney (DA donor) into a PVG rat (PVG recipient), was peculiar in that donor-specific anti-Class I and II MHC monoclonal antibodies[1] were available and had been applied previously for identifying specifically the induction of donor Class I and II MHC antigens during acute rejection by immunohistochemistry.

In this research work, the donor-specific anti-Class I and II MHC antibodies were used radiolabelled with ^{111}In as in vivo probes to follow expression of donor Class I and II MHC antigens in rejecting or cyclosporine-treated transplants without interference from the recipient's infiltrating cells or surrounding tissues.

The model was also suitable for the use of an ^{111}In anti-T cell[2] (CD5) and an ^{111}In anti-IL-2 receptor[3] McAb, as markers for T lymphocytes and activated T

---

1 MN4-91-6 : Anti-DA-rat Class I MHC, F17-23-2 : Anti-DA Class II MHC.
2 MRC OX-19 McAb.
3 MRC OX-39 McAb.

lymphocytes respectively, in order to test the involvement of these cells in the rejection process by external monitoring using the scintillation camera.

12.2 Description of the major histocompatibility complex of the rat and the MHC of the donor (DA or WAG) and recipient (PVG) rats used in this study

The major histocompatibility complex of the rat, designated RT1 (IAWSR 1979), has been found to include the RT1A, RT1B and RT1D regions, and is located between two marker enzyme loci glyoxalate 1 (Glo-1) and neuraminidase 1 (Neu-1) (see Figure 12.1).

Figure 12.1. The genes of the major histocompatibility complex in the rat; a comparison with mouse and human MHC.

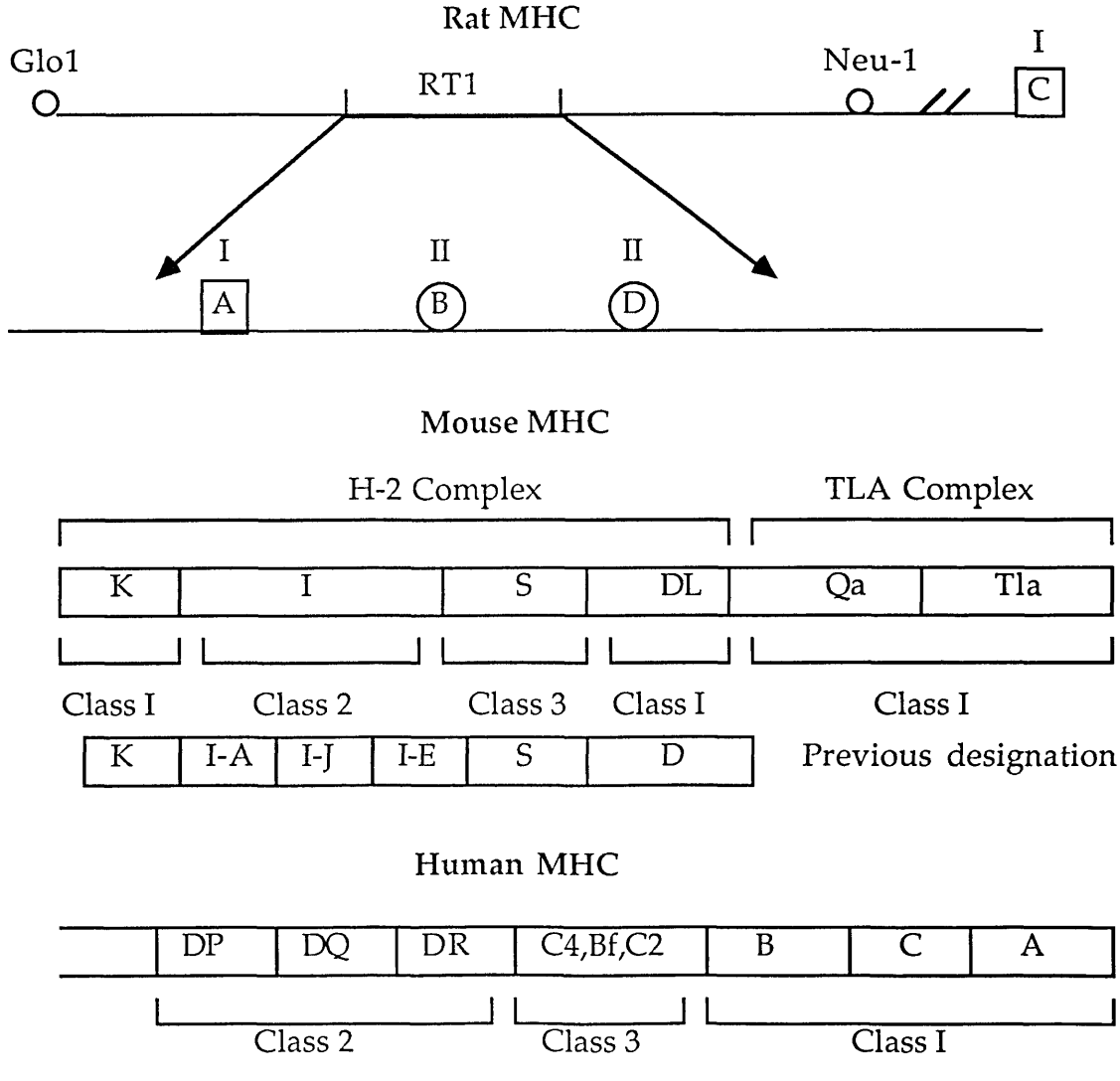

The RT1A subregion encodes for MHC Class I antigens while RT1B and RT1D encode for MHC Class II antigens.

12.2.1 The Class I molecules

The RT1A gene product is a classic transplantation Class I antigen. It is ubiquitously expressed among tissues and incompatibility at this gene region is known to cause acute skin graft rejection (Gunther and Stark 1977). Functionally, the RT1A molecule is a restriction element for cytotoxic T-cell activity (Gunther and Wurst 1984).

The Class I MHC molecule is composed of two non-covalently associated polypeptides : The alpha chain containing 3 extracellular domains a transmembrane region and a cytoplasmic tail, and the beta-2 microglobulin comprising one extracellular domain (β2 microglobulin is not encoded by the MHC region).

12.2.2 The Class II molecules

The gene products of RT1B and RT1D give the strongest stimulation for graft rejection in allograft transplantation (Kohoutava et al 1980, Paris and Gunther 1980).

The RT1B has been shown to be homologous to H-2 I-A in the mouse Class II MHC and RT1D homologous to H-2 I-E. The Class II MHC molecule is a dimer consisting of an alpha and beta chain. Each chain consists of two extracellular domains (alpha-1, alpha-2, beta-1 and beta-2), a connecting peptide, a transmembrane region and a cytoplasmic tail (Figueroa and Klein 1986).

The rat strains used in the present study differ from each other in both the Class I and Class II MHC antigens : DA is $RT1^{av1}$, WAG $RT1^{u}$ and PVG $RT1^{c}$.

Allogeneic unmodified grafts of DA or WAG kidneys into PVG recipients are rejected and become non-functional within 7-10 days of transplantation.

12.3 Materials and Methods

12.3.1 Animals

Adult male DA ($RT1^{av1}$, $RT2^{b}$ & $RT3^{a}$), WAG ($RT1^{u}$ & $RT2^{b}$) and PVG/c ($RT1^{c}$, $RT2^{b}$ & $RT3^{a)}$ rats were purchased from Harlan-Olac Ltd, England and used when they were between 200-350 g.

12.3.2. The monoclonal antibodies

Four monoclonal antibodies labelled with ^{111}In were used : MRC OX-19 (CD5, Pan T in the rat), MRC OX-39 (anti-IL-2 receptor in the rat), MN4-91-6 (anti-Class I MHC DA specific) and F17-23-2 (anti-Class II MHC DA rat specific).

For details on antibody specificity, radiolabelling with ^{111}In, immunoreactivity and binding of each McAb to the relevant cell population see the previous chapter.

12.3.3 The transplantation procedure[1]

Orthotopic left kidney transplantation in the rat was performed. The left kidney of the donor (the transplant, Tx) was grafted in the place of the left kidney of the recipient by end to end anastomosis of the renal artery, vein and ureter. The right kidney of the recipient was left in place (native control). The ischaemia time was usually 30 min and did not exceed 45 minutes.

---

1 For details of the traansplant procedure, see Appendix, page 350.

12.3.4 Cyclosporine treatment of the transplanted rats

Cyclosporine[1] was diluted in oil at 10 mg/ml and was given orally by gavage under ether anaethesia to a group of the transplanted rats at 10 mg/kg/day from the day of transplantation until the day of sacrifice of the animals. The animals were weighed daily to monitor weight gain and adjust the dose of cyclosporine given accordingly.

12.3.5 In vivo administration of the antibodies, scintillation camera imaging and tissue sampling

12.3.5.1 The experimental setting (see Figure 12.2)

The experimental approach to using the ^{111}In McAbs (MRC OX-19, MRC OX-39, MN4-91-6 or F17-23-2) involved intravenous injection in the following groups of animals :

1) Non-transplanted intact controls : These were either DA or PVG rats.

2) Allogeneic-kidney transplanted rats : All transplants were DA-donor kidney into a PVG-recipient rat combination, except one experiment that used a WAG donor kidney into a PVG recipient rat (see Table 12.1 below).

3) Isogenic kidney transplanted rats : Both donor and recipient in this group were PVG rats.

4) Cyclosporine-treated allogeneic-kidney transplanted rats : These were DA-donor kidney into PVG recipient rat combination treated with cyclosporine.

5) Cyclosporine-treated isogenic-kidney transplanted rats : Both donor and recipient in this group were PVG rats. The animals were treated with cyclosporine after transplantation.

---

1 Sandimmune, Sandoz, Switzerland. Cyclosporine in oil at 100 mg/ml.

Two protocols were used for the injection of the antibodies. In the first, ^{111}In-labelled McAbs were injected intravenously into transplanted rats via a lateral tail vein at set times after transplantation and the rats were imaged and sacrified at 24 hr after ^{111}In McAb injection (except rats injected with ^{111}In MRC OX-19, which were sacrificed at 70 hr post Ab injection).

The second protocol differed from that described above in that the animals were sacrificed at 4 hr (instead of 24 hr) after the intravenous injection of the of the ^{111}In McAb (see Table 12.1 for details on the animals used).

In this setting, the right kidney of the recipient (native kidney) provided an internal control in each rat by giving a reference for the images and the uptake of each ^{111}In McAb used.

Figure 12.2. The experimental setting used for in vivo administration of ^{111}In McAbs in the transplanted rats.

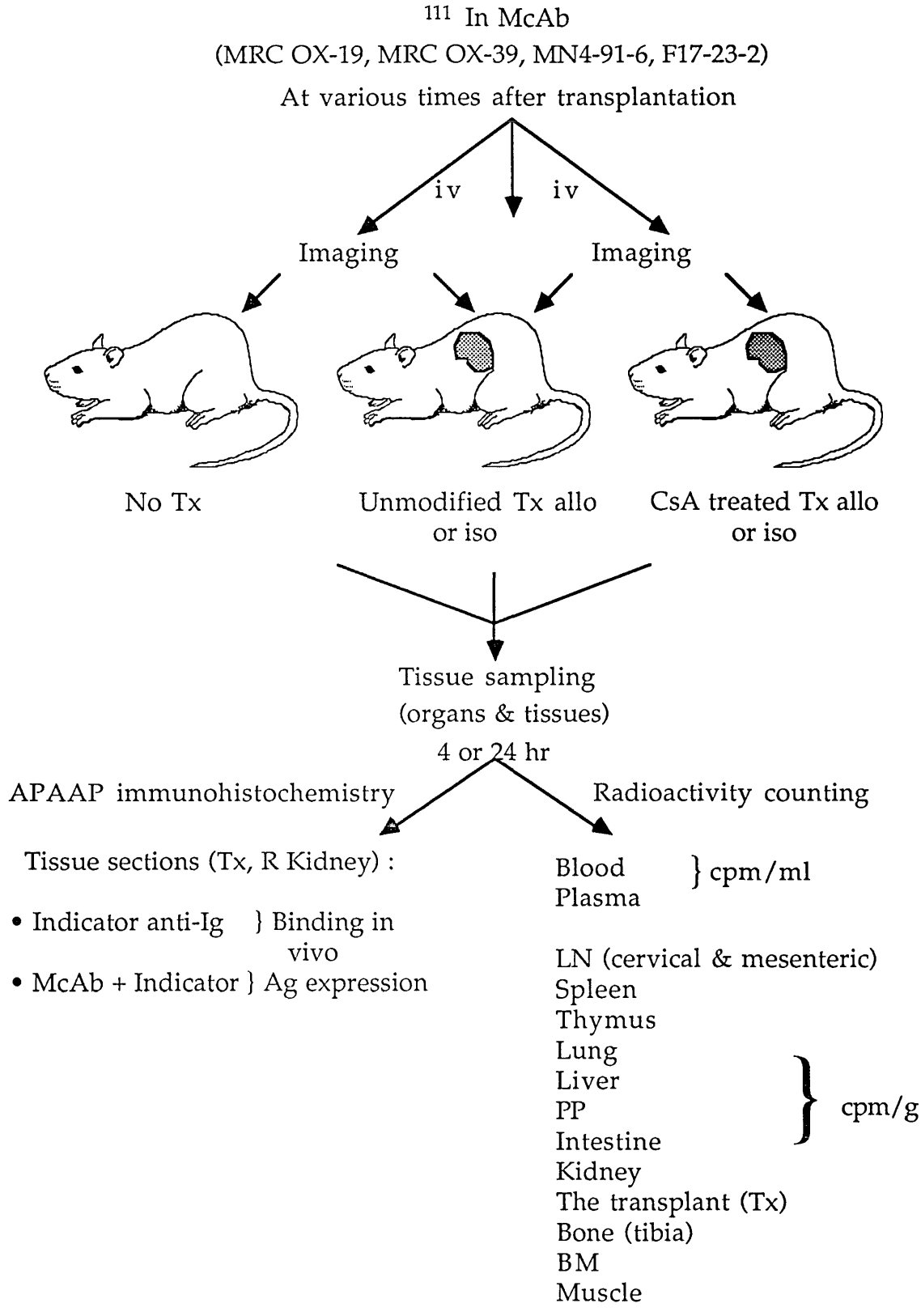

Abbreviations : Tx : Transplant, allo : allogeneic, iso : isogeneic, LN : lymph nodes, PP : Peyer's patches, BM : bone marrow, CsA : cyclosporine, iv : intravenous, McAb : monoclonal antibody, Ag : antigen. Ig : immunoglobulin.

Table 12.1. List of experiments performed, rats included, injection time after transplantation, cyclosporine treatment, time of sacrifice and the preparation used (specificity, dose and radioactivity).

Expt	Rat	Injection time (days post Tx[b])	CsA[a]	^{111}In McAb	Dose (µg/kg)	Radioactivity (MBq)	Time of sacrifice (hr post Ab injection)
1	PVG Control	NA[c]	NO	OX-19	20	5	70
	DA--->PVG	3	NO	OX-19	20	5	70
	DA--->PVG	5	NO	OX-19	20	5	70
2	PVG Control	NA	NO	OX-39	20	4	24
	DA Control	NA	NO	OX-39	20	4	24
	DA--->PVG	4	NO	OX-39	20	4	24
3	DA--->PVG	4	NO	OX-39	20	1	24
	PVG--->PVG	4	NO	OX-39	20	1	24
4	DA--->PVG	4	NO	OX-39	20	1.5	24
5	DA--->PVG	2	NO	OX-39	20	2	24
	DA--->PVG	2	YES	OX-39	20	2	24
6	PVG Control	NA	NO	MN4	20	3.5	24
	DA Control	NA	NO	MN4	20	3.5	24
7	DA--->PVG	1	NO	MN4	20	2.5	24
	DA--->PVG	4	NO	MN4	20	1.3	24
8	DA--->PVG	3	NO	MN4	20	1.5	24
9	PVG--->PVG	1	NO	MN4	20	1	24
10	DA--->PVG	3	NO	MN4	20	0.5	4
	PVG--->PVG	3	NO	MN4	20	0.5	4

Table 12.1. Continued.

Expt	Rat	Injection time (days post Tx)	CsA	^{111}In McAb	Dose (µg/kg)	Radioactivity (MBq)	Time of sacrifice (hr post Ab injection)
11	DA--->PVG	3	NO	MN4	20	0.5	4
	WAG--->PVG	3	NO	MN4	20	0.5	4
12	DA--->PVG	3	YES	MN4	20	1	4
13	DA--->PVG	7	YES	MN4	20	1	4
	PVG--->PVG	7	YES	MN4	20	1	4
14	DA--->PVG	14	YES	MN4	20	6	4
	DA--->PVG	21	YES	MN4	20	2	4
15	PVG Control	NA	NO	F17	20	5	24
	DA Control	NA	NO	F17	20	5	24
16	DA--->PVG	6	NO	F17	20	5	24
17	DA--->PVG	4	NO	F17	20	3	24
	DA--->PVG	4	NO	F17	4	0.5	24
18	DA--->PVG	4	NO	F17	20	12	4
	DA--->PVG	4	NO	F17	20	3	4
19	DA--->PVG	4	YES	F17	20	6	4
	DA--->PVG	7	YES	F17	20	3	4
20	DA--->PVG	14	YES	F17	20	5	4

a CsA : Cyclosporine.
b Tx : transplant.
c NA : Not applicable.

12.3.5.2 Scintillation camera imaging

The rats were imaged at 4 or 24 hr after the injection of the antibodies. The same imaging equipment described in Chapter 8 for imaging ^{111}In MRC OX-19 distribution in the rat was used (Toshiba LFOV scintillation camera, pinhole collimator & on-line computer acquisition).

Whole body static images were taken, as well as spot-views of the chest, abdomen & pelvis in anterior or posterior projections. Obliques views were also taken to clarify further the anatomical elements in the images obtained. Acquisition time was set usually to 10 minutes for each view. The images were displayed on a colour monitor screen for analysis or photography.

12.3.5.3 Tissue sampling

At the time of sacrifice of each animal, blood was taken into a heparin-containing syringe by cardiac puncture under terminal anaesthesia. The following organs were dissected, cleaned and kept on a wet tray for weighing: lymph nodes, thymus, lung, spleen, the transplant, the right kidney, Peyer's patches, intestine, bone, bone marrow and muscle. Each organ/tissue was weighed in a preweighed scintillation vial and counted for ^{111}In radioactivity in a gamma well counter. Also, aliquots of 1 ml blood and 1 ml plasma, obtained by blood centrifugation at 1000 g for 10 minutes, were counted similarly.

In some experiments, samples of the transplant, right kidney (the native kidney) and spleen were frozen in liquid nitrogen after weighing of the tissues and were used to prepare tissue sections for immunohistology staining.

During dissection of the animals, a graph showing the anatomical position of the transplant and the spleen was drawn. Also, the macrosopic appearance of the transplant in terms of size and colour was noted.

12.3.6 Immunohistochemistry staining of tissue sections

Tissue sections from the transplant, the native kidney and the spleen were prepared and stained by the APAAP technique as described earlier (see Chapter 8, Paragraph 8.2.9 page 132).

For each tissue sampled, staining of the sections was done with or without in vitro addition of the antibody that had been used in vivo to check, respectively, antigen presence and in vivo binding of the antibody to the cells (see Chapter 8 page 132).

12.4 Results

12.4.1 ^{111}In MRC OX-19 (CD5, anti-Pan rat T cell) in the transplanted rats

A) Imaging :

Imaging ^{111}In MRC OX-19 distribution showed intense uptake in the spleen noted previously in non-transplanted rats (see Chapter 8). Also, uptake was seen in the abdomen corresponding to the mesenteric chain of lymph nodes. Uptake in the transplant was not, however, seen even on scans performed at 24 and 48 hr or on the oblique views (Figure 12.3).

Figure 12.3. Images of ^{111}In MRC OX-19 in control and transplanted rats.

Right panel : Images of a control PVG rat 24 hr after injection of ^{111}In MRC OX-19. Top right : Anterior abdomen. Bottom right : Left anterior oblique. Bottom left : Right anterior oblique. Note the high uptake in the spleen, uptake in liver and the mesenteric lymph nodes.
Left panel : Images of DA-->PVG rat transplanted 5 days before the injection of ^{111}In MRC OX-19 and imaged 24 hr PI. Top left : Anterior abdomen. Top R : Posterior abdomen. Bottom R: Anterior whole body, Bottom L : Posterior WB. High uptake is seen in the spleen which is lying across the abdomen. Uptake in the liver is also seen but no clear uptake in the transplant.

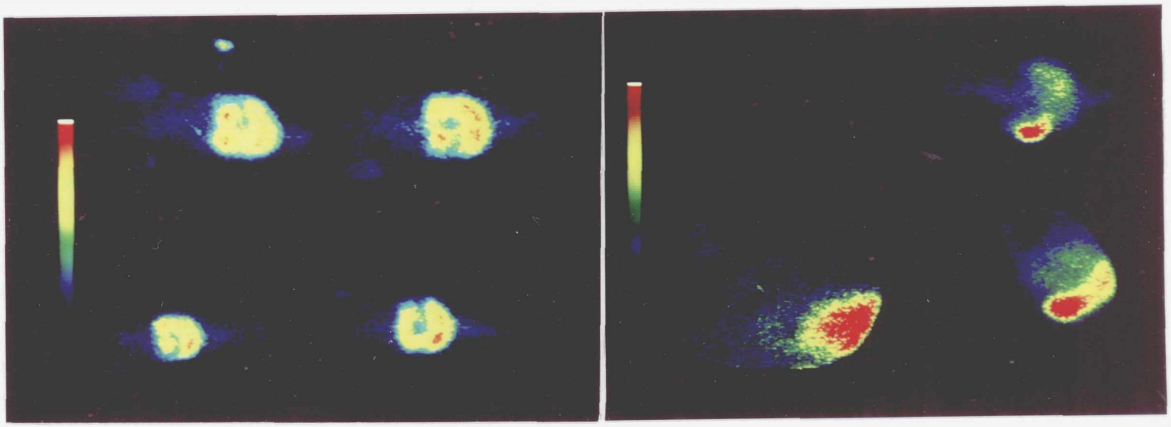

Tail ⟶ Head

B) Tissue sampling

Sampling of the transplant showed an enlarged oedematous kidney which had a pale colour as compared to the native kidney. Also, an enlarged spleen was noted.

The results of tissue sampling in the control and the unmodified transplanted rats after injection of ^{111}In MRC OX-19 are shown in Table 12.2.

Table 12.2. Tissue uptake[a] in the rats injected with ^{111}In MRC OX-19

	Expt 1		
Rat	PVG Control	DA--->PVG (Tx 6d)	DA--->PVG (Tx 8d)
Blood[b]	0.12 ± 0.0005	0.18 ± 0.001	0.16 ± 0.001
Plasma[b]	0.17 ± 0.0006	0.28 ± 0.002	0.22 ± 0.001
CLN[c]	3.81 ± 0.02	2.64 ± 0.02	2.31 ± 0.02
Spleen[c]	13.69 ± 0.05	6.73 ± 0.03	5.23 ± 0.02
Spleen total[d]	6.57 ± 0.02	5.16 ± 0.02	5.89 ± 0.02
Liver[c]	1.47 ± 0.01	2.12 ± 0.02	2.45 ± 0.02
Liver total[d]	12.23 ± 0.08	17.38 ± 0.16	22.69 ± 0.19
R Kidney[c]	3.56 ± 0.01	5.64 ± 0.03	5.15 ± 0.02
R Kid total[d]	3.25 ± 0.01	4.92 ± 0.03	6.01 ± 0.02
Transplant[c]	NA	2.66 ± 0.006	1.15 ± 0.003
Tx total[d]	NA	2.93 ± 0.007	2.02 ± 0.005
Ratio Tx/Kid	NA	0.47 ± 0.003	0.22 ± 0.001
Ratio Tx/Kid (total)	NA	0.60 ± 0.004	0.34 ± 0.001

a The results of uptake in the other tissues sampled, ie lung, intestine, etc, are shown in Table A12.1, Appendix, page 351.
b The results are shown as percent injected dose per millilitre (%ID/ml).
c The results are shown as percent injected dose per gramme (%ID/g).
d The results are shown as percent injected dose per total organ (%ID total).

In Tables 12.2 and A12.1, uptake of ^{111}In MRC OX-19 at 70 hr after injection was documented in the spleen (per unit weight and total organ) and lymph nodes. Uptake in the liver was also noted. The uptake in the transplant compared to the right kidney was low, both per unit weight and total organ and the ratio of the uptake in the transplant to that in the right kidney was significantly less than one. The right kidney accumulated the tracer to a rather high degree in the transplanted animals compared to the kidney in the control intact rat. This was most probably due to localisation of antibody degradation products in the single functional kidney.

12.4.2 ^{111}In MRC OX-39 (anti-IL-2 receptor McAb)

A) Imaging :

The images obtained at 24 hr after the injection of ^{111}In MRC OX-39 in unmodified rats 2 and 4 days post transplantation showed positive uptake in the transplant. Uptake in the liver and spleen was also seen. The uptake in the rejecting transplant was readily identifiable (Figure 12.4), however, no uptake in the isograft or the graft in the rat treated with cyclosporine was seen (Figure 12.4).

Figure 12.4. Images of ^{111}In MRC OX-39 in control, transplanted and cyclosporine treated transplanted rats.

Fig 12.4A. Control (intact) PVG rat injected with ^{111}In MRC OX-39 and imaged 24 hr after injection. Left panel : Whole body image (L : Ant, R : Post) showing uptake in the liver and spleen. Right panel : Close-up view of the abdomen (L: Post, R: Ant).

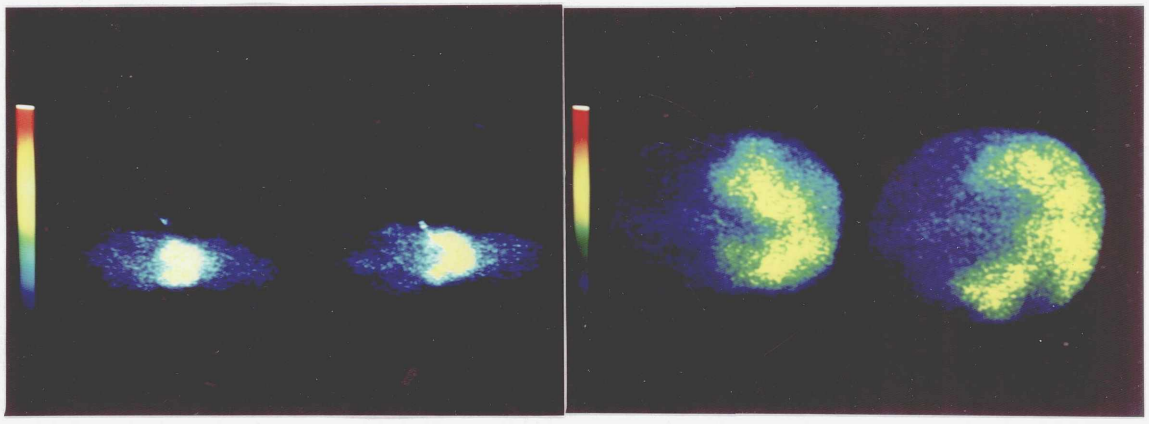

Tail ⟶ Head

Fig 12.4B. DA-->PVG rat transplanted 3 days before injection of ^{111}In MRC OX-39 and imaged 24 hr PI. Left panel : Whole body image (L : Post, R : Ant) showing clear uptake in the rejecting transplant. Uptake in the liver is also seen. Right panel : Close-up view of the abdomen (L : Post, R : Ant) showing uptake in the transplant. The spleen is lying medial to the inferior pole of the transplant (comma shaped).

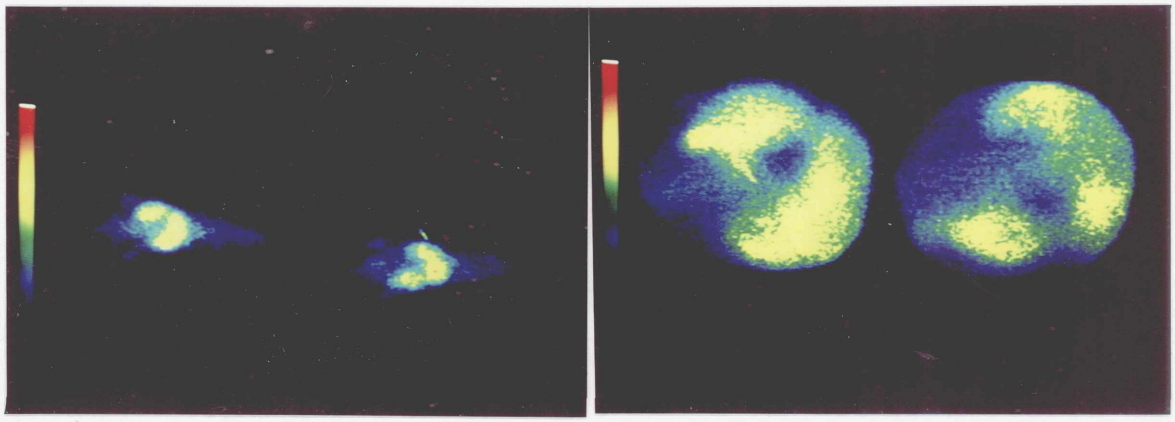

Tail ⟶ Head

Fig 12.4C. Cyclosporine treated DA-->PVG rat transplanted 2 days before injection of ^{111}In MRC OX-39 and imaged 4 hr PI. Left panel : Whole body image (L : Ant, R : Post). Uptake is only seen in the liver and blood pool (heart). Right panel : Close-up view of the abdomen (L : Post, R : Ant). Uptake in the liver is seen. No uptake in the transplant.

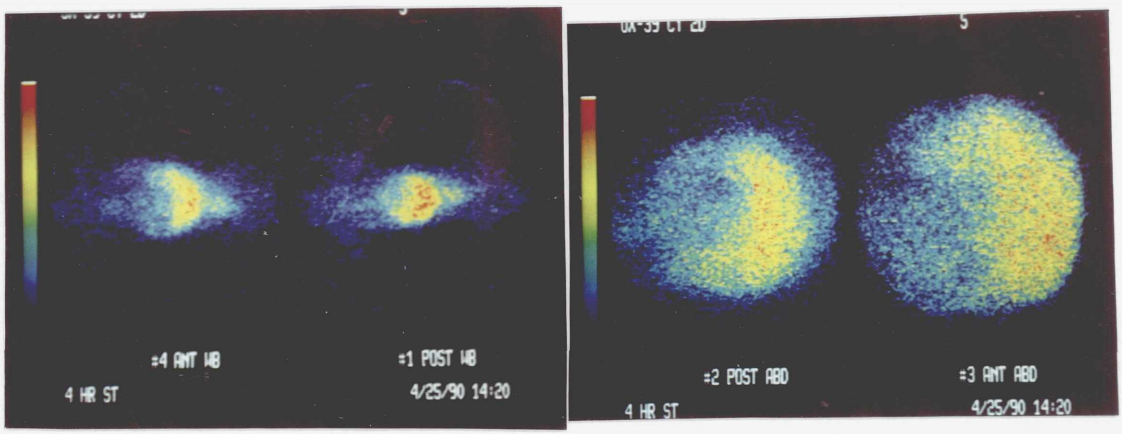

Tail ⟶ Head

B) Tissue sampling :

The results of tissue sampling in control, unmodified- and cyclosporine treated-transplanted rats after injection of ^{111}In MRC OX-39 are shown in Table 12.3.

The distribution of ^{111}In MRC OX-39 in the rats was mainly in the liver and to a minor extent the spleen. Uptake in the right kidney was rather high about 3-5% of the injected dose. Comparatively, uptake in the rejecting transplant was similar or marginally higher, especially when uptake in the total organ was considered for comparison. On the other hand, uptake in the isografts or cyclosporine treated grafts was much lower than that in the rejecting graft and the right native kidney. In one case, increased uptake in the spleen was noted in an animal bearing a rejecting graft on day 4 (Expt 2).

Macroscopically, the rejecting transplants were enlarged and oedematous and had a pale colour as compared to the contralateral native kidney. The spleen was also enlarged in some of the animals undergoing rejection.

C) Immunohistochemistry of tissue sections :

Immunohistochemistry staining of the transplant, kidney and spleen sections using the APAAP technique and addition of MRC OX-39 as first layer antibody showed presence of high numbers of MRC OX-39 positive cells in the transplant and the spleen. However, in vivo binding of MRC OX-39 to the cells in the sections studied was not demonstrable using the same technique having omitted the first layer antibody from the staining sequence (see Figure 12.5).

Table 12.3. Tissue uptake[a] in the rats injected with ^{111}In MRC OX-39 McAb (anti-IL 2 receptor in the rat).

Expt	Rat	Blood[b]	Plasma[b]	Spleen[c]	Spleen[d] total	Liver[c]	Liver[d] total	R kidney[c]	R kidney[d] total	Tx[c]	Tx[d] total	Tx/R kid	Tx/R kid total
2	PVG Control	0.51 ±0.002	0.89 ±0.005	3.71 ±0.01	1.54 ±0.004	2.90 ±0.01	22.73 ±0.08	4.89 ±0.01	3.57 ±0.007	NA	NA	NA	NA
	DA Control	ND	ND	3.94 ±0.01	1.13 ±0.003	3.02 ±0.008	21.29 ±0.06	3.91 ±0.01	3.01 ±0.008	NA	NA	NA	NA
	DA->PVG (Tx 5d)	0.48 ±0.002	0.70 ±0.004	8.39 ±0.02	3.04 ±0.008	2.91 ±0.01	ND	6.48 ±0.01	5.00 ±0.008	4.56 ±0.01	6.87 ±0.02	0.70 ±0.002	1.37 ±0.005
3	DA->PVG (Tx 5d)	0.22 ±0.001	0.34 ±0.002	2.72 ±0.009	2.02 ±0.007	1.36 ±0.006	14.73 ±0.06	4.74 ±0.02	4.44 ±0.02	2.75 ±0.009	4.06 ±0.01	0.58 ±0.003	0.91 ±0.005
	PVG->PVG (Tx 5d)	0.43 ±0.002	0.72 ±0.003	2.88 ±0.01	1.84 ±0.006	1.67 ±0.007	18.70 ±0.08	3.48 ±0.01	2.42 ±0.007	1.09 ±0.004	1.31 ±0.005	0.31 ±0.001	0.54 0.003
4	DA->PVG (Tx 5d)	0.21 ±0.0005	0.31 ±0.0007	2.97 ±0.01	2.27 ±0.008	1.27 ±0.01	14.40 ±0.11	3.91 ±0.01	4.33 ±0.01	2.20 ±0.007	4.73 ±0.02	0.56 ±0.002	1.09 ±0.005
5	DA->PVG (Tx 3d)	0.57 ±0.004	1.00 ±0.006	3.67 ±0.01	2.09 ±0.006	2.06 ±0.01	23.00 ±0.11	4.35 ±0.01	4.28 ±0.01	2.10 ±0.007	1.77 ±0.006	0.48 ±0.002	0.41 ±0.002
	DA->PVG (Tx 3 d CsA)	0.68 ±0.004	1.12 ±0.006	3.34 ±0.01	1.83 ±0.005	2.13 ±0.01	25.22 ±0.12	4.01 ±0.01	4.49 ±0.01	1.31 ±0.01	1.37 ±0.01	0.33 ±0.003	0.31 ±0.002

a The results of uptake in the other tissues sampled, ie lymph nodes, lung, intestine etc, are shown in Table A12.2, Appendix A, page 351.
b %ID/ml.
c %ID/g.
d %ID/total organ.

Figure 12.5. Immunohistochemistry after injection of ^{111}In MRC OX-39 in the DA->PVG rat (Tx 5d). Sampling at 24 hr PI (Frozen sections, X40).

Fig 12.5A. Left panel: Haematoxylin staining of the right native kidney (normal kidney). Right panel : Haematoxylin staining of the transplant. Note the cellular infiltration and disruption of the normal histology.

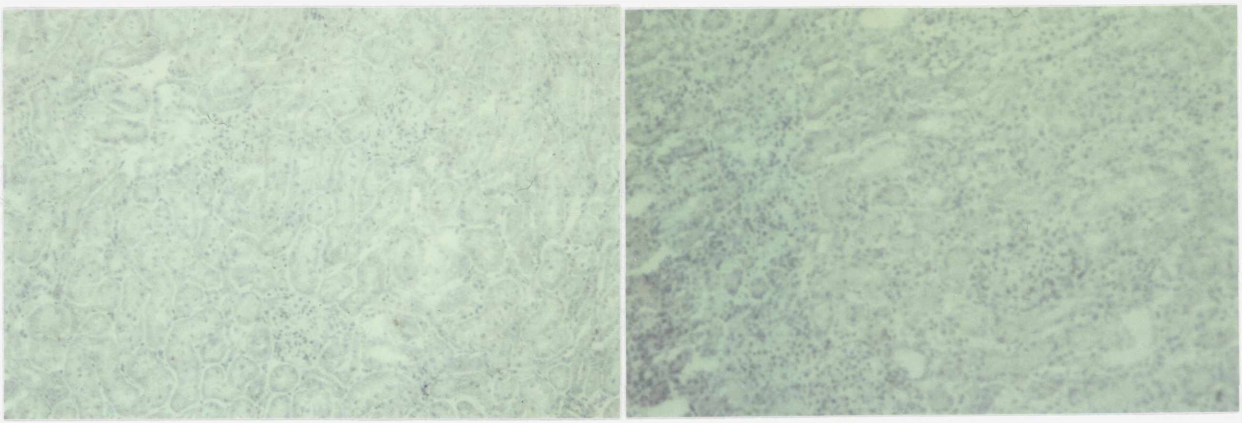

Fig 12.5B. L panel : APAAP staining of the R kidney after addition of MRC OX-39 in vitro. Negative. R panel : APAAP staining of the Tx after addition of MRC OX-39 in vitro. Note the positive staining of individual cells scattered in the section.
Fig 12.5 C. R panel only : APAAP staining of the Tx to detect in vivo binding of ^{111}In MRC OX-39 (no MRC OX-39 in vitro). Negative.

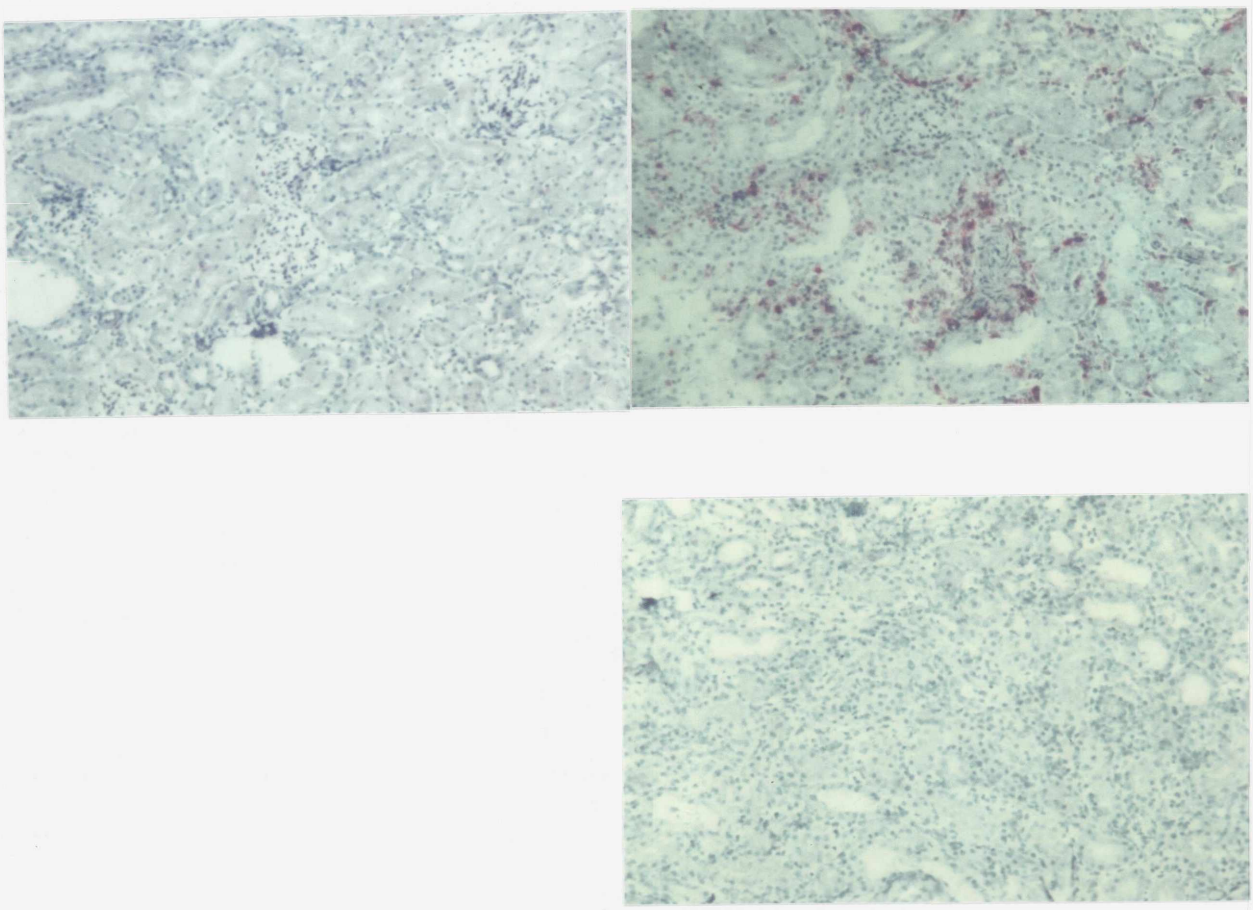

12.4.3. ^{111}In MN4-91-6 (anti-Class I MHC donor specific McAb)

A) Imaging :

Intense uptake of radioactivity in the kidney graft was seen in all allogeneic transplants (unmodified and cyclosporine treated)(Figure 12.6). This was associated with low radioactivity in liver and blood pool. In the isogenic PVG into PVG grafts, no uptake was seen in the transplant (Figure 12.6). Also, using a donor kidney from a third-party rat belonging to WAG ($RT1^u$) strain into a PVG rat and imaging the animal after injection of ^{111}In MN4-91-6 no uptake in the graft could be elicited.

Imaging at 4 hr instead of 24 hr after injection of the antibody did not show great difference using the ^{111}In MN4-91-6 McAb. Intense uptake in the transplant was seen using either protocol. Uptake in liver was relatively higher in the late images, while blood pool activity in the heart was more prominent in the early images.

Figure 12.6. Images of ^{111}In MN4-91-6 in a control rat and in allogeneic and isogeneic grafts.

Fig 12.6A. Control PVG rat, 24 hr post ^{111}In MN4-91-6. L panel : Whole body image (L : Ant, R : Post). Activity is seen mainly in liver, spleen and blood pool (posterior image is faint due to technical fault). R panel : Close-up view of the abdomen (L : Ant, R : Post) with uptake in liver and spleen.

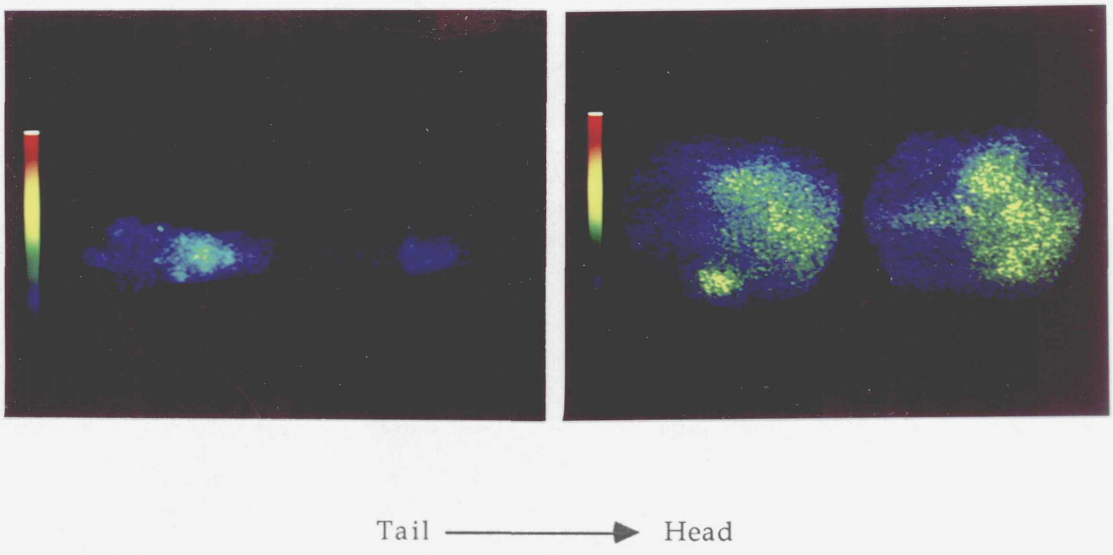

Fig 12.6B. DA-->PVG Tx 4 d, 24 hr PI. Left panel : whole body image (L : Ant, R : Post). The transplant has taken the tracer very avidly and no other structure is seen. R panel : Close-up view of the abdomen (L : Ant, R : Post). Intensive uptake is seen in the transplant. Very faint background in liver.

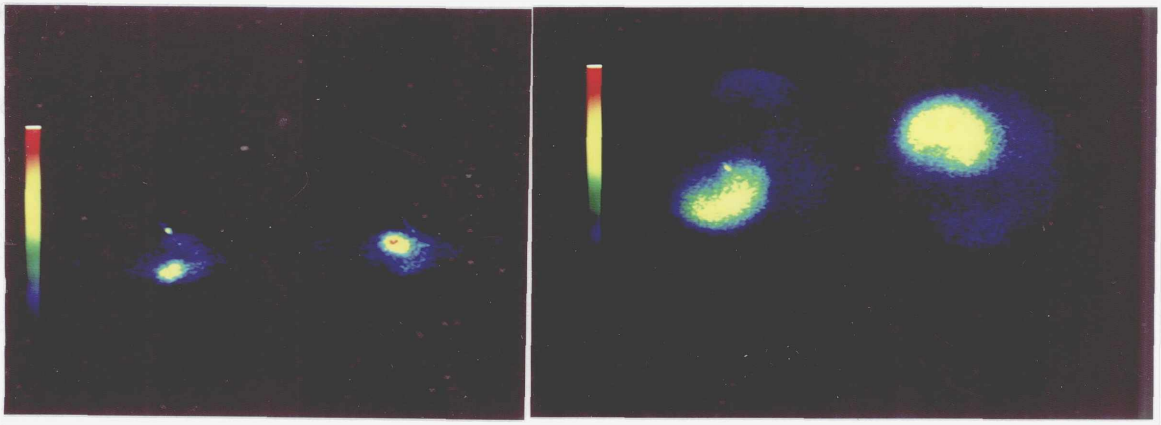

Tail ⟶ Head

Fig 12.6C. PVG-->PVG, Tx 4 d, 4 hr PI. L panel : Whole body image (L : Post, R : Ant). No uptake in the transplant (isograft). Uptake is seen in liver, spleen and blood pool (heart). R panel : Close-up view of the abdomen (L : Ant, R : Post) showing diffuse radioactivity in the liver and spleen. No uptake in the isograft.

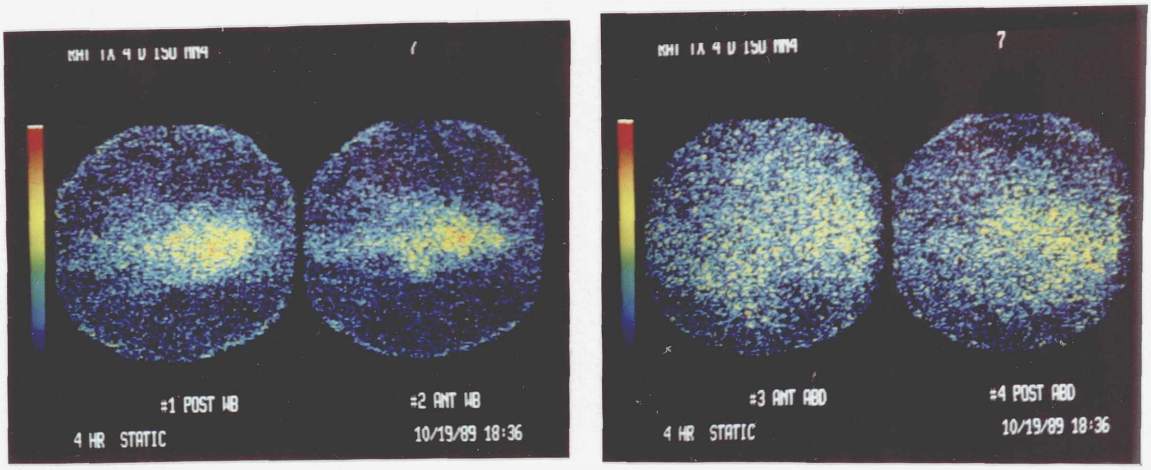

Tail ⟶ Head

B) Tissue sampling

Rejecting kidneys in unmodified rats showed signs of swelling and discolouration at the time of sampling. In contrast, transplants in cyclosporine-treated rats or the isografts were not significantly different from the native contralateral kidney of the recipient. Uptake in the transplant and other tissues sampled in the rats injected with ^{111}In MN4-91-6 is shown in Table 12.4.

From Table 12.4, intensive uptake of ^{111}In MN4-91-6 was seen in allogeneic grafts from DA-donor rats. This uptake amounted to about a third of the injected dose. The ratio of uptake in the transplant to that in the right kidney ranged between 5-30. Sampling at 4 hr after injection showed higher uptake in the graft and lower background in the right kidney compared to sampling at 24 hr PI. Both unmodified and cyclopsorine-treated DA grafts showed high uptake. However, graft uptake in cyclosporine-treated animals was less than in non-treated rats sampled at the same time after transplantation. In contrast, PVG into PVG isografts and the rejecting WAG-donor allograft in the PVG rat did not accumulate the tracer and the ratio of uptake in the transplant to the contralateral native kidney did not point to a difference in uptake of antibody between the two organs.

Table 12.4. Tissue uptake[a] in the rats injected with ^{111}In MN4-91-6 anti-Class I MHC DA specific McAb.

Expt	Rat	Blood[b]	Plasma[b]	Spleen[c]	Spleen[d] total	Liver[c]	Liver[d] total	R kidney[c]	R kidney[d] total	Tx[c]	Tx[d] total	Tx/R kid	Tx/R kid total
I. Sampling 24 hr after Ab injection													
6	PVG Control	1.67 ±0.006	2.81 ±0.01	1.77 ±0.008	0.91 ±0.004	1.06 ±0.004	9.35 ±0.04	2.58 ±0.009	2.01 ±0.007	NA	NA	NA	NA
	DA Control	2.91 ±0.01	1.67 0.01	5.55 ±0.02	2.06 ±0.007	2.14 ±0.009	12.99 ±0.05	3.98 ±0.01	2.35 ±0.006	NA	NA	NA	NA
7	DA->PVG (Tx 2d)	0.63 ±0.003	1.09 ±0.004	5.94 ±0.02	2.97 ±0.01	1.06 ±0.005	8.80 0.04	3.54 ±0.01	3.50 ±0.01	25.15 ±0.09	23.59 ±0.08	7.10 ±0.03	6.74 ±0.03
	DA->PVG (Tx 5d)	0.62 ±0.003	1.03 ±0.004	2.38 ±0.008	1.86 ±0.006	0.94 ±0.004	9.90 ±0.04	3.73 ±0.01	4.91 ±0.01	12.13 ±0.04	24.25 ±0.08	3.25 ±0.01	4.94 ±0.02
8	DA->PVG (Tx 4d)	0.66 ±0.005	0.94 ±0.006	1.79 ±0.01	1.26 ±0.007	0.63 ±0.008	6.09 ±0.08	2.20 ±0.01	2.46 ±0.01	14.17 ±0.05	20.27 ±0.07	6.44 ±0.04	8.24 0.04
9	PVG->PVG (Tx 2d)	1.22 ±0.004	1.95 ±0.006	1.92 ±0.006	1.24 ±0.004	1.06 ±0.004	11.05 ±0.04	2.17 ±0.007	2.30 ±0.007	1.49 ±0.005	1.46 ±0.005	0.69 ±0.003	0.63 ±0.003
II. Sampling 4 hr after Ab injection													
10	DA->PVG (Tx 3d)	2.17 ±0.007	3.49 ±0.01	2.40 ±0.007	1.68 ±0.005	0.86 ±0.004	8.22 ±0.04	1.38 ±0.004	1.41 ±0.004	33.90 ±0.11	44.47 ±0.14	24.57 ±0.11	31.54 ±0.13
	PVG->PVG (Tx 3d)	4.07 ±0.01	6.06 ±0.02	1.17 ±0.004	0.58 ±0.002	1.05 ±0.005	9.50 ±0.05	1.62 ±0.005	1.45 ±0.004	1.60 ±0.005	1.68 ±0.005	0.99 ±0.003	1.16 ±0.005
11	DA->PVG (Tx 3d)	2.24 ±0.009	3.47 ±0.01	3.09 ±0.01	1.76 ±0.006	0.89 ±0.005	8.44 ±0.05	1.18 ±0.004	1.17 ±0.004	27.16 ±0.08	32.25 ±0.09	23.02 ±0.10	27.56 ±0.12
	WAG->PVG (Tx 3d)	4.08 ±0.02	5.92 ±0.02	1.39 ±0.004	1.06 ±0.003	1.46 ±0.007	13.72 ±0.07	1.62 ±0.005	1.70 ±0.005	1.55 ±0.005	1.87 ±0.006	0.96 ±0.004	1.10 ±0.005

Table 12.4. Continued.

Expt	Rat	Blood[b]	Plasma[b]	Spleen[c]	Spleen[d] total	Liver[c]	Liver[d] total	R kidney[c]	R kidney[d] total	Tx[c]	Tx[d] total	Tx/R kid	Tx/R kid total
12	DA->PVG	1.94	3.09	1.91	1.03	0.77	7.44	1.14	1.21	24.68	25.99	21.65	21.48
	(Tx 3d CsA)	±0.007	±0.01	±0.005	±0.003	±0.003	±0.03	±0.003	±0.003	±0.05	±0.05	±0.07	±0.07
13	DA->PVG	2.04	3.09	0.95	0.52	0.64	5.25	1.48	1.18	29.04	24.64	19.69	20.88
	(Tx 7d CsA)	±0.008	±0.01	±0.007	±0.004	±0.006	±0.05	±0.009	±0.007	±0.05	±0.04	±0.12	±0.13
	PVG->PVG	3.72	5.68	1.00	0.45	0.82	6.56	1.71	1.43	1.64	1.28	0.96	0.90
	(Tx 7d CsA)	±0.01	±0.02	±0.003	±0.001	±0.007	±0.06	±0.007	±0.006	±0.007	±0.005	±0.006	±0.005
14	DA->PVG	2.38	3.43	0.94	0.57	0.74	9.13	1.47	1.69	38.23	36.44	26.01	21.56
	(Tx 14d CsA)	±0.01	±0.01	±0.005	±0.003	±0.005	±0.06	±0.006	±0.007	±0.11	±0.10	±0.13	±0.11
	DA->PVG	2.00	3.17	0.90	0.49	0.59	6.28	1.42	1.53	29.28	31.08	20.62	20.31
	(Tx 21d CsA)	±0.008	±0.01	±0.005	±0.003	±0.003	±0.03	±0.003	±0.003	±0.09	±0.10	±0.08	±0.08

a The results of uptake in the other tissues sampled. ie lymph nodes, lung, intestine etc, are shown in Table A12.3, Appendix, page 352.
b %ID/ml.
c %ID/g.
d %ID/total organ.

C) Immunohistochemistry of tissue sections :

Staining of tissue sections from rats bearing an untreated allogeneic DA into PVG kidney grafts was done to check in vivo binding of ^{111}In MN4-91-6 to the cells and the antigen expression in the tissue. Positive patchy staining of the glomeruli and tubules was seen in the sections that were tested for in vivo binding of the antibody (no first layer antibody, staining by anti-mouse Ig, APAAP & substrate)(see Figure 12.7). In sections where MN4-91-6 was added as first layer in the staining procedure, generalised staining was seen.

Figure 12.7. Immunohistochemistry after injection of ^{111}In MN4-91-6 in the DA--> PVG rat (TX 5d). Sampling at 24 hr PI (Frozen sections, X40).

Fig 12.7A. L Panel : APAAP staining of the R kidney after addition of MN4-91-6 in vitro. Generally negative, faint staining in the glomeruli. R Panel : APAAP staining of the Tx after addition of MN4-91-6 in vitro. Generalised staining of the tubules.

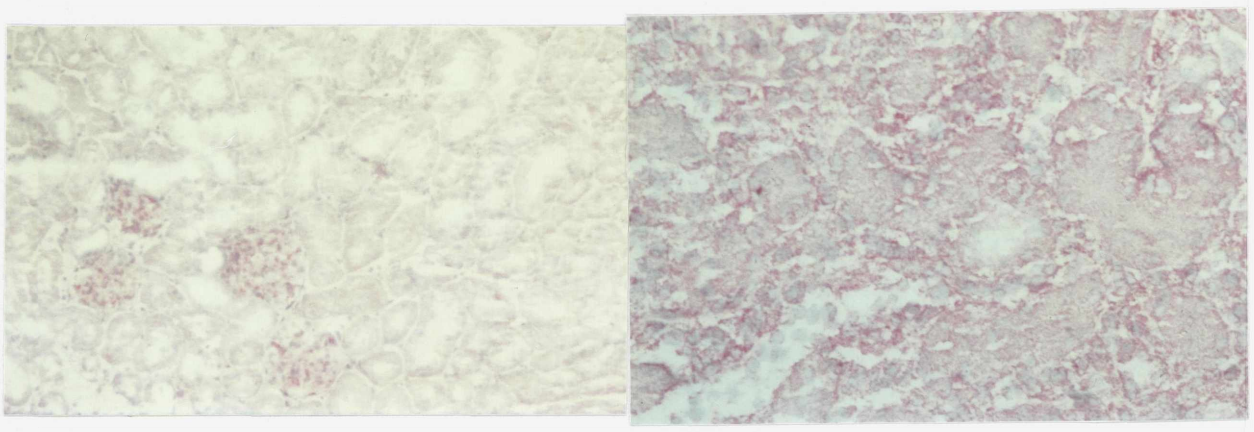

Fig 12.7B. Right panel only : APAAP staining of the Tx to detect in vivo binding of ^{111}In MN4-91-6. Patchy positive staining around the tubules and in the glomerulus.

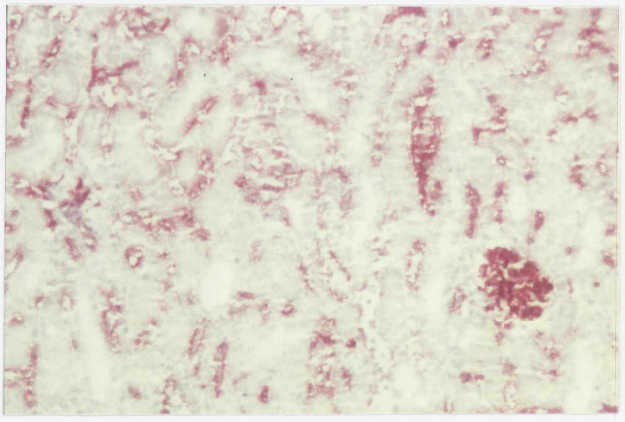

12.4.4 ^{111}In F17-23-2 (anti-Class II MHC donor specific McAb)

A) Scintillation camera imaging :

The results of imaging using ^{111}In F17-23-2 anti-Class II DA-specific McAb showed clear uptake in the unmodified allogeneic kidney transplants at 4 days post transplant (Figure 12.8). However, high background in liver and spleen was also seen. Uptake in the rejecting transplant was more clearly seen in a rat injected with a rather lower dose of antibody, 1 μg instead of 5 μg used in the other transplanted animals. In cyclosporine treated rats no uptake was seen in the transplant and images obtained were similar to images of the control PVG rat.

Figure 12.8. Images of ^{111}In F17-23-2 in transplanted rats.

Fig 12.8A. DA-->PVG (Tx 4d), 24 hr PI. Left panel : Whole body image (L : Ant, R : Post) showing uptake in the transplant and high uptake in liver and blood pool. Rght panel : Close-up abdominal view (L : Ant, R : Post) showing uptake in the transplant, liver and spleen (lying across the abdomen).

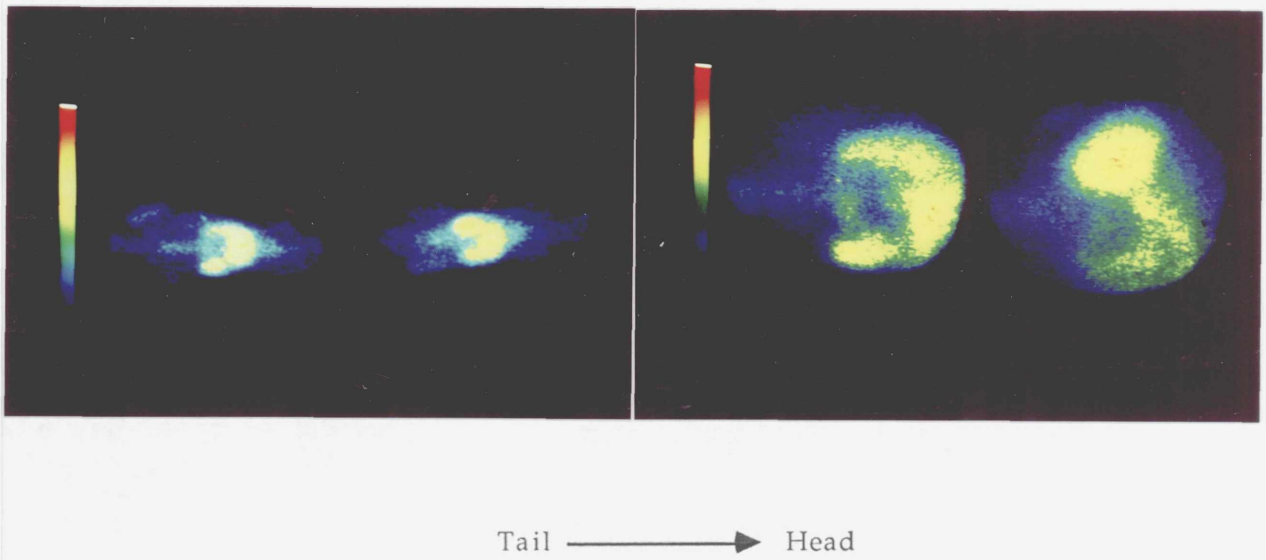

Fig 12.8B. DA-->PVG (Tx 7d), 24 hr PI. Left panel : Whole body image (L : Post, R : Ant) showing intense uptake in liver and moderate uptake in the graft. R panel : Close-up view of the abdomen (L : Post, R : Ant). Uptake is noted mainly in the liver. Faded uptake in the transplant is seen.

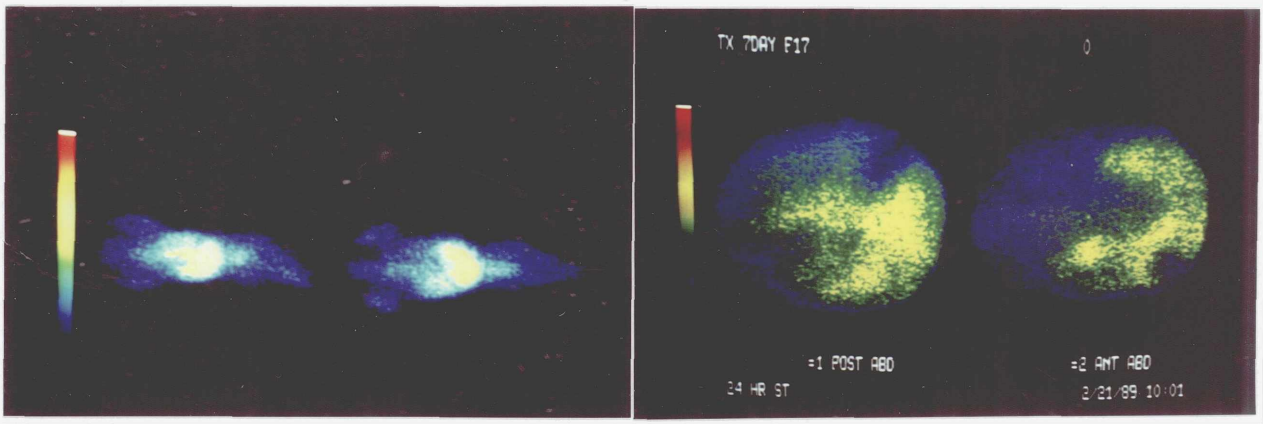

Tail ⟶ Head

B) Tissue sampling :

Unmodified allogeneic kidney transplants were enlarged and oedematous. Patchy discolouring was also noted. The transplants taken from cyclosporine treated rats were of normal size and their weight was similar to the native kidney and, if any, showed a slight pallor as compared to the contralateral kidney.

The results of the tissue sampling in non-modified and cyclosporine treated animals are shown in Table 12.5.

Table 12.5. Tissue uptake[a] in the rats injected with ^{111}In F17-23-2 anti-Class II MHC DA specific McAb.

Expt	Rat	Blood[b]	Plasma[b]	Spleen[c]	Spleen[d] total	Liver[c]	Liver[d] total	R kidney[c]	R kidney[d] total	Tx[c]	Tx[d] total	Tx/R kid	Tx/R kid total
I. Sampling 24 hr after Ab injection													
15	PVG Control	ND	ND	1.90 ±0.02	0.91 ±0.01	2.39 ±0.006	23.65 ±0.06	3.70 ±0.008	2.91 ±0.006	NA	NA	NA	NA
	DA Control	1.20 ±0.03	1.86 0.005	14.44 ±0.04	6.31 ±0.02	3.24 ±0.01	27.66 ±0.09	2.82 ±0.006	2.75 ±0.006	NA	NA	NA	NA
16	DA->PVG (Tx 7d)	1.26 ±0.008	1.73 ±0.01	1.79 ±0.06	1.57 ±0.05	1.88 ±0.01	16.17 0.09	3.20 ±0.01	2.90 ±0.009	0.94 ±0.003	2.74 ±0.009	0.29 ±0.001	0.94 ±0.004
17	DA->PVG (Tx 4d, 5 μg)	0.93 ±0.005	1.59 ±0.009	1.71 ±0.01	1.13 ±0.007	2.13 ±0.01	22.85 ±0.11	3.33 ±0.01	3.51 ±0.01	3.31 ±0.008	6.71 ±0.02	0.99 ±0.004	1.91 ±0.008
	DA->PVG (Tx 4d, 1 μg)	1.00 ±0.01	1.03 ±0.02	1.89 ±0.02	1.29 ±0.01	2.24 ±0.02	22.83 ±0.20	3.35 ±0.02	3.53 ±0.02	5.07 ±0.02	7.60 ±0.03	1.51 ±0.01	2.15 0.01
II. Sampling 4 hr after Ab injection													
18	DA->PVG (Tx 4d)	2.23 ±0.009	3.47 ±0.01	1.14 ±0.004	0.91 ±0.003	1.89 ±0.009	20.02 ±0.10	1.64 ±0.006	2.04 ±0.007	1.66 ±0.005	2.73 ±0.008	1.01 ±0.005	1.34 ±0.006
	DA->PVG (Tx 4d)	1.76 ±0.007	2.88 ±0.01	1.01 ±0.003	0.79 ±0.002	1.50 ±0.007	17.75 ±0.08	1.71 ±0.006	2.14 ±0.008	1.53 ±0.005	2.74 ±0.001	0.89 ±0.004	1.28 ±0.006
19	DA->PVG (Tx 4d CsA)	2.55 ±0.01	4.26 ±0.02	1.20 ±0.003	0.76 ±0.002	2.00 ±0.009	23.14 ±0.10	1.77 ±0.006	2.11 ±0.007	1.34 ±0.005	1.36 ±0.005	0.76 ±0.004	0.64 ±0.003
	DA->PVG (Tx 7d CsA)	2.48 ±0.01	4.06 ±0.02	1.12 ±0.003	0.63 ±0.002	1.85 ±0.01	20.01 ±0.10	1.68 ±0.009	2.02 ±0.01	1.39 ±0.003	1.22 ±0.003	0.83 ±0.005	0.61 ±0.004
	DA->PVG (Tx 14d CsA)	3.38 ±0.01	5.48 ±0.02	2.37 ±0.005	1.69 ±0.004	2.14 ±0.01	25.27 ±0.12	2.14 ±0.007	2.26 ±0.007	2.01 ±0.007	2.01 ±0.007	0.94 ±0.005	0.89 ±0.004

a The results of uptake in the other tissues sampled. ie lymph nodes, lung, intestine etc, are shown in Table A12.3, Appendix, page 353.
b %ID/ml, c : %ID/g, d : %ID/total organ.

C) Immunohistochemistry staining of tissue sections :

Using APAAP for staining the tissue sections, in vivo binding of ^{111}In F17-23-2 and the extent of antigen expression in the transplant were studied. Positive staining was obtained when in vitro F17-23-2 was added to the sections as first-layer antibody in the staining procedure indicating high expression of Class II in the transplant, especially on the renal tubules (Figure 12.9). Staining with rabbit-anti-mouse Ig, APAAP and substrate only did not show, in contrast, clear staining as was seen using MN4-91-6 McAb for the detection of antibody binding in vivo.

Figure 12.9. Immunohistochemistry after the injection of ^{111}In F17-23-2 in DA-->PVG rat (Tx 4d). Sampling at 24 hr PI (Frozen sections, X40).

Fig 12.9A. Left panel : APAAP staining of the R kidney after addition of F17-23-2 in vitro. Negative. R panel : APAAP staining of the Tx after addition of F17-23-2 in vitro. Intensive staining of the tubules is seen.

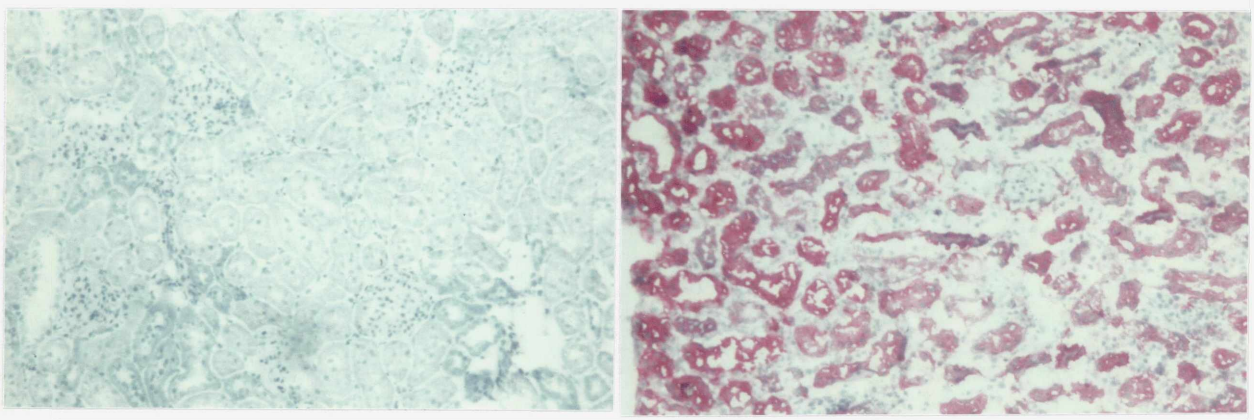

Fig 12.9B. Right panel only : APAAP staining of the Tx to detect in vivo binding of ^{111}In F17-23-2. Negative.

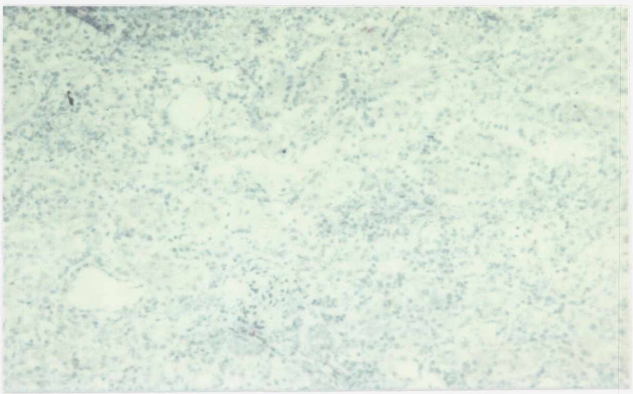

12.5 Discussion

In this chapter, immunopathological events occurring during the progression of acute allogeneic transplant rejection, ie graft infiltration with activated lymphocytes and induction of MHC antigens therein, were followed by using a novel in vivo method in which the respective cell population was radiolabelled with a specific McAb.

Also, this work provided a basis for a new means for the detection and discrimination of allogeneic-kidney-transplant rejection especially that it employed a strictly defined transplant model, a variety of controls and cyclosporine as anti-rejection agent.

12.5.1 Anti-Pan T (rat CD5, ^{111}In MRC OX-19) and anti-activated T cell (^{111}In MRC OX-39) McAbs

Based on the fact that rejecting transplants usually infiltrated with lymphocytes, ^{111}In MRC OX-19 was used to radiolabel the lymphocytes present in the graft. This approach was rather similar to injecting in-vitro-^{111}In-labelled lymphocytes reported previously by Martin-Comin 1986.

In this model, however, the high uptake in the spleen and in the abdominal lymphoid structures observed on scintillation camera images prevented clear distinction of the transplant located in the left flank of the animal. Also, tissue sampling of the transplanted rats showed that there was less uptake of the antibody in the transplant compared to the contralateral native kidney, although uptake in spleen and lymph nodes was similar to that seen in non-transplanted rats. This observation was in agreement with what was found by Armstrong et al 1987. They showed that the staining of tissue sections of rejecting kidney grafts for MRC OX-19 was not proportional to the degree of infiltration of the transplant with lymphocytes.

These difficulties made further investigation with a non-selective pan T cell appear unrewarding and, therefore, the use of ^{111}In MRC OX-19 in transplanted animals was ended.

The use of ^{111}In anti-interleukin 2 receptor McAb to label activated T cells in kidney transplanted rats provided a more specific reagent for the detection of graft rejection. As the rejecting graft provided a terrain for active immune reactions, the presence of T cells bearing the IL-2 receptor would be expected to occur in high numbers. This infiltration by IL-2 R-positive cells was noticed previously and its presence or absence was advocated to indicate, respectively, actively rejecting or enhanced (non-rejecting) allografts (Armstrong et al 1987).

In vivo use of ^{111}In MRC OX-39 gave positive results in terms of imaging the rejecting transplant and increased uptake in it. Corroborative evidence was also obtained by immunohistochemistry showing high numbers of IL-2 R-positive cells in the graft. The positive results after use of this tracer, however, were not adequate as marginal increases in the uptake of the transplant over that measured in the native kidney were noted. This was most probably related to the numbers of IL-2 R positive cells in the graft, which could not sustain the quantitative requirement of radioactive uptake for providing a high target to non-target ratio.

12.5.2 ^{111}In anti-Class I and Class II MHC McAb (^{111}In MN4-91-6 & ^{111}In F17-23-2)

The allogeneic transplants accumulated ^{111}In MN4-91-6 (anti-Class I MHC McAb) avidly showing intense uptake on the images and substantial radioactivity in the graft measured by direct tissue sampling. This positive uptake was seen early after transplantation and was still present at 3 weeks afterwards in cyclosporine-treated rats.

These findings were in agreement with previously reported data in the same model especially those concerning induction and expression of donor Class I MHC in unmodified grafts. However no striking difference in Class I MHC expression as measured by tissue sampling and assessed by imaging was noted between unmodified and cyclosporine treated animals. This finding compared to some extent to an earlier observation by Milton et al (1986) and raised the issue of the value of monitoring Class I MHC expression in the graft for the follow-up of rejection.

The use of ^{111}In F17-23-2 in this experimental work provided the best available tracer among those used in this experimental work for addressing the question of kidney graft rejection and its follow-up.

In the allogeneic transplants undergoing rejection, increased uptake of radioactivity in the graft after injection of ^{111}In F17-23-2 was documented by scintillation camera imaging and direct tissue sampling. The cyclosporine-treated transplants, however, did not show this increased uptake and, in fact, the accumulation of tracer was less than that in the native kidney. Thus, most probably, induction of Class II MHC did not occur in the cyclosporine-treated animals and therefore monitoring Class II expression could be of value in following the progression of rejection.

12.5.3 Summary

In this chapter, radiotracing of both circulating cells and molecules on fixed cells involved in allogeneic transplant rejection by in vivo administration of ^{111}In labelled McAbs was shown to enable early detection of immunopathological events closely and specifically associated with graft rejection. The ability of each antibody to provide images of the rejecting graft differed among the antibodies tested. The ^{111}In Pan T McAb used (MRC OX-19) did not show sufficient uptake in the transplant for a clear image to

be seen and the images obtained included interference from uptake in the spleen and other lymphoid tissues.

The use of the ^{111}In anti-interleukin 2-receptor McAb (MRC OX-39) gave better results than the anti-Pan T (MRC OX-19) McAb. Uptake in the rejecting transplant was clearly seen on the scintillation camera images. However, total uptake in the transplant, measured directly by tissue sampling, marginally exceeded that in the contralateral kidney. The ^{111}In anti-Class I MHC McAb (MN4-91-6) gave impressive results in unmodified and cyclosporine treated allograft recipients. Imaging showed intensive uptake in the graft in both situations and tissue sampling established that between 20-45% of the injected dose was found in the transplant. However, failure of cyclosporine to alter significantly the uptake of ^{111}In MN4-91-6 in the graft made the use of this antibody rather inadequate for the discrimination of rejection. Finally, ^{111}In anti-Class II MHC McAb provided a radiotracer for imaging rejection with an acceptable margin of uptake in the rejecting kidney above that in the native kidney. The value of decreasing the dose of antibody injected was noted in reducing background, thereby enhancing target to non-target ratio. In cyclosporine-treated animals the transplant failed to show on the images and contained less radioactive counts than the native kidney. Therefore, the use of ^{111}In anti-Class II McAb in vivo would provide the best radiotracer, among those tested so far, for the detection and discrimination of allogeneic transplant rejection.

It remains to be said that the work presented in this thesis has been on the whole exploratory for the role of ^{111}In McAbs in providing tracers for imaging events occurring during transplant rejection. The value of these reagents in the diagnosis and management of transplant rejection in the human would need to be tested and established in a suitable clinical and experimental setting.

Section Five :

General Discussion and Conclusions

Chapter 13 :

The Value of in Vivo Use of ^{111}In McAbs in Radiolabelling Platelets, Lymphocytes and Fixed Cells Expressing MHC Molecules

Implications for Imaging Cell Distribution and Following the Kinetics of Various Cell Populations

13.1 Introduction:

The aim of this thesis was to address the question of in vivo use of ^{111}In McAbs for labelling blood cells, namely platelets and lymphocytes, and for labelling fixed cells displaying antigens of the major histocompatibility complex on their surface. This was for the purpose of imaging the respective cell populations using a scintillation camera and following their behaviour in vivo.

The goals were achieved experimentally and the results of using various ^{111}In McAbs were discussed separately in the relevant sections of this thesis.

For radiolabelling platelets, ^{111}In P256 McAb and its F(ab)'$_2$ fragment proved to be very effective in binding to the cells in vitro and in vivo. Thus, the use of ^{111}In P256 or ^{111}In P256 F(ab)'$_2$ provided images of platelet distribution which were similar to those observed previously using ^{111}In oxine/tropolone labelled platelets. The major outcome of the use of this McAb clinically was in imaging thrombus in man. Areas of abnormal platelet deposition in the vasculature were detected by scintillation camera imaging and the findings were documented in some cases by angiography.

Lymphocyte radiolabelling with ^{111}In McAbs was approached from two angles. The first was a consideration of the effectiveness of antibody binding to the relevant cell population and potential effect of the radiolabel on cell function. Binding parameters gave an idea of the expected situation for cell

labelling in vivo and the effect of the ^{111}In anti-lymphocyte McAbs on mitogen induced cell proliferation was tested experimentally to provide an indication of any toxic effect the radiolabelled antibodies had on the cells.

The second approach studied in vivo use of anti-lymphocyte McAbs. An anti- T cell McAb (MRC OX-19) was traced in various lymphoid tissues after its intravenous injection in increasing amounts in the rat using available techniques of immunofluorescence and immunochemistry. This enabled the documentation of in vivo antibody binding to the relevant target and the uncovering of a modulation effect on the cells. The use of the ^{111}In anti-T cell McAb (^{111}In MRC OX-19) in the rat produced images of spleen and lymph nodes. Tissue sampling of the animals gave a quantitative assessment of the uptake in each tissue and identified sites of non-specific uptake such as liver and kidney.

In the experimental application of the ^{111}In McAbs in allogeneic kidney transplantation in a rat model, we showed that such use could provide an effective means for imaging rejection if antibodies of the right specificities were used. Monoclonal antibodies specific for activated T lymphocytes (anti-IL-2 receptor) or against the molecules of the major histocompatibility complex were found to be most suitable for radiotracing the immunopathological events during the progression of allograft rejection. Peculiarities of the use of each antibody in transplanted rats were identified especially in those animals treated with cyclosporine to prevent rejection of their grafts.

13.2 Blood cell radiolabelling and the place of radiolabelled antibodies reacting with various blood cells as in vivo cell tracers

The concern of physiologists, immunologists and clinicians regarding blood cell behaviour has been to explore where blood cells go, how they migrate in tissues and once there what they do. The answers to these questions using non-invasive means that enable accurate identification and localisation of blood cell populations have stemmed from application of various cell tracing methods mainly cell radiolabelling and scintillation camera imaging.

The study of granulocytes has benefited from such application especially using the ^{111}In oxine/tropolone labelling method. Conforming to the strict requirements of the ideal cell tracer, ^{111}In oxine/tropolone labelling of granulocytes has enabled a full and accurate description of granulocyte behaviour in man in normal and disease conditions using available imaging technology of scintillation camera imaging and its allied techniques, ie tomography, SPECT, etc.

Labelling other blood cells using ^{111}In oxine/tropolone or similar methods, however, has not achieved the same satisfactory results obtained with labelling granulocytes. The problems of specific cell labelling, particularly the functionally different lymphocytes or cells involved in a certain pathological condition such as activated platelets or lymphocytes, called for alternative ways of cell tracing.

Radiolabelled monoclonal antibodies against various cell surface molecules on platelets and lymphocytes have provided, to some extent, the in vivo tracer that can target cells specifically. The pattern of cell labelling with ^{111}In monoclonal antibodies injected in vivo and reported in this experimental work, shows the following characteristics :

1) Specific blood cell radiolabelling is unambiguously obtained. Thus, cells bearing a specific surface marker are radiolabelled with the antibody directed against this surface marker.

2) Both kinetics of the free and cell bound ^{111}In antibody are observed in blood and whole body at the same time. Thus, non-specific uptake in liver and kidney and high background in plasma are noted.

3) The kinetics of the cell-bound fraction of the antibody shows a peculiar pattern when it is followed over time. For circulating platelets and lymphocytes, it is related to the life span of the cells and to the kinetics of the antibody and its antigen on the cell surface, affinity of binding, internalisation, turnover of the receptor, antibody re-binding to other cells etc. Therefore, a distorted picture of the behaviour of the traced cell population emerges upon use of the radiolabelled antibody as the cell tracer and no firm conclusion as to the time course of cell migration into tissue or life-span of the cell population in blood can be made.

The value of radiolabelled anti-blood cell McAbs lies mainly in giving a map of distribution of the relevant cell population in the body at a given time. It can therefore localise abnormal accumulation of cells in certain sites such as platelet deposition in thrombus and activated lymphocytes in rejecting grafts. This property makes imaging the most useful application of the ^{111}In anti-platelet/lymphocytes McAbs.

The main implication for use of the method in clinical practice will be, therefore, as an investigation for localising abnormalities involving blood cells such as thrombi by using anti-platelet antibodies and immunopathologic events in which lymphocyte infiltration occurs by anti-lymphocyte McAbs.

Theoretically, repetition of these investigations at reasonably close intervals (1-2 weeks) should be possible in order to provide follow-up of each situation studied. The main determinant in this case will be background radioactivity in tissues remaining from the previous use of the method or other investigations using radionuclides. However in practice, problems related mainly to generation of human anti-mouse Ig antibodies (HAMA) restrict the repetitive use of murine McAbs in man. The modern trends of using human or humanised antibodies will probably provide a solution to this major obstacle.

13.3 In vivo study of the physiology or pathophysiology of platelets and lymphocytes using ^{111}In McAbs

The main question this thesis has answered is the ability of in vivo ^{111}In anti-platelet, lymphocyte or MHC-molecule McAbs to radiolabel the relevant cells and to provide the means for imaging these cells using a scintillation camera.

Equally important is the issue of how this approach can be useful in providing information on the physiology and pathophysiology of a cell population by targeting it with a certain ^{111}In McAb. The first step would be adequate knowledge of antibody reactivity and binding characteristics to the cell population studied in a suitable setting in vitro. Examples of such primary testing are the binding assays of ^{111}In P256 McAb to platelets and ^{111}In anti-lymphocyte antibodies to lymphoid cell lines and blood. Other in vitro tests are designed so that they test functional alterations of the cell population studied upon use of the radiolabelled antibody. For instance, binding of P256 to platelets has increased aggregation, ^{111}In anti-human T lymphocyte McAb has caused antigenic modulation and a reduction in lymphocyte mitogen-induced proliferation. Once satisfactory in vitro tests have been obtained, application in appropriate models of experimental

animals will provide the opportunity to gather information before use of the method in man. Thus a primate model for thrombus induction has been used by Lavender et al (1988) for testing ^{111}In P256 anti-platelet McAb further. The rat has been used in this thesis as the experimental animal for testing ^{111}In anti-lymphocyte and anti-Class I or II MHC McAbs in vivo.

It is by relating the resulting images to tissue function in vivo using ^{111}In McAbs as probes detecting the presence of specific molecules on the surface of a certain cell population during the execution of a recognised function, that the potential of the new method in studying physiologic and pathologic events lies. Notwithstanding problems of cross-reactivity of antibodies with different cells, the investigator can choose to follow in this way the cells displaying the specific marker on their surface; the population that seems to be involved in the phenomenon of interest. Thus, we have succeeded in this experimental work in adapting the in-vivo ^{111}In McAb approach to study by scintillation camera imaging reactive events involving platelet deposition in thrombus in man, lymphocyte distribution in the rat, activated lymphocyte infiltration of rejecting grafts and the induction of Class I and II MHC molecules in unmodified and cyclosporine treated allogeneic transplants in the rat.

13.4 Scintillation camera imaging of radiolabelled blood cells and MHC molecules after in vivo administration of ^{111}In McAbs

The generation of an image truly reflecting the pathophysiology of an abnormality is a valuable addition to means of medical investigation.

In this thesis, emphasis has been on obtaining scintillation camera images after the injection of the labelled monoclonal antibodies using the equipment available and by altering the experimental setting in each case, the optimal conditions have been achieved. Also, the imaging data using

^{111}In McAbs have been compared with alternative cell labelling methods such as ^{111}In tropolone labelled cells. In the work on the experimental animal, imaging results have been compared directly to tissue sampling data, thereby documenting the results and identifying areas of weakness in the procedure and ways of improving on the outcome of imaging in terms of optimal target to background ratio. For instance, sequential imaging and tissue sampling of rats injected with ^{111}In anti-T cell McAb, ^{111}In MRC OX-19, show very early uptake in the spleen. However, a clear picture of the lymph nodes emerges only after the decline of background activity in the circulation 24 hr after injection of that antibody. In contrast to the situation with lymph nodes however, early imaging of the transplanted rats at 4 hr after antibody injection has been found to give a higher target to non-target ratio, Transplant/Native Kidney, than that obtained using late imaging (24 hr) after the injection of ^{111}In anti-Class I or II McAb.

The generation of images for as small an animal as the rat, has benefited from the great versatility and manoeuvrability of the scintillation camera system, especially the use of the pinhole collimator. Image magnification and improvement in system resolution have occurred enabling relatively simple localisation and differentiation of anatomical structures. In addition, whole body and close-up views of the imaged rats have been possible by simply adjusting the distance of the pinhole from the imaging plane.

Dynamic imaging has been used mostly in man after injection of the ^{111}In anti-platelet McAb (^{111}In P256 or ^{111}In P256 F(ab')$_2$). The uptake of radioactivity after intravenous injection of ^{111}In P256 or ^{111}In P256 F(ab')$_2$ increases steadily in the spleen to reach a plateau at 1 hr but decreases over the heart (blood pool). Liver uptake shows essentially a plateau throughout the dynamic study.

Comparison of uptake in different parts of the static images has been readily done by comparing count-rates in regions of interest drawn manually over chosen organs or tissues on the monitor screen. The results of such analysis show that ^{111}In McAbs have achieved the ratios of target to background or target of non-target uptake in the range of 2 : 1 to 30 : 1. These data compare favourably with other imaging investigations employing radionuclides, especially radiolabelled cells (^{111}In granulocytes, platelets), and radiolabelled antibodies for targeting tumours.

Finally, with more refinements of the imaging equipment and the preparations of antibody used, the in vivo radiolabelled approach may prove of great benefit as a non-invasive investigational means as has been shown in our experimental work.

13.5 In vivo ^{111}In McAbs anti-platelets, lymphocytes and MHC molecules; notes of caution and reservations for use in man.

It has become obvious during the progress of the experimental work in this thesis that the use of ^{111}In labelled McAbs in vitro and in vivo is not without undesirable effects.

The anti-platelet McAb P256 has been found to cause platelet aggregation when its concentration exceeds a certain level. However at doses lower than 500 Ab molecules/ptlt (100 μg per person), it appears to be safe and still provides good scintillation camera images. Anti-T cell monoclonal antibodies used in vivo in the rat and tested in vitro with human lymphocytes have caused antigen modulation on the cell surface. This makes cell labelling more difficult due to loss of the CD5 molecule from the surface. The use of other anti-lymphocyte McAbs has also been reported to induce functional changes in the cells. The effects range from cell activation to complete block of cellular function.

The damaging effect of the radiolabel, indium-111, on the cells has been addressed particularly in the case of ^{111}In anti-lymphocyte McAbs. Previous reports using different radiolabelling methods such as ^{111}In oxine/tropolone have emphasised the issue of radiotoxicity to lymphocytes and limits of ^{111}In radioactivity permissible per cell. Dose estimates for ^{111}In McAb binding to lymphocytes have indicated a lower risk of damage to DNA by virtue of antibody binding to the cell surface as compared to intracellular deposition of ^{111}In after oxine/tropolone labelling. The risk of malignancy induction in the labelled cells remains, however, unclear and further studies are needed to establish its significance.

Whole body and target organ dosimetry from the ^{111}In McAb method within the limits of radioactivity used in this thesis, ie 4-10 MBq (100-300 μCi) compare favourably with other investigations using ^{111}In labelled blood cells (platelets & granulocytes).

Finally, using murine monoclonal antibodies in man brings the issue of the generation of human anti-mouse antibodies, which prevents efficient repetitive use of the murine McAbs in man. To this end, the use of antibody fragments ($F(ab')_2$ & Fab) and the introduction of modified antibodies such as the mouse-human heteroantibodies hold promise for a solution to this problem.

Chapter 14 :

Conclusions

1) It is possible to radiolabel platelets in man by the intravenous injection of an ^{111}In anti-platelet glycoprotein monoclonal antibody (^{111}In P256 or ^{111}In P256 F(ab')$_2$). Scintillation camera imaging of platelet distribution in the body can be obtained after the administration of this tracer. The method enables the detection of platelet deposition in thrombus and holds promise for an early and non-invasive diagnostic test for this condition.

2) Lymphocyte subsets can be targeted with ^{111}In McAbs for the purpose of scintillation camera imaging. The binding of an ^{111}In anti-T cell McAb to T lymphocytes in various lymphoid tissues has been documented experimentally in the rat by imaging and tissue sampling. However, antibody binding to T lymphocytes has been found to cause modulation of the antigen that binds the antibody. Dosimetry of ^{111}In labelled anti-lymphocyte antibodies has been addressed considering surface binding to the cells and in vitro experimental data on cell binding and proliferation. Accordingly, ^{111}In anti-lymphocyte McAbs are thought to expose the cells less to short range particulate emissions than conventional labelling with ^{111}In oxine. This factor will favour the use of ^{111}In McAbs for labelling lymphocytes.

3) The involvement of lymphocytes in immunopathological events and the alteration in tissues undergoing certain inflammatory reactions such as induction of the molecules of the major histocompatibility complex in allogeneic transplant rejection have been studied successfully using in vivo administration of ^{111}In McAbs in an experimental rat model of kidney transplantation. ^{111}In anti-IL-2 receptor McAb as tracer for activated T cells and donor specific ^{111}In anti-Class I and II MHC McAbs are accumulated in rejecting allogeneic transplants giving clear images of the graft using the

scintillation camera. Treatment of the transplanted animals with cyclosporine to prevent rejection has resulted in little alteration in the expression of Class I MHC in their grafts compared to grafts in unmodified recipients (non-cyclosporine treated) as judged by the imaging and tissue sampling data. However, abrogation of the uptake of the ^{111}In anti-Class II MHC McAb in the cyclosporine-treated transplants has occurred giving a clear distinction between rejecting and non-rejecting allogeneic kidney transplants in the rat model used. This has implications for adopting the ^{111}In anti-Class II MHC McAbs for the diagnosis and discrimination of kidney transplant rejection in man.

References

Aas KA and Gardner FH, Survival of blood platelets labelled with chromium-51. J Clin Invest 37 : 1257-1268, 1958.

Abrahamsen AF, Survival of ^{51}Cr labelled autologous and isologous platelets as differential diagnosis aid in thrombocytopenic states. Scand J Haematol 7 : 525-528, 1970.

Agarwal KC, Wahner HW, Dewanjee MK, Fuster V, Puga FJ, Danielson GK, Chesebro JH and Feldt RH, Imaging of platelets in right-sided extracardiac conduits in humans. J Nucl Med 23 : 342-347, 1982.

Ahmed-Ansari A, Tadros TS, Knopf WD, Murphy DA, Hertzler G, Feighan J, Leatherbury A and Sell KW, A major histocompatibility complex class I and class II expression by myocytes in cardiac biopsies posttransplantation. Transplantation 45 : 972-978, 1988.

Anderson RE, Sprent J and Miller JFAP, Radiosensitivity of T and B lymphocytes. 1. Effect of irradiation on cell migration. Eur J Immunol 4 : 199-203, 1974.

Andres RY and Schubiger PA, Radiolabelling of antibodies. Methods and limitations. Nuklearmedizin 25 : 162-166, 1986.

Ansell JD and Micklem HS, Genetic markers for following cell populations. In Handbook of Experimental Immunology, Vol 2 Cellular Immunology, Chapter 56, Weir DM ed, 4th edition, Blackwell Scientific Publications, 1986.

Armstrong HE, Bolton EM, McMillan I, Spencer SC and Bradley JA, Prolonged survival of actively enhanced rat renal allografts despite accelerated cellular infiltration and rapid induction of both class I and class II MHC antigens. J Exp Med 164 : 891-907, 1987.

Asherson GI and Allwood GG, Inflammatory lymphoid cells : Cells in immunized lymph nodes that move to sites of inflammation. Immunology 22 : 493-502, 1972.

Aster RH, Pooling of platelets in the spleen : Role in the pathogenesis of "hypersplenic" thrombocytopenia. J Clin Invest 45 : 645-657, 1966.

Athens JW, Mauer AM, Ashenbrucker H, Cartwright GE and Wintrobe MM, Leukokinetic studies. I. A method for labeling leukocytes with di-isopropyl fluorophosphate (DFP 32). Blood 15 : 303-333, 1959.

Ault KA and Towle M, Human B lymphocyte subsets, I. IgG-bearing B cell response to pokeweed mitogen. J Exp Med 153 : 339-351, 1981.

Bai Y, Durbin H and Hogg N, Monoclonal antibodies specific for platelet glycoproteins react with human monocytes. Blood 64 : 139-146, 1984.

Baine Y, Ponzio NM and Thorbecke GJ, Transfer of memory cells into antigen-pretreated hosts II. Influence of localized antigens on the migration of specific memory B cells. Eur J Immunol 11 : 990-996, 1981.

Balaban EP, Simon TR, Sheehan RG and Frenkel EP, The effect of the radiolabel mediator tropolone on lymphocyte structure and function. J Lab Clin Med 107 : 306-314, 1986.

Balaban EP, Simon TR and Frenkel EP, Toxicity of indium-111 on the radiolabeled lymphocyte. J Nucl Med 28 : 229-233, 1987.

Bassano DA and McAfee JG, Cellular radiation doses of labeled neutrophils and platelets. J Nucl Med 20 : 255-259, 1979.

Bazerbashi MB, Reeve J and Chanarin I, Studies in chronic lymphocytic leukaemia-The kinetics of ^{51}Cr labelled lymphocytes. Scand J Haematol 20 : 37-51, 1978.

Benjamin RJ, Cobbold SP, Clark MR and Waldmann H, Tolerance to rat monoclonal antibodies. Implications for serotherapy. J Exp Med 163 : 1539-1552, 1986.

Bennett JS, Vilaire G and Cines DB, Identification of fibrinogen receptor of human platelets by photoaffinity labeling. J Biol Chem 257 : 8049-8054, 1982.

Bentley SA and Miller DT, Radionuclide blood cell survival studies. In Radionuclides in Haematology, Lewis SM and Bayly RJ eds. Methods in Hematology series vol 14, Churchill Livinstone, London pp 245-254, 1986.

Bergman SR, Lerch RA, Carlson EM Saffitz JE and Sobel BE, Detection of cardiac transplant rejection with radiolabelled lymphocytes. Circulation 65 : 591-599, 1982.

Bergman SR, Lerch RA, Mathias CJ, Sobel BE and Welch MJ, Non invasive detection of coronary thrombi with In-111 platelets : Concise communication. J Nucl Med 24 : 130-135, 1983.

Bernard A, Boumsell L, Dausset J, Milstein C and Schlossman SF, Leucocyte Typing, Springer-Verlag Berlin, 1984.

Berndt MC, Chong BH, Bull HA, Zola H and Castaldi PA, Molecular characterization of quinine/quinidine drug-dependent antibody platelet interaction using monoclonal antibodies. Blood 66 : 1292-1301, 1985.

Bernstein ID, Eary JF, Badger CC, Press OW, Appelbaum FR, Martin PJ, Krohn KA, Nelp WB, Porter B, Fisher D, Miller R, Brown S, Levy R and Thomas ED, High dose radiolabeled antibody therapy of lymphoma. Cancer Res (suppl) 50 : 1017s-1021s, 1990.

Bevan DJ and Chisholm PM, Co-expression of CD4 and CD8 molecules and de novo expression of MHC Class II antigens on activated rat T cells. Immunology 59 : 621-625, 1986.

Beverley PCL and Callard RE, Re-definition of human T cells by monoclonal antibodies. Protides of Biological Fluids 29 : 653-658, 1981.

Beverley PCL, Hybridoma, monoclonal cells and analysis of the immune system. Br Med Bull 40 : 213-217, 1984.

Bloom BR and Bennett B, Mechanism of a reaction in vitro associated with delayed-type hypersensitivity. Science 153 : 80-82, 1966.

Bolhuis PA, Sakariassen KS, Sander HJ, Bouma BN and Sixma JJ, Binding of factor VIII-von Willebrand factor to human arterial subendothelium precedes increased platelet adhesion and enhances platelet spreading. J Clin Lab Med 97 : 568-576, 1981.

Bond VP, Cronkite EP, Fliedner TM and Schork PK, Deoxyribonucleic acid synthesizing cells in peripheral blood of normal human beings. Science 128 : 202-203, 1958.

Borel JF, Comparative study of in vitro and in vivo drug effects on cell-mediated cytotoxicity. Immunology 31 : 631-641, 1976.

Bosslet K, Luben G, Schwarz A, Hundt E, Harthus HP, Seiler FR, Muhrer C, Kloppel G, Kayser K and Sedlacek HH, Immunohistochemical localisation and molecular characterisation of three monoclonal antibody-defined epitopes detectable on carcino-embryonic antigen (CEA). Int J Cancer 36 : 75-84, 1985.

Boulianne GL, Hozumi N and Shulman MJ, Production of functional chimaeric mouse/human antibody. Nature 312 : 643-646, 1984.

Boven E, Lindmo T, Mitchell JB and Bunn PA Jr, Selective cytotoxicity of ^{125}I-labeled monoclonal antibody T101 in human malignant T cell lines. Blood 67 : 429-435, 1986.

Branehog I, Kutti J and Weinfeld A, Platelet survival and platelet function in idiopathic thrombocytopenic purpura (ITP). Br J Haematol 27 : 127-143, 1974.

Bremer K, Fliedner TM and Schick P, Kinetic difference of autotransfused (^{3}H)-cytidine labelled blood lymphocytes in leukemic and non-leukemic lymphoma patients. Eur J Cancer 9 : 113-124,1973a.

Bremer K, Wack O and Schick P, Impaired recirculation of autotransfused blood lymphocytes via thoracic duct lymph in patients with chronic lymphoid leukemia. Biomedicine 18 : 393-400, 1973b.

Brent L and Medawar PB, Quantitative studies on tissue transplantation immunity. V. The role of antiserum in enhancement and desensitization. Proc Roy Soc [Biol] 55 : 392, 1962.

Brown BA, Davis GL, Salzgaber-Muller J, Simon P, Ho M-K, Shaw PS, Stone BA, Sands H and Moore GP, Tumor-specific genetically engineered murine/human chimeric monoclonal antibody. Cancer Res 47 : 3577-3583, 1987.

Brownell GL, Berman M and Robertson JS, Nomenclature for tracer kinetics, Int J appl Radiat Isot 19 : 249-262, 1968.

Buchsbaum DJ, Nelson LA, Hanna DE, Vallera DA, Human leukemia cell binding and killing by anti-CD5 radioimmunotoxins. Int J Radiation Oncology Biol Phys 13 : 1701-1712, 1987.

Buinauskas P, McCredie JA, Brown ER and Cole WH, Experimental treatment of tumors with antibodies. AMA Arch Surg Chicago 79 : 432-437, 1959.

Bunn PA Jr, Carrasquillo JA, Keenan AM, Schroff RW, Foon KA, Hsu SM, Gazdar AF, Reynolds JC, Perentesis P and Larson SM, Imaging of T-cell lymphoma by radiolabelled monoclonal antibody. The Lancet Nov 24, 1219-1221, 1984.

Busch GJ, Schamberg JF, Moretz RC, Strom TB, Tilney NL, and Carpenter CB, T and B cell patterns in irreversibly rejected human renal allografts; correlation of morphology with surface markers and cytotoxic capacity of the isolated lymphoid infiltrate. Lab Invest 35 : 272-280, 1976.

Butcher EC and Ford WL, Following cellular traffic : Methods of labeling lymphocytes and other cells to trace their migration in vivo. In Handbook of Experimental Immunology, Vol 2 Cellular Immunology, Chapter 57, Weir DM ed, 4th Ed, Blackwell Scientific Publications, London 1986.

Caen JP, Nurden AT, Jeanneau C, Michel H, Tobelem C, Levy-Toledano S, Sultan Y, Valeusi F and Bernard J, Bernard-Soulier syndrome : A new platelet glycoprotein abnormality. Its relationship with platelet adhesion to subendothelium and with the factor VIII von Willebrand protein. J Lab Clin Med 87 : 586-596, 1976.

Calne RY, Mechanisms in the acceptance of organ grafts. Br Med Bull 32 : 107-112, 1976.

Campbell AM, Monoclonal Antibody Technology, Elsevier Science Publishers BV, Amsterdam 1984.

Carrasquillo JA, Krohn KA, Beaumier P, McGuffin RW, Brown JP, Hellstrom KE, Hellstrom J and Larson M, Diagnosis of and therapy for solid tumors with radiolabeled antibodies and immune fragments. Cancer Treat Rep 68 : 317-328, 1984.

Carrasquillo JA, Bunn PA Jr, Keenan AM, Reynolds JC, Schroff RW, Foon KA, Ming-Hsu S, Gazdar A, Mulshine JL, Oldham RK, Parentesis P, Horowitz M, Eddy J, James P and Larson SM, Radioimmunodetection of cutaneous T-cell lymphoma with ^{111}In-labeled T101 monoclonal antibody. N Engl J Med 135 : 673-680,1986.

Carrasquillo JA, Mulshine JL, Bunn PA Jr, Reynolds JC, Foon KA, Schroff RW, Perentesis P, Steis RG, Keenan AM and Horowitz M, Indium-111 T101 monoclonal antibody is superior to iodine-131 T101 in imaging of cutaneous T-cell lymphoma. J Nucl Med 28 : 281-287,1987.

Catafau AM, Lomeno FJ, Ricart MJ, Pons F, Piera C, Pavia J, Moragas M, Garcia A, Herranz R, Andreu J and Setoain J, Indium-111-labeled platelets in monitoring human pancreatic transplants. J Nucl Med 30 : 1470-1475, 1989.

Catovsky D, Melo JV and Matutes E, Biological markers in lymphoproliferative disorders. In Chronic and acute leukaemias in adults, Bloomfield CD Ed, Martinus Nijhoff Publishers, Boston, pp69-112, 1985.

Charlton DE, Calculation of single and double strand DNA breakage from incorporated I-125. Proc Intl Workshop on Auger emitters in DNA : Implications and Applications, Baverstock KF and Charlton DE eds, Taylor and Francis p89, 1987.

Chatenoud L, Bandrihaye MF, Kreis H, Goldstein G, Schindler J and Bach JF, Human in-vivo antigenic modulation induced by the anti-T-cell OKT3 monoclonal antibody. Eur J Immunol 12 : 979-982, 1982.

Chatenoud L and Bach JF, Antigenic modulation - a major mechanism of antibody action. Immunol Today 5 : 20, 1984.

Chatenoud L, The immune response against therapeutic monoclonal antibodies. Immunology Today 7 : 367-368, 1986.

Chin GW and Hay JB, A comparison of lymphocyte migration through intestinal lymph nodes, subcutaneous lymph nodes and chronic inflammatory sites of sheep. Gastroenterology 79 : 1231-1242, 1980.

Chisholm PM, Danpure HJ, Healey G and Osman S, Cell damage resulting from the labeling of rat lymphocytes and HeLa S3 cells with ^{111}In oxine. J Nucl Med 20 : 1308-1311, 1979.

Clevers H, Alarcon B, Wileman T and Terhorst C, The T cell receptor/CD3 complex : A dynamic protein ensemble. Ann Rev Immunol 6 : 629-662, 1988.

Coller BS, Interaction of normal, thrombasthenic and Bernard-Soulier platelets with immobilized fibrinogen : Defective platelet interaction in thrombasthenia. Blood 55 : 169-178, 1980.

Coller BS, Peerschke EI, Scudder LE and Sullivan CA, A murine monoclonal antibody that completely blocks the binding of fibrinogen to platelets produces a thrombasthenic-like state in normal platelets and binds to glycoproteins IIb and/or IIIa. J Clin Invest 72 : 325-338, 1983.

Coller BS, A new murine monoclonal antibody reports an activation dependent change in the conformation and/or microenvironment of the platelet glycoprotein IIb/IIIa complex. J Clin Invest 76 : 101-108, 1985.

Courtenay-Luck NS, Epenetos AA, Moore R, Larche M, Pectasides D, Dhokia B and Ritter MA, Development of primary and secondary immune responses to mouse monoclonal antibodies used in the diagnosis and therapy of malignant neoplasms. Cancer Res 46 : 6489-6493, 1986.

Crowther D, Hamilton Failey G, Sewell R, Significance of the changes in the circulating lymphoid cells in Hodgkin's disease. Brit Med J 2 : 473-477, 1969.

Crowther D and Wagstaff J, Lymphocyte migration in malignant disease. Clin Exp Immunol 51 : 413-420, 1983.

Dacie JV and Lewis SM, Estimation of the life-span of red cells in vivo. In Practical Haematology 6th ed. Churchill Livingstone London pp 297-307, 1984.

Dallman MJ, Thomas ML and Green JR, MRC OX-19 : A monoclonal antibody that labels rat T lymphocytes and augments in vitro proliferation responses. Eur J Immunol 14 : 260-267, 1984.

Danpure HJ, Osman S and Brady F, The labelling of blood cells in plasma with ^{111}In tropolonate. Br J Radiol 543 : 247-249, 1982.

Davis HH II, Siegel BA, Sherman LA, Heaton WA and Welch MJ, Scintigraphy with ^{111}In labeled autologous platelets in venous thromboembolism. Radiology 136 : 203-207, 1980a.

Davis HH II, Siegel BA, Sherman LA, Heaton WA, Naidich TP, Joist JH and Welch MJ, Scintigraphic detection of atherosclerosis with ^{111}In labeled autologous platelets. Circulation 61 : 982-988, 1980b.

DeNardo SJ, DeNardo GL, O'Grady LF, Levy NB, Mills SN, Macey DJ, McGahan JP, Miller CH and Epstein AL, Pilot studies of radioimmunotherapy of B-cell lymphoma and leukemia using I-131 Lym-1 monoclonal antibody. Antibody Immunoconj Radiopharm 1 : 17-33, 1986.

Deshpande SV, DeNardo SJ, Meares CF, McCall MJ, Adams GP, Moi MK and DeNardo GL, Copper-67-labeled monoclonal antibody Lym-1, A potential radiopharmaceutical for cancer therapy : Labeling and biodistribution in RAJI tumored mice. J Nucl Med 29 : 217-225, 1988.

Desir G, Bia MJ, Lange RC, Smith EO, Kashgarian M, flye W, Schiff M and Ezekowitz MD, Detection of acute allograft rejection by indium-111 labeled platelet scintigraphy in renal transplant patients. Transplant Proc 19 : 1677-1680, 1987.

Dewanjee MK, Rao SH and Didisheim P, Indium-111 tropolone, a new high affinity platelet label; preparation and evaluation of labeling parameters. J Nucl Med 22 : 981-987, 1981.

Dewanjee MK, Fuster V, Rao SA, Forshaw PL and Kaye MP, Non-invasive radioisotopic technique for detection of platelet deposition in mitral valve prostheses and quantitation of visceral microembolism in dogs. Mayo Clin Proc 58 : 307-314, 1983.

Dewanjee MK, Non invasive radioisotopic techniques for detection of platelet deposition in mechanical and bovine pericardial mitral valve prostheses and in vitro quantitation of visceral microembolism, In Blood cells in nuclear medicine part I cell kinetics and bio-distribution, Hardeman MR and Najean Y eds, Martinus Nijhoff Publishers Boston, pp262-288, 1984.

Dillman RO, Shawler DL, Dillman JB and Royston I, Therapy of chronic lymphocytic leukemia and cutaneous T-cell lymphoma with T101 monoclonal antibody. J Clin Oncology 2 : 881-891, 1984.

Dillman RO, Shawler DL, Johnson DE, Meyer DL, Koziol JA and Frincke JM, preclinical trials with combinations and conjugates of T101 monoclonal antibody and doxorubicin. Cancer Research 46 : 4886-4891, 1986.

Doney K, Martin P, Storb R, Whitehead J, Smith A, Hansen JA, Appelbaum F, Buckner CD and Thomas ED, A randomized trial of anti-human thymocyte globulin versus murine monoclonal anti-human T-cell antibodies as immunosuppressive therapy for aplastic anaemia. Exp Hematol 13 : 520-524, 1985.

Drayson MT, The entry of lymphocytes into stimulated lymph nodes; the site of selection of alloantigen specific cells. Transplantation 41 : 745-751, 1986.

Dyer MJS, Hale G, Hayhoe FGJ, Waldsmann H, Effects of CAMPATH-1 antibodies in vivo in patients with lymphoid malignancies : Influence of antibody isotype. Blood 73 : 1431-1439, 1989.

Ebaugh FG Jr, Emerson CP and Ross JF, The use of radioactive chromium-51 as an erythrocyte tagging agent for the determination of red cell survival in vivo. J Clin Invest 32 : 1260-1276, 1953.

Eger RR, Covell DG, Carrasquillo JA, Abrams PG, Foon KA, Reynolds JC, Schroff RW, Morgan AC, Larson SM and Weinstein JN, Kinetic model for the biodistribution of an ^{111}In labeled monoclonal antibody in humans. Cancer Res 47 : 3328-3336, 1987.

Engeset A, Froland SS and Bremer K, Studies of human peripheral lymph II. Low lymphocyte count and few B-lymphocytes in peripheral lymph of patients with chronic lymphocytic leukemia. Scand J Haematol 13 : 93-100, 1974.

Evans EA, Self-decomposition of radiochemicals : Principles, control, observations and effects. Review 16, Amersham International plc UK, 1984.

Everett NB, Reinhardt WO and Yoffey JM, The appearance of labeled cells in the thoracic duct lymph of the guinea pig after administration of tritiated thymidine. Blood 15 : 82-94, 1960.

Ey PL, Prowse SJ and Jenkins CR, Isolation of pure IgG_1, IgG_{2a}, IgG_{2b} immunoglobulins from mouse serum using protein A sepharose. Immunochemistry 15 : 429-436, 1978.

Farrands PA, Perkins AC, Pimm MV, Hardy JD, Embleton MJ, Baldwin RW and Hardcastle JD, Radioimmunodetection of human colorectal cancers by an antitumor monoclonal antibody. Lancet ii 397-400,1982.

Fasman GD, Molar absorptivity and $A_{1cm}^{1\%}$ values for proteins at selected wave lengths of the ultraviolet and visible region, immunoglobulins, In Handbook of Biochemistry and Molecular Biology, Vol II, Proteins, Fasman GD ed, 3rd ed, Chemical Rubber Company, pp383, 452-457, 1976.

Favour CB, Antigen-antibody reactions in tissue culture. In Immunological methods, Ackroyd JR ed, Blackwell Scientific Publications, Oxford 195-223, 1964.

Fedullo PF, Moser KM, Moser KS, Konopka R and Hatman MT, Indium-111 labeled platelets : Effect of heparin on uptake by venous thrombi and relationship to the activated partial thromboplastin time. Circulation 66 : 632-637, 1982.

Feinendegen LE, Odartchenko N, Cottier H and Bond VP, Kinetics of megakaryocyte proliferation. Proceedings of the Society of Experimental Biology and Medicine 111 : 177-182, 1962,

Fenech A, Hussey JK, Smith FW, et al, Diagnosis of deep vein thrombosis using autologous indium-111 labeled platelets. Br Med J 282 : 1020-1022, 1981.

Ferrero D and Rovera G, Human leukaemic cell lines. Clin Haematol 13 : 461-487, 1984.

Figueroa F and Klein J, The evolution of MHC class II genes. Immunol Today 7 : 78-81, 1986.

Fishman M, Antibody formation in vitro. J Exp Med 114 : 837-856, 1961.

Flad HD, Huber C, Bremer K, Menne HD and Huber H, Impaired recirculation of B lymphocytes in chronic lymphocytic leukemia. Eur J Immunol 3 : 688-693, 1973.

Ford WL, Lymphocyte migration and immune responses. Prog Aller, 19 :1-59, 1975.

Ford WL, The preparation and labelling of lymphocytes, In Handbook of Experimental Immunology, Volume 2 Cellular Immunology, Chapter 23, Weir DM ed, 3rd ed, Blackwell Scientific Publications, London 1977.

Forstrom LE, Locken MK, Cook A, Chandler R and McCullough J, In-111-labeled leukocytes in the diagnosis of rejection and cytomegalovirus infection in renal transplant patients. Clin Nucl Med 6 : 146-149, 1981.

French ME and Batchelor JR, Immunological enhancement of rat kidney grafts. Lancet 2, 1103-1106, 1969.

Frost H, Frost P, Wilcox C and Thrall J, Lymph node scanning in sheep with indium-111 labelled lymphocytes. Int J Nucl Med Biol 9 : 60-67, 1979.

Gallego J, Price MR and Baldwin RW, Preparation of four daunomycin monoclonal antibody 191T/36 conjugates with antitumor activity. Int J Cancer 33 : 737-744, 1984.

Geigy Scientific Tables, Volume 3, 8th edition, p212, Ciba-Geigy, Basel, 1984.

George JN, Nurden AT and Phillips DR, Molecular defects in interactions of platelets with the vessel wall. N Engl J Med 311 : 1084-1098, 1984.

Ghose T, Norvell ST, Guclu A, Cameron D, Ddurtha D and MacDonald AS, Immunochemotherapy of cancer with chlorambucil carrying antibody. Br Med J 3 : 495-499,1972.

Goldenberg DM, DeLand F, Kim E, Bennett S, Primus FJ, van Nagell JR, Estes N, De Simone P and Raysburn P, Use of radiolabeled antibodies for carcinoembryonic antigen for the detection and localisation of diverse cancers by external photoscanning. N Engl J Med 298 : 1384-1386, 1978.

Goodwin DA, Bushberg JT, Doherty PW, Lipton MJ, Conley FK, Diamanti CI and Meares CF, Indium-111 labeled autologous platelets for location of vascular thrombi in humans. J Nucl Med 19 : 626-634, 1978.

Goodwin DA, Heckman JR, Fajardo LF, Calin A, Propst SJ and Diamanti CI, Kinetics and migration of indium-111 labeled human lymphocytes. In Proceedings of the International Symposium on Medical Radionuclide Imaging, International Atomic Energy Agency SM-247/95 Vienna pp 487-497, 1981a.

Goodwin DA, Finston RA and Smith SI, The distribution and dosimetry of In-111 labeled leukocytes and platelets in humans. In Third International Radiopharmaceutical Dosimetry Symposium, HHS Publications, FDA 81-8166, pp88-101, 1981b.

Goodwin DA and Meares CF, Indium-111 labeled cells new approaches and radiation dosimetry. In Radiolabeled Cellular Blood Elements, Pathophysiology, Techniques and Scintigraphic Applications. Thakur ML ed, Plenum Press, New York pp 343-362, 1985.

Goodwin DA, Meares CF, McCall MJ, Haseman MK, McTigue M, Diamanti CI and Chaovapong W, Chelate conjugates of monoclonal antibodies for imaging lymphoid structures in the mouse. J Nucl Med 26 : 493-502, 1985.

Gorer PA, Genetic and antigenic basis of tumour transplantation. J Pathol Bacteriol 44 : 691-697, 1937.

Gorer PA, Antigenic basis of tumour transplantation. J Pathol Bacteriol 47 : 231-252, 1938.

Gorer PA, Lyman S and Snell GD, Studies on the genetic and antigenic basis of tumour transplantation : Linkage between a histocompatibility gene and "fused" in mice. Proc Roy Soc of London Series B 135 : 499-505, 1948.

Gowans JL, The recirculation of lymphocytes from blood to lymph in the rat. J Physiol 146 : 54-69, 1959.

Gray SJ and Sterling K, The tagging of red cells and plasma proteins with radioactive chromium. J Clin Invest 29 : 1604-1613, 1950.

Greaves MF, Delia D, Robinson J, Sutherland R and Newman R, Exploitation of monoclonal antibodies : "Who's Who" of Haemopoietic malignancy. Blood Cells 7 : 257-280, 1981.

Greenberg ML, Chanana AD, Cronkite EP, Schiffr LM and Stryckmans PA, Extracorporeal irradiation of blood in man : Radiation resistance of circulating platelets. Radiat Res 35 : 147-154, 1968.

Griscelli C, Vassalli P and McCluskey RT, The distribution of large dividing lymph node cells in syngeneic recipient rats after intravenous injection. J Exp Med 130 : 1427-1451, 1969.

Grob D, Lilienthal JL Jr, Harvey AM and Jones BF, The administration of di-isopropyl fluorophosphate to man. Bull Johns Hopkins Hosp 81 : 217-244, 1947.

Gunther E and Stark O, The major histocompatibility system of the rats (AgB or H-1), In : The major histocompatibility system in man and animals, Gotze D ed, Springer-Verlag, New York, p102, 1977.

Gunther E and Wurst W, Cytotoxic T lymphocytes of the rat are predominantly restricted by RT1A and not RT1C-determined major histocompatibility class I antigens. Immunogenetics 20 : 1-12, 1984.

Guthrie CC, Applications of blood vessel surgery. In Blood vessel surgery, New York, Longman's Green & Co p113, .

Guy-Grand D, Griscelli C and Vassalli P, The gut associated lymphoid system : Nature and properties of the large dividing cells. Eur J Immunol 4 : 435-443, 1974.

Hafler DA, Ritz J, Schlossman SF and Weiner HL, Anti-CD4 and anti-CD2 monoclonal antibody infusions in subjects with multiple sclerosis. Immunosuppressive effects and human anti-mouse responses. J Immunol 141 : 131-138, 1988.

Hahn PF and Hevesy G, A method for blood volume determination. Acta Physiol Scand 1 : 3-10, 1940.

Hall JG, Hopkins J and Orlans W, Studies on the lymphocytes of sheep III. Destination of lymph-borne immunoblasts in relation to their tissue of origin. Eur J Immunol 7 : 30-37, 1977.

Hall BM, Dorsch S and Roser B, The cellular basis of allograft rejection in vivo. I. The cellular requirements for first-set rejection of heart grafts. J Exp Med 148 : 878-889, 1978a.

Hall BM, Dorsch S and Roser B, The cellular basis of allograft rejection in vivo. II. The nature of memory cells mediating second-set heart graft rejection. J Exp Med 148 : 890-902, 1978b.

Hall BM, Bishop GA, Farnsworth A, Duggin GG, Howarth JS, Sheil AGR and Tiller DJ, Identification of the cellular subpopulation infiltrating rejecting cadaver renal allografts. Transplantation 35 : 564-570, 1984.

Halpern SE, Haindt W, Beauregard J, Hagan P, Clutter M, Amox D, Merchant B, Uniger M, Mongovi C, Bartholomew R, Jue R, Carlo D and Dillman R, Scintigraphy with In-111 labeled monoclonal antitumor antibodies : Kinetics, biodistribution and tumor detection. Radiology 168 : 529-536, 1988.

Hancock WW, Analysis of intragraft effector mechanisms associated with human renal allograft rejection : Immunohistological studies with monoclonal antibodies. Immunol Rev 77 : 61-84, 1984.

Harker LA and Finch CA, Thrombokinetics in man. J Clin Invest 48 : 963-974, 1969.

Harker LA, The kinetics of platelets production and distribution in man. Clin Haematol 6 : 671-693, 1977.

Hart DNJ and Fabre JW, MHC antigens in rat kidney, ureter and bladder; localisation with monoclonal antibodies and demonstration of Ia positive dendritic cells. Transplantation 31 : 318-325, 1981.

Heaton WA, Davis HH, Welch MJ, Mathias CJ, Joist JH, Sherman LA and Siegel BA. Indium-111 : A new radionuclide label for studying human platelet kinetics. Br J Haematol 42 : 613-622, 1979.

Hegge FN, Hamilton GW, Larson SM, Ritchie JL and Richards P, Cardiac chamber imaging : Comparison of red blood cells labeled with Tc-99m in vitro and in vivo. J Nucl Med 19 : 129-134, 1978.

Herbertson BM, The morphology of allograft reactions, In Immunological aspects of transplantation surgery, Calne RY ed, Medical and Technical Publishing, Lancaster, 4-38, 1973.

He'ricourt J and Richet C, Physiologie pathologique de la serotherapie dans le traitement du cancer. C r hebd Seanc Acad Sci Paris 121 : 567-569, 1895.

Herlyn D, Lubeck M, Sears H and Koprowski H, Specific detection of anti-idiotypic immune responses in cancer patients treated with murine monoclonal antibody. J Immunol Meth 85 : 27-38, 1985.

Hersey P, The separation and ^{51}chromium labeling of human lymphocytes with in vivo studies of survival and migration. Blood 38 : 360-371, 1971.

Herzog CH, Walker CH, Pichler W, Aeschlimann A, Wassmer P, Stockinger H, Knapp W, Rieber P and Muller W, Monoclonal anti-CD4 in arthritis. Lancet Dec 14, 1461-1462, 1987.

Heyns duP A, Lotter MG, Badenhorst PN, van Reenen OR, Pieters H, Minaar PC and Retief FP, Kinetics, distribution and sites of destruction of indium-111 labeled human platelets. Br J Haematol 44 : 269-280, 1980.

Heyns duP A, Lotter MG, Badenhorst PN, de Kock F, Pieters H, Herbst C, van Reenen OR, Kotze H and Minaar PC, Kinetics and sites of destruction of ^{111}Indium oxine labeled platelets in idiopathic thrombocytopenic purpura : A quantitative study. Am J Haematol 12 : 167-177, 1982.

Hnatowich DJ, Layne WW and Childs RL, The preparation and labeling of DTPA-coupled albumin. Int J Appl Radiat Isotop 33 : 327-332, 1982.

Hnatowich DJ, Layne WW, Childs RL, Lanteigne D, Davis MA, Griffin TW and Doherty PW, Radioactive labeling of antibody: A single and efficient method. Science 220 : 613-615, 1983.

Hnatowich DJ, Griffin TW, Koscinczyk C, Rusckowski M, Childs RL, Mattis JA, Shealy D and Doherty PW, Pharmacokinetics of and indium-111 labeled monoclonal antibody in cancer patients. J Nucl Med 26 : 849-858, 1985.

Hofer KG, Harris CR and Smith JM, Radiotoxicity of intracellular ^{67}Ga, ^{125}I and ^{3}H : Nuclear versus cytoplasmic radiation effects in murine L1210 leukemia. Int J Radiat Biol 28 : 225-241, 1975.

Hofer KG, Microdosimetry of labeled cells. In Blood Cells in Nuclear Medicine, Vol II Migratory Blood Cells, Fueger GF ed, Martinus Nijhoff Publishers, Boston pp 224-243, 1984.

Horton MA and Hogg N, Platelet antigens : New and previously defined clusters, In Leucocyte typing III, McMichael AJ, Beverley PCL, Cobbold S, Crumpton MJ, Gilks W, Gotch FM, Hogg N, Ling N, MacLennan ICM, Mason DY, Milstein C, Spiegelhalter D and Waldmann H eds, Oxford University Press, Oxford pp733-787, 1987.

Houston LL, Nowinski RC, Bernstein ID, Specific in vivo localisation of monoclonal antibodies directed against the Thy 1.1 antigen. J Immunol 125 : 837-843, 1980.

Hurley PJ, Red cell and plasma volumes in normal adults. J Nucl Med 16 : 46-52, 1975.

Imbasciati E, Banfi G, Egidi F, Tarantino A and Ponticelli C, Morphologic patterns of renal allograft rejection. Contr Nephrol (Karger, Basel) 55 : 105-122, 1987.

ICRP (International Commission on Radiological Protection) Reference man : Anatomical, physiological and metabolic characteristics, Publication 23, Oxford Pergamon Press 1975.

ICSH (International Committee for Standardization in Haematology), The Panel on Diagnostic Application of Radioisotopes in Haematology. Recommended methods for radioisotope red cell survival studies. Br J Haematol 21 : 241-250, 1971.

ICSH (International Committee for Standardization in Haematology), The Panel on Diagnostic Application of Radioisotopes in Haematology. Recommended method for radioisotope platelet survival studies. Blood 50 : 1137-1144, 1977.

ICSH (International Committee for Standardization in Haematology), The Panel on Diagnostic Application of Radioisotopes in Haematology. Recommended methods for radioisotope red cell survival studies. Br J Haematol 45 : 659, 1980.

ICSH (International Committee for Standardization in Haematology), The Panel on Diagnostic Application of Radioisotopes in Haematology. Recommended method for indium-111 platelet survival studies. J Nucl Med 29 : 564-566, 1988.

IWASR (International Workshop on Alloantigenic Systems in the Rat), Transplantation Proc 1663-1664, 1979.

Isaacs A and Lindemann J, Virus interference 1. The interferon. Proceedings of the Royal Society of London (Series B) 259-67, 1957.

Issekutz T, Chin W and Hay JB, Measurement of lymphocyte traffic with indium-111. Clin Exp Immunol 39 : 215-221, 1980.

Jain RK and Baxter LT, Mechanisms of heterogenous distribution of monoclonal antibodies and other macromolecules in tumors : Significance of elevated interstitial pressure. Cancer Res 48 : 7022-7032, 1988.

Janossy G and Campana D, Monoclonal antibodies in the diagnosis of acute leukaemia. In the leukemic cells, Catovsky D ed, Methods in Hematology, Churchill Livinstone, Edinburgh 1-22, 1989.

Jennings LK, Phillips DR and Walker WS, Monoclonal antibodies to human platelet glycoprotein IIbβ that initiate distinct platelet responses. Blood 65 : 1112-1119, 1985.

Johansson L, Mattson S and Nosslin B, Effective dose equivalent from radiopharmaceuticals. Eur J Nucl Med 9 : 485-489, 1984.

Johnston A and Thorpe R ed, Immunochemistry in practice, 2nd ed, Blackwell Scientific Publications, London, p2, 1987.

Jones HB, Chaikoff IL, and Lawrence JH, Phosphorus metabolism of the soft tissues of the normal mouse as indicated by radioactive phosphorus. Am J Cancer 40 : 235-242, 1940.

Kaplan ME and Clark C, An improved rosetting assay for detection of human T lymphocytes. J Immunol Meth 5 : 131-135, 1974.

Keenan AM, Weinstein JN, Carrasquillo JA, Bunn Pa Jr, Reynolds JC, Foon KA, Smarte NC, Ghosh B, Fejka RM, Larson SM and Mulshine JL, Immunolymphoscintigraphy and the dose dependence of ^{111}In labeled T101 monoclonal antibody in patients with cutaneousT-cell lymphoma. Cancer Research 47 : 6093-6099, 1987.

Kincade PW and Cooper MD, Development and distribution of immunoglobulin-containing cells in the chicken. An immunofluorescent analysis using purified antibodies to mu, gamma and light chains. J Immunol 106 : 371-382, 1971.

Kincade-Smith P, Histological diagnosis of rejection of renal homografts in man. Lancet ii, 849-852, 1967.

Kinlough-Rathbone RL, Packham MA and Mustard JF, Platelets aggregation, In Measurement of platelet function, Harker LA, Zimmerman TS eds, Methods in Hematology, Churchill Livingstone, Edinburgh 1983.

Kipps TJ, Parham P, Punt J and Herzenberg LA, Importance of immunoglobulin isotype in human antibody dependent cell mediated cytotoxicity directed by murine monoclonal antibodies. J Exp Med 161 : 1-17, 1985.

Klonizakis I, Peters AM, Fitzpatrick ML, Kensett MJ, Lewis SM and Lavender JP, Radionuclide distribution following injection of ^{111}Indium labelled platelets. Br J Haematol 46 : 595-602, 1980.

Kohler G and Milstein C, Continuous cultures of fused cells secreting antibody of predefined specificity. Nature 256 : 495-497, 1975.

Kohoutava M, Gunther E and Stark O, Genetic definition of a further gene region of at least three different histocompatibility genes in the rat major histocompatibility system. Immunogenetics 11 : 483-490, 1980.

Knapp W, Leucocyte Typing IV, White Cell Differentiation Antigens, Oxford University Press, Oxford 1989.

Kraal G and Geldof AA, Radiotoxicity of ^{111}Indium. J Immunol Meth 31 : 193-195, 1979.

Kradin RL, Boyle LA, Preffer FI, Callahan RJ, Barlai-Kovach M, Strauss HW, Dubinett S and Kurnick JT, Tumor-derived interleukin-2 dependent lymphocytes in adoptive therapy of lung cancer. Cancer Immunol Immunther 24 : 76-85, 1987.

Kunicki TJ, Pidard D, Rosa JP and Nurden AT, The formation of Ca^{++} dependent complexes of platelet membrane glycoprotein IIb and IIIa in solution as determined by crossed immunoelectrophoresis. Blood 58 : 268-278, 1981.

Kunicki TJ, Montgomery RR and Kristopeit SM, Polyclonal and monoclonal antibodies used in the rapid detection of platelet defects, In monoclonal antibodies and human blood platelets, INSERM Symposium No 27. McGregor JL ed, Elsevier Science Publishers, Amsterdam pp 297-305, 1986.

Laemmli UK, Cleavage of structural proteins during the assembly of the head of bacteriophage T4. Nature 227 : 680-685, 1970.

Lamoyi E and Nisonoff A, Preparation of $F(ab')_2$ fragments from mouse IgG of various subclasses. J Immunol Meth 56 : 235-243, 1983.

Landsteiner K and Levine P, On inheritance and racial distribution of agglutinable properties of human blood. J Immunol 18 : 87-94, 1930.

Laurent G, Maraninchi D, Gluckman E, Vernant JP, Derocq JM, Gaspard MH, Ris B, Michalet M, Reiffers J, Dreyfus E, Casellas P, Schneider P{, Blythman HE, Boulax C and Janssen Fk, Donor bone marrow treatment with T101 Fab fragment-ricin-A-chain immunotoxin prevents graft-versus-host disease. Bone Marrow Transplantation 4 : 367-371, 1989.

Lavender JP, Goldman JM, Arnot RN and Thakur ML, Kinetics of indium-111 labelled lymphocytes in normal subjects and patients with Hodgkin's disease. Br Med J 2 : 797-799, 1977.

Lavender JP, Stuttle AWJ, Peters AM, O 'Donnell CJ, Davies GJ, Harrison R and Hogg N, In vivo studies with an anti-platelet monoclonal antibody; P256. Nucl Med Comm 9 : 817-822, 1988.

Leithner C, Sinzinger H, Schwartz M, Pohana E and Syne G, Increased deposition of ^{111}In labelled platelets in chronically rejected kidney transplants. Clinical Nephrology 18 : 311-313, 1982.

Lerch RA, Bergmann SR, Carlson EM, Saffitz JE and Sobel BE, Monitoring of cardiac anti-rejection therapy with In-111 lymphocytes. J Nucl Med 23 : 496-500, 1982.

Levin J and Evatt BL, Humoral control of thrombopoiesis. Blood Cells 5 : 105-119, 1979.

Lexer E, Free Transplantation. Ann Surg 60 : 166-194, 1914.

Lindmo T, Boven E, Cuttita F, Fedorko J and Bunn PA Jr, Determination of the immunoreactive fraction of radiolabeled monoclonal antibodies by linear extrapolation to binding at infinite antigen excess. J Immunol Meth 72 : 77-89, 1984.

Lindmo T and Bunn PA Jr, Determination of the true immunoreactive fraction of monoclonal antibodies after radiolabeling. Meth Enzymology 121 : 678-691, 1986.

Little CC and Tizzer EE, Experimental studies on the inheritance of susceptibility to a transplantable tumor, Carcinoma (J.W.A.) of the Japanese Waltzing mouse. J Med Res Bost 33 : 393-453, 1916.

Little JR, Brecher G, Bradley TR and Rose S, Determination of lymphocyte turnover by continuous infusion of ^{3}H-thymidine. Blood 19 : 236-242, 1962.

Lombardo VT, Hodson E, Roberts JR, Kunicki TJ, Zimmerman TS and Ruggeri ZM, Independent modulation of von Willebrand factor and fibrinogen binding to the platelet membrane glycoprotein IIb/IIIa complex as demonstrated by monoclonal antibody. J Clin Invest 76:1950-1958, 1985.

Lotze MT, Line BD, Mathisen DJ and Rosenberg SA, The in vivo distribution of autologous human and murine lymphoid cells grown in T cell growth factor (TCGF); implications for the adoptive immunotherapy of tumors. J Immunol 125 : 1487-1493, 1980.

Lumley P and Humphrey PA, A method for quantitating platelet aggregation and analyzing drug receptor interaction on platelets in whole blood in vitro. J Pharmacological Methods 6 : 153-166, 1981.

McAfee JG and Thakur ML, Survey of radioactive agents for in vitro labeling of phagocytic leukocytes I. Soluble agents. J Nucl Med 17 : 480-487, 1976a.

McAfee JG and Thakur ML, Survey of radioactive agents for in vitro labeling of phagocytic leukocytes II. Particles. J Nucl Med 17 : 488-492, 1976b.

McEver RP, Baenziger NL and Majerus PL, Isolation and quantitation of the platelet membrane protein deficient in thrombasthenia using a monoclonal antibody. J Clin Invest 66 : 1311-1318, 1980.

McEver RP and Martin MN, A monoclonal antibody to a membrane glycoprotein binds only to activated platelets. J Biol chem 259 : 9799-9804, 1984.

MacGregor DD and Logie PS, The mediator of cellular immunity VII Localisation of sensitized lymphocytes in inflammatory exudates. J Exp Med 139 : 1415-1430, 1974.

McGregor JL, Brochier J, Wild F, Follea G, Trzeciak MC, James E, Dechavanne M, McGregor L and Clementson KJ, Monoclonal antibodies against platelet membrane glycoproteins, characterization and effect on platelet function. Eur J Biochem 131 : 427-436, 1983.

Mach JP, Carrel S, Forni M, Ritschard J, Donath A and Alberto P, Tumor localisation of radiolabeled antibodies against carcino-embryonic antigen in patients with carcinoma. A critical evaluation. N Engl J Med 303 : 5-10, 1980.

Machac J, Vallabhajosula S, Goldman ME and Goldsmith SJ, Value of blood pool subtraction in cardiac indium-111 labeled platelet imaging. J Nucl Med 30 : 1445-1455, 1989.

McKillop JH, Wallwork J, Reitz, BA, Billingham ME, Miller R and McDougall IR, The use of In-111 labeled lymphocyte imaging to evaluate graft rejection following cardiac transplantation in dogs. Eur J Nucl Med 7 : 162-165, 1982.

McMichael AJ, Beverley PCL, Cobbold S, Crumpton MJ, Gilles W, Gotch FM, Hogg N, Horton M, Ling N, MacLennan ICM, Mason DY, Milstein C, Speigelhalter D and Waldmann H, Leucocyte Typing III, White Cell Differentiation Antigens, Oxford University Press, Oxford 1987.

McPherson GG, Development of megakaryocytes in bone marrow of the rat : An analysis by electron microscopy and high resolution autoradiography. Proc of the Royal Society of London B 177 : 265-274, 1971.

Makrigioros GM, Adelstein SJ and Kassis AI, Limitations of conventional internal dosimetry at the cellular level. J Nucl Med 30 : 1856-1864,1989.

Marcus CS, Koyle MA, Darcourt J and Vivian M, Evaluation of the utility of indium-111 oxine platelet imaging in renal transplant patients on cyclosporine. Clin Nucl Med 11 : 834-839, 1986.

Marguerie GA, Edgington TS and Plow EF, Interaction of fibrinogen with its platelet receptor as part of a multistep reaction in ADP-induced platelet aggregation. J Biol Chem 255 : 154-161, 1980.

Mariano Garcia A, Gagne GM, Ames IH, Stiteler W, Tomar RH and McAfee JG, Migratory patterns of different indium-111 labeled leukocyte populations (chiefly lymphocytes) from control nad thymectomized rats. J Nucl Med 29 : 83-90, 1988.

Martin-Comin J, Roca M, Grino JM, Paradell C and Caralps C, Indium-111 oxine autologous labeled platelets in the diagnosis of kidney graft rejection. Clin Nucl Med 8 : 7-10, 1983.

Martin-Comin J, Kidney graft rejection studies with labeled platelets and lymphocytes. Nucl Med Biol (Int J Radiat Appl Instrum Part B) 13 : 173-181, 1986.

Mason DW and Williams AF, Kinetics of antibody reactions and the analysis of cell surface antigens, In Handbook of Experimental Immunology, Vol 1 Immunochemistry, Chapter 38, Weir DM ed, 4th edition, Blackwell Scientific Publications, London 1986.

Masui H, Moroyama T and Mendelsohn J, Mechanism of antitumor activity in mice for anti-epidermal growth factor receptor monoclonal antibodies with different isotypes. Cancer Res 46 : 5592-5598, 1986.

Matzku S, Brocker EB, Bruggen J, Dippold WG and Tilgen W, Modes of binding and internalization of monoclonal antibodies to human melanoma cell lines. Cancer Research 46 : 3848-3854, 1986.

Mausner LF, Straub RF and Srivastava SC, Production and use of prospective radionuclides for radioimmunotherapy. In Radiolabeled Monoclonal Antibodies for Imaging and Therapy, Srivastava SC ed, Plenum Press, New York 1988.

Mazumder A, Eberlein TJ, Grimm EA, Wilson DJ, Keenan AM, Modt RAA and Rosenberg SA, Phase I study of the adoptive immunotherapy of human cancer with lectin activated autologous mononuclear cells. Cancer 53 : 896-905, 1984.

Medawar PB, The behaviour and fate of skin autografts and skin homografts in rabbits. J Anat 78 : 176-199,1944.

Melamed MR, Clifton EG, Mercer C and Koss LG, The megakaryocyte blood count. Am J of the Medical Sciences 252 : 301-309, 1966.

Mertz T, Tatum J and Hirsh J, Technetium99-m labeled lymphocytes. A radiotoxicity study. J Nucl Med 27 : 105-110, 1986.

Micklem HS, Ford CE, Evans EP and Gray J, Interrelationship of myeloid and lymphoid cells : Studies with chromosome-marked cells transfused into lethally irradiated mice. Proc Roy Soc Lond (B) 165 : 78-102, 1966.

Milgram R and Goodwin DA, Human scanning with In-111 oxine labeled autologous lymphocytes. Clinical Nuclear Medicine 10 : 30-34, 1985.

Miller JFAP, Analysis of the thymus influence in leukaemogenesis. Nature 191 : 248-250, 1961a.

Miller JFAP, Immunological functions of the thymus. Lancet ii 748-749, 1961b.

Miller RA, Gartner S and Kaplan HS, Stimulation of mitogenic responses in human peripheral blood lymphocytes by lipopolysaccharide : Serum and helper T cell requirements. J Immunol 121 : 2160-2164, 1978.

Miller RA, Coleman CN, Fawcett HD, Hoppe RT and McDougall IR, Sezary syndrome : A model for migration of T lymphocytes to skin. N Engl J Med 303 : 89-92, 1980.

Milton AD and Fabre JW, Massive induction of donor-type class I and class II majopr histocompatibility complex antigens in rejecting cardiac allografts in the rat. J Exp Med 161 : 98-112, 1985.

Milton AD, Spencer SC and Fabre JW, Detailed analysis and demonstration of differences in the kinetics of induction of class I and class II major histocompatibility complex antigens in rejecting cardiac and kidney allografts in the rat. Transplantation 41 : 499-508, 1986.

Milton AD, Spencer SC and Fabre JW, The effects of cyclopsorine on the induction of donor class I and class II MHC antigens in heart and kidney allografts in the rat. Transplantation 42 : 337-347, 1986.

Modderman PW, Tetteroo PAT, Leuksma OC, Bos MJE, van Mourik JA, Huisman JG and von dem Borne AEG, Differences in functional effects of monoclonal antibodies against platelet membrane glycoproteins IIb/IIIa, In Monoclonal antibodies and human blood platelets, INSERM symposium No 27, McGregor JL ed, Elsevier Science Publishers BV, Amsterdam, pp131-142, 1986.

Moore A, Cooper SA and Jones DB, Use of monoclonal antibody WR-17, identifying the CD37 gp40-45 kD antigen complex in the diagnosis of B lymphoid malignancy. J Pathol 152 : 13-21, 1987.

Morrison SL, Transfectomas provide novel chimeric antibodies. Science 229 : 1202-1207, 1985.

Murphy JB, The lymphocyte in resistance to tissue grafting, malignant disease and tuberculous infection. Monogr Rockefeller Inst Med Res No 21, 1926.

Murphy S, Oski FA, Naiman JL, Lusch CJ, Goldberg S and Gardner FH, Platelet size and kinetics in hereditary and acquired thrombocytopenia. N Engl J Med 289 : 499-504, 1972.

Murray G, Experiments in immunity in cancer. Can Med Ass J 79 : 249-259, 1958.

Murray JE, Merrill JP, Harrison JH, Wilson RE and Demmin GJ, Prolonged survival of human kidney homografts by immunosuppressive drug therapy. N Engl J Med 268 : 1315-1323, 1963.

Mustard JF and Packham MA, In Inflammation, immunity and hypersensitivity, Movat HZ ed, Harper and Row publishers, New York, pp 557-564, 1979.

Nachman RL and Leung LL, Complex formation of platelet membrane glycoproteins IIb and IIIa with fibrinogen. J Clin Invest 69 : 263-269, 1982.

Neuberger MS and Plasensky K, Activation of mouse complement by monoclonal mouse antibodies. Eur J Immunol 11 : 1012-1016, 1981.

Neuberger MS, Williams GT and Fox RD, Recombinant antibodies possessing novel effector functions. Nature 312 : 604-608, 1984.

Nurden AT and Caen JP, Specific roles for platelet surface glycoproteins in platelet function. Nature (Lond) : 255 :720-722, 1975.

Nurden AT and Caen JP, The different glycoprotein abnormalities in thrombasthenic and Bernard-Soulier platelets. Sem Hematol 16 : 234-250, 1979.

Oi VT, Vvong TM, Hardy R, Reidler J, Dangle L, Herzenberg A and Stayer L, Correlation between segmental flexibility and effector function of antibodies. Nature 307 : 136-139, 1984.

Oster ZH, Srivastava SC, Som P, Meinken GE, Scudder LE, Yamamoto K, Atkins HL, Brill AB and Coller BS, Thrombus radioimmunoscintigraphy : An approach using monoclonal antiplatelet antibody. Proc Natl Acad Sci USA 82 : 3465-3468, 1985.

Ottaway CA and Parrott DMV, Regional blood flow and its relationship to lymphocytes and lymphoblast traffic during a primary immune reaction. J Exp Med 150 : 218-230, 1979.

Ottesen J, On the age of human white cells in peripheral blood. Acta Physiol Scand 32 : 75-93, 1954.

Palou A, Remesar X, Arola Ll and Alemany M, Body and organ size and composition during late foetal and postnatal development of rat. Comp Biochem Physiol 75A : 597-601, 1983.

Paris A and Gunther E, Kidney grafting between rats which carry recombinant major histocompatibility haplotypes. Immunogenetics 10 : 205-209, 1980.

Parker BA, Vassos AB, Halpern SE, Miller RA, Hupf H, Amox DG, Simoni JL, Starr RJ, Green MR and Royston I, Radioimmunotherapy of human B-cell lymphoma with ^{90}Y-conjugated antiidiotype monoclonal antibody. Cancer Research (suppl) 50 : 1022s-1028s, 1990.

Parnham P, Androlewicz MJ, Brodsky FM, Holmes NJ and Ways JP, Monoclonal antibodies : Purification, fragmentation and application to structural and functional studies of class I MHC antigens. J Immunol Meth 53 : 133-173, 1982.

Parnham P, Preparation and purification of active fragments of mouse monoclonal antibodies. In Handbook of Experimental Immunology, vol 1, Chapter 14, Weir DM ed. 4th Ed, Blackwell Scientific Publications, 1986.

Parrott DMV de Sousa MAB and East J, Thymus-dependent areas in the lymphoid organs of neonatally thymectomised mice. J Exp Med 123 : 191-204, 1966.

Parrott DMV and de Sousa M, Thymus-dependent and thymus independent populations : Origin, migratory patterns and lifespan. Clin Exp Immunol 8 : 663-684, 1971.

Parrott DMV and Fergusson A, Selective migration of lymphoblasts within the small intestine. Immunology 26 : 571-588, 1974.

Parrott DMV and Wilkinson PC, Lymphocyte locomotion and migration. Prog Allergy 28 : 193-284, 1981.

Pasternack A, Fine-needle aspiration biopsy of human renal homografts. Lancet ii, 82-84, 1968.

Paterson DJ, Jefferies WA, Green JR, Brandon MR, Corthesy P, Puklavec M, and Williams AF, Antigens of activated rat T lymphocytes including a molecule of 50000 Mr detected only on CD4 positive T blasts. Molecular Immunology 24 : 1280-1291, 1987.

Pauly JL, Sokal JE and Han T, Whole blood culture technique for functional studies of lymphocyte reactivity to mitogens, antigens and homologous lymphocytes. J Lab Clin Med 82 : 500-512, 1973.

Pavel DG, Zimmer AM and Patterson VN, In vivo labeling of red blood cells with Tc-99m : A new approach to blood pool visualisation. J Nucl Med 18 : 305-308, 1977.

Pearson HA, The binding of ^{51}Cr to hemoglobin I. In vitro studies. Blood 22 : 218-230, 1963.

Perkins AC and Pimm MV, Difference in tumor and normal tissues concentration of iodine and indium labeled monoclonal antibody. 1. The effect on image contrast in clinical studies. Eur J Nucl Med 11 : 295-299, 1985.

Peters AM, Klonizakis I, Lavender JP and Lewis SM, Use of ^{111}In-labeled platelets to measure spleen function. Br J Haematol 46 : 587-593, 1980.

Peters AM, Saverymuttu SH, Wonke B, Lewis SM and Lavender JP, The interpretation of platelet kinetic studies for the identification of sites of abnormal platelet destruction. Br J Haematol 57 : 637-649, 1984.

Peters AM, Saverymuttu SH, Bell RN and Lavender JP, The kinetics of short-lived indium-111 radiolabelled platelets. Scand J Haematol 34 : 137-145, 1985.

Peters AM, Danpure HJ, Osman S, Hawker RJ, Henderson BL, Hodgson HJ, Kelly JD, Neirinckx RD and Lavender JP, Clinical experience with $^{99}Tc^{m}$-hexamethyl-propylene-amine-oxime for labelling leucocytes and imaging inflammation. Lancet ii, 946-949, 1986.

Peters AM, Roddie ME, Danpure HJ, Osman S, Zacharopoulos GP, George P, Stuttle AWJ, and Lavender JP, $^{99}Tc^{m}$-HMPAO labelled leucocytes : Comparison with ^{111}In tropolonate labelled granulocytes. Nucl Med Comm 9 : 449-463, 1988.

Phillips DR and Agin PP, Platelet membrane defects in Glanzmann's thrombasthenia. Evidence for decreased amounts of two major glycoproteins. J Clin Invest 60 : 535-545, 1977.

Pidard D, Montgomery RR, Bennett JS and Kunicki TJ, Interaction of AP-2, a monoclonal antibody specific for the human platelet glycoprotein IIb-IIIa complex with intact platelets. J Biol Chem 258 : 12582-12586, 1983.

Pimm MV, Perkins AC, Armitage NC and Baldwin RW, The characteristics of blood-borne radiolabels and the effect of anti-mouse IgG antibodies on localization of radiolabeled monoclonal antibodies in cancer patients. J Nucl Med 26 : 1011-1023, 1985.

Pober JS, Gimbrone MA Jr, Cotran RS, Reiss CS, Burakoff SJ, Fiers W and Ault KA, Ia expression by vascular endothelium is inducible by activated T cells and by human γ-interferon. J Exp Med 157 : 1339-1353, 1983.

Powers WJ, Siegel DA, Davis HH II, Mathias CJ, Clark HB and Welch MJ, In-111 platelet scintigraphy in cerebrovascular disease. Neurol 32 : 938-943, 1982.

Pressman D and Korngold L, The in vivo localisation of anti-Wagner osteogenic sarcoma antibodies. Cancer 6 : 619-623, 1953.

Price MR, Hannant D, Embleton MJ and Baldwin RW, Icrew workshop report : Detection and isolation of tumour associated antigens, Br J Cancer 41 : 843, 1980.

Rainsbury RN and Westwood JH, Tumor localisation with monoclonal antibody radioactively labeled with metal chelate rather than iodine. Lancet ii: 1347-1348, 1982.

Rannie GH and Donald KJ, Estimation of the migration of thoracic duct lymphocytes to non-lymphoid tissues. A comparison of the distribution of radioactivity at intervals following iv transfusion of cells labelled with ^{3}H, ^{14}C, ^{75}Se, ^{99m}Tc, ^{125}I and ^{51}Cr in the rat. Cell Tissue Kinet 10 : 523-541, 1977.

Rannie GH, Thakur ML and Ford WL, An Experimental comparison of radioactive labels with potential application to lymphocyte migration studies in patients. Clin Exp Immunol 29 : 509-514, 1977.

Rao DV, Sastry KSR, Grimmond HE, Howell RW, Govelitz GF, Lanka VK and Mylavapu VB, Cytotoxicity of some indium radiopharmaceuticals in mouse testes. J Nucl Med 29 : 375-384, 1988.

Read EJ, Keenan AM, Carter CS, Yolles PS and Davey RJ, In vivo traffic of indium-111-oxine labeled human lymphocytes collected by automated apheresis. J Nucl Med 31 : 999-1006, 1990.

Reinherz EL, Haynes BJ, Bernstein ID and Nadler LM, Leucocyte Typing II, Springer-Verlag, New York 1986.

Reynolds J, Heron I, Dudler L and Trnka Z, T cell recirculation in the sheep : Migratory properties of cells from lymph nodes. Immunology 47 : 415-421, 1982.

Ritchie JL, Stratton JR, Thiele B, Hamilton GW, Warrick LN, Huang TW and Harker LA, Indium-111 platelet imaging for detection of platelet deposition in abdominal aneurysms and prosthetic arterial grafts. Am J Cardiol 47 : 882-889, 1981.

Ritz J, Pesando JM, Notis-McConarty J and Schlossman SF, Modulation of human acute lymphoblastic leukemia antigen induced by monoclonal antibody in vitro. J Immunol 125 : 1506-1514, 1980.

Robertson JS, Dewanjee MK, Brown ML, Fuster V and Chesebro JJ, Distribution and dosimetry of ^{111}In labeled platelets. Radiology 140 : 169-176, 1981.

Romson JL, Hook BG, Rigot VH, Schork MA, Swanson DP and Lucchesi BR, The effect of Ibuprofen on accumulation of indium-111 labeled platelets and leukocytes in experimental myocardial infarction. Circulation 66 : 1002-1011, 1982.

Rose ML, Parrott DMV and Bruce RG, Migration of lymphoblasts to the small intestine II. Divergent migration of mesenteric and peripheral immunoblasts to sites of inflammation in the mouse. Cell Immunol 27 : 36-46, 1976.

Rosen ST, Zimmer AM, Goldman-Leikin R, Gordon LI, Kazikiewicz JM, Kaplan EH, Variakojis D, Marder RJ, Dykewicz MS, Piergies A, Silverstein EA, Roenigk HH Jr and Spies SM, Radioimmunodetection and radioimmunotherapy of cutaneous T cell lymphomas using and ^{131}I-labeled monoclonal antibody : An Illinois cancer council study. J Clin Oncology 5 : 562-573, 1987.

Rosenberg S, Lymphokine-activated killer cells. A new approach to immunotherapy of cancer. J N C I 75 : 75 : 595-603, 1985.

Rosenberg SA, Spiess P and Lafreniere R, A new approach to the adoptive immunotherapy of cancer with tumor infiltrating lymphocytes. Science 233: 1318-1321, 1986.

Rosenblum MG, Murray JL, Haynie TP, Glenn HJ, Jahns MF, Benjamin RS, Frincke JM, Carlo DJ and Hersh EM, Pharmacokinetics of ^{111}In labeled anti-p97 monoclonal antibody in patients with metastatic melanoma. Cancer Res 45 : 2382-2386, 1985.

Roysten I, Majda JA, Baird SM et al, Human T-cell antigens defined by monoclonal antibodies : The 65000 dalton antigen of T cells (T65) is also found on chronic lymphocytic leukemia cells bearing surface immunoglobulin. J Immunol 125 : 725-731, 1980.

Ruggeri ZM, The use of monoclonal antibodies to probe the receptor function of the glycoprotein IIb/IIIa complex, In Monoclonal antibodies and human blood platelets, McGregor JL ed, INSERM symposium No 27 Elsevier Scientific Publishers BV, Amsterdam, pp83-91, 1986.

Russell P, Colvin RB and Cosimi AB, Monoclonal antibodies for the diagnosis and treatment of transplant rejection. Ann Rev Med 35 : 63-81, 1984.

Sastry KSR and Rao DV, Dosimetry of low energy electrons, In : Rao DV, Chandra R and Graham MC eds, Physics of nuclear medicine : Recent advances. American Association of Physicists in Medicine, Monograph No 10, New York, American Institute of Physics, 169-208, 1984.

Sastry KSR, Howell RW, Rao DV et al, Dosimetry of Auger emitters : Physical and phenomenological approaches. Proc Intl Workshop on Auger emitters in DNA : Implications and Applications, Baverstock KF and Charlton DE, Taylor and Francis, p15, 1987.

Scheffel U, Tsan MF, Mitchell TG, Camargo EE, Braine H, Ezekowitz MD, Nickoloff EL, Hill-Zobel R, Murphy E and McIntyre PA, Human platelets labeled with In-111 8-hydroxyquinoline : Kinetics, distribution and estimates of radiation dose. J Nucl Med 23 : 149-159, 1982.

Schmidt KG, Rasmussen JW, Rasmussen AD and Arendrup H, Comparative studies of the in vivo kinetics of simultaneously injected ^{111}In and ^{51}Cr labelled human platelets. Scand J Haematol 30 : 69-77, 1983a.

Schmidt KG, Rasmussen JW, Rasmussen AD, Arendrup H and Lorentzen M, Comparative studies of the function and morphology of ^{111}In and ^{51}Cr labelled human platelets. Scand J Haematol 31 : 69-77, 1983b.

Schoene G, Die Heteroplastische und Homoeoplastische Transplantation, 73-74, Springer Verlag, Berlin 1912.

Schroff RW, Foon RA, Beatty SM, Oldham RK and Morgan AC Jr, Human anti-murine immunoglobulin response in patients receiving monoclonal antibody therapy. Cancer Res 45 : 879-885, 1985.

Scott JL, Davidson JG, Marino JV and McMillan R, Leukocyte labeling with ^{51}chromium. III The kinetics of normal lymphocytes. Blood 40 : 276-281, 1972.

Scott JL, McMillan R, Marino JV and Davidson JG, Leukocyte labeling with ^{51}chromium. IV The kinetics of chronic lymphocytic leukemic lymphocytes. Blood 41 : 155-162, 1973.

Sedlacek HH, Gronski P, Hofstaetter T, Kanzy EJ, Schorlemmer HV and Seiler FR, The biological properties of immunoglobulin G and its split products $(F(ab)'_2$ and Fab). Klin Wschr 61 : 723-736, 1983.

Segal AW, Deteix P, Garcia R, Tooth P, Zanelli GD and Allison AC, Indium-111 labeling of leukocytes : A detrimental effect on neutrophil and lymphocyte function and an improved method of cell labeling. J Nucl Med 19 : 1238-1244, 1978.

Shawler DL, Miceli MC, Wormsley SB, Royston I, Dillman RO, Induction of in vitro and in vivo antigenic modulation by the anti-human T-cell monoclonal antibody T101. Cancer Research 44 : 5921-5927, 1984.

Shawler DL, Bartholomew RM, Smith LM and Dillman RO, Human immune response to multiple injections of murine monoclonal IgG. J Immunol 135 : 1530-1535, 1985.

Silvester DJ and Waters SL, Dosimetry of radiolabelled blood cells. Int J Nucl Med Biol 10 : 141-144, 1983.

Sinn H and Silvester DJ, Simplified cell labelling with ^{111}In acetylacetone. Br J Radiol 52 : 758-759, 1979.

Sivolapenko GB, Kanariou M, Edwards RJ, Epenetos AA and Ritter MA, Immunosuppression by immunoglobulin deaggregation is not effective in reducing the anti-xenogeneic immunoglobulin response : Experimental and clinical studies. Br J Cancer 60 : 511-516, 1989.

Smith N, Chandler S, Hawker RJ, Hawker LM and Barnes AD, Indium labeled autologous platelets as diagnostic aid after renal transplantation. Lancet ii 1241-1242, 1979a.

Smith CIE, Hammerstrom L, Bird AG, Kunori T, Gustafsson B and Holme T, Lipopolysaccharide and lipid A induced human blood activation as detected by a protein A plaque assay. Eur J Immunol 9 : 619-625, 1979b.

Smith ME and Ford WL, The recirculating lymphocyte pool of the rat : A systematic description of the migratory behaviour of recirculating lymphocytes. Immunology 49 : 83-94, 1983.

Snell GD, Methods for the study of histocompatibility genes. J Genet 49 : 87-103, 1948.

Snyder WS, Ford MR, Warner GG and Watson SB, "S" absorbed dose per unit cumulated activity for selected radionuclides and organs, MIRD pamphlet No 11, Society of Nuclear Medicine, New York 1975.

Som P, Oster ZH, Zamora PO, Yamamoto K, Sacker DF, Brill AB, Newel KD and Rhodes BA, Radioimmunoimaging of experimental thrombi in dogs using technetium-99m labeled monoclonal antibody fragments reactive with human platelets. J Nucl Med 27 : 1315-1320, 1986.

Sparshott SM, Sharma H, Kelly JD and Ford WL, Factors influencing the fate of In-111 labelled lymphocytes after transfer to syngeneic rats. J Immunol Meth 41 : 303-320, 1981.

Spivak J and Perry S, Lymphocyte kinetics in chronic lymphatic leukemia. Br J Haematol 18 : 511-522, 1970.

Sprent J, Anderson RE and Miller JFAP, Radiosensitivity of T and B lymphocytes. II. Effect of irradiation on response of T cells to alloantigens. Eur J Immunol 4 : 204-210, 1974.

Sprent J, Migratory properties and radiosensitivity of lymphocytes, In : Radiolabeled cellular blood elements : Pathophysiology, techniques and scintigraphic applications, Thakur ML ed, Plenum Press, New York pp31-50, 1985.

Stefanini M, Enzymes, isozymes and enzyme variants in the diagnosis of cancer : A short review. Cancer 55 : 1931-1936, 1985.

Steiner M and Baldini M, Subcellular distribution of ^{51}Cr and characterisation of its binding sites in human platelets. Blood 35 : 727-739, 1970.

Sterling K and Gray SJ, Determination of the circulating red cell volume or mass by radioactive chromium. J Clin Invest 29 : 1614-1619, 1950.

Stokeley EM, Parkey RW and Bonte FJ, Gated blood pool imaging following Tc-99m stannous pyrophosphate imaging. Radiology 120 : 433-434, 1975.

Stratton JR, Thiele BL and Ritchie JL, Platelet deposition on aortic bifurcation grafts in man : Quantitation with ^{111}In labeled platelet imaging. Circulation 66 : 1287-1293, 1982.

Strom TB, Tilney NL, Carpenter CB and Busch GJ, Identity and cytotoxic activity of cells infiltrating renal allografts. N Engl J Med 292 : 1257-1263, 1975.

Strykmans PA, Chanana AD, Cronkite EP, Greenberg ML, and Schiffer LM, Studies on lymphocytes IX. The survival of autotransfused labeled lymphocytes in chronic lymphocytic leukemia. Eur J Cancer 4 : 241, 1968.

Strykmans PA, Debusscher L and Collard E, Cell kinetics in chronic lymphocytic leukaemia. Clinics in Haematology, 6 : 159-167, 1977.

Stuart FP, Siatoh R and Fitch GW, Rejection of renal allografts : Specific immunologic suppression. Science 160 : 1463-1465, 1968.

Stuttle AWJ, Peters AM, Loutfi I, Lumley P, George P and Lavender JP, Use of an anti-platelet monoclonal antibody F(ab')$_2$ fragment for imaging thrombus. Nucl Med Comm 9 : 647-655, 1988a.

Stuttle AWJ, Ritter JM, Peters AM and Lavender JP, In vitro studies with an anti-platelet monoclonal antibody; P256. Nucl Med Comm 9 : 813-815, 1988b.

Sutherland GK, King ME, Peerless SJ, et al, Platelet interaction within giant intracranial aneurysms. J Neurosurg 56 : 53-61, 1982.

Taylor-Papadimitriou J, Peterson JA, Arklie J, Burchell J, Ceriani RC and Bodmer WF, Monoclonal antibodies to epithelium specific components of the milk fat globule membrane : Production and reaction with cells in culture. Int J Cancer 28 : 17-24, 1981.

ten Berge RJM, Natarajan AT, Hardeman MR, van Royen EA and Schellekens PThA, Labeling with indium-111 has detrimental effects on human lymphocytes : concise communication. J Nucl Med 24 : 615-620, 1983.

Thakur ML, Welch ML and Joist H, Indium-111 labeled platelets : Studies on preparation and evaluation on in vitro and in vivo functions. Thromb Res 9 : 345-357, 1976.

Thakur ML, Lavender JP, Arnot RN, Silvester DJ and Segal AW, Indium-111 labeled autologous leukocytes in man. J Nucl Med 18 : 1012-1019, 1977a.

Thakur ML, Segal AW, Louis L, Welch MJ, Hopkins J and Peters TJ, Indium-111 labeled cellular blood components : Mechanisms of labeling and intracellular location in human neutrophils. J Nucl Med 18 : 1022-1026, 1977b.

Thistlethwaite JR, CosimiAB, Delmonico RH, Rubin N, Tolkoff-Rubin PW, Nelson L, Fang , Russell PS, Evolving use of OKT3 antibody for treatment of renal allograft rejection. Transplantation, Baltimore, 38 : 695-702, 1984.

Thorpe PE, Mason DW, Brown ANF, Simmonds J, Ross WCJ, Cumber AJ and Forrester JA, Selective killing of malignant cells in a leukaemic rat bone marrow using an antibody-ricin conjugate. Nature (Lond) 297 : 594-596, 1982.

Tilgen W, Matzku S, Kaufmann I, Engstner M, Brueggen J, Dippold W and Petzoldt D, Modulation of melanoma-associated antigens by monoclonal antibodies as visualized by radioimmunoelectron microscopy and radioantibody binding assay. Arch Dermatol Res 279 : s116-s126, 1987.

Tingaard Pedersen N, The pulmonary vessels as a filter for circulating megakaryocytes in rats. Scand J Haematol 13 : 225-231, 1974.

Tisdale PL, Collier BD, Kauffman HM, Adams MB, Isitman AT, Hellman RS, Hoffman RG, Rao SA, Joetgen T and Krohn L, Early diagnosis of acute postoperative renal transplant rejection by indium-111 labeled platelet scintigraphy. J Nucl Med 27 : 1266-1272, 1986.

Travers P and Bodmer WF, Preparation and characterisation of monoclonal antibodies against placental alkaline phosphatase and other human trophoblast associated determinants. Int J Cancer 33 : 633-641, 1984.

Trowbridge EA, Martin JF and Slater DN, Evidence for a theory of physical fragmentation of megakaryocytes implying that all platelets are produced in the pulmonary circulation. Thrombosis Research 28 : 461-475, 1982.

Trowbridge EA and Martin JF, A biological approach to the platelets survival curve with criticism of previous interpretation. Phys Med Biol 28 : 1349-1368, 1983.

Ullman E, Experimentelle Nierentransplantation. Wien Klin Wochenschr 15 : 281, 1902.

Unkeless JC, Fleit H and Mellman IS, Structural aspects and heterogeneity of immunoglobulin Fc receptors. Adv Immunol 31 : 247-270, 1981.

van Dinther-Janssen ACHM and Scheper RJ, Restriction to the use of ^{111}Indium-oxine as a radiolabel in lymphocyte migration studies. J Immunol Meth 46 : 353-360, 1981.

von dem Borne AEGKr, De Bruijne-Admiraal LG, Modderman PW, Nieuwenhuis HK, Platelet antigens, In Leucocyte typing IV, Knapp W, Dorken B, Gilks WR, Rieber EP, Schmidt RE, Stein H and von dem Borne AEGKr, Oxford University Press, Oxford, part 6, pp950-1046, 1989.

Wagstaff J, Gibson C, Thatcher N, Ford WL, Sharma H, Benson H and Crowther D, A method for following human lymphocyte traffic using indium-111 oxine labelling. Clin Exp Immunol 43 : 435-442, 1981a.

Wagstaff J, Gibson C, Thatcher N, Ford WL, Sharma H and Crowther D, Human lymphocyte traffic assessed by indium-111 oxine labelling : Clinical observations. Clin Exp Immunol 43 : 443-449, 1981b.

Wagstaff J, Gibson C, Thatcher N and Crowther D, The migratory properties of indium-111 oxine labelled lymphocytes in patients with chronic lymphocytic leukaemia. Br J Haematol 49 : 283-291, 1981c.

Waldmann H ed, Monoclonal Antibody Therapy. Prog Aller 45, 1988.

Wang TST, Oluwole S, Fawwaz RA, Wolff M, Kuromoto N, Satake K, Hardy MA and Alderson PO, Cellular basis of In-111 labeled leukocytes and platelets in rejecting cardiac allografts. J Nucl Med 23 : 993-997, 1982.

Warnke RA, Slavin S, Coffman RL, Butcher EC, Knapp MR, Strober S and Weissman I, The pathology and homing of a transplantable murine B cell leukaemia (BCL1). J Immunol 123 : 1181-1188, 1979.

Watson EE, Cell Labeling : Radiation dose and effects. J Nucl Med 24 : 637-640, 1983

Weetman AP and Rees AJ, Synergistic effects of recombinant tumor necrosis factor and interferon-gamma on rat thyroid cell growth Ia antigen expression. Immunology 63 : 285-289, 1988.

Weiss L, A scanning electron microscopic study of the spleen. Blood 43 : 665-691, 1974.

Williams AF, Galfre G and Milstein C, Analysis of cell surface by xenogeneic myeloma-hybrid antibodies : Differentiation antigens of rats lymphocytes. Cell 12 : 663-673, 1977.

Williams LR and Leggett RW, Reference values for resting blood flow to organs of man. Clin Phys Physiol Meas 10 : 187-217, 1989.

Williamson CS, Some observations on the length of survival and function of homogeneous kidney transplants. Premilinary report. J Urol 10 : 275, 1923.

Winzelberg GG, McKussik KA, Strauss HW, Waltman AC and Greenfield AJ, Evaluation of gastrointestinal bleeding by red blood cells labeled in vivo with technetium-99m. J Nucl Med 20 : 1080-1086, 1979.

Wong GH, Clark-Lewis WI, Harris AW and Schnader JW, Effect of cloned interferon gamma on expression of H-2 and Ia antigens on cell lines of haemopoietic, lymphoid, epithelial, fibroblastic and neuronal origin. Eur J Immunol 14 : 52-56, 1984.

Wright JH, The morphogenesis of the blood platelets. Journal of Morphology 21 : 263-278, 1906.

Wu PTT and Mann F, Histologic studies of autologous and homogenous tranplants of the kidney. AMA Arch Surg 28, 889, 1934.

Yoffey JM and Courtice FC, Lymphatics, lymph and lymphoid tissue, Edward Arnold London, 1956.

Zatz MM, White A and Goldstein AL, Alterations in lymphocyte populations in tumorigenesis I. Lymphocyte trapping. J Immunol 3 : 706-711, 1974.

Zimmer AM, Rosen ST, Spies SM, Goldman-Leikin R, Kazikiewicz JM, Silverstein EA, Kaplan EH, Radioimmunotherapy of patients with cutaneous T-cell lymphoma using an iodine-131-labeled monoclonal antibody : Analysis of retreatment following plasmapheresis. J Nucl Med 29 : 174-180, 1988.

Zinkernagel EM and Doherty PC, H-2 compatibility requirement for T cell mediated lysis of target cells infected with lymphocytic choriomeningitis virus : Different cytotoxic specificities are associated with structures coded for in either H-2K or H-2 D. J Exp Med 141 : 1427-1432, 1975.

Zucker MB and Nachmias VT, Platelet activation. Arteriosclerosis 5 : 2-18, 1985.

Appendix

Including : Experimental Protocols, Techniques and Additional Results Related to Experiments in the Thesis

Experimental protocols and data relating to Chapter 5 : In Vitro Testing of an ^{111}In Labelled Anti-Platelet Glycoprotein Monoclonal Antibody

Coupling of P256 F(ab')$_2$ to DTPA :

Same protocol described in page 50 was used. The results are shown in Table A5.1:

Table A5.1. Elution fractions of P256-F(ab')$_2$-DTPA reaction mixture on the Sephadex G-50 column in PBS. P256 F(ab')$_2$: 5 mg, DTPA : 0.7 mg.

Fraction No	Fraction volume (ml)	OD	Protein content (mg/ml)
BG[a]	--	0.00	0.00
1	2	0.00	0.00[b]
2	2	0.01	0.00[b]
3	2	0.02	0.01
4	2	1.25	0.92[c]
5	2	0.96	0.70[c]
6	2	0.08	0.06[d]
7	2	0.01	0.00[b]
8	2	0.01	0.00[b]
9	2	0.01	0.00[b]

a Background level was set at zero with PBS. This gave 3 reproducible readings of 0.000 before starting to measure the OD of the elution fractions.

b Fractions giving low readings, OD <0.010 (<10μg), were considered to be non-different from background.

c Fractions 4 & 5 were pooled together; OD : 1.06, final McAb concentration : 0.78 mg/ml, total : 3.13 mg, recovery of protein : 65%.

d Fraction 6 was not pooled with fractions 4+5 in order to keep the antibody-DTPA solution as concentrated as possible.

P256 test labelling with ^{111}In :

P256-DTPA : 0.1mg, 124 μl; ^{111}In in citrate buffer : 115MBq (3.11 mCi), 234 μl.

Table A5.2. Elution of the P256-DTPA-^{111}In mixture on the Sephadex G 50 column :

Fraction	Fraction volume (ml)	^{111}In radioactivity (MBq)
1	2.36	0.0
2	2.00	0.0
3	2.00	0.0
4	2.00	5.7[a]
5	2.00	73.8[a]
6	2.00	10.5[a]
7	2.00	0.4
8	2.00	0.6[b]
9	2.00	3.2[b]
10	2.00	9.4[b]

a ^{111}In radioactivity associated with the McAb. Fractions 4, 5 & 6 were pooled together. Specific activity 900 MBq/mg (24.3 mCi/mg).

b Free ^{111}In eluting in late fractions giving a second peak of radioactivity.

Experiment to measure the number of DTPA bound to P256 F(ab')$_2$:

The same experimental protocol to that used for testing DTPA bound to the whole P256 antibody was used. Table A5.3 shows the results of this experiment.

Table A5.3. Elution of ^{111}In+DTPA+P256 F(ab')$_2$-reaction mixture[a] on the Sephadex G-50 column in PBS. Labelling of the test sample (10µl) for calculation of the number of DTPA molecules bound per Ab.

Fraction No	Fraction volume (ml)	Radioactivity (MBq)	Count-rate (cpm-BG[b])
1	2.21	0.0	10[c]
2	2.00	0.0	-6[c]
3	2.00	0.0	14[c]
4	2.00	0.1	827[d]
5	2.00	0.9	5691[d]
6	2.00	0.2	1348[d]
7	2.00	0.0	235
8	2.00	0.4	2159
9	2.00	6.2	38374
10	2.00	11.5	70526
11	2.00	14.0	86130
12	2.00	6.9	42763
13	2.00	2.9	17314
14	2.00	0.6	3571
15	2.00	0.1	408
16	2.00	0.0	95
17	2.00	0.0	57
18	2.00	0.0	34[c]
19	2.00	0.0	21[c]
20	2.00	0.0	9[c]

a Reaction mixture 10 µl; 25 mg/ml P256 F(ab')$_2$, 3.5 mg/ml DTPA, Mol DTPA : Ab; 39 : 1, ^{111}In : 45 MBq (1.1 mCi) in 200 µl.

b Background (BG) was subtracted. Average BG : 150 cpm (n=3, se=7).

c Count-rates corrected for background and falling within 3 standard errors of the calculated difference (99% confidence limits) were considered to be non-significant and were ignored.

d Radioactivity in elution fractions 4, 5 & 6 (first peak) was associated with DTPA-Ab bound. The radioactive count in the following fractions 7-20 (second peak) was associated with free DTPA. The ratios Ab-DTPA/DTPA (MBq) = 1.25/43.8 = 0.03, Ab-DTPA/DTPA (cpm) = 7866/269498 = 0.03. The number of DTPA molecules bound per P256 F(ab')$_2$ molecule = 1.17 DTPA/Ab.

P256 $F(ab')_2$ test labelling with ^{111}In :

P256 $F(ab')_2$-DTPA : 0.1mg, 128 µl; ^{111}In in citrate buffer : 97MBq (2.62 mCi), 195 µl.

Table A5.4. Elution of the P256 $F(ab')_2$-DTPA-^{111}In mixture on the Sephadex G 50 column :

Fraction	Fraction volume (ml)	^{111}In radioactivity (MBq)
1	2.32	0.0
2	2.00	0.0
3	2.00	0.0
4	2.00	4.8[a]
5	2.00	58.1[a]
6	2.00	2.1[a]
7	2.00	0.3
8	2.00	0.4[b]
9	2.00	6.4[b]
10	2.00	14.2[b]

a ^{111}In radioactivity associated with the McAb. Fractions 4, 5 & 6 were pooled together. Specific activity 650 MBq/mg (17.6 mCi/mg).

b Free ^{111}In eluting in late fractions giving a second peak of radioactivity.

^{111}In P256 $F(ab')_2$ immunoreactivity testing.

Table A5.5. Setting of the experiment for measurement of the immunoreactivity of ^{111}In P256 $F(ab')_2$[a] with PRP[b].

Tube No[c]	Ptlt/ml[d]	^{111}In P256 $F(ab')_2$[e] µg/ml	^{111}In P256 $F(ab')_2$/ptlt	Cold P256 $F(ab')_2$[f] µg/ml (tubes C&D)
1 A,B,C,D.	$2X10^8$	0.13	4000	13
2 A,B,C,D.	10^8	0.13	8000	13
3.A,B,C,D.	$5X10^7$	0.13	16000	13
4.A,B,C,D.	$2.5X10^7$	0.13	32000	13
5.A,B,C,D.	$1.25X10^7$	0.13	64000	13
6.A,B,C,D.	$6.25X10^6$	0.13	128000	13

a ^{111}In P256 $F(ab')_2$; 25 µg/ml, 218 MBq/mg (5.9 mCi/mg).

b PRP obtained after centrifugation of whole blood contained $2.8X10^8$ ptlt/ml. Platelet poor plasma (PPP) was obtained by spinning 40 ml of anticoagulated blood at 1500 g for 10 min and was used for diluting PRP.

c Quadruplicate tubes were used for every tube number : 1A, 1B, 1C, 1D, 2A, etc. Two tubes (A&B) were used to measure the extent of binding of ^{111}In P256 $F(ab')_2$ to platelets, the other two (C&D) contained unlabelled P256 $F(ab')_2$ as well (dispensed in the tubes before addition of ^{111}In P256 $F(ab')_2$) and were used to measure the Ab non-specific binding.

d Doubling dilutions of PRP in cell free plasma of the number of platelets in tubes No 1 were dispensed in tubes 2-6. The total volume of the reaction mixture was made up to 1 ml with PPP.

e ^{111}In P256 $F(ab')_2$ was added to all the tubes at 0.13 µg/ml in a volume of 5.2 µl. A reference standard was left for comparison.

f Unlabelled (cold) P256 $F(ab')_2$ was added to tubes C&D of every number group at 13 µg/ml (100 fold excess over ^{111}In P256 $F(ab')_2$) for measuring non-specific binding of ^{111}In P256 $F(ab')_2$.

Table A5.6. ^{111}In P256 F(ab')$_2$ platelet bound and values of ^{111}In P256 F(ab')$_2$ T/B for the calculation of the antibody's immunoreactive fraction.

Tube No	^{111}In P256 F(ab')$_2$ptlt bound[a,b] cpm ± 1 se	Non-specific binding[c] cpm ± 1 se	T/B[d] ± 1 se
1	52600 ± 200	170 ± 300[e]	1.17 ± 0.006
2	50700 ± 210	70 ± 300[e]	1.21 ± 0.006
3	47300 ± 210	230 ± 300[e]	1.30 ± 0.007
4	40500 ± 230	180 ± 300[e]	1.52 ± 0.010
5	33200 ± 240	110 ± 300[e]	1.85 ± 0.015
6	21400±270	250 ± 300[e]	2.87 ± 0.037

a All radioactive counts were corrected for background (BG). Average BG=130 cpm (n=3, se=6).

b Count-rate from ^{111}In P256 F(ab')$_2$ platelet bound was obtained indirectly by counting the 500 µl aliquots of the supernatant in tubes (A&B), correcting the resulting count-rate for BG, taking the average of the two count-rates (A&B) and multipying this average by 2 to get a value for the total unbound count-rate in the supernatant (the volume of the platelet pellet was ignored). Subtraction of unbound count-rate from the count-rate in the reference standard resulted in the count-rate in the pellet (platelet-bound count).

c Same method described in b above was used to obtain cell bound count-rate in the presence of excess unlabelled P256 F(ab')$_2$.

d Reference standard count-rate was obtained by counting an equal amount of ^{111}In P256 F(ab')$_2$ to that added to the test tubes (count was obtained in duplicate). Std 61500, n=2, se=180.

e The values of radioactive count-rates, differences in counts, ratios etc. that did not lie within three standard errors (se) representing 99% confidence limits were considered to be non-significant and were ignored.

Figure A5.1 :

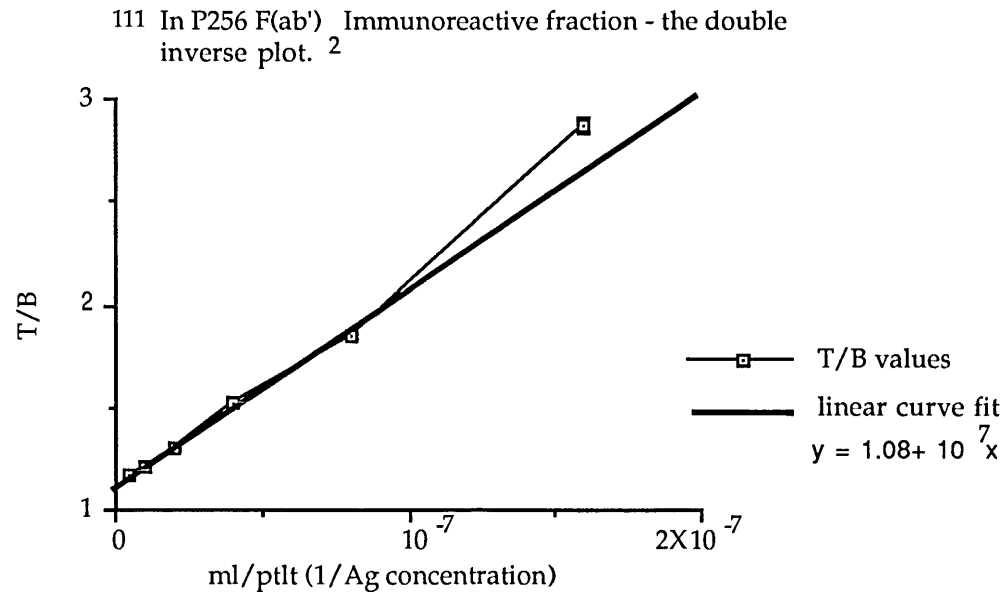

Intercept 1.08, immunoreactive fraction 1/1.08 = 0.924.

Non-specific binding of ^{111}In P256 to platelets in PRP :

Table A5.7: Results of ^{111}In P256[a] vs PRP[b] (I) non-specific binding[c].

Tube	Std ^{111}In P256 added cpm ± 1 se	Bound cpm ± 1 se	B/T ± 1 se
9	84500 ± 290	400 ± 500	0.005 ± 0.006
10	42400 ± 210	170 ±360	0.004 ± 0.008
11	20980 ± 150	130 ± 250	0.006 ± 0.012
12	10600 ± 100	150 ± 180	0.014 ± 0.017
13	5230 ± 70	110 ± 130	0.020 ± 0.024
14	2650 ± 50	60 ± 90	0.023 ± 0.036
15	1400 ± 40	80 ± 70	0.057 ± 0.051
16	710 ±30	30 ±40	0.045 ± 0.051

a ^{111}In P256 : 150 µg/ml, 182 MBq/mg (4.9 mCi/mg).

b PRP : 3.5X10^{8}ptlt/ml.

c Setting is the same as in Table 5.5 except that P256 (unlabelled) was added in X20 excess over ^{111}In P256. All cpm were corrected for background count-rate; BG = 170, n =3, se =7.

Repeat ^{111}In P256 vs PRP radioimmunoassay :

Table A5.8. Setting and results of ^{111}In P256[a] vs PRP[b] (II) radiobinding assay[c].

Tube No[d]	^{111}InP256 conc µg/ml	^{111}In P256 /ptlt	Std cpm ± 1 se	Bound cpm ± 1 se	B/T ± 1 se
1	50	10^6	68400 ± 190	11000 ± 300	0.16 ± 0.004
2	25	5X10^5	34000 ± 130	7500 ± 210	0.22 ± 0.006
3	12.5	2.5X10^5	17100 ± 90	6100 ± 140	0.36 ± 0.009
4	6.25	1.25X10^5	8600 ± 70	4000 ± 100	0.47 ± 0.012
5	3.13	6.25X10^4	4300 ± 50	2800 ± 60	0.65 ± 0.017
6	1.56	3.13X10^4	2200 ± 30	1700 ± 50	0.78 ± 0.024
7	0.78	1.56X10^4	1120 ± 30	920 ± 40	0.82 ± 0.037
8	0.39	7.8X10^3	550 ±20	500 ±30	0.86 ± 0.060

a ^{111}In P256 : 180 µg/ml, 384 MBq/mg (9.4 mCi/mg).

b Stock PRP : 2.7X10^{8}ptlt./ml.

c All cpm were corrected for background count-rate; BG = 150, n =3, se = 7.

d Tubes prepared in duplicate. Each tube contained 2X10^8 ptlt/ml. A separate set containing 2X10^8 ptlt/ml + 20 fold excess of cold P256 over ^{111}In P256 was prepared to measure non-specific binding (see Table A5.9).

Non-specific binding of ^{111}In P256 to platelets in PRP, Repeat experiment:

Table A5.9: Results of ^{111}In P256 vs PRP (II) non-specific binding[a].

Tube	Std ^{111}In P256 added cpm ± 1 se	Bound cpm ± 1 se	B/T ± 1 se
9	68600	270	0.005
	± 260	± 450	± 0.008
10	33700	340	0.010
	± 180	±320	± 0.009
11	17100	240	0.014
	± 130	± 230	± 0.013
12	8700	130	0.014
	± 90	± 160	± 0.018
13	4300	160	0.038
	± 70	± 120	± 0.027
14	2240	110	0.051
	± 50	± 90	± 0.039
15	1190	100	0.084
	± 40	± 70	± 0.056
16	600	80	0.140
	±30	±50	± 0.086

a Same setting as in Table A5.8. Excess of unlabelled P256 (X20) was added to measure non-specific binding of ^{111}In P256. All cpm were corrected for background ; BG = 150, n =3,se =7.

Table 5.10. Setting and results of ^{111}In P256 F(ab')$_2$[a] vs PRP[b] assay.

Tube No[c]	^{111}InP256 conc µg/ml	^{111}In P256 /ptlt	Std cpm[d] ± 1 se	Bound cpm[d] ± 1 se	B/T ± 1 se
1	32	10^6	78600	11800	0.15
			± 200	± 330	0.004
2	16	$5X10^5$	39400	7900	0.20
			± 140	± 230	± 0.006
3	8	$2.5X10^5$	19900	6400	0.32
			± 100	±.150	± 0.008
4	4	$1.25X10^5$	10000	4100	0.41
			± 70	± 110	± 0.011
5	2	$6.25X10^4$	5000	2800	0.56
			± 50	± 70	± 0.015
6	1	$3.13X10^4$	2500	1700	0.67
			± 40	± 50	± 0.022
7	0.5	$1.56X10^4$	1220	900	0.75
			± 30	± 40	± 0.034
8	0.25	$7.8X10^3$	640	500	0.77
			±20	±30	± 0.053

a ^{111}In P256 F(ab')$_2$: 100 µg/ml, 140 MBq/mg (3.8 mCi/mg).

b PRP prepared from ACD-blood by centrifugation contained $3.1X10^8$ptlt/ml.

c Tubes prepared in duplicate. Each tube contained $2X10^8$ ptlt/ml. A separate set containing $2X10^8$ ptlt/ml + 20 fold excess of cold P256 F(ab')$_2$ over ^{111}In P256 F(ab')$_2$ was prepared to measure non-specific binding (see text).

d All count-rates were corrected for background. BG = 140, n = 3, se = 7.

Non-specific binding of ^{111}In P256 F(ab')$_2$ to platelets in PRP:

Table A5.11: Results of ^{111}In P256 F(ab')$_2$ [a]vs PRP[b] (I) non-specific binding[c].

Tube	Std ^{111}In P256 F(ab')$_2$ added cpm ± 1 se	Bound cpm ± 1 se	B/T ± 1 se
9	78600	360	0.005
	± 280	± 490	± 0.007
10	40000	290	0.007
	± 200	±350	± 0.008
11	20000	240	0.012
	± 140	± 240	± 0.012
12	10000	180	0.018
	± 100	± 180	± 0.017
13	5000	150	0.029
	± 70	± 130	± 0.025
14	2500	70	0.029
	± 50	± 90	± 0.036
15	1250	110	0.090
	± 40	± 70	± 0.054
16	670	60	0.088
	±30	±50	± 0.078

a ^{111}In P256 F(ab')$_2$: 100 µg/ml, 140 MBq/mg (3.8 mCi/mg).

b PRP : 3.1X10^{8}ptlt/ml.

c Setting is the same as in Table 5.7 except that P256 F(ab')$_2$ (unlabelled) was added in X20 excess over ^{111}In P256 F(ab')$_2$. All cpm were corrected for background ; BG = 140, n =3, se =7.

Repeat ^{111}In P256 F(ab')$_2$ vs PRP radioimmunoassay :

Table A5.12. Setting and results of ^{111}In P256 F(ab')$_2$ [a]vs PRP[b] (II) radiobinding assay[c].

Tube No[d]	^{111}InP256 F(ab')$_2$ conc µg/ml	^{111}In P256 F(ab')$_2$/ptlt	Std cpm ± 1 se	Bound cpm ± 1 se	B/T ± 1 se
1	50	10^6	92700	13900	0.15
			± 220	± 350	± 0.004
2	25	5X10^5	46500	9800	0.21
			± 150	± 250	± 0.005
3	12.5	2.5X10^5	23200	7000	0.30
			± 110	± 170	± 0.007
4	6.25	1.25X10^5	11700	4900	0.42
			± 80	± 110	± 0.010
5	3.13	6.25X10^4	5900	3400	0.57
			± 60	± 80	± 0.014
6	1.56	3.13X10^4	3000	2100	0.69
			± 40	± 54	± 0.020
7	0.78	1.56X10^4	1500	1130	0.76
			± 30	± 60	± 0.044
8	0.39	7.8X10^3	780	600	0.78
			±20	±30	± 0.047

a ^{111}In P256 F(ab')$_2$: 100 µg/ml, 286 MBq/mg (7.7 mCi/mg).

b Stock PRP : 2.6X10^{8}ptlt/ml.

c All cpm were corrected for background count-rate; BG = 140, n =3, se = 7.

d Tubes prepared in duplicate. Each tube contained 2X10^8 ptlt/ml. A separate set containing 2X10^8 ptlt/ml + 20 fold excess of cold P256 F(ab')$_2$ over ^{111}In P256 F(ab')$_2$ was prepared to measure non-specific binding.

Non-specific binding of ^{111}In P256 F(ab')$_2$ to platelets in PRP Repeat experiment:

Table A5.13: Results of ^{111}In P256 F(ab')$_2$ vs PRP (II) non-specific binding[a].

Tube	Std ^{111}In P256 F(ab')$_2$ added cpm ± 1 se	Bound cpm ± 1 se	B/T ± 1 se
9	92800	590	0.006
	± 300	± 530	± 0.005
10	47200	360	0.008
	± 220	±380	± 0.008
11	23500	430	0.018
	± 150	± 270	± 0.011
12	11800	270	0.023
	± 110	± 190	± 0.016
13	6000	140	0.024
	± 80	± 140	± 0.023
14	3000	90	0.030
	± 60	± 100	± 0.033
15	1500	70	0.045
	± 40	± 70	± 0.048
16	780	60	0.107
	±30	±60	± 0.072

a Same setting as in Table A5.11. Excess of unlabelled P256 F(ab')$_2$ (X20) was added to measure non-specific binding of ^{111}In P256 F(ab')$_2$. All cpm were corrected for background ; BG = 140, n =3, se = 7.

Non-specific binding of ^{111}In P256 to platelets in anticoagulated whole blood:

Table A5.14: Results of ^{111}In P256[a] vs whole blood[b] (I) non-specific binding[c].

Tube	Cpm in 0.5 ml blood ± 1 se	Bound cpm ± 1 se	B/T ± 1 se	Cpm in PRP ± 1 se	PRP/T ± 1 se
9	71300	710	0.010	70600	0.99
	± 270	± 380	± 0.053	± 270	± 0.005
10	35800	250	0.007	38700	1.08
	± 190	±270	± 0.008	± 200	± 0.008
11	18000	230	0.013	17800	0.99
	± 130	± 190	± 0.011	± 130	± 0.011
12	9000	150	0.017	8800	0.98
	± 100	± 130	± 0.015	± 90	± 0.015
13	5000	130	0.026	4800	0.97
	± 70	± 100	± 0.020	± 70	± 0.020
14	2300	90	0.041	2250	0.99
	± 50	± 70	± 0.030	± 50	±0.030
15	1200	80	0.066	1150	0.98
	± 40	± 50	± 0.043	± 40	± 0.043
16	570	60	0.111	560	0.98
	±30	±40	±0.066	±30	± 0.066

a ^{111}In P256 : 300 µg/ml, 302 MBq/mg (8.2 mCi/mg).

b Hct : 0.40, Ptlt. No : 2.85X10^{8}ptlt/ml.

c Setting is the same as in Table 5.9 except that P256 (unlabelled) was added in X20 excess over ^{111}In P256. All cpm were corrected for background ; BG = 110, n =3, se = 6.

Binding of ^{111}In P256 to platelets in anticoagulated whole blood, Repeat experiments:

Table A5.15: Results of ^{111}In P256[a] vs whole blood[b] (II)[c].

Tube	Cpm in 0.5 ml blood ± 1 se	Bound cpm ± 1 se	B/T ± 1 se	Cpm in PRP ± 1 se	PRP/T ± 1 se
1	92400	9200	0.11	79500	0.86
	± 300	± 420	± 0.005	± 280	± 0.004
2	48100	9100	0.19	43800	0.91
	± 220	±300	± 0.006	± 210	± 0.006
3	23900	8100	0.34	19800	0.83
	± 160	± 200	± 0.009	± 140	± 0.008
4	12000	4900	0.41	11500	0.96
	± 110	± 140	± 0.012	± 110	± 0.013
5	5900	3500	0.59	5300	0.90
	± 80	± 90	± 0.018	± 70	± 0.017
6	3140	2100	0.68	2700	0.87
	± 60	± 70	± 0.025	± 50	± 0.023
7	1500	1100	0.73	1270	0.85
	± 40	± 50	± 0.037	± 40	± 0.034
8	780	600	0.76	630	0.81
	±30	±40	±0.055	±30	± 0.048

a ^{111}In P256 : 260 µg/ml, 247 MBq/mg (6.7 mCi/mg).

b Hct : 0.42, Ptlt No : 3.0X10^{8}ptlt/ml.

c Setting is the same as in Table 5.9 except that P256 (unlabelled) was added in X20 excess over ^{111}In P256. All cpm were corrected for background ; BG = 130, n =3, se = 7.

Table A5.16: Results of ^{111}In P256 vs whole blood (II) non-specific binding[a].

Tube	Cpm in 0.5 ml blood ± 1 se	Bound cpm ± 1 se	B/T ± 1 se	Cpm in PRP ± 1 se	PRP/T ± 1 se
9	92500	650	0.007	91600	0.99
	± 300	± 430	± 0.005	± 300	± 0.005
10	47900	480	0.010	46900	0.98
	± 220	±310	± 0.006	± 220	± 0.006
11	24200	250	0.010	23200	0.99
	± 160	± 220	± 0.009	± 160	± 0.009
12	12500	190	0.015	12400	0.99
	± 110	± 160	± 0.013	± 110	± 0.013
13	60	220	0.036	5860	0.97
	± 80	± 110	± 0.018	± 80	± 0.018
14	3000	140	0.048	2930	0.98
	± 60	± 80	± 0.026	± 60	± 0.026
15	1500	80	0.055	1500	0.98
	± 40	± 60	± 0.038	± 40	± 0.038
16	800	40	0.048	780	0.97
	±30	±40	±0.054	±30	±0.054

a Same setting as in Table A5.14 Excess of unlabelled P256 (X20) was added to measure non-specific binding of ^{111}In P256. All cpm were corrected for background ; BG = 130, n =3, se = 7.

Table A5.17: Results of ^{111}In P256[a] vs whole blood[b] (III)[c].

Tube	Cpm in 0.5 ml blood ± 1 se	Bound cpm ± 1 se	B/T ± 1 se	Cpm in PRP ± 1 se	PRP/T ± 1 se
1	101200	11100	0.11	90100	0.89
	± 320	± 440	± 0.004	± 300	± 0.004
2	53200	10600	0.20	49500	0.93
	± 230	±310	± 0.006	± 220	± 0.006
3	26400	9000	0.34	22200	0.84
	± 160	± 210	± 0.008	± 150	± 0.008
4	13500	5419	0.40	12200	0.90
	± 120	± 150	± 0.011	± 110	± 0.011
5	7000	4300	0.61	6050	0.86
	± 80	± 100	± 0.016	± 80	± 0.015
6	3500	2400	0.69	2850	0.82
	± 60	± 70	± 0.023	± 60	± 0.021
7	1700	1270	0.74	1500	0.87
	± 40	± 50	± 0.035	± 40	± 0.033
8	900	700	0.77	820	0.92
	±30	±40	±0.051	±30	± 0.049

a ^{111}In P256 : 280 µg/ml, 276 MBq/mg (7.5 mCi/mg).

b Hct : 0.37, Ptlt No : 2.45X10^{8}ptlt/ml.

c Setting is the same as in Table 5.9 except that P256 (unlabelled) was added in X20 excess over ^{111}In P256. All cpm were corrected for background ; BG = 140, n =3, se = 7.

Table A5.18: Results of ^{111}In P256 vs whole blood (III) non-specific binding[a].

Tube	Cpm in 0.5 ml blood ± 1 se	Bound cpm ± 1 se	B/T ± 1 se	Cpm in PRP ± 1 se	PRP/T ± 1 se
9	99700	520	0.005	103700	1.04
	± 320	± 450	± 0.004	± 320	± 0.005
10	50700	350	0.007	50200	0.99
	± 230	±320	± 0.006	± 220	± 0.006
11	25200	330	0.013	24700	0.98
	± 160	± 220	± 0.009	± 160	± 0.009
12	12900	170	0.013	12800	0.99
	± 110	± 160	± 0.012	± 110	± 0.012
13	6800	130	0.019	6700	0.98
	± 80	± 120	± 0.017	± 80	± 0.017
14	3400	80	0.023	3300	0.98
	± 60	± 80	± 0.025	± 60	± 0.025
15	1700	100	0.063	1600	0.97
	± 40	± 60	± 0.036	± 40	± 0.035
16	870	50	0.060	860	0.99
	±30	±50	±0.052	±30	± 0.052

a Same setting as in Table A5.16 Excess of unlabelled P256 (X20) was added to measure non-specific binding of ^{111}In P256. All cpm were corrected for background ; BG = 140, n =3, se = 7.

Table A5.19. Setting and results of the ^{111}In P256 F(ab')$_2$ [a] vs ACD-blood[b] radiobinding assay[c].

Tube	^{111}In P256 F(ab')$_2$ µg/ml	Ab/ptlt	cpm 500µl WB ± 1 se	cpm cell bound 500 µl WB ± 1 se	B/T ± 1 se
1	50	10^6	86300 ± 300	8600 400	0.10 ± 0.005
2	25	$5X10^5$	43500 ± 210	7000 ± 280	0.16 ± 0.007
3	12.5	$2.5X10^5$	22000 ± 150	6400 200	0.29 ± 0.009
4	6.25	$1.25X10^5$	11300 ± 110	4000 ± 140	0.36 ± 0.013
5	3.13	$6.25X10^4$	5800 ± 80	3100 ± 100	0.53 ± 0.018
6	1.56	$3.13X10^4$	3000 ± 60	1900 ± 70	0.62 ± 0.025
7	0.78	$1.56X10^4$	1500 ± 40	1000 50	0.69 ± 0.037
8	0.38	$7.8X10^3$	800 ±30	600 ±40	0.72 ± 0.054

a ^{111}In P256 F(ab')$_2$: 280 µg/ml, 198 MBq/mg (5.4 mCi/mg).

b Hct = 0.41, Ptlt No = $2.90X10^8$/ml.

c All count-rates were corrected for background. BG = 120, n = 3, se = 6.

Table 5.20. Radioactive counts in PRP and their ratio to ^{111}In P256 F(ab')$_2$ counts in ACD-Whole blood[a].

Tube	cpm 500µl WB ± 1 se	cpm PRP in 500 µl WB ± 1 se	PRP/T ± 1 se
1	86300 ± 300	82800 ± 290	0.96 ± 0.005
2	43500 ± 210	41000 ± 200	0.94 ± 0.006
3	22000 ± 150	20100 ± 140	0.91 ± 0.009
4	11300 ± 110	9800 ± 100	0.87 ± 0.012
5	5800 ± 80	5200 ± 70	0.89 ±0.017
6	3000 ± 60	2800 ± 50	0.92 ± 0.025
7	1500 ± 40	1250 ± 40	0.86 ± 0.035
8	800 ±30	700 ±30	0.90 ± 0.051

a Same experiment as in the previous Table.

Table A5.21: Results of ^{111}In P256 F(ab')$_2$[a] vs whole blood[b] (I) non-specific binding[c].

Tube[d]	Cpm in 0.5 ml blood ± 1 se	Bound cpm ± 1 se	B/T ± 1 se	Cpm in PRP ± 1 se	PRP/T ± 1 se
9	86800	230	0.005	86000	0.99
	± 290	± 420	± 0.009	± 290	± 0.005
10	44200	370	0.008	45900	1.04
	± 210	±300	± 0.007	± 210	± 0.007
11	22500	290	0.013	22000	0.98
	± 150	± 210	± 0.009	± 150	± 0.009
12	11100	200	0.018	11000	0.99
	± 110	± 150	± 0.013	± 110	± 0.013
13	5700	110	0.020	5700	0.99
	± 80	± 110	± 0.019	± 80	± 0.019
14	2800	150	0.052	2700	0.97
	± 50	± 80	± 0.027	± 50	± 0.028
15	1460	110	0.075	1440	0.99
	± 40	± 60	± 0.038	± 40	± 0.039
16	690	80	0.117	680	0.98
	±30	±40	±0.058	±30	± 0.059

a ^{111}In P256 F(ab')$_2$: 280 µg/ml, 198 MBq/mg (5.4 mCi/mg).

b Hct : 0.41, Ptlt No : 2.90X10^{8}ptlt/ml.

c All cpm were corrected for background count-rate; BG = 120, n =3, se = 6.

d Setting was the same as in Table 5.12 except that 20 fold excess of cold P256 F(ab')$_2$ over ^{111}In P256 F(ab')$_2$ was added to measure non-specific binding.

Binding of ^{111}In P256 F(ab')$_2$ to platelets in anticoagulated whole blood, Repeat experiments:

Table A5.22: Results of ^{111}In P256 F(ab')$_2$[a] vs whole blood[b] (II)[c].

Tube	Cpm in 0.5 ml blood ± 1 se	Bound cpm ± 1 se	B/T ± 1 se	Cpm in PRP ± 1 se	PRP/T ± 1 se
1	69600	6300	0.09	65500	0.94
	± 260	± 370	± 0.005	± 260	± 0.005
2	35300	5600	0.16	32100	0.91
	± 190	±260	± 0.007	± 180	± 0.007
3	17600	4900	0.28	15500	0.88
	± 130	± 170	± 0.010	± 130	± 0.010
4	8900	3200	0.36	7670	0.86
	± 100	± 120	± 0.014	± 90	± 0.014
5	4400	2300	0.52	4100	0.92
	± 70	± 80	± 0.020	± 70	± 0.020
6	2300	1400	0.61	1960	0.85
	± 50	± 60	± 0.029	± 50	± 0.027
7	1140	780	0.68	990	0.87
	± 40	± 40	± 0.043	± 30	± 0.041
8	530	370	0.71	440	0.83
	±30	±30	±0.070	±20	± 0.063

a ^{111}In P256 F(ab')$_2$: 240 µg/ml, 215 MBq/mg (5.8 mCi/mg).

b Hct : 0.43, Ptlt No : 3.25X10^{8}ptlt/ml.

c Setting was the same as in Table 5.12. All cpm were corrected for background count-rate; BG = 130, n =3, se = 7.

Table A5.23: Results of ^{111}In P256 F(ab')$_2$ vs whole blood (II) non-specific binding[a].

Tube	Cpm in 0.5 ml blood ± 1 se	Bound cpm ± 1 se	B/T ± 1 se	Cpm in PRP ± 1 se	PRP/T ± 1 se
9	70000	470	0.007	71400	1.02
	± 260	± 370	± 0.005	± 270	± 0.005
10	35900	240	0.007	35600	0.99
	± 190	±270	± 0.007	± 190	± 0.007
11	17700	270	0.015	18600	1.05
	± 130	± 190	± 0.011	± 140	± 0.011
12	8800	140	0.016	8600	0.98
	± 90	± 130	± 0.015	± 90	± 0.015
13	4500	140	0.032	4500	0.99
	± 70	± 100	± 0.021	± 70	± 0.021
14	2240	120	0.052	2200	0.97
	± 50	± 70	± 0.031	± 50	± 0.030
15	1230	100	0.079	1200	0.98
	± 40	± 50	± 0.042	± 40	± 0.043
16	660	70	0.111	650	0.98
	±30	±40	±0.061	±30	± 0.061

a Same setting as in Table A5.19 Excess of unlabelled P256 F(ab')$_2$ (X20) was added to measure non-specific binding of ^{111}In P256 F(ab')$_2$. All cpm were corrected for background ; BG = 130, n =3, se = 7.

Table A5.24: Results of ^{111}In P256 F(ab')$_2$[a] vs whole blood[b] (III)[c].

Tube	Cpm in 0.5 ml blood ± 1 se	Bound cpm ± 1 se	B/T ± 1 se	Cpm in PRP ± 1 se	PRP/T ± 1 se
1	81600	8160	0.10	78400	0.96
	± 290	± 390	± 0.005	± 280	± 0.005
2	41200	7000	0.17	37900	0.92
	± 200	±280	± 0.007	± 200	± 0.007
3	20800	6200	0.30	18500	0.89
	± 140	± 190	± 0.009	± 140	± 0.009
4	10200	3900	0.38	9300	0.91
	± 100	± 130	± 0.013	± 100	± 0.013
5	5620	3000	0.54	4840	0.86
	± 80	± 90	± 0.018	± 70	± 0.017
6	2800	1800	0.64	2430	0.87
	± 50	± 60	± 0.026	± 50	± 0.025
7	1400	1000	0.70	1330	0.93
	± 40	± 50	± 0.038	± 40	± 0.038
8	750	550	0.73	630	0.84
	±30	±40	±0.057	±30	± 0.051

a ^{111}In P256 F(ab')$_2$: 265 µg/ml, 284 MBq/mg (7.7 mCi/mg).

b Hct : 0.38, Ptlt No : 2.75X10^{8}ptlt/ml.

c Setting was the same as in Table 5.12. All cpm were corrected for background count-rate; BG = 140, n =3, se = 7.

Table A5.25: Results of ^{111}In P256 F(ab')$_2$ vs whole blood (III) non-specific binding[a].

Tube	Cpm in 0.5 ml blood ± 1 se	Bound cpm ± 1 se	B/T ± 1 se	Cpm in PRP ± 1 se	PRP/T ± 1 se
9	81200	330	0.004	88500	1.09
	± 290	± 400	± 0.005	± 300	± 0.005
10	41000	360	0.009	40200	0.98
	± 200	±290	± 0.007	± 200	± 0.007
11	20500	280	0.013	21100	1.03
	± 140	± 200	± 0.010	± 150	± 0.010
12	10400	210	0.020	10300	0.99
	± 100	± 140	± 0.014	± 100	± 0.014
13	5500	190	0.034	5400	0.99
	± 80	± 110	± 0.019	± 70	± 0.019
14	2800	140	0.050	2730	0.97
	± 50	± 80	± 0.027	± 50	± 0.027
15	1400	110	0.077	1360	0.98
	± 40	± 60	± 0.040	± 40	± 0.040
16	680	70	0.102	680	0.99
	±30	±40	± 0.060	±30	± 0.060

a Same setting as in Table A5.21 Excess of unlabelled P256 F(ab')$_2$ (X20) was added to measure non-specific binding of ^{111}In P256 F(ab')$_2$. All cpm were corrected for background ; BG = 140, n =3, se = 7.

Effect of P256 F(ab')$_2$ on spontaneous platelet aggregation in PRP

Table A5.26. Platelet counts[a] pre and post P256 F(ab')$_2$ addition to PRP[b].

	Pre P256			Post P256		
Tube No	Single Ptlt[c]	Aggreg[d]	Total[e]	Single Ptlt[c]	Aggreg[d]	Total[e]
1	258	5	263	11	46	57
	± 11	± 1.6	± 11	± 2.4	± 4.8	± 5.3
2	233	8	241	27	31	58
	± 11	± 2	± 11	± 3.7	± 3.9	± 5.4
3	216	12	228	19	54	73
	± 10	± 2.5	± 11	± 3.1	± 5.2	± 6.0
4	224	18	242	68	37	105
	± 11	± 3	± 11	± 5.8	± 4.3	± 7.2
5	246	7	253	82	43	125
	± 11	± 1.9	± 11	± 6.4	± 4.6	± 8
6	238	14	252	157	23	180
	± 11	± 2.7	± 11	± 9	± 3.4	± 9
7	211	22	233	196	17	213
	± 10	± 3.3	± 11	± 10	± 2.9	± 10
8	205	19	224	219	13	232
	±10	±3.0	±11	±10	±2.6	± 11

a Counts done in duplicate using the two chambers of the haemocytometer.
b Stock PRP contained 2.50X10^{8}ptlt/ml.
c Single platelets counted in the 25 large square area of the haemocytometer.
d Aggregates of platelets (two or more platelets together) counted in the same area as c above.
e The total number of particles (single + platelet aggregates) counted in 25 large squares of the haemocytometer.

Table A5.27. Platelet aggregation after the addition of P256 F(ab')$_2$.

Tube No	1	2	3	4	5	6	7	8
PA (%)	96 ± 0.9	88 ± 1.7	91 ± 1.5	70 ± 3.0	67 ± 3.0	34 ± 4.8	7 ± 6.5	-9 ± 7.3

Figure A5.2. Platelet aggregation versus P256 F(ab')$_2$ concentration in PRP.

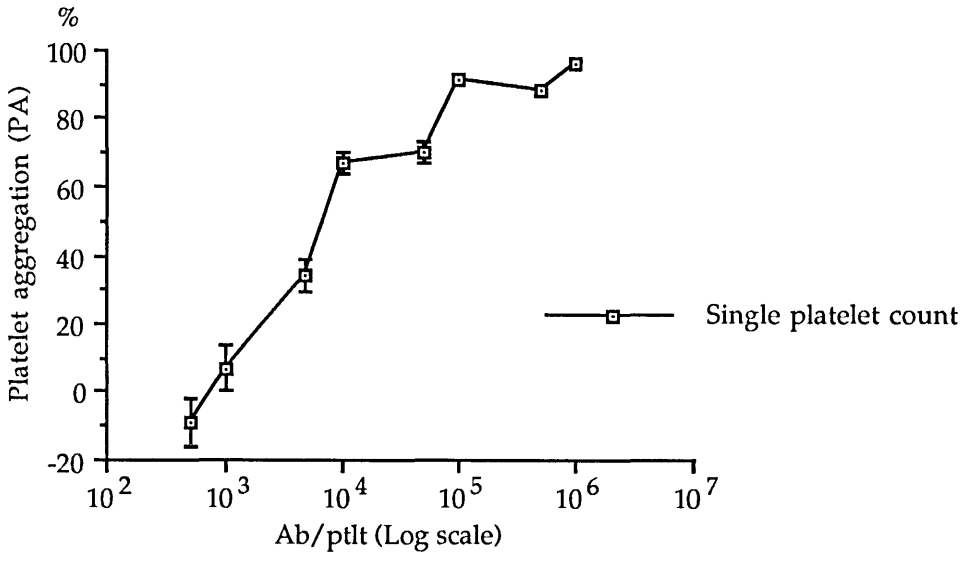

Experimental details of the measurement of spontaneous and induced platelet aggregation in whole blood in the presence of P256 or P256 F(ab')$_2$ using Ultraflo 100

Blood was collected from a healthy male volunteer who had received no medication for at least 2 weeks prior to collection. Blood was anticoagulated with trisodium citrate[1] (1 : 9) to give a final concentration in whole blood of 12.9 mmol/l. An initial platelet count was obtained for the citrated blood. Aliquots of 0.5 ml citrated blood were transferred to polystyrene vials[2] containing aspirin[3] ($2X10^{-3}$ mol/l). The mixture was flushed with a mixture of 5% CO_2 in air, sealed and placed in a water bath[4] for 30 min at 37°C with continuous mixing. Following this incubation period, a 10 µl sample of blood was withdrawn from an aliquot, mixed in a pre-filled diluent pot (Clay Adams), and the platelets counted (control count). For this and all subsequent 10 µl samples, two counts were always performed and the mean count recorded. The tested compound (aggregating agent, Ab, etc) was then added (time 0) to one of the aliquots, the tube regassed with 5% CO_2 in air, resealed and returned to the water bath. At set time points, further 10 µl samples were taken and a platelet count for each sample was performed in the counter after appropriate dilution. Platelet counts obtained at these various times were expressed as a percentage of the control count.

1 BDH, England.
2 Raven Scientific.
3 Aspirin, O-acetylsalicylic acid BDH-England, was dissolved in 100 mmol/l Tris buffer pH 8.5.
4 Grant instruments, England.

P256 diluted in PBS[1] was added to aliquots of citrated blood prepared as above in the following concentrations 800, 1600, 2400, 3200 and 4000 Ab/ptlt[2] (Ab dilutions were prepared after the performance of the initial platelet count). Platelet counts at 10 minutes after addition of the antibody showed a fall in platelet number as shown in Table A5.28.

Table A5.28. Results of P256 on platelet spontaneous aggregation in whole blood.

Ab/ptlt	% fall in ptlt count at 10 min	Range	No of observations
0	1.3	0 - 1.9	4
800	0	--	1
1600	0.4	-1.2 - 2.0	2
2400	4.7	0 - 15.0	5
3200	9.0	4.2 - 17.0	4
4000	74.0	--	1

Another similar test using whole P256 antibody and its F(ab')$_2$ fragment was reported by Stuttle et al (1988). A fall in platelet count was found after the addition of whole P256 Ab. This fall was more pronounced as the concentration of Ab increased (see Table A5.29). In contrast to the effect of the whole antibody on spontaneous aggregation, the F(ab')$_2$ fragment of the antibody did not cause intensive platelet aggregation when similar concentrations to those used with whole antibody were tested. See Table A5.29 for setting and results.

Table A5.29. Effect of P256 and P256 F(ab')$_2$ on spontaneous aggregation in whole blood.

I) P256 whole Ab

Ab/ptlt	% fall in ptlt count					
	5 min	10 min	15 min	20 min	25 min	30 min
350	- 0.74	2.96	5.93	6.67	7.41	ND
	± 1.48	± 2.22	± 2.96	± 1.48	± 0.74	ND
700	4.44	2.96	4.44	8.15	8.89	ND
	± 0.74	± 2.22	± 2.96	± 1.48	± 0.74	ND
1400	8.15	8.89	7.41	17.78	14.81	22.22
	± 4.44	± 5.19	± 2.96	± 4.44	± 5.93	± 8.89
2100	21.48	33.33	37.78	40	43.70	46.67
	± 10.37	± 9.63	± 13.33	± 10.37	± 11.85	± 16.30
3500	37.04	51.11	62.22	68.15	70.37	71.85
	± 5.93	± 8.15	± 7.41	± 6.67	± 5.93	± 7.41

II) P256 F(ab')$_2$

Ab/ptlt	% fall in ptlt count				
	5 min	10 min	15 min	20 min	25 min
350, 700,	1.85	1.67	1.48	3.70	ND
1400 & 2100	± 1.30	± 2.04	± 1.30	± 1.48	ND
3500	10.37	11.85	14.81	22.22	21.48
	±2.22	±2.96	±3.70	±7.41	± 8.89

a ND : not done.

b Average values of % fall in platelet count for the concentrations of F(ab')$_2$ between 350 and 2100 Ab/ptlt were taken due to the minimal effect observed on the platelet count using this concentration range.

1 Flow Labs, England.

2 These values were used as they represented respectively 2, 4, 6, 8 & 10% of the number of GPIIb/IIIa found on the platelet surface (100% = $5X10^4$/ptlt)(See paragraph 6.4.1 and Footnote 1 page 96).

The effect of preincubation of citrated blood with whole P256 antibody or P256 F(ab')$_2$ on induced platelet aggregation by proaggregants such as ADP, collagen and U-46619[1] was recorded in terms of the EC50 of the proaggregant with or without Ab addition[2].

The experiment was repeated in the same way as was done for measurement of spontaneous aggregation except that blood was preincubated with P256 or P256 F(ab')$_2$ 10 min before the addition of the proaggregant (for Ab concentrations see Table 5.30).

Table A5.30. Setting and results of the effect of P256 on induced aggregation in vitro in whole blood.

Donor	Ab/ptlt	U-46619 (µmol/l)		Collagen (µg/ml)		ADP (µmol/l)	
		Control	P256	Control	P256	Control	P256
1	2560	0.36	0.15	0.42	0.80	1.60	1.30
2	3000	0.56	0.35	1.40	0.58	2.90	4.70
3	2720	0.64	0.18	0.62	0.16	0.69	0.64

Another test reported by Stuttle et al (1988), using a single concentration of 1400 Ab/ptlt of P256 whole antibody or P256 F(ab')$_2$ gave EC50 values for the same proaggregants as shown in Table A5.31.

Table A5.31. The effect of P256[a] or P256 F(ab')$_2$[a] on induced aggregation in vitro in whole blood. Values of EC50 for each proaggregant are shown.

	EC50		
Proaggregant	Control	P256	F(ab')$_2$
ADP (µM)	1.6	1.9	2.4
	2.6	2.0	2.6
	1.4	1.8	2.0
Collagen (µg/ml)	0.2	0.2	0.2
	1.6	1.1	1.6
	0.5	0.6	0.6
U-46619 (µM)	0.2	0.2	0.2
	0.5	0.4	0.5
	0.3	0.2	0.5

a A concentration of 1400 Ab/ptlt was used.

1 U-46619 is a stable prostaglandin endoperoxide analog.

2 EC50 is the concentration of the proaggregant that causes 50% of the maximal platelet aggregation observed with this proaggregant.

Experimental protocols and data relating to Chapter 6 : In vivo Use of ^{111}In P256 and ^{111}In P256 F(ab')$_2$ in Man.

Table A6.1. ^{111}In radioactivity in blood and plasma after the injection of ^{111}In P256 in the normal volunteer (JPL).

Sample	Time PI[a] (hr)	whole blood count[b] in 1 ml	plasma count (1 ml)	cell associated count in 1 ml whole blood	RatioB/T[c]
1	0.08	4240 ± 70[d]	890 ± 40	3730 ± 80	0.88 ± 0.02
2	0.67	3220 ± 60	780 ± 40	2780 ± 70	0.86 ± 0.03
3	1.42	2790 ± 60	1020 ± 40	2200 ± 70	0.79 ± 0.03
4	2.75	2060 ± 50	880 ± 40	1560 ± 60	0.76 ± 0.04
5	4.67	1760 ± 50	1000 ± 40	1200 ± 60	0.68 ± 0.04
6	19.42	1130 ± 40	690 ± 40	730 ± 50	0.65 ± 0.08
7	27.50	900 ± 40	670 ± 40	520 ± 50	0.58 ± 0.06
8	45.92	670 ± 40	540 ± 40	360 ± 40	0.54 ± 0.07
9	49.67	600 ±40	280 ±30	280 ±50	0.47 ±0.10

a PI: Post antibody injection.
b All counts were done in 10 minutes, corrected for background (BG=640, n=3, se =10) and for radioactive decay.
c Ratio of cell associated to total added radioactivity. This was calculated by subtraction of the count-rate in the volume of plasma contained in 1 ml whole blood (1-Hct ml) from the count-rate in 1 ml whole blood (Hct : 0.43).
d 1 se.

Table A6.2. ^{111}In radioactivity in blood and plasma after the injection of ^{111}In P256 in patient SH.

Sample	Time PI[a] (hr)	whole blood count[b] in 1 ml	plasma count (1 ml)	cell associated count in 1 ml whole blood	RatioB/T[c]
1	1	24700 ± 160[d]	9100 ± 100	18360 ± 170	0.74 ± 0.01
2	19.5	18900 ± 140	5000 ± 70	15380 ± 150	0.82 ± 0.01
3	43.5	16400 ± 130	6150 ± 80	12150 ± 140	0.74 ± 0.01
4	72.5	10900 ± 110	3800 ± 70	8310 ± 120	0.76 ± 0.01
5	114.75	7200 ± 90	2250 ± 50	5640 ± 90	0.78 ± 0.02
6	166	4300 ±70	1750 ±50	3080 ±80	0.72 ±0.02

a PI: Post antibody injection.
b All counts were done in 5 minutes, corrected for background (BG=340, n=3, se =10) and for radioactive decay.
c Ratio of cell associated to total added radioactivity (Hct : 0.308).
d 1 se.

Figure A6.1. ^{111}In radioactivity in blood versus time after the injection of ^{111}In P256 in patient SH.

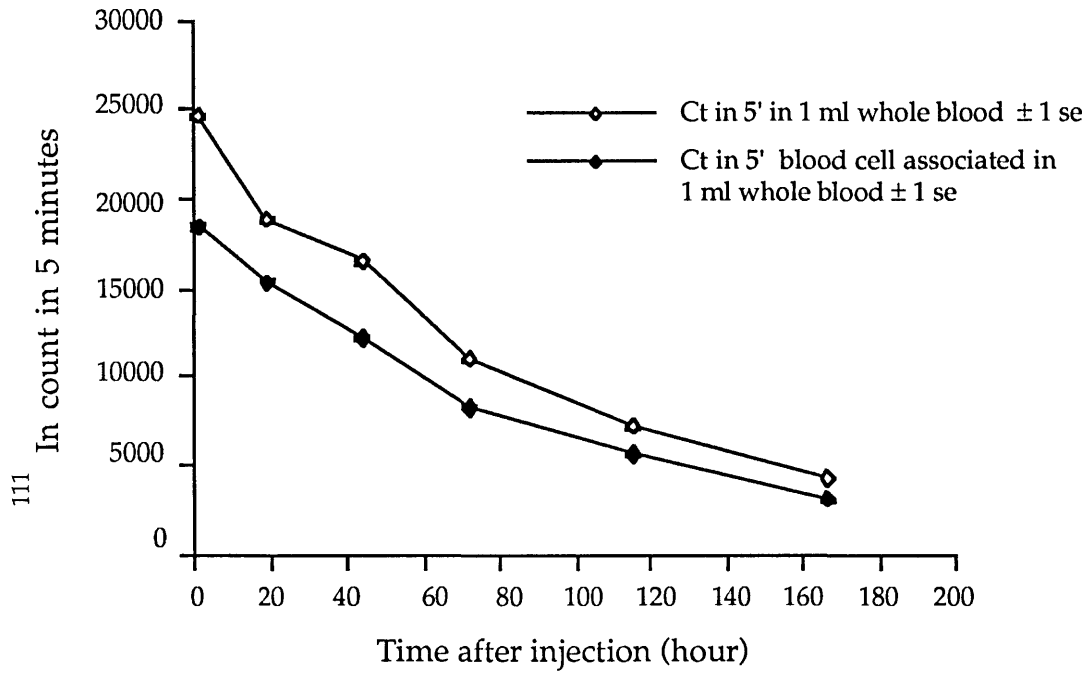

Table A6.3. ^{111}In radioactivity in blood and plasma after the injection of ^{111}In P256 in patient CN.

Sample	Time PI[a] (hr)	whole blood cpm[b] in 1 ml	plasma cpm (1 ml)	cell associated cpm in 1 ml whole blood	RatioB/T[c]
1	0.17	18800	6830	15000	0.79
		± 140[d]	± 80	± 150	± 0.01
2	0.33	15800	6320	12200	0.77
		± 130	± 80	± 130	± 0.01
3	0.50	14600	5720	11300	0.78
		± 120	± 80	± 130	± 0.02
4	19	9000	5200	6060	0.67
		± 100	± 100	± 110	± 0.01
5	46.50	6400	1600	5500	0.86
		± 80	± 40	± 80	± 0.02
6	72	6350	1500	5500	0.87
		± 110	± 60	± 120	± 0.02
7	96	3440	910	2920	0.85
		±90	±50	±90	±0.04

a PI: Post antibody injection.
b All counts were corrected for background (BG=65, n=6, se =3) and for radioactive decay.
c Ratio of cell associated to total added radioactivity (Hct : 0.43).
d 1 se.

Figure A6.2, ^{111}In radioactivity in blood versus time after the injection of ^{111}In in patient CN.

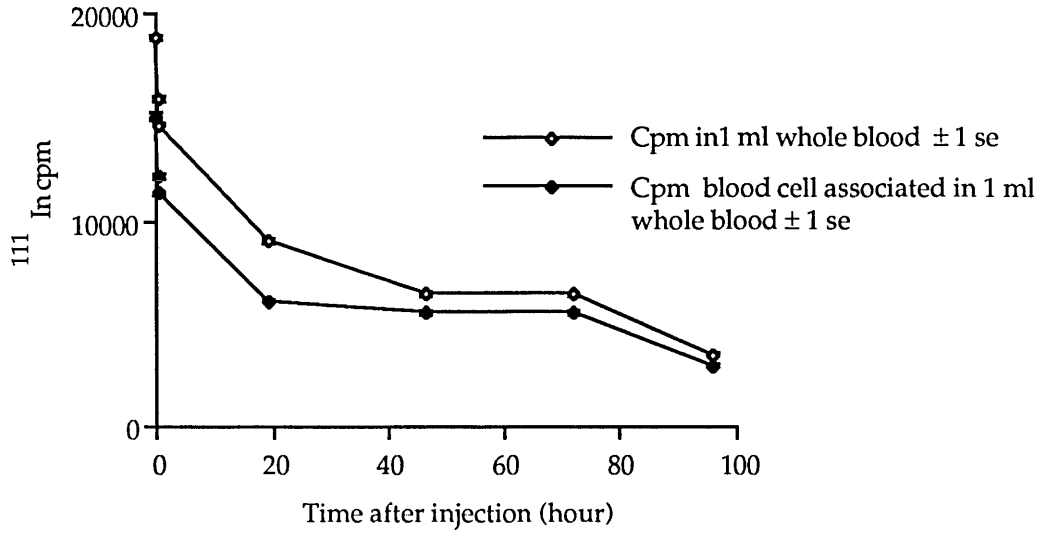

Table A6.4. ^{111}In radioactivity in blood and plasma after the injection of ^{111}In P256F(ab')$_2$ in patient JC.

Sample	Time PI[a] (hr)	whole blood cpm[b] in 1 ml	plasma cpm (1 ml)	cell associated cpm in 1 ml whole blood	RatioB/T[c]
1	0.08	15600 ± 130[d]	6000 ± 80	11800 ± 130	0.75 ± 0.010
2	0.25	14100 ± 120	5700 ± 80	10500 ± 130	0.74 ± 0.011
3	0.50	12900 ± 110	5380 ± 70	9500 ± 120	0.74 ± 0.012
4	21.5	8200 ± 90	2750 ± 50	6480 ± 100	0.79 ± 0.015
5	50	5560 ± 80	1950 ± 40	4320 ± 80	0.78 ± 0.018
6	120	2800 ± 50	970 ± 30	2190 ± 60	0.78 ± 0.025
7	144	2370 ± 50	1150 ± 30	1640 ± 50	0.69 ± 0.027
8	170	1930 ±40	820 ±30	1400 ±50	0.73 ±0.030

a PI: Post antibody injection.
b All counts were corrected for background (BG=64, n=6, se =3) and for radioactive decay.
c Ratio of cell associated to total added radioactivity (Hct : 0.364).
d 1 se.

Table A6.5. ^{111}In radioactivity in blood and plasma after the injection of ^{111}In P256F(ab')$_2$ in patient AM.

Sample	Time PI[a] (hr)	whole blood count[b] in 1 ml	plasma count (1 ml)	cell associated count in 1 ml whole blood	RatioB/T[c]
1	0.50	101900 ± 320[d]	75000 ± 280	56900 ± 360	0.56 ± 0.004
2	0.25	51100 ± 230	26500 ± 170	35200 ± 250	0.69 ± 0.006
3		25100 ± 160	9700 ± 100	19300 ± 170	0.77 ± 0.009
4	21.5	14800 ± 130	5750 ± 80	11000 ± 140	0.74 ± 0.011
5	50	11400 ±110	4880 ±80	8500 ±120	0.74 ± 0.013

a PI: Post antibody injection.
b All counts were done in 10 minutes, corrected for background (BG=740, n=3, se =16) and for radioactive decay.
c Ratio of cell associated to total added radioactivity (Hct : 0.40).
d 1 se.

Figure A6.3. ^{111}In radioactivity in blood versus time after the injection of ^{111}In P256F(ab')$_2$ in patient AM.

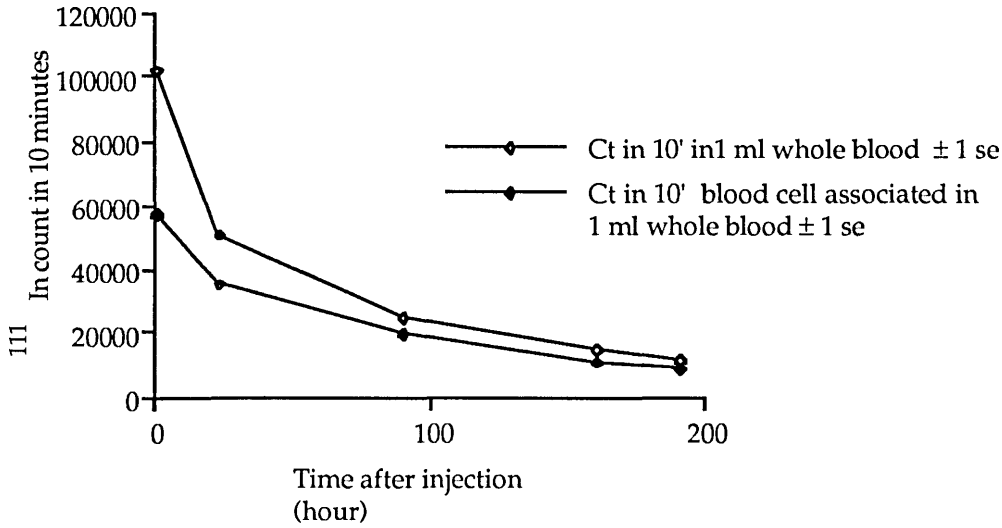

Figure A6.4. Kinetics of ^{111}In P256 F(ab')$_2$ uptake in the blood pool (heart), spleen and liver from 1-30 minutes after iv injection in patient WM. A dynamic study using the scintillation camera.

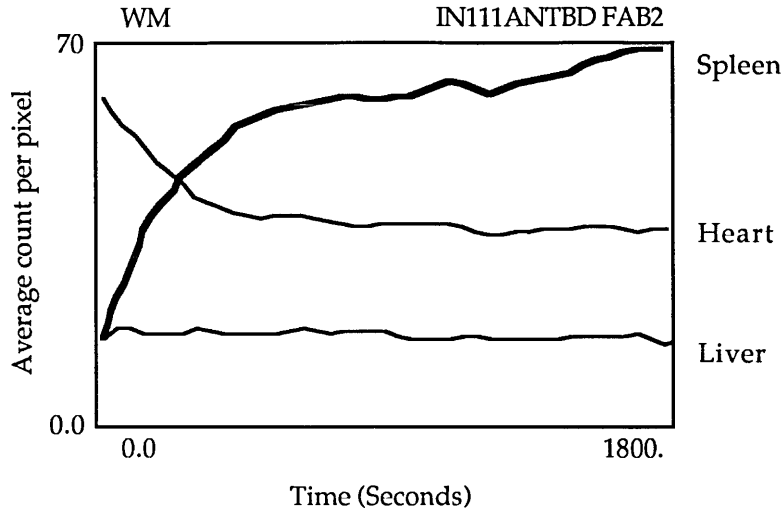

Table A6.6. Platelet count before and after[a] injection of ^{111}In P256 or ^{111}In P256 F(ab')$_2$. Test of significance using the paired t-test[b].

Patient	Pre ptlt ct (X10^9)	Post ptlt ct (X10^9)	Difference (X10^9)
I. ^{111}In P256			
1. JPL	247	234	-13
2. JW	167	165	-2
3. GM	233	241	7
4. AS	260	256	-4
5. SH	323	317	-6
6. VH	381	372	-9
7. HQ	243	248	5
8. DS	220	224	4
9. CN	135	129	-6
10. CC	277	271	-6
II. ^{111}In P256 F(ab')$_2$			
11. AM	196	202	6
12. ML	270	265	-5
13. EK	244	246	2
14. JC	226	215	-11
15. MD	263	258	-5
16. DA	186	182	-4
17. WM	230	227	-3
18. RW	319	310	-9

a Values are for samples collected at 24 hr after antibody injection.

b Difference after injection of P256 : $t = \frac{-3}{1.94} = 2.04$, degrees of freedom =9, $p<0.1$ non-significant.

Difference after injection of P256 F(ab')$_2$: $t = \frac{-3.625}{1.945} = 1.86$, degrees of freedom =7, $p<0.2$ non-significant.

Experimental protocols and data relating to Chapter 8 : In Vitro Tests and in Vivo Use of an ^{111}In Anti-T Lymphocyte Monoclonal Antibody in the Rat.

Sodium dodecyl sulphate polyacrylamide gel electrophoresis (SDS-PAGE) of MRC OX-19 ascites fluid :

Slab gel discontinuous electrophoresis according to the method of Laemmli (1970) was applied. The equipment used was the minigel slab electrophoresis cell (Mighty Small II, Hofer, San Francisco, USA) linked to a constant-current-power supply. The resolving gel (10% acrylamide) was cast in place and left to polymerise for 30 min. The stacking gel was added afterwards and the comb (0.5 cm-wide wells) was placed on the top of the stacking gel and left for 10-20 min to allow polymerisation. Afterwards, the comb was removed and the ascites fluid diluted 1/100 in the sample buffer (see below) was added to one well and a sample of mouse IgG_1 (Sigma, England) was loaded in another well using a Hamilton syringe. Finally, the cell was filled with the electrophoretic buffer (see below) and the electric current was started at 10 mA (50 V) then the current was increased to 20 mA (100 V). At the end of the run (about 1 hr), the gel was stained in 0.1% Coomassie blue and then destained in water-ethanol-acetic acid mixture (5:4:1). The gel was dried on a sheet of filter paper in a gel drier (Biorad) and was cut and photographed for analysis.
Electrophoresis buffer : 0.025 M Tris (3.03 g/l), 0.192 M glycin (14.42 g/l), 0.1% SDS (1 g/l), adjust to pH 8.3.
Sample buffer : 0.5 ml 10% SDS, 0.5 ml glycerol, 0.4 ml 1 M Tris pH 6.8, 3.1 ml H_2O, 500 µl Bromophenol blue.

Immunofluorescence results of the assay for the presence of MRC OX-19 McAb in FPLC elution fractions of the ascites fluid

Twenty-six LP3 tubes containing $2X10^6$ lymph node cells from a Wistar rat in each were prepared for testing 10 elution fractions of FPLC, a blank negative control of PBS (BG), a negative control of H17E2 McAb abd a positive control of MRC OX-19 ascites fluid. The first-layer reagents were used at 1:5 and 1:10 dilutions in PBS. The second layer was rabbit anti-mouse Ig $F(ab')_2$ FITC conjugate 1/120 dilution (QB.AR 9, Serotec, England).

Results of the immunofluorescence test :

	1 : 5 dilution	1 : 10 dilution
BG	-ve	-ve
H17E2	-ve	-ve
MRC OX-19	Strong +ve	Strong +ve
Fraction 1	-ve	-ve
2	-ve	-ve
3	-ve	-ve
4	Weak +ve	Weak +ve
5	Strong +ve	Strong +ve
6	Weak +ve	Weak +ve
7	-ve	-ve
8	-ve	-ve
9	-ve	-ve
10	-ve	-ve

The fraction No 5 was taken and its protein content was measured using light absorption at 280 nm; OD : 0.47, protein content : 0.35 mg/ml, total volume : 6 ml, Antibody content : 2 mg.

Testing of the positive FPLC elution fraction No 5 using the FACS (EPICS)

Sample	%fluorescence	Peak channel
BG (PBS)	0.33	--
-ve (H17E2)	0.77	--
+ve (MRC OX-19)	68.49	397
Fraction No 5	65.68	382

Coupling of MRC OX-19 to DTPA

Same protocol as that described in page 50 was used. The results are shown in Table A8.1.

Table A8.1. Elution fractions of MRC OX-19+DTPA reaction mixture on the Sephadex G-50 column in PBS. MRC OX-19 : 2 mg, DTPA : 0.24 mg.

Fraction No	Fraction volume (ml)	OD	Protein content (mg/ml)
BG[a]	--	0.00	0.00
1	2	0.00	0.00[b]
2	2	0.00	0.00[b]
3	2	0.00	0.00[b]
4	2	0.12	0.09[c]
5	2	0.46	0.34[d]
6	2	0.24	0.18[d]
7	2	0.00	0.00[b]
8	2	0.00	0.00[b]
9	2	0.00	0.00[b]
10	2	0.00	0.00[b]

a Background level was set at zero with PBS. This gave 3 reproducible readings of 0.000 before starting to measure the OD of the elution fractions.

b Fractions giving low readings, OD <0.010 (<10μg), were considered to be non-different from background.

c Fractions 5 & 6 were pooled together; OD : 0.34, final McAb concentration : 0.25 mg/ml, total : 1 mg, recovery of protein : 50%

d Fraction 4 was not pooled with fractions 5+6 in order to keep the antibody-DTPA solution as concentrated as possible.

Experiment to measure the number of DTPA bound to MRC OX-19:

The same experimental protocol described in page 52 was used. Table A8.2 shows the results of this experiment.

Table A8.2. Elution of ^{111}In+DTPA+MRC OX-19-reaction mixture[a] on the Sephadex G-50 column in PBS. Labelling of the test sample (10µl) for calculation of the number of DTPA molecules bound per Ab.

Fraction No	Fraction volume (ml)	Radioactivity (MBq)	Count-rate (cpm-BG[b])
1	2.21	0.0	1[c]
2	2.00	0.0	12[c]
3	2.00	0.0	21[c]
4	2.00	0.1	1013[d]
5	2.00	0.3	2082[d]
6	2.00	0.1	537[d]
7	2.00	0.0	318
8	2.00	0.6	4440
9	2.00	4.8	38102
10	2.00	9.9	76034
11	2.00	5.1	40189
12	2.00	1.2	9487
13	2.00	0.2	1706
14	2.00	0.1	529
15	2.00	0.0	173
16	2.00	0.0	64
17	2.00	0.0	36[c]
18	2.00	0.0	23[c]
19	2.00	0.0	22[c]
20	2.00	0.0	19[c]

a Reaction mixture 10 µl; 10 mg/ml MRC OX-19, 1.2 mg/ml DTPA, Mol DTPA : Ab; 40 : 1, ^{111}In : 25 MBq (0.7 mCi) in 200 µl.

b Background (BG) was subtracted. Average BG : 140 cpm (n=3, se=7).

c Count-rates corrected for background and falling within 3 standard errors of the calculated difference (99% confidence limits) were considered to be non-significant and were ignored.

d Radioactivity in elution fractions 4,5 & 6 (first peak) was associated with DTPA-Ab bound. The radioactive count in the following fractions 7-20 (second peak) was associated with free DTPA. The ratios Ab-DTPA/DTPA (MBq) = 0.5/22.4 = 0.02. Ab-DTPA/DTPA (cpm) = 3950/174674 = 0.02. The number of DTPA molecules bound per MRC OX-19 molecule = 0.9 DTPA/Ab.

MRC OX-19 test labelling with ^{111}In :
MRC OX-19-DTPA : 50 µg, 200 µl; ^{111}In in citrate buffer : 85MBq (2.3 mCi), 225 µl.
Table A8.3. Elution of the MRC OX-19-DTPA-^{111}In mixture on the Sephadex G 50 column :

Fraction	Fraction volume (ml)	^{111}In radioactivity (MBq)
1	2.43	0.0
2	2.00	0.0
3	2.00	0.0
4	2.00	0.4[a]
5	2.00	22.9[a]
6	2.00	9.0[a]
7	2.00	0.4
8	2.00	0.2
9	2.00	1.0[b]
10	2.00	5.5[b]

a ^{111}In radioactivity associated with the McAb. Fractions 5 & 6 were pooled together. Specific activity 656 MBq/mg (17.7 mCi/mg).
b Free ^{111}In eluting in late fractions giving a second peak of radioactivity.

H17E2 test labelling with ^{111}In :
H17E2-DTPA : 100 µg, 50 µl; ^{111}In in citrate buffer : 50MBq (1.4 mCi), 150 µl.
Table A8.4. Elution of the H17E2-DTPA-^{111}In mixture on the Sephadex G 50 column :

Fraction	Fraction volume (ml)	^{111}In radioactivity (MBq)
1	2.20	0.0
2	2.00	0.0
3	2.00	0.0
4	2.00	0.6[a]
5	2.00	13.8[a]
6	2.00	10.2[a]
7	2.00	0.5[a]
8	2.00	0.1
9	2.00	1.4[b]
10	2.00	6.9[b]

a ^{111}In radioactivity associated with the McAb. Fractions 5 & 6 were pooled together. Specific activity 251 MBq/mg (6.8 mCi/mg).
b Free ^{111}In eluting in late fractions giving a second peak of radioactivity.

^{111}In MRC OX-19 immunoreactivity testing
Thoracic duct lymphocytes were collected overnight from a cannulated Wistar rat[1] in a sterile flask containing 200 iu of heparin[2]. The lymph was centrifuged at 150 g for 7 minutes and the cells were washed once with Tris balanced salt solution (Favour 1964) containing 1% bovine serum albumin[3] (BSA), pH 7.45. The cells were then resuspended in buffer and their number was counted using a haemocytometer[4]. ^{111}In MRC OX-19 was added at 10 ng/ml to a set of seven LP3[5] tubes containing suspensions of TDLs dispensed in doubling dilutions starting with 2.5X10^7 cells/ml in Tris buffer (total volume per tube 1 ml) (see Table A8.5 for the experimental setting). The antibody was left to incubate with the cells for 2 hr at 37°C in a

1 See thoracic duct cannulation page 318.
2 Pularin, heparin sodium injection BP (mucous), 1000 iu/ml, containing no bactericide, Duncan Flockhard, England.
3 Sigma, England.
4 Improved Neubauer, Gallenkamp, England.
5 Luckham, England.

water bath[1]. Thereafter, cell bound radioactivity was measured having washed the cells twice in the same buffer. An identical group of tubes was set with excess unlabelled antibody to measure non-specific binding, which was subtracted from the values obtained above. The data obtained (see Table A8.5) was plotted as the inverse relative cell-bound radioactivity versus the inverse cell concentration and extrapolated to intercept the y-axis at a point representing the inverse of the immunoreactive fraction (see Figure A8.1).

Table A8.5. Setting and results of the assay for measuring ^{111}In MRC OX-19[a] immunoreactivity with rat thoracic duct lymphocytes.

Tube No	TDL/ml	Cpm bound[b]	Non-specific cpm	Specific bound cpm	Ratio T/B
1	$2.5X10^7$	5400±40	290±10	5110±40	2.27±0.03
2	$1.25X10^7$	4900±40	240±10	4660±40	2.49±0.03
3	$6.25X10^6$	3800±40	180±10	3660±40	3.17±0.04
4	$3.13X10^6$	3200±30	150±10	3060±30	3.80±0.06
5	$1.56X10^6$	1800±25	100±10	1710±25	6.81±0.12
6	$7.8X10^5$	1300±20	80±10	1220±20	9.56±0.20
7	$3.9X10^5$	900±20	120±10	770±20	15.12±0.42

a ^{111}In MRC OX-19 : 382 MBq/mg (10 mCi/mg) was added at 10 ng/ml giving a total count-rate of 11700±100 cpm.

b Count-rates corrected for background, BG = 130, n =3, se = 7.

Figure A8.1. ^{111}In MRC OX-19 immunoreactive fraction, the double inverse plot.

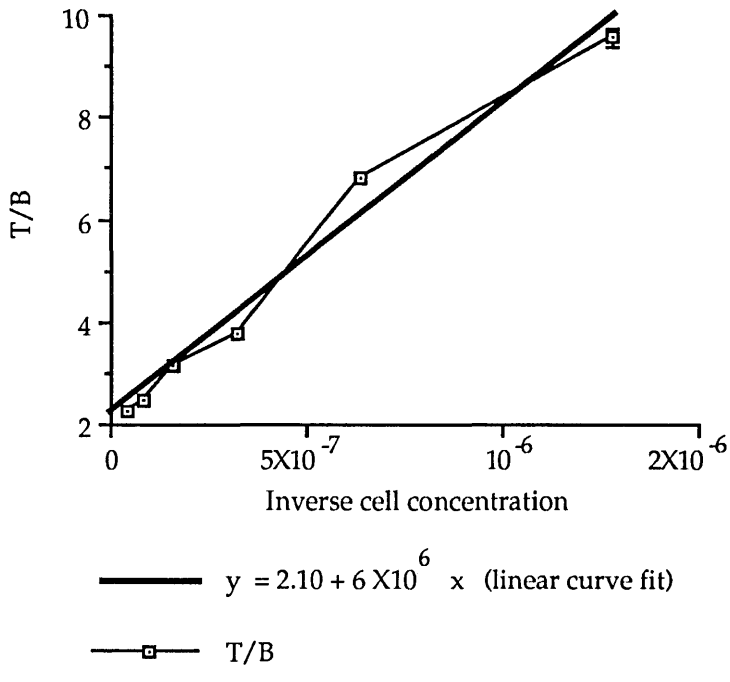

Intercept = 2.10, the immunoreactive fraction ≈ 50%.

Thoracic duct cannulation in the rat

A rat was anesthetised using ether or by intraperitoneal injection of an anaesthetic mixture[2] and the animal was fixed to a dissecting board on its back. A left infracostal incision was

1 Grant, England.

2 Hypnorm (fentanyl citrate and fluanisone), Janssen, Denmark, 1 part, Hypnovel (midazolam hydrochloride) Roche 1 part, and water for injection BP 2 parts. The mixture was given at 2.5 ml/kg body weight IP. Narcan (naloxone hydrochloride), Dupont was given as antidote at 400 µg/kg in case of overdosage of the anaesthetic.

made and the thoracic duct was exposed after gentle displacement of the left kidney into the right flank. A plastic cannula[1] was inserted into the thoracic duct in its abdominal section just above the point of emergence of the renal artery from the aorta. The cannula was passed outside the abdomen through the skin of the left flank and the animal was closed-up and left restrained in a Bollman cage. During lymph collection the rat was given an intravenous infusion of phosphate buffered saline with added calcium and magnesium and containing 1 unit/ml of heparin (DAB-1 solution) through a lateral tail vein.

Tissue sampling and the preparation of cell suspensions, Group A

Blood was taken from the inferior vena cava under terminal anaesthesia into a 10 ml syringe containing heparin. Afterwards, the cervical lymph nodes and the spleen were dissected and removed. One quarter of the spleen and one or two lymph nodes were snap frozen in a hexane-liquid N_2 bath for preparation of frozen tissue sections. Touch imprints of spleen and lymph nodes were prepared on microscope slides as well as several blood smears. The rest of the spleen was cut into small pieces with surgical scissors and the resulting bits were then forced through a fine nylon mesh using a plastic pestle (syringe plunger) to obtain a suspension of spleen cells. The lymph nodes were teased and a suspension of lymph node cells was obtained. The spleen cell suspension and the blood (diluted 1 : 1 in saline) in 6 ml volumes were centrifuged on density gradients made up of a mixture of Histopaque[2] 1119 and 1083 at a ratio of 1 : 2 in 15 ml centrifuge tubes[3] to separate the mononuclear cells in each preparation from the granulocytes and the red blood cells. The resulting mononuclear cells (MNC) from blood or spleen were washed once (150 g for 7 minutes) in Hank's balanced salt solution containing 1% BSA pH 7.4 and the cells were resuspended in buffer and counted using a haemocytometer.

Cytospin preparation for APAAP staining

The cells were resuspended at $5X10^5$ cells/ml and 2 drops from a Pasteur pipette filled with the cell suspension in question were loaded in the bucket of the cytospin centrifuge[4]. The cytospins were obtained after spinning the bucket-slide assembly for 1 minute at 150 g (1000 rpm). Five slides were prepared for each cell suspension and every slide was checked under the microscope for its suitability for staining. The slides were left to dry for 4-5 hours, then they were fixed with acetone for 10 minutes at 4 °C.

Figure A8.2. The thyroid phantom 3602 used for testing the scintillation camera system.

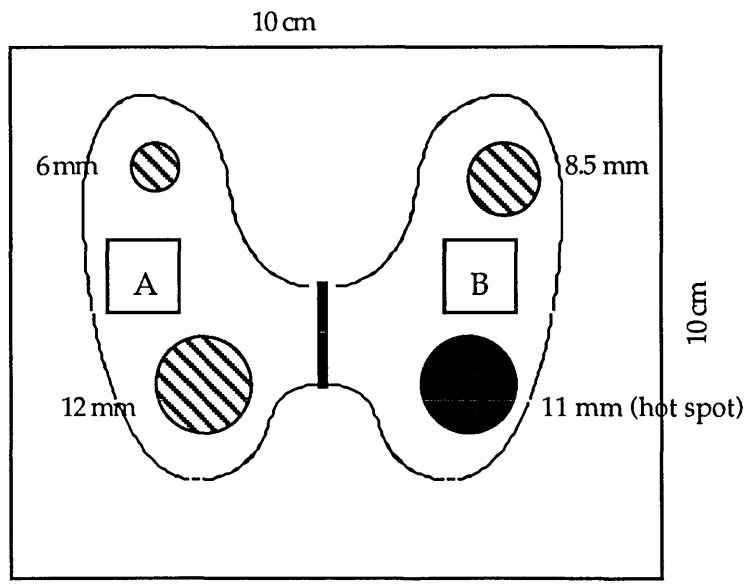

1 Tubing pp50, Portland Plastic Ltd, England.
2 Sigma, England.
3 Falcon, USA.
4 Shandon, England.

Table A8.5. Radioactive counts and ratios of counts[a] in different parts of the phantom versus collimator distance from it (see Figure A8.2 above).

Distance	Whole image	Hot spot	Region A	Region B
5cm	239260 (1.00)	11197 (0.05)	12865 (0.05)	9258 (0.04)
7cm	183299 (1.00)	9991 (0.05)	12666 (0.07)	9013 (0.05)
10cm	108797 (1.00)	4382 (0.04)	6417 (0.04)	3620 (0.02)
13cm	70959 (1.00)	3320 (0.05)	5582 (0.08)	3132 (0.04)

a The ratio of the count in the region studied to the count in the whole phantom is give in brackets.

Table A8.6. Distribution of radioactivity after injection of ^{111}In MRC OX-19, ^{111}In tropolone labelled lymph nodes cells or ^{111}In H17E2 in intact rats.

		%ID/ml		%ID/g			
Expt	Rat	WB	Pl	CLN	Spl	Liver	Muscle
C1	C1a	1.25	1.82	4.11	12.96	1.14	0.04
		±0.006	±0.01	±0.02	±0.04	±0.01	±0.001
	C1b	0.27	0.44	6.89	13.32	1.63	0.08
		±0.002	±0.008	±0.03	±0.04	±0.006	±0.002
	C1c	0.42	0.22	7.43	69.83	1.40	0.03
		±0.006	±0.01	±0.09	±0.56	±0.01	±0.004
	C1d	0.23	0.17	37.60	63.75	2.18	0.06
		±0.004	±0.02	±0.02	±0.52	±0.02	±0.006
C2	C2a	3.44	4.49	0.42	0.73	1.69	0.07
		±0.007	±0.01	±0.003	±0.002	±0.004	±0.0003
	C2b	0.39	0.45	0.26	0.51	4.87	0.03
		±0.0007	±0.0009	±0.001	±0.001	±0.008	±0.0003

Table A8.7. Whole body dosimetry of an ^{111}In anti-T cell McAb in man based on data using ^{111}In MRC OX-19 in the rat.

	Rat			Man			
Organ	%ID/g	Organ Wt (g)	%uptake	Uptake for 100 MBq administered (MBq)	mGy/MBq	Weighting factor	mSv/ MBq
LN	8	0.02	0.16	0.16	0.002	-.-	0.002
Spleen	13	0.6	8	8	24.3	0.006	11.7
Lung	0.75	0.9	0.7	0.7	4.3	0.12	0.4
Liver	1.8	7.2	13	13	4.2	0.06	3.3
Kidney	2	1.6	3	3	-.-	-.-	-.-
Bone	0.5	30	15	15	-.-	-.-	-.-
BM	0.07	6	0.4	0.4	3.3	-.-	0.2
Muscle	0.03	88	3	3	-.-	-.-	-.-
Blood	0.4	13	5	5	-.-	-.-	-.-
Bone surface[a]				0.4[b]	12	0.09	0.1
Breast[a]					0.8	0.15	0.6
Thyroid[a]					0.7	0.03	0.1
Gonads[a]					0.5	0.25	0.15
							20 mSv/ 100 MBq[c]

a Other organs of interest (irradiated by other organs).
b In the bone marrow.
c Total effective dose equivalent = 0.2 mSv/MBq.

Experimental protocols and data relating to Chapter 9 : Radiolabelling of Human T or B Lymphocytes with ^{111}In Monoclonal Antibodies. In Vitro Tests and Action Plan for Use in Vivo.

Coupling of UCHT2 (Pan T) to DTPA

Same protocol as that described in page 50 was used. The results are shown in Table A9.1.

Table A9.1. Elution fractions of UCHT2+DTPA reaction mixture on the Sephadex G-50 column in PBS. UCHT2 : 12 mg, DTPA : 1.2 mg.

Fraction No	Fraction volume (ml)	OD	Protein content (mg/ml)
BG[a]	--	0.00	0.00
1	2	0.00	0.00[b]
2	2	0.00	0.00[b]
3	2	0.00	0.00[b]
4	2	0.02	0.01[b]
5	2	O.R[c]	>2[d]
6	2	1.08	0.79[d]
7	2	0.15	0.11[d]
8	2	0.02	0.01[b]
9	2	0.01	0.00[b]
10	2	0.00	0.00[b]

a Background level was set at zero with PBS. This gave 3 reproducible readings of 0.000 before starting to measure the OD of the elution fractions.

b Fractions giving low readings, OD <0.010 (<10μg), were considered to be non-different from background.

c OR : Overreading (>2.00).

d Fractions 5, 6 & 7 were pooled together; OD : 1.09, final McAb concentration : 0.80 mg/ml, total : 4.81 mg, recovery of protein : 40%

Experiment to measure the number of DTPA bound to UCHT2:

The same experimental protocol described in page 52 was used. Table A9.2 shows the results of this experiment.

Table A9.2. Elution of ^{111}In+DTPA+UCHT2-reaction mixture[a] on the Sephadex G-50 column in PBS. Labelling of the test sample (10µl) for calculation of the number of DTPA molecules bound per Ab.

Fraction No	Fraction volume (ml)	Radioactivity (MBq)	Count-rate (cpm-BG[b])
1	2.09	0.0	-9[c]
2	2.00	0.0	21
3	2.00	0.0	25
4	2.00	0.1	112[d]
5	2.00	0.5	503[d]
6	2.00	0.2	158[d]
7	2.00	0.3	296
8	2.00	0.4	411
9	2.00	2.1	934
10	2.00	4.9	4856
11	2.00	10.5	9471
12	2.00	2.8	2690
13	2.00	0.6	604
14	2.00	0.2	176
15	2.00	0.1	82
16	2.00	0.0	51
17	2.00	0.0	53
18	2.00	0.0	45
19	2.00	0.0	10[c]
20	2.00	0.0	2[c]

a Reaction mixture 10 µl; 60 mg/ml UCHT2, 6 mg/ml DTPA, Mol DTPA : Ab; 40 : 1, ^{111}In : 25 MBq (0.7 mCi) in 75 µl.

b Background (BG) was subtracted. Average BG : 152 cpm (n=3, se=5).

c Count-rates corrected for background and falling within 3 standard errors of the calculated difference (99% confidence limits) were considered to be non-significant and were ignored.

d Radioactivity in elution fractions 4,5 & 6 (first peak) was associated with DTPA-Ab bound. The radioactive count in the following fractions 7-20 (second peak) was associated with free DTPA. The ratios Ab-DTPA/DTPA (MBq) = 0.8/22.7 = 0.04. Ab-DTPA/DTPA (cpm) = 819/20493 = 0.04. The number of DTPA molecules bound per UCHT2 molecule = 1.60 DTPA/Ab.

UCHT2 test labelling with ^{111}In :

UCHT2-DTPA : 0.1 mg, 125 µl; ^{111}In in citrate buffer : 75MBq (2 mCi), 300 µl.

Table A9.3. Elution of the UCHT2-DTPA-^{111}In mixture on the Sephadex G 50 column :

Fraction	Fraction volume (ml)	^{111}In radioactivity (MBq)
1	2.43	0.0
2	2.00	0.0
3	2.00	0.0
4	2.00	18.3[a]
5	2.00	18.7[a]
6	2.00	0.6[a]
7	2.00	0.1
8	2.00	0.2[b]
9	2.00	0.5[b]
10	2.00	0.9[b]

a ^{111}In radioactivity associated with the McAb. Fractions 4 & 5 were pooled together. Specific activity 376 MBq/mg (10 mCi/mg).

b Free ^{111}In eluting in late fractions giving a second peak of radioactivity.

Coupling of WR-17 (Pan B) to DTPA

Same protocol as that described in page 50 was used. The results are shown in Table A9.4.

Table A9.4. Elution fractions of WR-17+DTPA reaction mixture on the Sephadex G-50 column in PBS. WR-17 : 10 mg, DTPA : 1.0 mg.

Fraction No	Fraction volume (ml)	OD	Protein content (mg/ml)
BG[a]	--	0.00	0.00
1	2	0.00	0.00[b]
2	2	0.00	0.00[b]
3	2	0.01	0.00[b]
4	2	0.02	0.20[c]
5	2	0.27	>2[c]
6	2	O.R[d]	>2[c]
7	2	0.92	0.68[c]
8	2	0.36	0.26[c]
9	2	0.02	0.01[b]
10	2	0.01	0.00[b]

a Background level was set at zero with PBS. This gave 3 reproducible readings of 0.000 before starting to measure the OD of the elution fractions.

b Fractions giving low readings, OD <0.010 (<10µg), were considered to be non-different from background.

c Fractions 5, 6, 7 & 8 were pooled together; OD : 0.76, final McAb concentration : 0.56 mg/ml, total : 4.47 mg, recovery of protein : 45%

d OR : Overreading (>2.00).

Experiment to measure the number of DTPA bound to WR-17:

The same experimental protocol described in page 52 was used. Table A9.2 shows the results of this experiment.

Table A9.5. Elution of ^{111}In+DTPA+WR-17-reaction mixture[a] on the Sephadex G-50 column in PBS. Labelling of the test sample (10µl) for calculation of the number of DTPA molecules bound per Ab.

Fraction No	Fraction volume (ml)	Radioactivity (MBq)	Count-rate (cpm-BG[b])
1	2.12	0.0	-2[c]
2	2.00	0.0	2[c]
3	2.00	0.0	21[d]
4	2.00	0.6	608[d]
5	2.00	0.1	133[d]
6	2.00	0.0	13[d]
7	2.00	0.1	72
8	2.00	0.7	704
9	2.00	9.6	9395
10	2.00	9.3	9263
11	2.00	2.3	2251
12	2.00	0.5	493
13	2.00	0.3	326
14	2.00	0.2	219
15	2.00	0.2	188
16	2.00	0.1	105
17	2.00	0.0	44
18	2.00	0.1	64
19	2.00	0.0	41
20	2.00	0.0	26

a Reaction mixture 10 µl; WR-17 : 50 mg/ml, DTPA : 6 mg/ml, Mol DTPA : Ab; 40 : 1, ^{111}In : 35 MBq (1 mCi) in 100 µl.

b Background (BG) was subtracted. Average BG : 152 cpm (n=3, se=5).

c Count-rates corrected for background and falling within 3 standard errors of the calculated difference (99% confidence limits) were considered to be non-significant and were ignored.

d Radioactivity in elution fractions 3, 4 & 5 (first peak) was associated with DTPA-Ab bound. The radioactive count in the following fractions 6-20 (second peak) was associated with free DTPA. The ratios Ab-DTPA/DTPA (MBq) = 0.7/23.9 = 0.03. Ab-DTPA/DTPA (cpm) = 762/23953 = 0.03. The number of DTPA molecules bound per UCHT2 molecule = 1.27 DTPA/Ab.

WR-17 test labelling with ^{111}In :

WR-17-DTPA : 0.1 mg, 180 µl; ^{111}In in citrate buffer : 95MBq (2.5 mCi), 350 µl.

Table A9.6. Elution of the WR-17-DTPA-^{111}In mixture on the Sephadex G 50 column :

Fraction	Fraction volume (ml)	^{111}In radioactivity (MBq)
1	2.53	0.0
2	2.00	0.0
3	2.00	0.1[a]
4	2.00	9.6[a]
5	2.00	38.6[a]
6	2.00	3.3[a]
7	2.00	0.17[a]
8	2.00	0.11
9	2.00	0.23[b]
10	2.00	0.56[b]

a ^{111}In radioactivity associated with the McAb. Fractions 4 5 & 6 were pooled together. Specific activity 518 MBq/mg (14 mCi/mg).

b Free ^{111}In eluting in late fractions giving a second peak of radioactivity.

^{111}In UCHT2 (Pan T) immunoreactivity testing

Table A9.7. Setting and results of the assay for measuring ^{111}In UCHT2[a] immunoreactivity with the cell line HPB ALL.

Tube No	Cell/ml	Cpm bound[b]	Non-specific cpm	Specific bound cpm	Ratio T/B
1	10^7	40800±100	2850±30	38000±120	3.57±0.01
2	$5X10^6$	32800±100	2500±30	30300±100	4.48±0.02
3	$2.5X10^6$	25400±100	1900±30	23500±100	5.76±0.02
4	$1.25X10^6$	18700±80	1700±20	17000±80	7.99±0.04
5	$6.25X10^5$	12800±70	1700±20	11000±70	12.29±0.08
6	$3.13X10^5$	8700±50	1300±20	7300±60	18.53±0.15
7	$1.56X10^5$	5800±40	1700±20	4100±50	32.86±0.41
8	$7.8X10^4$	4200±40	1200±20	3000±40	45.02±0.65
9	$3.9X10^4$	3300±30	1400±20	1900±40	72.05±1.56
10	$2X10^4$	3300±30	1400±20	1900±40	70.53±1.50

a ^{111}In UCHT2 : 476 MBq/mg (12.9 mCi/mg) was added at 10 ng/ml giving a total count-rate of 135700±150 cpm.

b Count-rates corrected for background, BG = 98, n =6, se = 4.

Figure A9.1. ^{111}In UCHT2 immunoreactive fraction tested with HPB ALL cells, the double inverse plot.

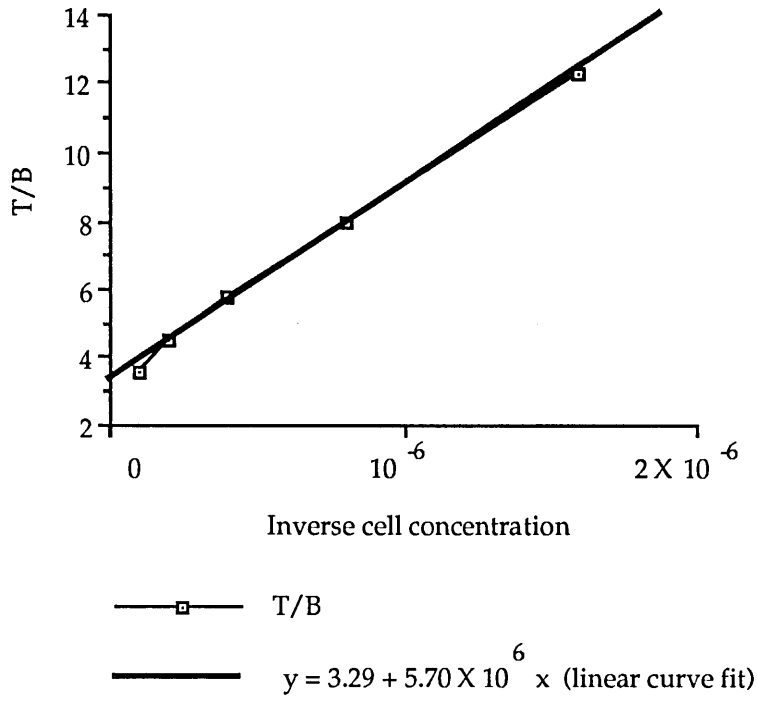

Intercept 3.29; the immunoreactive fraction ≈ 30%.

Table A9.8. Setting and results of the assay for measuring ^{111}In UCHT2[a] immunoreactivity with the cell line MOLT4.

Tube No	Cell/ml	Cpm bound[b]	Non-specific cpm	Specific bound cpm	Ratio T/B
1	10^7	31700±100	2400±30	29300±100	3.60±0.01
2	$5X10^6$	24700±90	1900±30	22900±100	4.60±0.02
3	$2.5X10^6$	17800±80	1500±20	16200±80	6.49±0.03
4	$1.25X10^6$	12200±60	1300±20	10900±70	9.68±0.06
5	$6.25X10^5$	8500±50	1300±20	7300±60	14.49±0.12
6	$3.13X10^5$	5200±40	1550±20	3700±50	28.61±0.38
7	$1.56X10^5$	4300±40	1350±20	3000±40	35.57±0.54
8	$7.8X10^4$	3100±30	1200±20	1900±40	54.83±1.12
9	$3.9X10^4$	2600±30	1260±20	1400±40	77.12±2.11
10	$2X10^4$	2070±30	1500±20	550±40	190.05±12.33

a ^{111}In UCHT2 : 370 MBq/mg (10 mCi/mg) was added at 10 ng/ml giving a total count-rate of 105200±130 cpm.

b Count-rates corrected for background, BG = 100, n =6, se = 4.

Figure A9.2. ^{111}In UCHT2 immunoreactive fraction tested with MOLT4 cells, the double inverse plot.

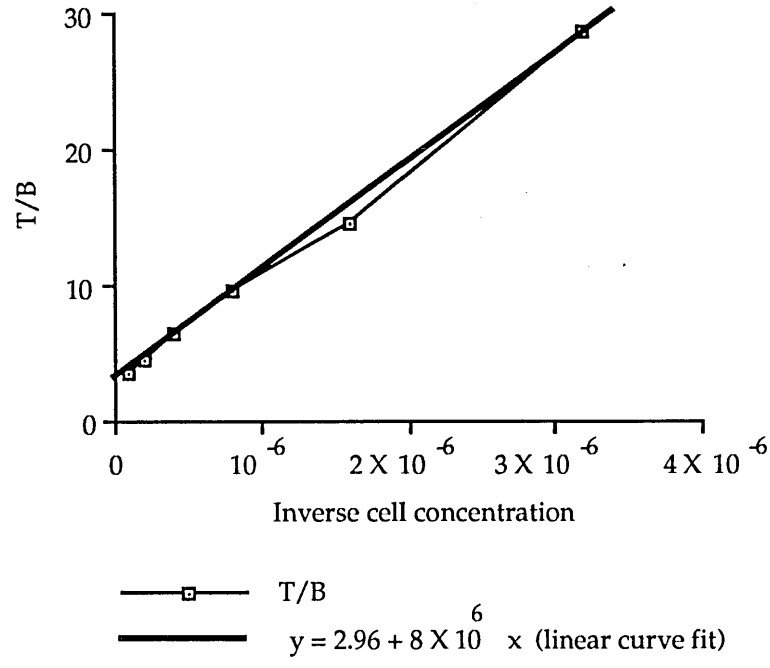

Intercept 2.96; the immunoreactive fraction ≈ 34%.

Table A9.9. Setting and results of the assay for measuring ^{111}In WR-17[a] immunoreactivity with the cell line EBV PGF.

Tube No	Cell/ml	Cpm bound[b]	Non-specific cpm	Specific bound cpm	Ratio T/B
1	10^7	59200±140	3200±30	56000±100	3.65±0.01
2	$5X10^6$	33700±100	2700±30	31000±100	6.59±0.02
3	$2.5X10^6$	20100±80	2500±20	17700±90	11.58±0.06
4	$1.25X10^6$	12200±60	2150±30	10100±40	20.26±0.08
5	$6.25X10^5$	7000±50	1900±30	5000±60	40.57±0.45
6	$3.13X10^5$	5500±40	2100±30	3400±50	60.82±0.93
7	$1.56X10^5$	3560±40	1800±30	1800±40	115.52±2.82
8	$7.8X10^4$	2500±30	1900±30	600±40	344.04±22.7
9	$3.9X10^4$	2900±30	1940±30	1000±40	206.56±8.63
10	$2X10^4$	2500±30	1700±25	800±40	252.6±12.05

a ^{111}In UCHT2 : 528 MBq/mg (14.3 mCi/mg) was added at 10 ng/ml giving a total count-rate of 204400±200 cpm.

b Count-rates corrected for background, BG = 86, n =4, se = 6.

Figure A9.3. ^{111}In WR-17 immunoreactive fraction tested with EBV PGF cells, the double inverse plot.

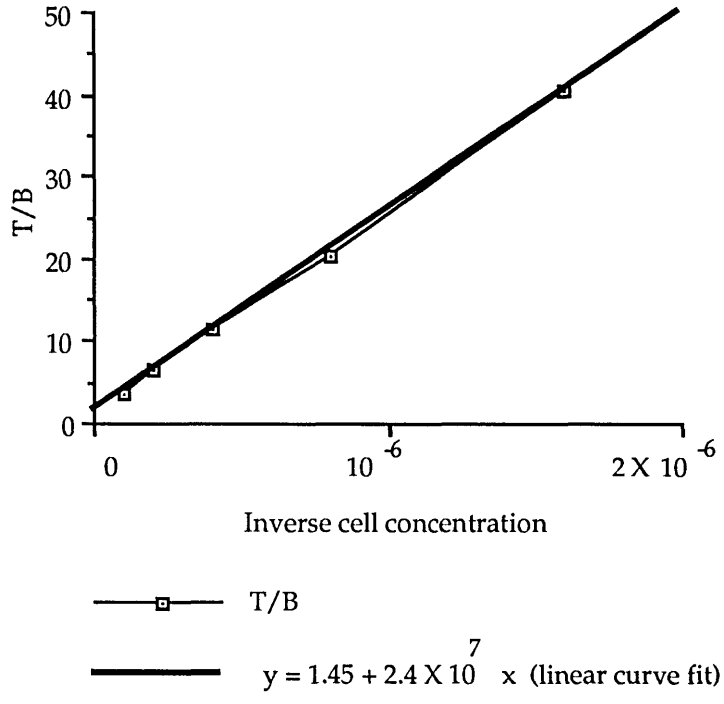

Intercept 1.45; the immunoreactive fraction ≈ 70%.

Table A9.10. Binding of ^{111}In UCHT2[a] (Pan T) to the HPB ALL T-cell line.

Tube No	Cell/ml	Std cpm added	Cpm bound[b]	Non-specific cpm	Specific bound cpm	Ratio B/T
1	10^7	92830000 ±126000	1088000 ±1200	1800 ±20	1086000 ±1200	0.012 ±0.00002
2	10^6	8310000 ±38000	321000 ±200	1700 ±20	319000 ±200	0.038 ±0.0002
3	10^5	902000 ±1100	102200 ±130	1100 ±15	101000 ±130	0.112 ±0.0002
4	10^4	75000 ±100	11300 ±400	370 ±10	11000 ±40	0.146 ±0.0006
5	10^3	8200 ±40	1600 ±20	50 ±5	1500 ±20	0.185 ±0.002
6	10^2	700 ±10	200 ±10	40 ±5	170 ±10	0.242 ±0.013

a ^{111}In UCHT2 : 100 MBq/mg (2.7 mCi/mg).

b All count-rates were corrected for background and for counting dead-time for counts above 10^5 cpm).

Table A9.11. Binding of ^{111}In UCHT2[a] (Pan T) to the MOLT4 T-cell line.

Tube No	Cell/ml	Std cpm added	Cpm bound[b]	Non-specific cpm	Specific bound cpm	Ratio B/T
1	10^7	58200000 ±70000	758000 ±800	1700 ±20	757000 ±800	0.013 ±0.00002
2	10^6	5800000 ±22000	240000 ±200	1400 ±20	240000 ±200	0.041 ±0.0002
3	10^5	594000 ±700	82000 ±100	800 ±10	81000 ±100	0.136 ±0.0003
4	10^4	62000 ±100	11000 ±40	500 ±10	10800 ±40	0.175 ±0.0008
5	10^3	6600 ±30	1700 ±20	80 ±5	1600 ±20	0.247 ±0.003

a ^{111}In UCHT2 : 50 MBq/mg (1.5 mCi/mg).
b All count-rates were corrected for background and for counting dead-time for counts above 10^5 cpm).

Table A9.12. Binding of ^{111}In WR-17[a] (Pan B) to the EBV PGF B-cell line.

Tube No	Cell/ml	Std cpm added	Cpm bound[b]	Non-specific cpm	Specific bound cpm	Ratio B/T
1	10^7	16536000 ±22000	190000 ±200	2000 ±20	190000 ±200	0.011 ±0.00002
2	10^6	1690000 ±7000	73000 ±100	1600 ±20	71000 ±100	0.042 ±0.0002
3	10^5	161000 ±200	14000 ±50	700 ±10	13000 ±50	0.081 ±0.0003
4	10^4	16000 ±50	2100 ±20	100 ±5	2000 ±20	0.128 ±0.0014
5	10^3	1500 ±20	300 ±10	40 ±5	230 ±10	0.146 ±0.006
6	10^2	150 ±5	80 ±5	30 ±5	50 ±10	0.335 ±0.053

a ^{111}In WR-17 : 227 MBq/mg (6.1 mCi/mg).
b All count-rates were corrected for background and for counting dead-time for counts above 10^5 cpm).

Table A9.13. Binding of ^{111}In UCHT2[a] (Pan T) to the whole blood[b].

Tube No	Ab/T cell[c]	Cpm 1 ml WB[d]	Cpm 1-Hct Pl	Cpm bound[e]	Ratio B/T
1	10^7	41680000	41560000	125000	0.003
		±84000	±84000	±120000	±0.003
2	10^6	3920000	3600000	320000	0.082
		±26000	±25000	±36000	±0.009
3	10^5	400000	321000	80000	0.199
		±1000	±700	±1000	±0.003
4	10^4	42000	32000	10000	0.236
		±100	±100	±200	±0.004
5	10^3	3600	2650	900	0.252
		±30	±30	±50	±0.013

a ^{111}In UCHT2 : 110 MBq/mg (3 mCi/mg).
b WBC 4.9X10^6/ml, lymphocytes 2.1X10^6/ml, monocytes 3X10^5/ml, Hct = 0.373.
c T-cell percentage of total lymphocytes was considered to be 64%.
d All count-rates were corrected for background and for counting dead-time for counts above 10^5 cpm).
e Non-specific binding was found to be low <1% of added count and was ignored (statistically non-significant <3 se).

Table A9.14. Distribution[a] of cell bound activity in the lymphocyte+monocyte fraction and between T & B cells after incubation of human blood with ^{111}In UCHT2.

Tube No	Cpm LM in 1 ml WB	Ratio LM/WB	Cpm 10^6 T cells	Cpm 10^6 B cells	Ratio cpm Tcell/ B cell
1	92000	0.002	61000	9500	6.46
	±400	±0.00004	±200	±200	±0.16
2	283000	0.072	78000	14000	5.43
	±500	±0.0005	±200	±200	±0.09
3	66000	0.165	47000	6000	8.10
	±300	±0.0007	±300	±300	±0.48
4	7500	0.810	6000	600	9.54
	±100	±0.0003	±100	±100	±1.99
5	700	0.191	500	200	2.20
	±40	±0.012	±20	±200	±1.73

a This experiment was the second part of the binding assay of ^{111}In UCHT2 to whole blood, see Table A9.13 above.

Table A9.15. Binding of ^{111}In Wr-17[a] (Pan B) to the whole blood[b].

Tube No	Ab/B cell[c]	Cpm 1 ml WB[d]	Cpm 1-Hct Pl	Cpm bound[e]	Ratio B/T
1	10^7	17000000	15900000	920000	0.054
		±23000	±31000	±63000	±0.004
2	10^6	1670000	1000000	600000	0.36
		±7000	±8000	±10000	±0.008
3	10^5	163000	90000	75000	0.459
		±200	±200	±400	±0.003
4	10^4	16000	4000	13000	0.795
		±50	±40	±80	±0.006
5	10^3	1600	270	1320	0.806
		±20	±10	±30	±0.018

a ^{111}In WR-17 : 330 MBq/mg (9 mCi/mg).
b WBC 7X10^6/ml, lymphocytes 2.8X10^6/ml, monocytes 3X10^5/ml, Hct = 0.424.
c B-cell percentage of total lymphocytes was considered to be 17.2%.
d All count-rates were corrected for background and for counting dead-time for counts above 10^5 cpm).
e Non-specific binding was subtracted from the values of cell-bound activity when statistically significant. Non-specific binding up to 2% was found (Tubes 1,3 &5).

Table A9.16. Distribution[a] of cell bound activity in the lymphocyte+monocyte fraction and between T & B cells after incubation of human blood with ^{111}In WR-17.

Tube No	Cpm LM in 1 ml WB	Ratio LM/WB	Cpm 10^6 B cells	Cpm 10^6 T cells	Ratio cpm B cell/ T cell
1	640000	0.037	800000	57000	14.42
	±1000	±0.00008	±2000	±300	±0.07
2	450000	0.271	750000	46000	16.37
	±2000	±0.002	±4000	±300	±0.13
3	57000	0.348	69000	7300	9.44
	±300	±0.002	±900	±70	±0.15
4	9000	0.567	14000	1000	11.53
	±200	±0.012	±300	±50	±0.60
5	740	0.453	600	280	2.18
	±50	±0.034	±170	±20	±0.64

a This experiment was the second part of the binding assay of ^{111}In WR-17 to whole blood, see Table A9.15 above.

Calculation of ^{111}In UCHT2 (Pan T) binding constant (the Ab equilibrium constant).
I. The association constant (K+1) :

Table A9.17 Binding of ^{111}In UCHT2[a] to MOLT4 cell line[b].

Time[c]	Cell bound cpm(1)[d]	Ratio B/T (1)	K+1[e]	Cell bound cpm (2)[f]	Ratio B/T (2)	K+1[f]
60	1265	0.0376	$2X10^6$	449	0.0405	$2X10^6$
120	1817	0.0540	$1.4X10^6$	616	0.0555	$1.4X10^6$
180	2653	0.0789	$1.3X10^6$	1226	0.1105	$1.8X10^6$
240	2834	0.0842	10^6	1384	0.1247	$1.6X10^6$

a ^{111}In UCHT2 : 330 MBq/mg (9 mCi/mg).
b The number of cells used was $2X10^6$/ml.
c Time after addition of the antibody in seconds.
d Antibody concentration used : 10^5 Ab/cell, Std count-rate (cpm) 33600±100.
e K+1 ($M^{-1}s^{-1}$) was calculated from Equation 9.2 :

$$K+1 = \frac{\text{Ratio B/T}}{[Ag] \,.\, t}$$

$$Ag = \frac{\text{Cell No/l X No of antigenic sites/cell}}{\text{Avogadro's Number}}$$

MOLT4 cells were considered to have 10^5 antigenic site/cell.
f Antibody concentration $5X10^4$ Ab/cell, Std count-rate (cpm) 11100±60.

Table A9.18 Binding of ^{111}In UCHT2[a] to HPB ALL cell line[b].

Time[c]	Cell bound cpm(1)[d]	Ratio B/T (1)	K+1[e]	Cell bound cpm (2)[f]	Ratio B/T (2)	K+1[f]
60	1378	0.0406	$2X10^6$	414	0.0370	$1.9X10^6$
120	2190	0.0645	$1.6X10^6$	758	0.0678	$1.7X10^6$
180	2786	0.0849	$1.4X10^6$	1067	0.1022	$1.7X10^6$
240	3094	0.0911	$1.1X10^6$	1232	0.1102	$1.4X10^6$

a ^{111}In UCHT2 : 330 MBq/mg (9 mCi/mg).
b The number of cells used was $2X10^6$/ml.
c Time after addition of the antibody in seconds.
d Antibody concentration used : 10^5 Ab/cell, Std count-rate (cpm) 34000±100.
e K+1 ($M^{-1}s^{-1}$) was calculated from Equation 9.2 :

$$K+1 = \frac{\text{Ratio B/T}}{[Ag] \,.\, t}$$

$$Ag = \frac{\text{Cell No/l X No of antigenic sites/cell}}{\text{Avogadro's Number}}$$

HPB ALL cells were considered to have 10^5 antigenic site/cell.
f Antibody concentration $5X10^4$ Ab/cell, Std count-rate (cpm) 11200±60.

II. The dissociation constant K-1 :

Table A9.19. Dissociation of ^{111}In UCHT2[a] from MOLT4 cells[b] after addition of excess unlabelled UCHT2.

Time[c]	Cell bound cpm(1)[d]	% bound cpm(1)	Log[e]	Cell bound cpm (2)[f]	% bound cpm (2)[g]	Log[f]
0	4912	8.04	0.91	3295	9.35	0.97
600	4529	7.41	0.87	3071	8.71	0.94
1800	4331	7.09	0.85	2866	8.13	0.91
3600	3857	6.31	0.80	2736	7.76	0.89
7200	3282	5.37	0.73	1981	5.62	0.75
10800	2549	4.17	0.62	1650	4.68	0.67
18000	1724	2.82	0.45	1114	3.16	0.50
125200	1167	1.91	0.28	705	2.00	0.30

a ^{111}In UCHT2 : 330 MBq/mg (9 mCi/mg).

b The number of cells used was $2X10^6$/ml.

c Time after addition of the antibody in seconds. The cells were incubated with ^{111}In UCHT2 for 2 hr beforehand.

d Antibody concentration used for the initial incubation : 10^5 Ab/cell, Std count-rate (cpm) 61000±150.

e The logarithm of the percentage cpm Bound/Total was plotted against the time (second) after addition of the unlabelled UCHT2 (see Figure A9.5 below). K-1 (s^{-1}) was obtained directly from the gradient of the curve linear fit or calculated using Equation 9.3 :

$$K\text{-}1 = \frac{0.693}{T_{1/2}}$$

f Antibody concentration used for the initial incubation at $5X10^4$ Ab/cell, Std count-rate (cpm) 35000±100.

g Non-specific binding was allowed for in the calculation.

Figure A9.4. Percentage cell (MOLT4) associated ^{111}In UCHT2 activity versus time after the addition of unlabelled UCHT2 to measure the Ab K-1.

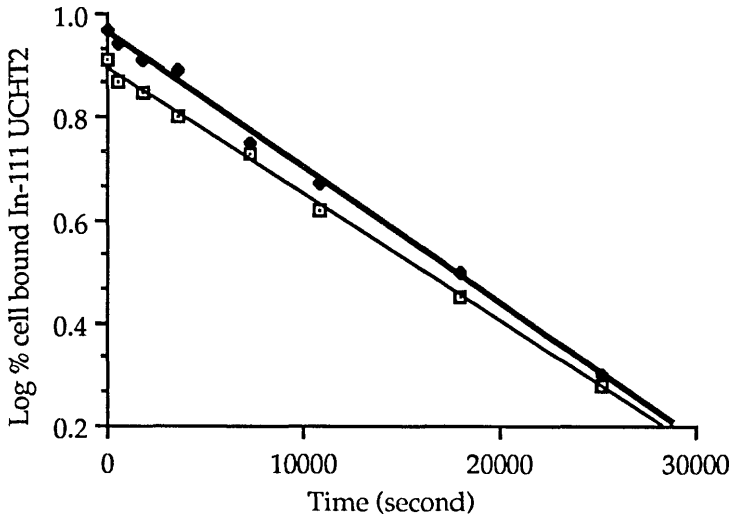

▫ ^{111}In UCHT2 added at 10^5 Ab/cell

——— Linear curve fit $y = 0.9 - 2.5 \times 10^{-5} x$ R^2 = 0.998

◆ ^{111}In UCHT2 added at 5×10^4 Ab/cell

——— Linear curve fit $y = 1.0 - 2.6 \times 10^{-5} x$ R^2 = 0.997

^{111}In UCHT2 K-1 ≈ 2.55×10^{-5} s^{-1}.

Table A9.20. Dissociation of ^{111}In UCHT2[a] from HPB ALL cells[b] after addition of excess unlabelled UCHT2.

Time[c]	Cell bound cpm(1)[d]	% bound cpm(1)	Log[e]	Cell bound cpm (2)[f]	% bound cpm (2)[g]	Log[f]
0	4786	7.83	0.89	4001	11.35	1.05
600	4639	7.59	0.88	3289	9.33	0.97
1800	4328	7.08	0.85	3215	9.12	0.96
3600	3949	6.46	0.81	2676	7.59	0.88
7200	3062	5.01	0.70	2383	6.76	0.83
10800	2928	4.79	0.68	1893	5.37	0.73
18000	2219	3.63	0.56	1340	3.80	0.58
125200	1534	2.51	0.40	885	2.51	0.40

a ^{111}In UCHT2 : 330 MBq/mg (9 mCi/mg).

b The number of cells used was $2X10^6$/ml.

c Time after addition of the antibody in seconds. The cells were incubated with ^{111}In UCHT2 for 2 hr beforehand.

d Antibody concentration used for the initial incubation : 10^5 Ab/cell, Std count-rate (cpm) 61000±150.

e The logarithm of the percentage cpm Bound/Total was plotted against the time (second) after addition of the unlabelled UCHT2 (see Figure A9.5 below). K-1 (s^{-1}) was obtained directly from the gradient of the curve linear fit or calculated using Equation 9.3 :

$$K\text{-}1 = \frac{0.693}{T_{1/2}}$$

f Antibody concentration used for the initial incubation at $5X10^4$ Ab/cell, Std count-rate (cpm) 35000±100.

g Non-specific binding was allowed for in the calculation.

Figure A9.5. Percentage cell (HPB ALL) associated ^{111}In UCHT2 activity versus time after the addition of unlabelled UCHT2 to measure the Ab K-1.

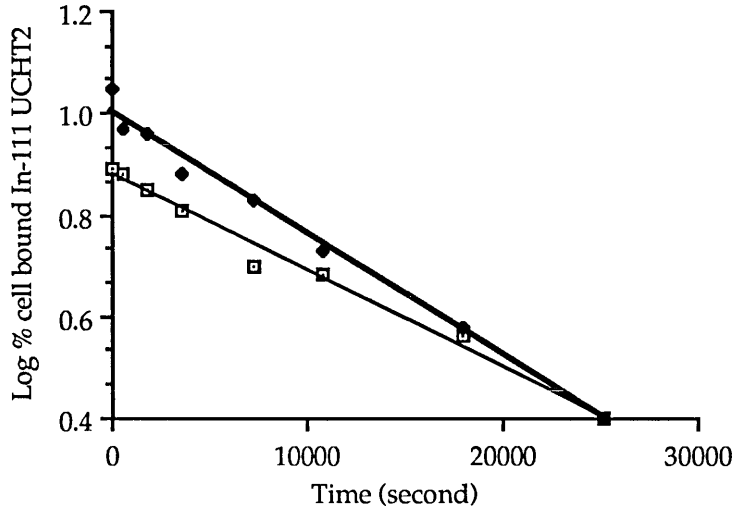

□ ^{111}In UCHT2 added at 10^5 Ab/cell

——— Linear curve fit $y = 0.88 - 2 \times 10^{-5} x$, $R^2 = 0.988$

◆ ^{111}In UCHT2 added at 5×10^4 Ab/cell

——— Linear curve fit $y = 1.00 - 2.4 \times 10^{-5} x$ $R^2 = 0.988$

^{111}In UCHT2 K-1 $\approx 2.2 \times 10^{-5}$ s^{-1}.

Calculation of ^{111}In WR-17 (Pan B) binding constant (the Ab equilibrium constant).
I. The association constant (K+1) :

Table A9.21 Binding of ^{111}In WR-17[a] to EBV PGF cell line[b].

Time[c]	Cell bound cpm(1)[d]	Ratio B/T (1)	K+1[e]	Cell bound cpm (2)[f]	Ratio B/T (2)	K+1[f]
60	737	0.0141	$7X10^5$	217	0.0116	$6X10^5$
120	1210	0.0232	$5X10^5$	391	0.0210	$5X10^5$
180	1573	0.0301	$5X10^5$	671	0.0360	$6X10^5$
240	2070	0.0396	$5X10^5$	795	0.0427	$5X10^5$

a ^{111}In WR-17 : 240 MBq/mg (6.5 mCi/mg).
b The number of cells used was $2X10^6$/ml.
c Time after addition of the antibody in seconds.
d Antibody concentration used : 10^5 Ab/cell, Std count-rate (cpm) 52000±150.
e K+1 ($M^{-1}s^{-1}$) was calculated from Equation 9.2 :

$$K+1 = \frac{\text{Ratio B/T}}{[Ag] \cdot t}$$

$$Ag = \frac{\text{Cell No/l X No of antigenic sites/cell}}{\text{Avogadro's Number}}$$

EBV PGFcells were considered to have 10^5 antigenic site/cell.
f Antibody concentration $5X10^4$ Ab/cell, Std count-rate (cpm) 18600±80.

II. The dissociation constant K-1 :

Table A9.22. Dissociation of ^{111}In WR-17[a] from EBV PGF cells[b] after addition of excess unlabelled WR-17.

Time[c]	Cell bound cpm(1)[d]	% bound cpm(1)	Log[e]	Cell bound cpm (2)[f]	% bound cpm (2)[g]	Log[f]
0	5331	8.98	0.95	3487	11.62	1.07
600	5080	8.56	0.93	2865	9.55	0.98
1800	4638	7.82	0.89	2554	8.51	0.93
3600	3834	6.46	0.81	2173	7.24	0.86
7200	2777	4.68	0.67	1504	5.01	0.70
10800	2309	3.89	0.59	1116	3.72	0.57
18000	961	1.62	0.21	573	1.91	0.28
125200	623	1.05	0.02	321	1.07	0.03

a ^{111}In WR-17 : 240 MBq/mg (6.5 mCi/mg).

b The number of cells used was $2X10^6$/ml.

c Time after addition of the antibody in seconds. The cells were incubated with ^{111}In WR-17 for 2 hr beforehand.

d Antibody concentration used for the initial incubation : 10^5 Ab/cell, Std count-rate (cpm) 59000±140.

e The logarithm of the percentage cpm Bound/Total was plotted against the time (second) after addition of the unlabelled WR-17 (see Figure A9.5 below). K-1 (s^{-1}) was obtained directly from the gradient of the curve linear fit or calculated using Equation 9.3 :

$$K\text{-}1 = \frac{0.693}{T_{1/2}}$$

f Antibody concentration used for the initial incubation at $5X10^4$ Ab/cell, Std count-rate (cpm) 30000±100.

g Non-specific binding was allowed for in the calculation.

Figure A9.6. Percentage cell (EBV PGF) associated ^{111}In WR-17 activity versus time after the addition of unlabelled WR-17 to measure the Ab K-1.

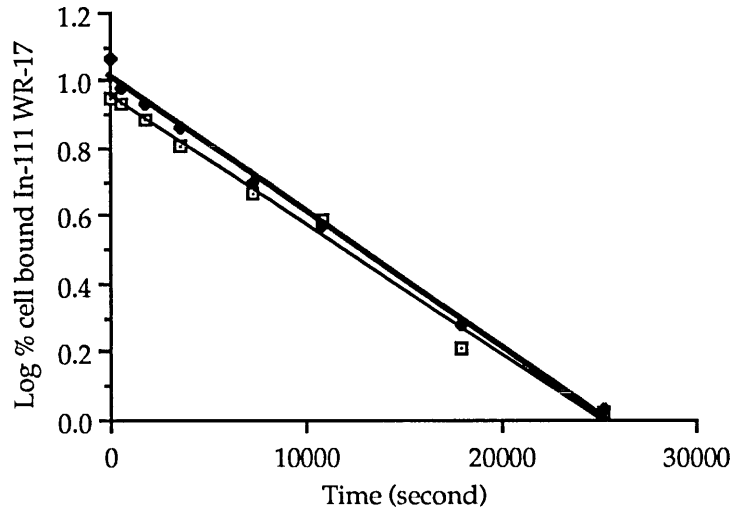

□ ^{111}In WR-17 added at 10^{5} Ab/cell

——— Linear curve fit $y = 1.0 - 3.8 \times 10^{-5} x$, $R^2 = 0.992$

◆ ^{111}In WR-17 added at 5×10^{4} Ab/cell

——— Linear curve fit $y = 1.0 - 4.0 \times 10^{-5} x$, $R^2 = 0.995$

^{111}In WR-17 K-1 $\approx 3.9 \times 10^{-5}$ s^{-1}.

Elution testing of the antibodies

Table A9.23. Elution of ^{111}In UCHT2[a] (Pan T) from the cell line HPB ALL.

Time	Std added cpm[b]	Cpm cell-bound
0	28900±100 (0.5 ml)	4900±30 (0.5 ml)
1 hr	1000±20 (0.2 ml)	740±10 (0.2 ml)
6 hr	990±20 (0.2 ml)	450±10 (0.2 ml)
19 hr	990±20 (0.2 ml)	430±10 (0.2 ml)
24 hr	1000±20 (0.2 ml)	440±10 (0.2 ml)

a ^{111}In UCHT2 : 42 MBq/mg (1.1 mCi/mg).
b All count-rates were corrected for background, BG = 65, n = 6, se = 3.

Table A9.24. Elution of ^{111}In WR-17[a] (Pan B) from the cell line EBV PGF.

Time	Std added cpm[b]	Cpm cell-bound
0	60500±140 (0.5 ml)	6360±30 (0.5 ml)
1 hr	1300±20 (0.2 ml)	940±10 (0.2 ml)
6 hr	1290±20 (0.2 ml)	240±10 (0.2 ml)
19 hr	1290±20 (0.2 ml)	180±10 (0.2 ml)
24 hr	1300±20 (0.2 ml)	180±10 (0.2 ml)

a ^{111}In WR-17 : 286 MBq/mg (7.7 mCi/mg).
b All count-rates were corrected for background, BG = 54, n = 6, se = 3.

Internalisation testing of the antibodies

Table A9.25. Internalisation testing of ^{111}In UCHT2[a] with the lymphoid cell line HPB ALL.

Time (hr)	Std added cpm	Pre-acid bound cpm	Post-acid bound cpm	Pre/Std	Post/Std
0	34000±100	2250±20	40±5	0.066±0.0006	0.0019±0.002
1	33000±100	5700±30	1200±15	0.174±0.001	0.210±0.003
2	33000±100	7000±35	1700±20	0.212±0.006	0.240±0.003
20	34500±100	5000±30	850±10	0.136±0.0009	0.180±0.003
24	32000±100	3500±25	630±10	0.110±0.0009	0.180±0.003

a ^{111}In UCHT2 : 70 MBq/mg (1.9 mCi/mg).

Table A9.26. Internalisation testing of ^{111}In WR-17[a] with the lymphoid cell line EBV PGF.

Time (hr)	Std added cpm	Pre-acid bound cpm	Post-acid bound cpm	Pre/Std	Post/Std
0	12400±65	275±10	10±5	0.028±0.0009	0.040±0.018
0.5	12300±65	620±10	30±5	0.050±0.003	0.052±0.009
1	12600±65	750±10	45±5	0.059±0.09	0.060±0.008
2	12200±65	1330±15	100±5	0.109±0.001	0.078±0.005
3	11850±65	1360±15	110±5	0.115±0.001	0.083±0.005
24	10200±60	2600±20	250±10	0.256±0.009	0.096±0.003

a ^{111}In WR-17 : 500 MBq/mg (13.5 mCi/mg).

Results of the mitogen induced proliferation tests in the presence of ^{111}In UCHT2 or WR-17.

Table A9.27. ^{3}H-thymidine incorporation[a] in the Con A stimulated plate used for testing the effect of ^{111}In UCHT2[b] on mitogen induced proliferation in whole blood[c].

Row	^{111}In UCHT2	UCHT2	HMFG2	RPMI
A	17810±174	47829±1347	48902±2912	48511±2478
B	50855±2181	52092±3288	50445±2207	50939±1817
C	46981±1901	51588±1048	53518±2090	51795±1163
D	51783±2037	49448±1320	53643±1456	56514±1152
E	53631±2248	52330±1706	54346±1701	ND
F	48643±2792	55574±2596	52903±2234	ND
G	54007±1238	48286±1402	56339±1579	ND
H	56948±1758	53335±1337	54262±1285	ND

a The count-rates in three well were measured and the average was taken.
b ^{111}In UCHT2 : 200 MBq/mg (5.5 mCi/mg).
c WBC 3.8 X10^{6}/ml, lymphocytes 2X10^{6}/ml.

Table A9.28. ^{3}H-thymidine incorporation[a] in the non-stimulated plate used for testing the effect of ^{111}In UCHT2[b] on mitogen induced proliferation in whole blood[c].

Row	^{111}In UCHT2	UCHT2	HMFG2	RPMI
A	211±72	147±42	236±67	65±21
B	119±17	145±50	125±8	57±26
C	108±14	104±40	55±15	22±7
D	150±31	84±10	44±21	56±12
E	117±56	83±28	29±11	ND
F	99±21	91±57	31±17	ND
G	61±31	78±46	19±16	ND
H	40±31	63±32	34±30	ND

a The count-rates in three well were measured and the average was taken.
b ^{111}In UCHT2 : 200 MBq/mg (5.5 mCi/mg).
c WBC 3.8 X10^{6}/ml, lymphocytes 2X10^{6}/ml.

Table A9.29. ^{3}H-thymidine incorporation[a] in the LPS+PWM stimulated plate used for testing the effect of ^{111}In WR-17[b] on mitogen induced proliferation in whole blood[c].

Row	^{111}In WR-17	WR-17	HMFG2	RPMI
A	123996±9311	115568±15261	125664±13053	128312±8837
B	121404±11981	132936±14837	134504±856	131936±13948
C	123092±14967	119197±14045	133481±14850	133540±13309
D	127123±11641	129371±21871	134415±2919	131263±7069
E	125237±3640	117154±6652	121954±11777	ND
F	124961±6758	114931±8025	128388±700	ND
G	118544±8363	118466±5479	139553±8584	ND
H	123278±26142	135738±6997	120451±9243	ND

a The count-rates in three well were measured and the average was taken.
b ^{111}In WR-17 : 217 MBq/mg (5.9 mCi/mg).
c WBC 5.2 X10^{6}/ml, lymphocytes 2.3X10^{6}/ml.

Table A9.30. ^{3}H-thymidine incorporation[a] in the non-stimulated plate used for testing the effect of ^{111}In WR-17[b] on mitogen induced proliferation in whole blood[c].

Row	^{111}In WR-17	WR-17	HMFG2	RPMI
A	676±604	865±574	1126±961	482±77
B	622±100	460±88	395±68	393±91
C	507±54	594±318	490±145	414±108
D	384±80	445±268	407±127	379±82
E	494±83	442±147	449±175	ND
F	341±41	350±198	533±247	ND
G	525±174	547±99	539±213	ND
H	683±81	566±124	438±92	ND

a The count-rates in three well were measured and the average was taken.
b ^{111}In WR-17 : 217 MBq/mg (5.9 mCi/mg).
c WBC 5.2 X10^{6}/ml, lymphocytes 2.3X10^{6}/ml.

Experimental protocols and data relating to Chapter 11 : ^{111}In Radiolabelling and in Vitro Tests of Monoclonal Antibodies against Lymphocytes, Activated Lymphocytes and Class I and II Major Histocompatibility Complex in the Rat.

Coupling of MRC OX-39 to DTPA

Same protocol as that described in page 50 was used. The results are shown in Table A11.1.

Table A11.1. Elution fractions of MRC OX-39+DTPA reaction mixture on the Sephadex G-50 column in PBS. MRC OX-39 : 3 mg, DTPA : 0.3 mg.

Fraction No	Fraction volume (ml)	OD	Protein content (mg/ml)
BG[a]	--	0.00	0.00
1	2	0.00	0.00
2	2	0.00	0.00
3	2	0.00	0.00
4	2	0.00	0.00
5	2	0.21	0.15[b]
6	2	0.29	0.22[b]
7	2	0.04	0.03
8	2	0.00	0.00
9	2	0.00	0.00

a Background level was set at zero with PBS. This gave 3 reproducible readings of 0.000 before starting to measure the OD of the elution fractions.

b Fractions 5 & 6 were pooled together; OD : 0.25, final McAb concentration : 0.18 mg/ml, total : 0.723 mg, recovery of protein : 24%

Experiment to measure the number of DTPA bound to MRC OX-39:

The same experimental protocol described in page 52 was used. Table A11.2 shows the results of this experiment.

Table A11.2. Elution of ^{111}In+DTPA+MRC OX-39-reaction mixture[a] on the Sephadex G-50 column in PBS. Labelling of the test sample (10µl) for calculation of the number of DTPA molecules bound per Ab.

Fraction No	Fraction volume (ml)	Radioactivity (MBq)	Count-rate (cpm-BG[b])
1	2.21	0.0	14[c]
2	2.00	0.0	5[c]
3	2.00	0.0	9[c]
4	2.00	0.0	49[d]
5	2.00	0.1	3857[d]
6	2.00	1.7	30976[d]
7	2.00	0.1	2975
8	2.00	0.0	944
9	2.00	0.0	772
10	2.00	0.0	2136
11	2.00	0.9	17537
12	2.00	1.8	41143
13	2.00	18.8	527440
14	2.00	18.5	507774
15	2.00	3.1	56112
16	2.00	0.7	14330
17	2.00	0.2	4384
18	2.00	0.0	647
19	2.00	0.0	110
20	2.00	0.0	60

a Reaction mixture 10 µl; 15 mg/ml MRC OX-39, 1.5 mg/ml DTPA, Mol DTPA : Ab; 40 : 1, ^{111}In : 50 MBq (1.4 mCi) in 200 µl.

b Background (BG) was subtracted. Average BG : 175 cpm (n=6, se=5).

c Count-rates corrected for background and falling within 3 standard errors of the calculated difference (99% confidence limits) were considered to be non-significant and were ignored.

d Radioactivity in elution fractions 5, 6 & 7 first peak) was associated with DTPA-Ab bound. The radioactive count in the following fractions 8-20 (second peak) was associated with free DTPA. The ratios Ab-DTPA/DTPA (MBq) = 1.9/45.9 = 0.04. Ab-DTPA/DTPA (cpm) = 38801/1211246 = 0.03. The number of DTPA molecules bound per MRC OX-39 molecule = 1.20 DTPA/Ab.

MRC OX-39 test labelling with ^{111}In :

MRC OX-39-DTPA : 50 µg, 280 µl; ^{111}In in citrate buffer : 40MBq (1.1 mCi), 200 µl.

Table A11.3. Elution of the MRC OX-39-DTPA-^{111}In mixture on the Sephadex G 50 column :

Fraction	Fraction volume (ml)	^{111}In radioactivity (MBq)
1	2.48	0.0
2	2.00	0.0
3	2.00	0.0
4	2.00	0.4[a]
5	2.00	3.8[a]
6	2.00	0.9[a]
7	2.00	0.1
8	2.00	0.0
9	2.00	0.3[b]
10	2.00	1.5[b]

a ^{111}In radioactivity associated with the McAb. Fractions 5 & 6 were pooled together. Specific activity 104 MBq/mg (2.81 mCi/mg).

b Free ^{111}In eluting in late fractions giving a second peak of radioactivity.

Coupling of MN4-91-6 to DTPA

Same protocol as that described in page 50 was used. The results are shown in Table A11.4.

Table A11.4. Elution fractions of MN4-91-6+DTPA reaction mixture on the Sephadex G-50 column in PBS. MN4-91-6 : 4 mg, DTPA : 0.38 mg.

Fraction No	Fraction volume (ml)	OD	Protein content (mg/ml)
BG[a]	--	0.00	0.00
1	2	0.00	0.00
2	2	0.00	0.00
3	2	0.00	0.00
4	2	0.03	0.02
5	2	0.99	0.73[b]
6	2	1.16	0.85[b]
7	2	0.16	0.12
8	2	0.01	0.00
9	2	0.00	0.00

a Background level was set at zero with PBS. This gave 3 reproducible readings of 0.000 before starting to measure the OD of the elution fractions.

b Fractions 5 & 6 were pooled together; OD : 0.77, final McAb concentration : 0.57 mg/ml, total : 3.4 mg, recovery of protein : 85%

Experiment to measure the number of DTPA bound to MN4-91-6:

The same experimental protocol described in page 52 was used. Table A11.5 shows the results of this experiment.

Table A11.5. Elution of ^{111}In+DTPA+MN4-91-6-reaction mixture[a] on the Sephadex G-50 column in PBS. Labelling of the test sample (10µl) for calculation of the number of DTPA molecules bound per Ab.

Fraction No	Fraction volume (ml)	Radioactivity (MBq)	Count-rate (cpm-BG[b])
1	2.21	0.0	18[c]
2	2.00	0.0	-10[c]
3	2.00	0.0	3[c]
4	2.00	0.0	16[c]
5	2.00	0.1	401[d]
6	2.00	2.5	9332[d]
7	2.00	0.2	1084[d]
8	2.00	0.1	715[d]
9	2.00	0.0	461
10	2.00	0.1	4159
11	2.00	0.6	3678
12	2.00	30.0	113105
13	2.00	29.0	108664
14	2.00	1.9	7638
15	2.00	0.3	2357
16	2.00	0.1	631
17	2.00	0.1	236
18	2.00	0.0	60
19	2.00	0.0	19
20	2.00	0.0	30

a Reaction mixture 10 µl; 20 mg/ml MN4-91-6, 1.9 mg/ml DTPA, Mol DTPA : Ab; 40 : 1, ^{111}In : 74 MBq (2 mCi) in 200 µl.

b Background (BG) was subtracted. Average BG : 175 cpm (n=6, se=5).

c Count-rates corrected for background and falling within 3 standard errors of the calculated difference (99% confidence limits) were considered to be non-significant and were ignored.

d Radioactivity in elution fractions 5, 6, 7 & 8 (first peak) was associated with DTPA-Ab bound. The radioactive count in the following fractions 9-20 (second peak) was associated with free DTPA. The ratios Ab-DTPA/DTPA (MBq) = 2.9/65 = 0.04. Ab-DTPA/DTPA (cpm) = 11532/252570 = 0.04. The number of DTPA molecules bound per MN4-91-6 molecule = 1.60 DTPA/Ab.

MN4-91-6 test labelling with ^{111}In :

MN4-91-6-DTPA : 50 µg, 90 µl; ^{111}In in citrate buffer : 40MBq (1.1 mCi), 200 µl.

Table A11.6. Elution of the MN4-91-6-DTPA-^{111}In mixture on the Sephadex G 50 column :

Fraction	Fraction volume (ml)	^{111}In radioactivity (MBq)
1	2.29	0.0
2	2.00	0.0
3	2.00	0.0
4	2.00	0.3[a]
5	2.00	4.2[a]
6	2.00	0.4[a]
7	2.00	0.1
8	2.00	0.0
9	2.00	0.1[b]
10	2.00	0.5[b]

a ^{111}In radioactivity associated with the McAb. Fraction 5 was pooled. Specific activity 98 MBq/mg (2.7 mCi/mg).

b Free ^{111}In eluting in late fractions giving a second peak of radioactivity.

Coupling of F17-23-2 to DTPA

Same protocol as that described in page 50 was used. The results are shown in Table A11.7.

Table A11.7. Elution fractions of F17-23-2+DTPA reaction mixture on the Sephadex G-50 column in PBS. F17-23-2 : 8 mg, DTPA : 0.76 mg.

Fraction No	Fraction volume (ml)	OD	Protein content (mg/ml)
BG[a]	--	0.00	0.00
1	2	0.00	0.00
2	2	0.00	0.00
3	2	0.01	0.00[b]
4	2	0.01	0.00[b]
5	2	0.68	0.50[c]
6	2	0.50	0.37[c]
7	2	0.01	0.00[b]
8	2	0.00	0.00
9	2	0.00	0.00

a Background level was set at zero with PBS. This gave 3 reproducible readings of 0.000 before starting to measure the OD of the elution fractions.

b Fractions 5 & 6 were pooled together; OD : 0.58, final McAb concentration : 0.43 mg/ml, total : 1.7 mg, recovery of protein : 20%

Experiment to measure the number of DTPA bound to F17-23-2:

The same experimental protocol described in page 52was used. Table A11.8 shows the results of this experiment.

Table A11.8. Elution of ^{111}In+DTPA+F17-23-2-reaction mixture[a] on the Sephadex G-50 column in PBS. Labelling of the test sample (10µl) for calculation of the number of DTPA molecules bound per Ab.

Fraction No	Fraction volume (ml)	Radioactivity (MBq)	Count-rate (cpm-BG[b])
1	2.21	0.0	16[c]
2	2.00	0.0	11[c]
3	2.00	0.0	32
4	2.00	0.0	138[d]
5	2.00	0.1	1849[d]
6	2.00	0.3	5673[d]
7	2.00	0.1	1779[d]
8	2.00	0.0	868[d]
9	2.00	0.0	661[d]
10	2.00	0.0	250
11	2.00	0.1	1827
12	2.00	0.6	11643
13	2.00	1.9	40116
14	2.00	3.8	78961
15	2.00	3.6	73208
16	2.00	1.6	32004
17	2.00	0.7	13175
18	2.00	0.2	3518
19	2.00	0.1	1729
20	2.00	0.0	363

a Reaction mixture 10 µl; 40 mg/ml F17-23-2, 3.8 mg/ml DTPA, Mol DTPA : Ab; 40 : 1, ^{111}In : 15 MBq (0.5 mCi) in 200 µl.

b Background (BG) was subtracted. Average BG : 170 cpm (n=4, se=6).

c Count-rates corrected for background and falling within 3 standard errors of the calculated difference (99% confidence limits) were considered to be non-significant and were ignored.

d Radioactivity in elution fractions 4, 5, 6, 7, 8 & 9 (first peak) was associated with DTPA-Ab bound. The radioactive count in the following fractions 10-20 (second peak) was associated with free DTPA. The ratios Ab-DTPA/DTPA (MBq) = 0.5/13.1 = 0.04. Ab-DTPA/DTPA (cpm) = 11250/267794 = 0.04. The number of DTPA molecules bound per F17-23-2 molecule = 1.68 DTPA/Ab.

F17-23-2 test labelling with ^{111}In :

F17-23-2-DTPA : 50 µg, 120 µl; ^{111}In in citrate buffer : 40MBq (1.1 mCi), 200 µl.

Table A11.9. Elution of the F17-23-2-DTPA-^{111}In mixture on the Sephadex G 50 column :

Fraction	Fraction volume (ml)	^{111}In radioactivity (MBq)
1	2.32	0.0
2	2.00	0.0
3	2.00	0.0
4	2.00	0.1[a]
5	2.00	5.7[a]
6	2.00	0.8[a]
7	2.00	0.0
8	2.00	0.0
9	2.00	0.1[b]
10	2.00	0.4[b]

a ^{111}In radioactivity associated with the McAb. Fraction 5 & 6 were pooled. Specific activity 132 MBq/mg (3.6 mCi/mg).

b Free ^{111}In eluting in late fractions giving a second peak of radioactivity.

^{111}In MRC OX-39 immunoreactivity testing

Table A11.10. Setting and results of the assay for measuring ^{111}In MRC OX-39[a] immunoreactivity with Con A-stimulated rat spleen cells.

Tube No	Cell/ml	Cpm bound[b]	Non-specific cpm	Specific bound cpm	Ratio T/B
1	$2.5X10^7$	13800±70	240±10	13500±70	1.73±0.01
2	$1.25X10^7$	10800±60	160±10	10600±60	2.20±0.02
3	$6.25X10^6$	8900±50	270±10	8300±60	2.81±0.02
4	$3.13X10^6$	5500±40	220±10	5250±50	4.46±0.04
5	$1.56X10^6$	3060±30	70±10	3000±30	7.83±0.1
6	$7.8X10^5$	2560±20	160±10	2300±30	10.21±0.15

a ^{111}In MRC OX-39 : 105 MBq/mg (2.8 mCi/mg) was added at 10 ng/ml giving a total count-rate of 23400±90 cpm.

b Count-rates corrected for background, BG = 136, n =6, se = 5.

Figure A11.1. ^{111}In MRC OX-39 immunoreactive fraction, the double inverse plot.

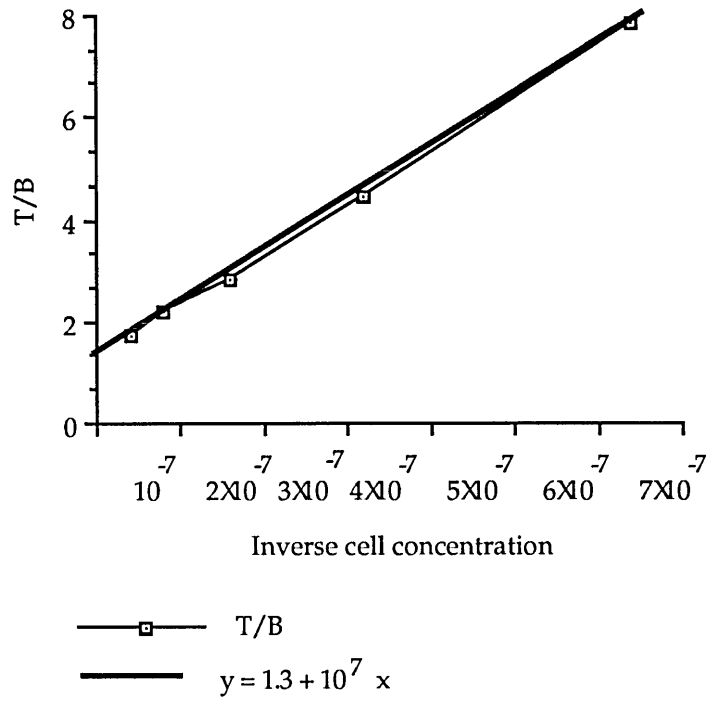

Intercept 1.3; the immunoreactive fraction ≈ 77%.

^{111}In MN4-91-6 immunoreactivity testing

Table A11.11. Setting and results of the assay for measuring ^{111}In MN4-91-6[a] immunoreactivity with DA-rat red blood cells.

Tube No	Cell/ml	Cpm bound[b]	Non-specific cpm	Specific bound cpm	Ratio T/B
1	10^8	14000±70	200±10	13700±70	1.15±0.008
2	$5X10^7$	11300±60	250±10	11100±60	1.42±0.01
3	$2.5X10^7$	9800±60	190±10	9650±60	1.63±0.01
4	$1.25X10^7$	5740±40	230±10	5500±50	2.85±0.03
5	$6.25X10^6$	3600±30	180±10	3160±40	4.98±0.06
6	$3.13X10^6$	1830±30	100±10	1720±30	9.14±0.15
7	$1.56X10^6$	1100±20	90±10	1000±20	15.80±0.37

a ^{111}In MN4-91-6 : 150 MBq/mg (4 mCi/mg) was added at 10 ng/ml giving a total count-rate of 15700±70 cpm.

b Count-rates corrected for background, BG = 125, n =6, se = 5.

Figure A11.2. ^{111}In MN4-91-6 immunoreactive fraction, the double inverse plot.

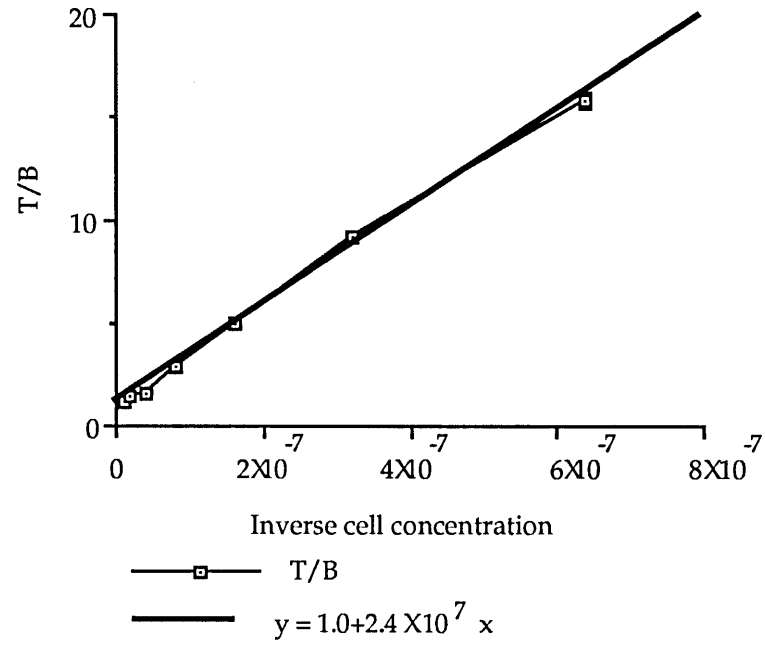

Intercept 1; the immunoreactive fraction ≈ 100%.

Table A11.12. Setting and results of the assay for measuring ^{111}In F17-23-2[a] immunoreactivity with DA-rat spleen cells.

Tube No	Cell/ml	Cpm bound[b]	Non-specific cpm	Specific bound cpm	Ratio T/B
1	$4X10^7$	11100±60	320±10	10800±60	1.74±0.01
2	$2X10^7$	9800±60	250±10	9600±60	1.97±0.02
3	10^7	8000±50	200±10	7750±50	2.43±0.02
4	$5X10^6$	5800±40	200±10	5600±50	3.38±0.03
5	$2.5X10^6$	3500±35	180±10	3350±40	5.62±0.07
6	$1.25X10^6$	2000±30	120±10	1900±30	9.81±0.16
7	$6.25X10^6$	1330±20	180±10	1150±25	16.45±0.37

a ^{111}In F17-23-2 : 125 MBq/mg (3.4 mCi/mg) was added at 10 ng/ml giving a total count-rate of 18800±80 cpm.

b Count-rates corrected for background, BG = 140, n =6, se = 5.

Figure A11.3. ^{111}In F17-23-2 immunoreactive fraction, the double inverse plot.

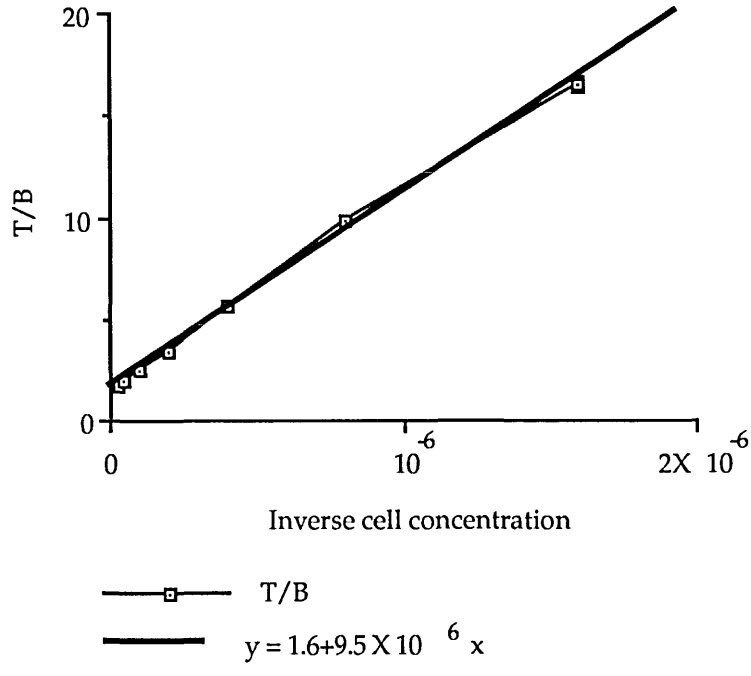

Intercept 1.6; the immunoreactive fraction ≈ 63%.

Experimental protocols and data relating to Chapter 12 : In Vivo Use of ^{111}In Anti-Lymphocyte, Activated Lymphocytes, Anti-Donor Class I & II MHC Monoclonal Antibodies for Scintillation Imaging of Rejection in Kidney Transplanted Rats. A Rat Model for the Early Diagnosis and Discrimination of Rejection in Unmodified and Cyclosporine Treated Allogeneic Kidney Transplants

The transplantation procedure

The procedure required two operators working closely together. The donor rat was anaethetised intraperitoneally and the animal was laid on its back and fixed to a dissecting cork board. A midline incision was made in the skin of the abdomen just below the xyphi sternum to the lower abdominal area. The muscle layer and peritoneum were opened by cutting the tissue with surgical scissors in the same way as the skin and the intestines were pulled out gently, wrapped in a piece of gauze moistened in saline and left on the left side of the abdominal incision (left hand side of the main operator). At this point, the dissecting microscope[1] was used. The left kidney was located and was freed from the posterior abdominal wall by cutting the surrounding renal fat with curved scissors. The renal pedicle was then cleared by gently dissecting the renal artery, vein and ureter using fine watch-maker forceps to provide suitable stumps for performing anastomoses with corresponding stumps in the recipient animal. Collateral arteries or veins were tied-off with 8/0 surgical-silk thread[2] so that they would not interfere with vessel suturing or cause excessive bleeding. The donor rat was afterwards put aside and the recipient rat was anaesthetised and treated in the same way as the donor. After clearing the kidney pedicle of the recipient rat, the renal artery was clamped as near to the aorta as possible using a Scoville-Lewis neurovascular clip. The kidney was observed for a short while afterwards to check complete blood stoppage and another clip was placed on the renal vein at a point as near to the inferior vena cava as possible. Using fine scissors, the ureter was transected at a point ≈ 7 mm of the pelvic-ureteric junction (PUJ) and the renal artery and vein were transected as close to the kidney as possible to provide stumps with reasonable lengths for the anatomoses.
The donor rat was injected intravenously with 250 iu of heparin in 1 ml PBS through the penile vein. After 5 minutes of the injection of heparin, the ureter was transected using fine scissors at ≈ 7 mm of the PUJ, the left renal artery in the donor was clamped by a tight hold of the artery using fine forceps and the artery was transected at a point as close to the aorta as possible. The left renal vein was also transected at the same distance. The kidney was removed, placed on a piece of gauze, gently squeezed and blotted of blood remaining in it. The donor rat was killed by severing the aorta under ether anaesthesia. The donor kidney (transplant) was placed in the recipient's left flank and the anastomosis was performed. Arterial anastomosis was done by putting 9 interrupted sutures to join the lips of both arterial stumps using a 10/0 Mersilk suture linked to a 4 or 6 mm curved needle[3]. In a few instances, a continuous suture of the artery was performed. For the venous anastomosis, the venous stumps were allowed to float in PBS added in the abdominal cavity and the lips of the venous stumps were joined by a continuous suture along their circumference. At the end of the venous anatomosis, the venous clamp was removed and bleeding was checked. In case it was present, a piece of fat was placed on its source which usually helped to stop it. Otherwise an extra suture was placed. The arterial clamp was then opened slowly keeping the clamp in place. If satisfactory flow was observed and no bleeding occurred, the clamp was removed altogether. If bleeding was noted a piece of fat was placed around the anastomosis and the clamp removed slowly making sure that bleeding had stopped. The ischemia time, ie time between removal of the donor kidney and restoration of blood flow after anastomosis, was always less than 45 min and usually ≈ 30 min. Ureteric anastomosis was done by joining the two ureteric stumps and putting 4 sutures around the circumference. The patency of the ureteric

---

1 Carl Zeiss, Germany.
2 Ethicon Ltd, Edinburgh, Scotland.
3 Ethicon Ltd, Edinburgh, Scotland.

anastomosis was checked after putting the third suture by allowing the tip of the fine forceps to enter the lumen of each stump on either side of the joining plane.
Having established satisfactory blood flow in the transplant both immediately and at 10 min after the anastomosis by inspection of the renal artery pulse and the brownish-red colour of the kidney, the operation was considered successful and the animal was closed. Closure of the wound was done after returning the viscera into the abdominal cavity, by suturing the muscle layer and peritoneum using a continuous 3/0 catgut suture and finally the skin using a 3/0 silk continuous suture. Afterwards, the animal was placed in a cage. A lamp was used as a source of heat to keep the animal warm during recovery from the surgical procedure.

Table A12.1. Uptake[a] of ^{111}In MRC OX-19 in the rest of the organs and tissues sampled in the studied rat.

	Expt 1		
Rat	PVG Control	DA--->PVG (Tx 6d)	DA--->PVG (Tx 8d)
MLN	3.65 ± 0.01	2.71 ± 0.02	2.13 ± 0.01
Thymus	0.16 ± 0.001	0.31 ± 0.008	0.21 ± 0.01
Lung	1.03 ± 0.005	0.80 ± 0.006	0.36 ± 0.006
Intestine	0.29 ± 0.002	0.22 ± 0.005	0.16 ± 0.004
Peyer's patches	1.54 ± 0.01	1.05 ± 0.03	0.70 ± 0.02
Tibia+BM	0.39 ± 0.002	0.48 ± 0.003	0.29 ± 0.002
Muscle	0.06 ± 0.0005	0.03 ± 0.0006	0.04 ± 0.0001

a The results are shown as percent injected dose per gramme (%ID/g).

Table A12.2. Uptake[a] of ^{111}In MRC OX-39 in the rest of the organs and tissues sampled in the studied rats.

Expt	Rat	CLN	MLN	Thy	Lung	Int	PP	Tib+BM	Tib	Muscle
2	PVG	1.95	1.97	0.30	1.92	0.98	1.36	0.69	0.23	0.11
	Ctrl	±0.02	±0.02	±0.003	±0.01	±0.009	±0.02	±0.005	±0.003	±0.002
2	DA	2.84	3.10	0.32	1.27	1.08	1.34	0.93	0.37	0.13
	Ctrl	±0.02	±0.04	±0.003	±0.01	±0.009	±0.03	±0.006	±0.004	±0.001
2	DA->PVG	1.80	ND	1.00	3.04	0.63	0.84	1.35	1.00	0.12
	(Tx 4d)	±0.02		±0.01	±0.02	±0.01	±0.03	±0.008	±0.006	±0.002
3	DA->PVG	0.96	1.18	0.32	0.57	0.53	0.71	0.19	0.14	0.05
	(Tx 4d)	±0.01	±0.01	±0.007	±0.007	±0.008	±0.02	±0.002	±0.002	±0.001
	PVG->PVG	1.47	1.41	0.38	0.58	0.65	1.65	0.22	0.12	0.03
	(Tx 4d)	±0.02	±0.02	±0.009	±0.01	±0.01	±0.05	±0.002	±0.001	±0.0009
4	DA->PVG	1.11	ND	0.22	0.67	ND	ND	ND	ND	0.04
	(Tx 4d)	±0.004		±0.002	±0.002					±0.0003
5	DA->PVG	1.92	ND	0.53	0.61	0.99	1.48	0.21	0.12	0.03
	(Tx 2d CsA)	±0.006		±0.004	±0.003	±0.004	±0.008	±0.0005	±0.0005	±0.0003
	DA->PVG	1.75	ND	0.52	0.54	0.94	1.57	0.25	0.06	0.08
	(Tx 2d)	±0.006		±0.003	±0.002	±0.004	±0.007	±0.0007	±0.0004	±0.0005

a %ID/g.

Table A12.3. Uptake[a] of ^{111}In MN4-91-6 in the rest of the organs and tissues sampled in the studied rats.

Expt	Rat	CLN	MLN	Thy	Lung	Int	PP	Tib+BM	Tib	Muscle
6	PVG	0.98	0.91	0.42	1.30	0.36	0.34	0.56	0.39	0.15
	Ctrl	±0.01	±0.01	±0.004	±0.01	±0.005	±0.01	±0.004	±0.004	±0.002
	DA	1.16	1.14	0.52	4.73	0.40	ND	0.95	0.36	0.27
	Ctrl	±0.01	±0.02	±0.004	±0.02	±0.005		±0.006	±0.004	±0.003
7	DA->PVG	0.66	0.88	0.38	0.68	0.64	0.56	0.35	0.21	0.07
	(Tx 2d)	±0.01	±0.01	±0.008	±0.007	±0.008	±0.01	±0.002	±0.002	±0.001
	DA->PVG	0.83	0.64	1.18	1.40	0.33	0.23	0.31	0.18	0.08
	(Tx 5d)	±0.01	±0.01	±0.01	±0.009	±0.006	±0.007	±0.002	±0.002	±0.001
8	DA->PVG	0.52	0.65	0.24	0.55	0.33	0.31	0.28	0.20	0.06
	(Tx 4d)	±0.003	±0.004	±0.002	±0.003	±0.003	±0.005	±0.001	±0.001	±0.0005
9	PVG->PVG	0.84	0.75	0.40	0.76	0.41	0.38	0.34	0.19	0.11
	(Tx 2d)	±0.006	±0.008	±0.003	±0.005	±0.005	±0.007	±0.001	±0.001	±0.0008
10	DA->PVG	0.58	ND	0.27	0.98	ND	ND	ND	ND	0.08
	(Tx 3d)	±0.009		±0.004	±0.007					±0.0009
	PVG->PVG	0.78	ND	0.34	1.40	ND	ND	ND	ND	0.08
	(Tx 3d)	±0.008		±0.005	±0.007					±0.001
11	DA->PVG	0.47	ND	0.25	1.53	0.30	0.40	0.31	0.15	0.05
	(Tx 3d)	±0.008		±0.004	±0.01	±0.006	±0.007	±0.002	±0.002	±0.0008
	WAG->PVG	0.72	ND	0.42	1.90	0.41	0.42	0.35	0.08	0.12
	(Tx 3d)	±0.008		±0.006	±0.01	±0.005	±0.01	±0.002	±0.001	±0.001
12	DA->PVG	0.41	ND	0.33	0.75	0.31	0.29	0.22	0.08	0.03
	(Tx 3d CsA)	±0.006		±0.005	±0.005	±0.004	±0.005	±0.002	±0.001	±0.005
13	DA->PVG	0.35	ND	0.27	1.02	0.25	0.31	0.25	0.21	0.05
	(Tx 7d CsA)	±0.002		±0.002	±0.003	±0.002	±0.003	±0.0008	±0.0008	±0.0003
	PVG->PVG	0.56	ND	0.34	1.24	0.36	0.48	0.30	0.21	0.07
	(Tx 7d CsA)	±0.003		±0.002	±0.004	±0.003	±0.005	±0.001	±0.0009	±0.0004
14	DA->PVG	0.47	ND	0.30	1.19	0.33	0.37	0.21	0.05	0.05
	(Tx 14d CsA)	±0.002		±0.001	±0.01	±0.001	±0.002	±0.0008	±0.0002	±0.0002
	DA->PVG	0.39	ND	0.17	0.90	0.30	0.32	0.21	0.08	0.05
	(Tx 21d CsA)	±0.002		±0.0009	±0.005	±0.001	±0.002	±0.002	±0.0004	±0.0002

a %ID/g.

Table A12.4. Uptake[a] of ^{111}In F17-23-2 in the rest of the organs and tissues sampled in the studied rats.

Expt	Rat	CLN	Thy	Lung	Int	PP	Tib+BM	Tib	Muscle
15	PVG	0.80	0.24	1.34	0.32	0.35	0.68	0.30	0.15
	Ctrl	±0.005	±0.002	±0.005	±0.003	±0.006	±0.003	±0.002	±0.001
	DA	2.03	1.20	1.86	0.74	4.61	0.67	0.75	0.07
	Ctrl	±0.01	±0.03	±0.005	±0.005	±0.05	±0.003	±0.004	±0.0006
16	DA->PVG	0.82	0.56	0.72	0.37	0.40	0.40	0.19	0.36
	(Tx 7d)	±0.02	±0.02	±0.01	±0.02	±0.02	±0.005	±0.004	±0.005
17	DA->PVG	0.61	0.69	0.85	0.21	0.08	0.40	0.27	0.10
	(Tx 4d 5µg)	±0.01	±0.02	±0.01	±0.01	±0.005	±0.004	±0.003	±0.002
	DA->PVG	0.72	0.47	0.72	0.27	0.23	0.42	0.24	0.19
	(Tx 4d 1µg)	±0.07	±0.02	±0.02	±0.02	±0.03	±0.01	±0.008	±0.008
18	DA->PVG	0.27	0.20	0.88	0.26	0.27	0.22	0.07	0.04
	(Tx 4d)	±0.001	±0.0009	±0.004	±0.001	±0.001	±0.001	±0.0003	±0.0002
	DA->PVG	0.35	0.21	0.67	0.21	0.24	0.19	0.07	0.04
	(Tx 4d)	±0.002	±0.01	±0.003	±0.001	±0.002	±0.001	±0.0003	±0.0002
19	DA->PVG	0.43	0.84	0.95	0.22	0.28	0.26	0.14	0.03
	(Tx 4d CsA)	±0.002	±0.006	±0.005	±0.0008	±0.002	±0.001	±0.0008	±0.0001
	DA->PVG	0.43	0.39	1.31	0.24	0.27	0.29	0.15	0.05
	(Tx 7d CsA)	±0.002	±0.003	±0.005	±0.002	±0.002	±0.001	±0.0007	±0.0003
20	DA->PVG	0.46	0.25	1.78	0.38	0.41	0.52	0.32	0.06
	(Tx 14d CsA)	±0.001	±0.0009	±0.007	±0.001	±0.002	±0.002	±0.002	±0.0002

a %ID/g.